Plant Molecular Biology **30**: 913–924, 1996.
© 1996 *Kluwer Academic Publishers. Printed in Belgium.*

Isolation, characterization and expression of the maize *Cat2* catalase gene

Lingqiang Guan, Alexis N. Polidoros and John G. Scandalios*
Department of Genetics, Box 7614. North Carolina State University, Raleigh, NC 27695-7614, USA
(author for correspondence)*

Received 19 October 1995; accepted in revised form 22 December 1995

Key *words:* catalase, gene expression, gene structure, isozyme, reactive oxygen

Abstract

The maize *Cat2* gene was isolated by direct cloning and PCR. The clones were mapped and sequenced. The start site of transcription was determined by primer extension. Computer analysis of the 1.6 kb *Cat2* promoter sequence has revealed an obvious TATA box, two GC boxes, a putative GA response element, and several ACGT core sequences known to have diverse regulatory functions in plants. Several other protein binding motifs were also identified within 800 bp upstream from the transcriptional start site. Five introns were identified in the *Cat2* coding region. All five *Cat2* introns are located in exactly the same position as five of the six introns in *Cat1*. Two of the *Cat2* introns are located in the same position as the two *Cat3* introns. The identical positioning of these introns suggests an evolutionary link between all three maize catalase genes. The response of the *Cat2* gene to plant growth regulators was examined. Results clearly showed that the response of *Cat2* to several environmental factors are developmental stage-dependent. Thus. complex regulatory mechanisms appear to be involved in the regulation of *Cat2* expression in maize.

Introduction

Catalase (H_2O_2:H_2O_2 oxidoreductase, EC 1.11.1.6; CAT) is a tetrameric, heme-containing enzyme found in all aerobic organisms. It provides protection against reactive oxygen toxicity by dismutating hydrogen peroxide to water and oxygen [1]. In maize (*Zea mays* L.), three unlinked structural genes, *Cat1*, *Cat2*, and *Cat3* encode three biochemically distinct isozymes, CAT-l, CAT-Z, and CAT-3 [2, 3]. Each of the *Cat* genes exhibits temporal and spatial specificity in its expression [4, 5, 6], and each responds differently to various environmental signals [1, 7]. In addition, the catalase isozymes exhibit cell and organelle specificities [1, and references therein]. For example, CAT-2 first appears during late kernel development and increases dramatically in the scutellum after germination. CAT-2 is absent in etiolated leaves, but rapidly accumulates upon exposure to light due to increased transcript accumulation and translation of the *Cat2* message.

The nucleotide sequence data reported will appear in the EMBL Nucleotide Sequence Database under the accession number Z54358.

Thus, unlike *Cat1* which does not respond to light and Cat3 which is controlled by a circadian clock, Cat2 is positively regulated by light in a tissue-specific manner [1, 8].

In order to understand the underlying mechanisms by which the *Cat* genes are regulated and expressed in response to various signals, their cDNAs were isolated and used, in turn, to isolate the respective genes. The *Cat1* and Cat3 genes were successfully isolated from a genomic library and fully characterized [9, 10]. The Cat2 gene was recently cloned by two different methods: direct cloning and PCR. Herein, we report on the isolation, characterization, and expression of the Car2 gene, and its comparison to the other maize catalase genes.

Materials and methods

Isolation and purification of digested genomic DNA

W64A genomic DNA was isolated from 14-day-old light grown leaves as described [11]. A large amount of total DNA (50 μg) was digested with the restriction enzymes *Bam*HI and *Xba*I and electrophoresed on a 0.4% agarose gel. Agarose slices containing DNA fragments between 2.0 to 4.0 kb in size were sliced into 6 agarose pieces. DNA purification was conducted by a special freeze-thaw method. The procedure proved to be an effective and efficient method in comparison to other commercially available DNA purification kits. This procedure is fast, inexpensive, and results in high-quality DNA ready for labeling and library construction. It can be effectively used for both low- and high-molecular-weight DNA purification. The detailed procedure is as follows: agarose slices were transferred into a microfuge tube and were quickly frozen in liquid N_2. Agarose slices were quickly thawed at 50 °C for 10 min. The tube was then centrifuged for 5 min and the aqueous solution containing eluted DNA was transferred into a new tube. The tube containing sliced agarose was frozen and thawed again to elute more DNA solution and the newly eluted liquid was transferred and combined with the previous eluted DNA. The efficiency of the DNA elution can be visualized under a UV light box. Phenol extraction was conducted to obtain pure DNA for genomic library construction. Ethidium bromide was removed from DNA by ethanol precipitation.

Preparation of the plasmid vector for genomic library construction

Because of the relatively small size of the insert DNA, we used plasmid pBluescript KS (–) as the vector for library construction. This plasmid was digested with the restriction enzymes *Xba*I/*Bam*HI and was purified by phenol/chloroform extraction.

Ligation and transformation

Genomic DNA fragments containing the *Cat2 5'* sequence were ligated into the *Bam*HI/*Xba*I-digested pBluescript vector. Ligation was set at 1:1 and 1:2 vector-to-insert ratio. Ligated plasmids were transformed into the XL-l Blue supercompetent cells according to the manufacturer's instructions (Stratagene). Transformation efficiency was 2 X 10' cfu/μg vector with supercompetent cells and 1:2 vector-to-insert ratio. The library was screened with a 5' end Cat2 cDNA fragment and positive clones were identified.

PCR primers

Two 21-mer primers for the genomic DNA PCR amplification reaction were synthesized (NCSU Molecular Genetics Facility). The 5' primer begins at the 22nd nucleotide of the known first *Cat2* intron (see Results for details) and its sequence is 5'-GTCTCAATTCGTGTTTCGTCG-3'. The 3' primer was selected to span 11 nucleotides in the 3'-untranslated region and the last 10 translated nucleotides of the *Cat2* cDNA. The 3' primer sequence is: 5'-GGTTGATCTTACATGCTCGGC-3'. Control PCR amplifica-

tion of the translated sequence of the *Cat2* cDNA was performed with plasmid p*Cat2*.1c template [12], the same 3' primer as in the genomic PCR and a 19-mer 5' primer from the start of translation with sequence 5'-CCATGGACCCGTACAAGCA-3'

Polymerase chain reaction

PCR was performed in a MJ Research PTC-100 programmable thermal controller, using either *Thermus aquaticus* DNA polymerase (*Taq* DNA polymerase; Stratagene) *or Thermoccocus litoralis* DNA polymerase (Vent; New England Biolabs). The reaction mixture, in a total volume of 100 μl, contained, when using *Taq* polymerase: 20 mM Tris-HCl pH 8.8, 10 mM $(NH_4)_2SO_4$, 10 mM KCl, 2 mM $MgSO_4$, 0.1% Triton X-100, 0.1 mg/ml nuclease-free BSA, 200 μM dNTPs, 1 μM of each primer, 5 units *Taq* Extender (Stratagene), 2.5 units *Taq* polymerase, and 0.5 μg template genomic DNA or 10 ng template plasmid DNA. The reaction mixture, when using Vent polymerase, was the same with the exceptions that the BSA and the *Taq* Extender were omitted and instead of *Taq*, 1 unit of Vent polymerase was used. The cycle program was, 3.5 min denaturation at 95 °C followed by 30 cycles of 1 min denaturation at 95 ° C, 1 min annealing at 60 ° C, and 1.5 min extension at 75 "C. The time of the last extension step was increased at 6 min to ensure that all the PCR products were complete double-stranded blunt-ended fragments. No differences were observed in the PCR products after the use of either Vent or *Taq* polymerases. Vent polymerase amplified DNA was used in further experiments, because Vent also contains a 3'-5' proofreading exonuclease activity resulting in higher fidelity of base incorporation compared to *Taq* polymerase, which lacks this function.

Purification and cloning of the PCR product

The PCR products were analyzed by agarose gel electrophoresis and the specific *Cat2* band was purified and directly cloned into the *Sma*I site of the pBluescript II KS(-) (Stratagene). That the PCR product was in fact *Cat2* was verified by hybridization with the Cat2 cDNA probe.

Sequencing

The DNA sequence of the *Cat2 5'* and the coding region clones were determined by the dideoxy nucleotide chain termination method [13]. Overlapping deletions for sequencing were generated using Exolll nuclease on double-stranded plasmid templates [14]. Template plasmids were isolated and purified by the Jetprep plasmid DNA isolation and purification kit (Genomed, Research Triangle Park, NC). Sequencing was performed by the Applied Biosystems Automated DNA Sequencer (Nucleic Acid Facility, Iowa State University).

Primer extension

Primer extension was used to determine the start site of transcription of *Cat2*. The procedure was according to Metraux *et* al. [15]. A 22-mer oligonucleotide primer (5'-TTGTACGGGTCCATGGCGGTGG-3') was synthesized (NCSU Molecular Genetics Facility) which is complementary to the 5' end of the *Cat2* cDNA. This primer was end-labeled with polynucleotide kinase. A 50 μg portion of total RNA (isolated from salicylic acid (SA)-treated scutella with increased *Cat2* transcript, 28 days after pollination [7]) was obtained. The modified procedure was described [9]. Extension products were electrophoresed on an 8% sequencing gel with sequencing reaction products of the *Cat2* promoter fragment using the same oligo primer.

Hormone treatment and RNA analysis

Maize W64A embryos were manually excised from germinating seed at 2 and 5 days post imbibition (dpi). Excised embryos were incubated

on MS basic salt plates [16] supplemented with 5 mM/10 mM of gibberellin (GA,), 100 mM abscisic acid (ABA) (5 dpi), and 1 mM/1.5 mM salicylic acid (2 dpi) for 24 h in the dark. After treatment, scutella were harvested, frozen in liquid nitrogen and stored at -70 "C. Total RNA was isolated from treated scutella by cold phenol extraction [17]. Total RNA (20 μg) from each sample was separated on denaturing 1.2% agarose gels, and transferred to either nitrocellulose or nylon membranes. The resulting blots were hybridized with ^{32}P-labeled *Cat2* gene-specific probe. After this analysis was performed, the probe was removed from the filters by repeated washes in boiling 0.1% SSC, 0.1% SDS. Equal sample loading was verified by reprobing the filters with a cloned fragment containing 18S rDNA [18].

Results

Isolation and characterization of the 5' end of the Cat2 *gene by direct cloning*

The *Cat1* and *Cat3 genes* of maize were previously isolated from a W64A genomic library and fully characterized [9, 10]. The maize *Cat2 gene* could not be isolated from the same library. We attempted a different approach in order to isolate the *Cat2* genomic clone. We have tested the possibility of isolating a partial genomic clone containing the 5' promoter region which is important for *Cat2* regulation by completely digesting with restriction enzymes. Preliminary results from Southern blot analysis indicated that a 2.3 kb *Xba*I/*Bam*HI genomic DNA fragment contained the 5' portion of the *Cat2* coding and 5' promoter regions. Genomic DNA was completely digested with *Xba*I/*Bam*HI and about 2.3 kb of this DNA was isolated and purified (Fig. 1A). Purified genomic DNA fragments were electrophoresed on a 1% agarose gel, transferred onto a nitrocellulose filter and probed with a *Cat2 5'* end cDNA fragment; one positive fraction was used for genomic library construction (Fig. 1B).

About 50000 colonies were screened with the

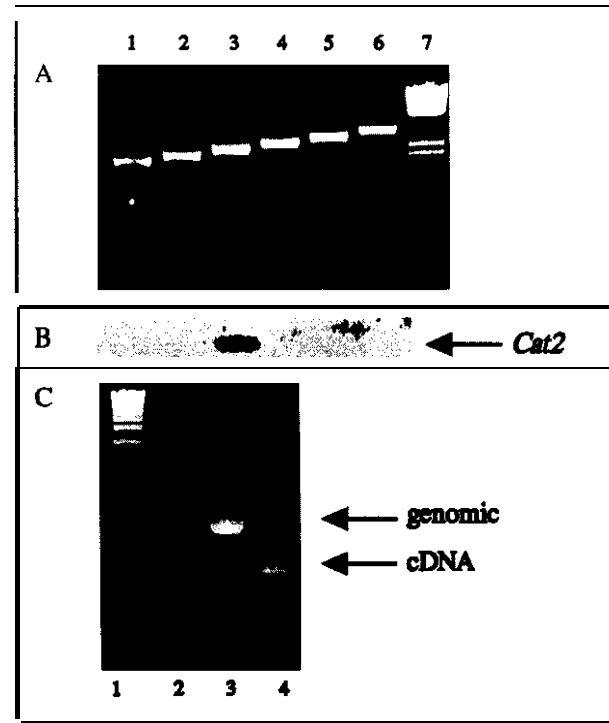

Fig. 1. W64A genomic DNA fragments purified by the freeze-thaw method. A. W64A genomic DNA (50 μg) was digested with *Bam*HI/*Xba*I and electraphoresed on a 0.4% agarose gel. Digested DNA fragments sized from 2.3 to 4 kb were sliced into 6 gel pieces and purified from agarose gels as described in Materials and methods. Fractions of purified DNA fragments were electrophoresed on a 1% agarose gel as indicated in lanes 1 to 6. Lane 7 is lambda *Hin*dIII DNA marker. B. The same DNA gel was transferred onto a nitrocellulose membrane and probed with a 5' *Cat2* cDNA fragment (*Eco*RI/*Bam*HI). Results indicate that lane 3 contains most of the *Cat2* genomic DNA fragments and was used for genomic library construction. C. Comparison of the PCR products using different Car2 templates. Lane I. 1 kb ladder (BRL) molecular weight markers. Lane 2, PCR amplification with Vent polymerase and 0.5 μg of maize genomic DNA as template. Lane 3, PCR amplification of *Cat2* genomic coding region using 10 ng of lane 2 PCR product DNA as template. Lane 4, PCR amplified *Cat2* cDNA using IO ng of lane 2 PCR product DNA as template. Lane 4, PCR amplified Car2 cDNA using 10 ng of p*Cat2*.1c plasmid as template. The *Cat2* genomic bands and the *Cat2* cDNA band are indicated by arrows. An apparent difference, ca. 400 bp in size can be observed suggesting the existance of intron(s) in the *Cat2* genomic coding region.

Cat2 5' end cDNA probe. Ten positive clones were identified and x-screened to eliminate any possible false positives. The plasmid DNA was

isolated in order to identify the proper insertion. Southern blots were used to confirm the positive clones and the restriction map was defined by digesting all positive clones with various restriction enzymes. Results indicated that all ten positive clones were identical. One of these clones was sequenced. On comparison to the Cat2 cDNA, this clone was found to contain a 1.6 kb 5' promoter sequence. The coding region ranged from the ATG start codon to the first *Bam*HI site (600 bp) (Fig. 2). Two introns were identified within that region by comparison with the Cat2 cDNA sequence. The first intron (92 bp long) was identified at five amino acids from the start of translation.

Isolation of the Cat2 gene *coding region by PCR*

In preliminary experiments, the primers designed for the Cat2 cDNA amplification were used in an attempt to amplify the Cat2 genomic coding region, with no success. After the genomic clone corresponding to the 5' of the *Cat2* coding region was isolated and sequenced, a 92 bp intron occurring 15 nucleotides from the first ATG codon was revealed. The last three nucleotides of the 5' cDNA primer were mismatching to the genomic DNA sequence due to the occurrence of that intro". Thus, a new 5' primer from the intron sequence was designed, to ensure that any PCR amplified sequence should represent *Cat2* genomic DNA. A single strong band about 1900 bp was observed after amplification ofgenomic DNA with the Vent polymerase. The 1900 bp band was excised from the gel to avoid any minor contamination and the recovered DNA was directly ligated into the *Sma*I site of the pBluescript vector. Plasmid DNA from clones with the correct insert served as template for PCR amplification to ensure that the insert is *Cat2* genomic DNA. Cat2 cDNA from the plasmid p*Cat2*.1c [12] was also amplified using the *Cat2* cDNA designed primers. The amplified *Cat2* genomic coding region migrated as a 1900 bp band from both templates used. The *Cat2* cDNA formed a 1480 bp band, as was expected. The apparent dissimilarity between the *Cat2* genomic coding region and the *Cat2* cDNA band suggested that one or more introns was responsible for the about 400 bp difference in length of the two bands (Fig. 1C). In order to gain more information about the number and possibly the location(s) as well as the orientation of the insert in one clone selected for further analysis, restriction digestion with several enzymes and sequencing were performed. Both indicated that in addition to the first intron which was used for making the 5' primer, four more introns were present. Comparison of the two clones isolated by direct cloning and by PCR as well as the *Cat2* cDNA revealed no mismatches in common regions.

Structure and expression ***of*** *the maize* Cat2 gene

Sequencing results showed that the overlapping regions of the two clones have identical sequences, indicating that both clones are part of the same gene. Previous results indicated that only one

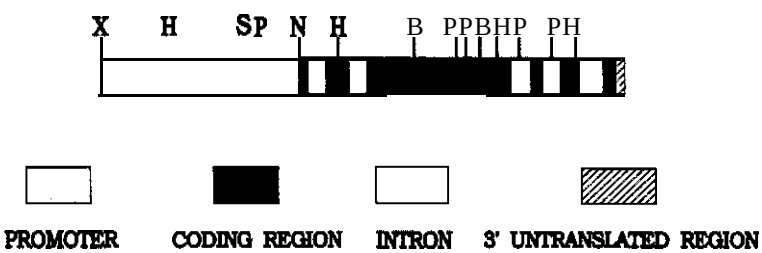

Fig. 2. Restriction map of the maize *Cat2* gene. The map was constructed from two clones isolated by direct cloning and PCR. The black box indicates the DNA fragments which hybridized to the full length *Cat2* cDNA probe. The introns, coding region, and 5'- and 3'-flanking regions are indicated. Restriction sites are: B, *Bam*HI; H, *Hin*dII; N, *Nco*I; P, *Pst*I; S, *Sac*I; X, *Xba*1.

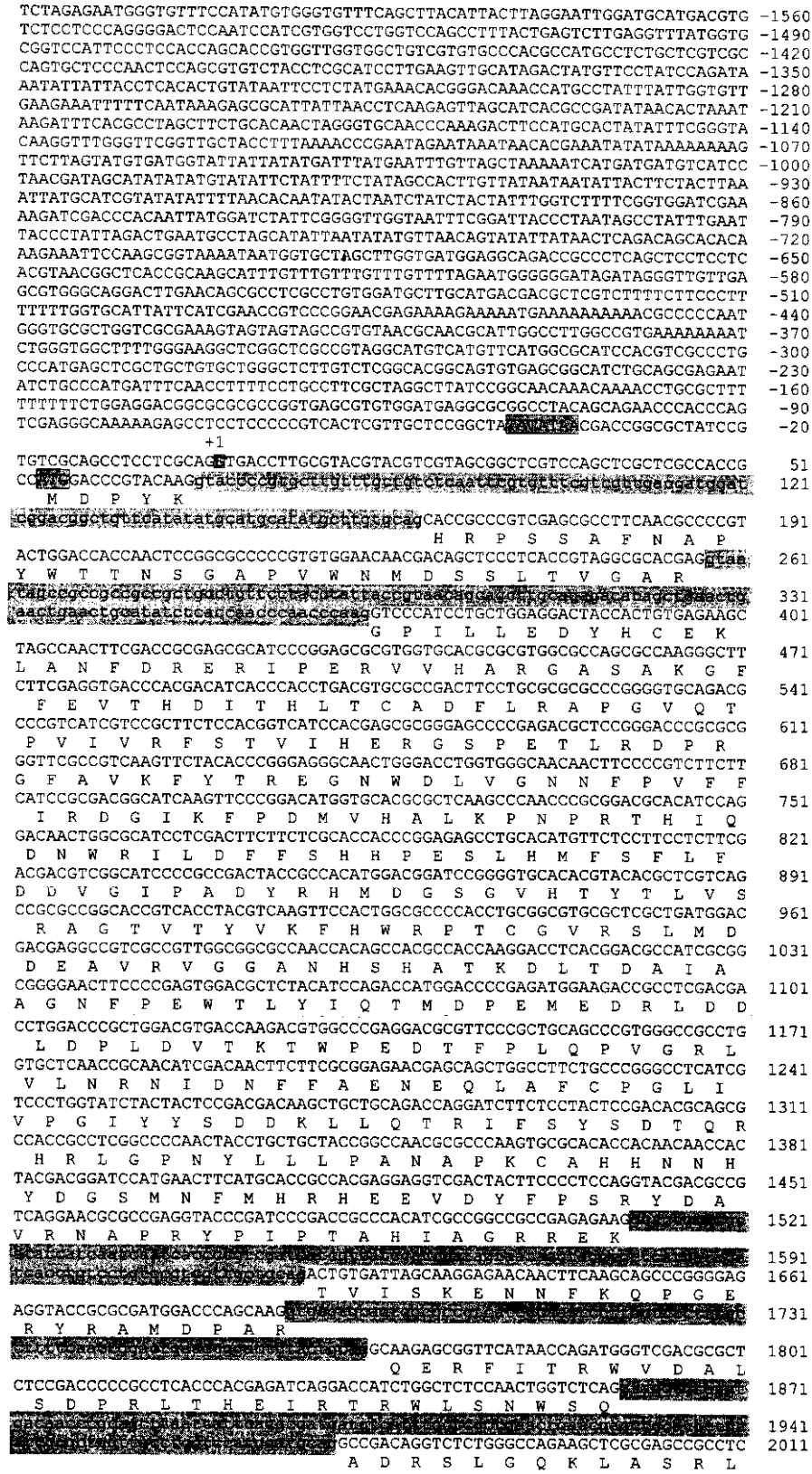

copy of the *Cat2* gene exists in the maize genome [11]. A restriction map (Fig. 2) was constructed based on a comparison of the Cat2 cDNA sequence with the Cat2 gene sequence (Fig. 3).

In order to map the 5' end of the Car2 transcript, primer extension was performed on total RNA isolated from 1 mM SA-treated scutella [7] 28 days after pollination in which the *Cat2* transcript was increased to high levels. The *Cat2* cDNA contains a short 5'-untranslated region. In order to obtain a fair size of extension product, a 22-mer oligonucleotide was synthesized which was complementary to both Cat2 cDNA and genomic DNA. It covered the portion of 5'-untranslated region and coding region up to the first intron. The primer extension product is about 45 bp and the 5' end is indicated as + 1 in Fig. 3. Upstream from the transcriptional start site, several motifs were found and are depicted in Fig. 4. A typical TATA box is located at -43. The CAAT consensus sequence cannot be found between -80 and -120; however, two sequence motifs (GCGCGG, GGGCAG), which are homologous to the consensus sequences for the Spl-binding site, GGGCGG (GC box) [19] were found around -114 and -570. The GC box has been found in promoters of many viral and cellular genes [20], and acts as a binding site of a protein, Spl, which is necessary for transcriptional activity. A pyrimidine box (CCTTT) and Box I (GCAGTG) which are part of the GA response complex [21] were found at -208 and -256. Two 8 bp sequences (CACGTCGC, CACGTAAC) which are similar to an ABA response element (ABRE, CACGTGGC) [22] were located at -308, -648 relative to the + 1 site. The core sequence of the ABA response element (ACGT) is the binding site for basic leucine zipper transcriptional factors or common plant regulatory factors (CPRFs) [23]. Promoter elements with a ACGT core are recognized by both homo- and heterodimers of leucine zipper transcriptional factors. A CEl-like element which was recently reported to enhance the ABA response [24], was located next to the second ABRE at -636 (Fig. 4). A 6 bp inverted repeat sequence (CGGCGC,GCGCCG) was also found. An 11 bp element (GGTGACCTTGC), which is identical to the antioxidant response element (ARE, PuGTGACNNNGC) of the rat glutathione *S*-transferase Ya subunit [25], was identified at a position close to the + 1 site. The ARE might represent a *cis*-acting element which activates genes that protect eukaryotic cells against oxidative stress. The ARE was also found at -470 of the maize *Cat1* promoter [9]. Two direct ACGT repeat sequences, which is the core sequence for leucine zipper protein binding sites, were located at about 15 bp downstream of the + 1 site. A DNA motif CAGGTG, which is identical to the core sequence for a class of transcriptional factors bHLH (CANNTG, basic helix-loop-helix proteins), was located near the + 1 site and overlapping with the 5' portion of the ARE motif. This transcriptional factor shares similarities with the basic, leucine zipper family and can form homo- and heterodimers to exert regulatory functions [26]. Two additional bHLH binding motifs (CATCTG, CATTTG) were also found at -245, and -625 relative to the + 1 site. Both of them are located down stream of the two leucine zipper core sequences ACGT. A DNA sequence (CGTCCCGGAACG) was located at -480 with 2 bp mismatch to the 12 bp metal responsive element (MRE, CGNCCCGGNCNC) core sequence [27]. This motif can be found in the promoter region of metallothionein proteins that bind heavy metal ions, and have been functionally implicated in heavy metal detoxification [28]. The putative regulatory motifs found in the 5' of the *Cat2* gene are summarized in Fig. 5.

The DNA coding sequence in the coding region of the *Cat2* genomic DNA is identical to the cDNA. The map and sequence of the *Cat2 gene*

Fig. 3. Nucleotide and deduced amino acid sequence of the maize Cad gene. The *Cat2* clones were sequenced by the dideoxynucleotide chain termination method. The deduced amino acid sequence is shown in single letter code below the nucleotide sequence. Introns are shown in lower-case letters. The transcriptional start site was determined by primer extension and is indicated as + 1. The translational codon (ATG) and TATA box are also indicated.

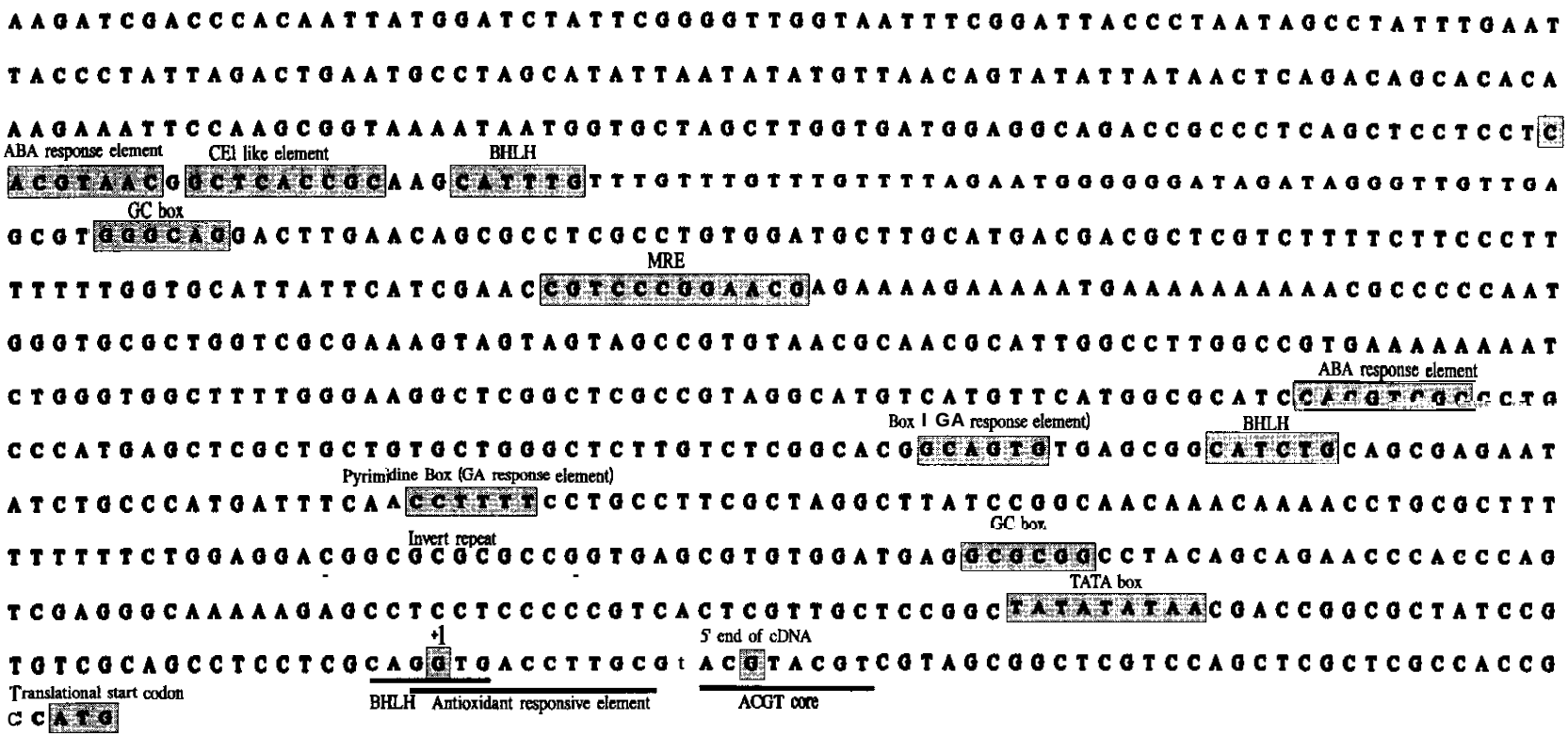

Fig. 4. Nucleotide sequence of the maize *Cat2* genomic DNA 5'-flanking region. This region extends from −860 (relative to the start of transcription + 1) to + 56, the translational start codon. The ATG codon, 5' end of the cDNA and + 1 site are indicated. Arrows indicate the direct repeat sequence. Some important motifs for plant gene regulation are also indicated and boxed, including TATA box, two GC boxes, two ABRE, CE1 like elements, metal responsive element (MRE), antioxidant-responsive element (ARE), three BHLH (basic helix-loop-helix), and part of the GA response element (pyrimidine box and box I).

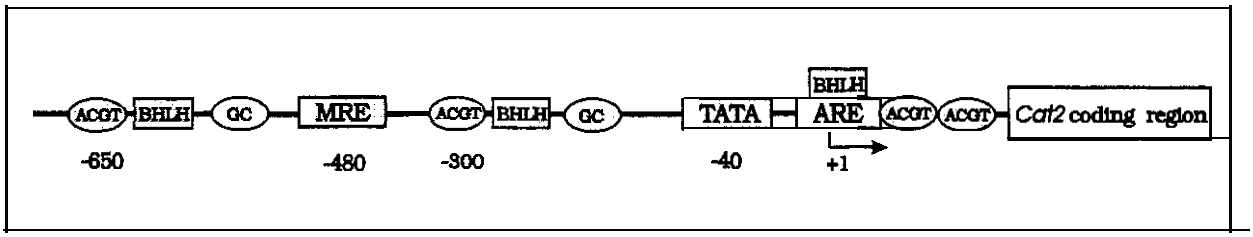

Fig. 5. Schematic representation of the putative motifs located in the promoter region of the Car2 gene. The abbreviations are: BHLH, basic helix-loop-helix protein binding site; ARE, antioxidant-responsive element: ACGT, ACGT core or leucine zipper protein binding site; GC, GC box or Spl-binding site; MRE, metal-responsive element.

indicated that the coding region contains five short introns. All introns possess the consensus 5' GT splice donor site and the 3' AG splice acceptor site described in other eukaryotic genes [29]. The properties of these five introns are indicated in Fig. 6. Intron sizes are relatively small ranging from 78 to 113 bp. The sequence at the 5' and 3' splice sites of the introns have low homologies to the consensus sequence (CAG/GTAAGT and TGCAG/GT) for plant introns [30]. In addition, all five introns are atypical from other plant introns in that they are not AT-rich. All five *Cat2* introns are located in exactly the same positions as five of the six introns in ***Carl.*** The number three intron in *Cat1* is missing in the *Cat2* gene (Fig. 7). In contrast to the *Cat1* introns, all *Cat2* introns are about 50% AT nucleotides and their sizes are relatively small in comparison to the *Cat1* introns. Introns 1 and 5 of the *Cat2* gene are located at the same position as the two introns in the *Cat3* gene. These results indicate evolutionary linkages among the three maize catalase genes.

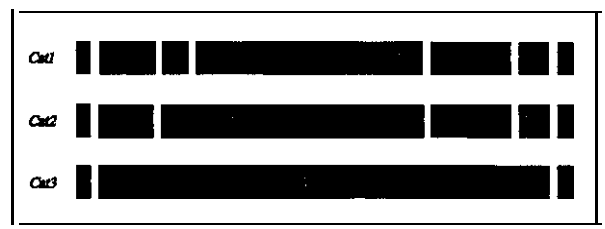

Fig. 7. Exon/intron structure of the three maize catalase genes. Exons (dark boxes) and intrans (gaps) are drawn schematically to indicate the relative position of the introns. The maize *Cat1* gene [9] possesses 6 introns, the Car2 gene (this study) has 5 intrans, and *Cat3* contains only 2 introns [10].

The expression of the maize *Cat2* gene is highly regulated developmentally and spatially [1]. The *Cat2* transcript can be detected during the late stages of seed development. Upon germination, the Cat2 transcript increases dramatically and reaches a peak at about 4 days after imbibition. The responses of *Cat2* to several environmental factors have also been examined. *Cat2* responds to the fungal toxin cercosporin differently at two distinct developmental stages: embryogenesis and

Properties of *Cat2* gene introns

Intron #	Junction sequence	Size (bp)	A+T (%)
1	CAAG/GTACCC.....TGCAG/CA	92	51
2	CGAG/GTAATA.....CCAAG/GT	108	47
3	GAAG/GTACTG.....TGCAG/AC	109	52
4	CAAG/GTGCGT.....TGCAG/GC	78	47
5	TCAG/GTAGGT.....TGCAG/GC	113	49

Fig. 6. Properties of the maize Car2 introns. The intron/exon junction sequences were located by comparison with the *Cat2* cDNA sequence. The size of *Cat2* introns varies from 78 to 113 bp.

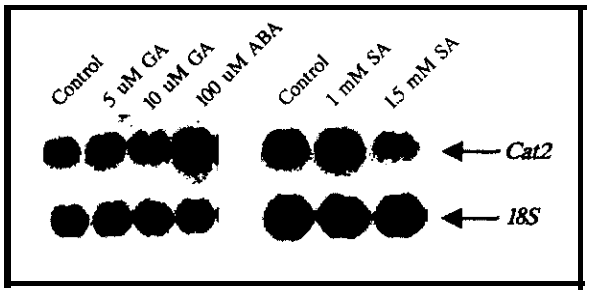

Fig. 8. Responses of the maize Car2 gene to GA,, ABA and SA in mature maize embryos. W64A embryos were excised from 5 dpi seeds and treated with 5 mM, 10 mM of gibberellic acid (GA_3), 100 mM ofabscisic acid (ABA); embryos were also excised from 2 dpi and treated with 1 mM/1.5 mM of salicylic acid (SA) as described. Scutella were isolated from treated embryos and examined for Car2 transcript accumulation with *Cat2* gene-specific probe and reprobed with a 18S DNA fragment as a loading control. Representative results from duplicate blots are shown.

germination [31]. The *Cat2 gene* also responds to SA differentially at these two stages [7]. In order to gain a better understanding of the developmental stage-dependent responses of *Cat2*, *we* extended our studies to examine the response of *Cat2* to plant growth regulators at later stages of germination. Germinating embryos were treated with GA, ABA at 5 dpi and SA at 2 dpi for 24 h. Northern blots were then performed with a *Cat2* gene-specific fragment. Results indicated that the *Cat2* transcript did not change upon GA treatment; however, the *Cat2* transcript from scutella 5 days after imbibition increased dramatically following ABA treatment, and *Cat2* transcript increased slightly after 1 mM SA treatment at 2 dpi (Fig. 8).

Discussion

The maize *Cat2* genomic DNA was isolated by direct cloning and PCR. A 2.3 bp genomic clone containing the 5' end of the *Cat2 gene* was isolated by the direct cloning method. The fragment includes 1.7 kb of sequence 5' of the Cat2 gene, two small introns shortly after the ATG start codon, and 600 bp of coding sequence. The small intron located 5 amino acids from the amino terminus is located exactly at the same position as the first introns of the *Carl* and *Cat3 genes. No* sequence similarity was found among the first introns of the three maize Cat genes. The coding region of the *Cat2* gene was cloned and isolated by PCR with the primer designed from the first intron. The resulting PCR product shared about 400 bp identical with the 3' portion of the 2.3 kb clone. This indicated that both clones are part of the same *Cat2* gene. Previous DNA blot data also suggested that only one copy of the *Cat2* gene exists in the maize genome [11]. In the coding region of the *Cat2* gene, 5 introns were located and their locations are exactly the same as five of the maize *Catl* introns. They also share the same locations with five castor bean introns [32]. The identical positions of the catalase introns between the monocot and dicot plants imply evolutionary links among plant catalases.

The *Cat2* gene promoter region revealed an obvious TATA box located 43 bp 5' from the end of the cDNA. No CAAT box was found within 120 bp upstream from the 5' end *Cat2* cDNA; however, several motifs involved in plant gene regulation were identified. Two putative ABA response elements (CACGTCGC, CACGTAAC) were identified in the Cat2 promoter region. One of the elements (CACGTCGC, -308) is almost identical to the ABA response element (CACGTGGC) of the wheat *Em gene* [22]. However, the *Cat2* gene responds negatively to ABA in scutella after pollination and the *Cat2* transcript failed to accumulate after 24 h of ABA treatment [33]. In this report, we found that the *Cat2* transcript increased after 24 h ABA treatment at 5 dpi, suggesting that the response of the *Cat2* gene to ABA is developmental stage specific. Whether the effect is direct or indirect still needs to be determined. This ABA response element contains the core **sequence** ACGT which is a *cis*-acting element for plant transcription factors. It is also the core element for response to light [34, 35], jasmonic acid [36], and salicylic acid [37]. The Cat2 gene responds positively to light [8] and salicylic acid [7]. It is possible that the ACGT core sequence in the *Cat2 gene* also serves as a light or SA response element. At 1 mM

of SA concentration, Cat2 transcript increased dramatically in 28 dpp scutella; however, the *Cat2* transcript failed to accumulate at 1 dpi with the same doses of SA treatment [7]. We extended our study to examine the effect of SA on *Cat2* at 2 dpi. Surprisingly, the *Cat2* transcript again increased slightly upon 1 mM SA treatment. The levels of transcript accumulation are not as dramatic as they are during embryogensis. **Thus,** the response of *Cat2* to the same doses of SA is not only different at two distinct developmental stages (i.e., embryogenesis and germination), but also differ at two time points of the same developmental stage. A pyrimidine box (CCTTTT) and box I (GCAGTG) of the GA response complex of a barley α-amylase [21] were also identified. Recently, new evidence indicated that the *Cat2 gene* is induced by a germination related regulator [7]. This regulator might be GA or some other plant hormone. To address this question, maize embryos from 5 dpi were isolated and incubated in culture plates containing GA, and the *Cat2* transcript level was examined by northern blots. Results showed that there are no changes in *Cat2* transcript levels between GA treated and non-treated maize embryos at 5 dpi. This is also the case with 28 dpp embryos (data not shown). These results suggest that GA is not the regulatory factor which induces *Cat2* expression upon germination.

Several regulatory motifs were found in the area around the transcription start site and 5′-untranslated region as well. Two repeat ACGT core sequences were located down stream of the + 1 site. An antioxidant responsive element and a bHLH binding site were located around the + 1 site. The function of these putative motifs at the + 1 and 5′-untranslated region still needs to be determined. It may be that they are involved in post-transcriptional mechanisms which regulate the *Cat2* gene. Further upstream in the *Cat2* promoter, two other bHLH motifs were also located near two ACGT core sequences. The same pattern was observed in the 5' region of the maize *Cat1* gene (two bHLH located near two ACGT core sequences) [9]. The role of the sequential presence of these elements in the two catalase gene promoters is being investigated. The expression of the maize *Cat2* gene is regulated at several different levels. The *Cat2* gene also responds to signals at specific developmental stages. Thus, tissue and stage specific regulatory factors might be involved in the regulation of *Cat2 gene.* Further experiments are underway to identify the *cis*-acting elements and the *trans*-acting factors responsible for *Cat2* expression.

Acknowledgements

We thank Stephanie Ruzsa and Sheri Kernodle for expert technical assistance. Research was supported in part by Grant 94-37-100-0690 from the National Research Initiative Competitive Grants Program, U.S.D.A., and North Carolina State University.

References

1. Scandalios JG: Regulation and properties of plant catalases. In: Foyer CH, Mullineaux PM (eds) Causes of Photooxidative Stress and Amelioration of Defense Systems in Plants, pp. 275-315. CRC Press, Boca Raton, FL (1994).
2. Scandalios JG: Subunit dissociation and recombination of catalase isozymes. Proc Natl Acad Sci USA 53: 1035–1040 (1965).
3. Scandalios JG, Tong WF, Roupakias DG: *Cat3*, a third gene locus coding for a tissue-specific catalase in maize: Genetics, intracellular location, and some biochemical properties. Mol Gen Genet 179: 33-41 (1980).
4. Scandalios JG, Tsaftaris AS, Chandlee JM, Skadsen RW: Expression of the developmentally regulated catalase (Cat) genes in maize. Devel Genet 4: 28 l-293 (1984).
5. Wadsworth GJ, Scandalios JG: Differential expression of the maize catalase genes during kernel development: the role of steady-state mRNA levels. Devel Genet 10: 304-310 (1989).
6. Redinbaugh MG, Sabre M, Scandalios JG: The distribution of catalase activity, isozyme protein, and transcript in the tissues of developing maize seedlings. Plant Physiol 92: 375-380 (1990).
7. Guan L, Scandalios JG: Developmentally related responses of maize catalase genes to salicylic acid. Proc Natl Acad Sci USA 92: 5930-5934 (1995).
8. Skadsen RW, Scandalios JG: Translational control of photo-induced expression of the Car2 catalase gene during leaf development in maize. Proc Natl Acad Sci USA 84: 2785-2789 (1987).

9. Guan L, Scandalios JG: Characterization of the catalase antioxidant defense gene *Cat1* of maize, and its developmentally regulated expression in transgenic tobacco. Plant J 3: 527-536 (1993).
10. Abler MA, Scandalios JG: Isolation and characterization of a genomic sequence encoding the maize Cad catalase gene. Plant Mol Biol 22: 1031–1038 (1994).
11. Redinbaugh MG, Wadsworth GJ, Scandalios JG: Characterization of catalase transcripts and their differential expression in maize. Biochim Biophys Acta 951: 104– 116 (1988).
12. Bethards LA, Skadsen RW, Scandalios JG: Isolation and characterization of a cDNA clone for the *Cat2* gene in maize and its homology with other catalases. Proc Natl Acad Sci USA 84: 6830-6834 (1987).
13. Sanger F, Nicklen S, Coulsen AR: DNA sequencing with chain-terminating inhibitors. Proc Natl Acad Sci USA 74: 5463-5467 (1977).
14. Henikoff S: Unidirectional digestion with exonuclease III creates targeted breakpoints for DNA sequencing. Gene 28: 351-359 (1984).
15. Metraux JP, Burkhart W, Moyer M, Dincher S, Middles&ad W, Williams S, Paune G, Carnes M, Ryals J: Isolation of a complementary DNA encoding a citinase with structural homology to a bifunctional lysozyme/chitinase. Proc Natl Acad Sci USA 86: 896-900 (1989).
16. Murashige T, Skoog F: A revised medium for rapid growth and bioassays with tobacco tissue cultures. Physiol Plant 15: 473-497 (1962).
17. Beachy RN, Chen Z-L, Horsch RB, Rogers SG, Horggman NL, Fraley RT: Accumulation and assembly of soybean β-conglycinin in seeds of transformed petunia plants. EMBO J 4: 3047-3053 (1985).
18. Jorgensen RA, Cuellar RE, Thompson WF, Kavanagh TA: Structure and variation in ribosomal RNA genes of pea. Characterization of a cloned rDNA repeat and chromosomal rDNA variants. Plant Mol Biol 8: 3-12 (1987).
19. Dynan WS, Tjian R: Control of eukaryotic messenger RNA synthesis by sequence-specific DNA-binding proteins. Nature 316: 774-778 (1985).
20. Kadonaga JT, Jones KA, Tjian R: Promoter-specific activation of RNA polymerase II transcription by Sp1. Trends Biochem Sci 11: 20-23 (1986).
21. Sutliff TD, Lanahan MB, Ho TH: Gibberellin treatment stimulates nuclear factor binding to the gibberellin response complex in a barley alpha-amylase promoter. Plant Cell 5: 1681-1692 (1993).
22. Guiltinan MJ, Marcotte WR Jr, Quatrano RS: A plant leucine ripper protein that recognizes and abscisic acid response element. Science 250: 267-271 (1990).
23. Armstrong GA, Weisshaar B, Hahlbrock K: Homodimeric and heterodimeric leucine zipper proteins and nuclear factors from parsley recognize diverse promoter elements with ACGT core. Plant Cell 4: 525-537 (1992).
24. Shen Q, Ho T-HD: Functional dissection of an ahscisic acid (ABA).inducible gene reveals two independent ABA-responsive complexes each containing a G-box and a novel *cis*-acting element. Plant Cell 7: 295-307 (1995).
25. Rushmore TH, Morton MR, Pickett CB: The antioxidant responsive element. J Biol Chem 266: 11632-11639 (1991).
26. Pabo CO: Transcription factors: structural families and principles of DNA recognition. Annu Rev Biochem 61: 1053–1095 (1992).
27. Stuart GW, Searle PF, Chen HY, Brinster RL, Palmiter RD: A 12-base-pair DNA motif that is repeated several times in metallothionein gene promoters confers metal regulation to a heterologous gene. Proc Natl Acad Sci USA 81: 7318-7322 (1984).
28. Westin G, Schaffner W: A zinc-responsive factor interacts with a metal-regulated enhancer element (MRE) of the mouse metallothinein-I gene. EMBO J 7: 3763-3770 (1988).
29. Shapiro MB, Senapathy P: RNA splice junctions of different classes of eukaryotes: Sequence statistics and functional implications in gene expression. Nucl Acids Res 15: 7155-7174 (1987).
30. Brown JWS: A catalogue of splice junction and putative branch point sequences from plant introns. Nucl Acids Res 14: 9549-9559 (1986).
31. Williamson JD, Scandalios JG: Response of the maize catalases and superoxide dismutases to cercosporin-containing fungal extracts: the pattern of catalase response in scutella is stage specific. Physiol Plant 88: 159-166 (1993).
32. Suzuki M, Ario T, Hattori T, Nakamura K, Asahi T: Isolation and characterization of two tightly linked catalase genes from castor bean that are differentially regulated. Plant Mol Biol 25: 507-516 (1994).
33. Williamson JD, Scandalios JG: Differential response of maize catalases to abscisic acid: *Vp1* transcriptional activator is not required for abscisic acid-regulated *Cat1* expression. Proc Natl Acad Sci USA 89: 8842-8846 (1992).
34. Oeda K, Salinas J, Chua N-H: A tobacco b-Zip transcription activator (TAF-I) binds to a G-box-like motif conserved in plant genes. EMBO J 10: 1793–1802 (1991).
35. Schulze-Lefert P, Becker-Andre M, Schulz W, Hahlbrock K, Dangl JC: Functional architecture of the light-responsive chalcone synthase promoter from parsley. Plant Cell 1: 707-714 (1989).
36. Mason HS, Dewald DB, Mullet JE: Identification of methyl jasmonate-responsive domain in the soybean *vspB* promoter. Plant Cell 5: 241–251 (1993).
37. Qin X-F, Holuigne L, Horvath DM, Chua N-H: Immediate early transcription activation by salicylic acid via the cauliflower mosaic virus *as-1* element. Plant Cell 6: 863–874 (1994).

Free Radical Biology & Medicine, Vol. 23, No. 3, pp. 497–504, 1997
Copyright © 1997 Elsevier Science Inc.
Printed in the USA. All rights reserved
0891-5849/97 $17.00 + .00

PII S0891-5849(97)00110-X

Forum

RESPONSE OF THE MAIZE CATALASES TO LIGHT

ALEXIS N. POLIDOROS and JOHN G. SCANDALIOS
Department of Genetics, North Carolina State University, Raleigh, NC, USA

Abstract—The three maize catalase genes respond differentially to light signals. Expression of *Cat1* is light independent while expression of *Cat2* and *Cat3* is light responsive. Upon exposure to light there is rapid accumulation of CAT-2 protein in leaves, due to both increased transcript accumulation and increased translation of the *Cat2* message. Short UV light pulses also cause a strong transient induction of *Cat2* gene expression, while long term exposure to UV does not affect the rate of *Cat2* transcription. The *Cat3* gene of maize exhibits a transcriptionally regulated circadian rhythm. The induction of the *Cat3* circadian expression in etiolated leaves is probably regulated by a very low fluence phytochrome response; the involvement of a blue light/UV-A and a UV-B photoreceptor is also possible. Regulatory elements located on the *Cat3* promoter have recently been identified and their significance in the complex light response of the gene is being investigated. Possible physiological role(s) of the light responding maize catalases *Cat2* and *Cat3* are discussed. © 1997 Elsevier Science Inc.

Keywords—*Zea mays*, Catalase, Light regulation, UV light, Free radicals, Circadian rhythm

INTRODUCTION

Light is an environmental signal that, in addition to providing energy for photosynthesis, serves as a trigger and modulator of complex regulatory mechanisms. The transition from an etiolated seedling to a fully green plant is one of the most dramatic events in the plant's life cycle.[1] During this transition the expression patterns for many genes are affected in various ways. Among the genes whose expression patterns are reprogrammed by exposure to light are two of the three catalases in maize.

Catalase (H_2O_2:H_2O_2 oxidoreductase, EC 1.11.1.6; CAT) is a tetrameric heme containing enzyme, that is found in all aerobic organisms, and degrades H_2O_2 at an extremely rapid rate.[2] Plants, unlike animals, have multiple enzymatic forms (isozymes) of catalase. In maize three unlinked nuclear structural catalase genes have been isolated and characterized.[3–5] These genes, namely *Cat1*, *Cat2*, and *Cat3* encode the three biochemically distinct catalase isozymes CAT-1, CAT-2, and CAT-3 respectively.[6–9] The function of catalase places the enzyme in the first line of the antioxidant defense mechanisms of the cell. Eukaryotic cells continuously produce reactive oxygen species (ROS) as by-products of electron transfer reactions. Several major metabolic processes of plants including photosynthesis, respiration, and β-oxidation of fatty acids are responsible for the production of ROS during normal metabolism. Antioxidant enzymatic and non-enzymatic mechanisms effectively remove ROS from different cellular compartments, preventing cellular damage. The antioxidant responses need to be finely tuned in order to be highly specific and efficient. Light is the signal that initiates a major transition from heterotrophic to autotrophic metabolism, and is also responsible for the initiation of ROS production during this metabolic process. Thus, it is not surprising that light also modulates and reprograms antioxidant gene expression in order to coordinate antioxidant defense responses to cope with the ROS produced during autotrophic metabolism.

The three maize catalase genes respond differentially to light. The expression of the *Cat1* gene is light independent throughout development.[2,11] In contrast, *Cat2* appears to be positively regulated by light[10–13] and *Cat3* exhibits a transcriptionally regulated circadian rhythm.[3,12–15] In this review we summarize the differential responses of maize catalases to light signals.

Address correspondence to: J. G. Scandalios, Department of Genetics, North Carolina State University, Raleigh, NC 27695-7614. E-mail: jgs@unity.ncsu.edu

CATALASE PHOTOINACTIVATION AND PHOTOREGULATED GENE EXPRESSION

Catalase is a light sensitive enzyme.[16] Purified catalase from bovine liver and catalase of isolated intact peroxisomes from rye leaves were shown to be inactivated *in vitro* by irradiation with visible light.[17] In the presence of isolated chloroplasts, catalase inactivation is mediated by light absorption in the chloroplasts. However, photoinactivation of catalase occurs only in the presence of non-photosynthesizing, but not in the presence of photosynthesizing, chloroplasts. Substantial and selective photoinactivation of catalase was also reported *in vivo*, when leaf sections from various plants, including maize, were irradiated with light of high intensity in the presence of translational inhibitors.[17] These results were verified in mature rye leaves, as the catalase polypeptide was shown to be increasingly degraded with increasing irradiance, although the steady state level of the enzyme remained fairly constant.[18] Degraded catalase was replaced by new synthesis that was also increasing with light intensity but was low in darkness.[18]

Regulation of catalase genes by light involves both induction and inhibition of gene expression. Photoregulated catalase gene expression has been reported in several plant species including maize,[10–15] *Arabidopsis*,[20,21] *N. plumbaginifolia*,[19,22] cotton,[23] and barley.[24] The maize CAT-2 catalase protein is synthesized in leaves only in the presence of light. *Cat2* mRNA can be isolated from both etiolated and light grown leaves. However, it is rendered translatable only after the leaves are exposed to white light, leading to a dramatic induction of the CAT-2 isozyme.[2,10] Further studies in our laboratory indicated that, in addition to this translational induction, transcriptional induction of *Cat2* gene expression also occurs after exposure to light.[13] The transcriptional induction of *Cat2* expression by light depends upon the presence of carotenoids. Carotenoid deficient maize mutants failed to accumulate detectable *Cat2* mRNA after exposure to light.[13] Such transcriptional and translational control mechanisms driven by light are known to regulate photosynthesis related genes.[1] The functional significance of the photoinduction of the *Cat2* gene during leaf development in maize is not clear. A possible role for CAT-2 is degradation of H_2O_2 produced in light grown maize leaves during photorespiration. However, the rate of photorespiration is not particularly high in maize, a C4 plant, and the constitutive expression of *Cat1* is likely sufficient to accommodate the H_2O_2 generated from photorespiration in green leaves as is suggested by the occurrence of normally growing CAT-2 null maize mutants. Thus, CAT-2 may play a significant role in protecting the plant under conditions that induce photooxidative stress, such as low temperature in combination with high light intensity. Such possibilities are currently under investigation in our laboratory using maize *Cat2* containing transgenic tobacco plants.

EFFECTS OF UV-LIGHT IN THE EXPRESSION OF THE MAIZE *CAT2* GENE

Differential light responses of the three maize catalases are also reflected in their expression pattern during photooxidative stress caused by UV-irradiation. We have recently shown[55] that UV light pulses in the range of 240–400 nm could entrain the *Cat3* circadian expression and cause a strong transient induction of *Cat2*. The most distinct response was obtained with UV-light in the range of 290 to 400 nm (containing UV-B and UV-A). This effect was reduced by 60‰ when the UV-B portion (240–310 nm) was removed. Expression of the *Cat2* gene was also induced by a UV-A/blue light pulse (310–400 nm). However, the maximal transcript level of *Cat2* was lower and appeared earlier than that observed by the full spectrum UV light pulse. Taken together these results suggest that the UV light induction of *Cat2* gene expression may be regulated by a UV-B and a UV-A/blue light photoreceptor.

A slight induction of *Cat2* was also observed after long term exposure to UV light. However, the level of *Cat2* transcript accumulation was lower than that obtained with UV light pulses, even though the transcript level remained slightly enhanced over the controls. Considering the stable circadian expression of *Cat3* under UV-light stress (see below), *Cat2* may ensure a basic level of H_2O_2 scavenging, particularly at the period when *Cat3* reaches a minimum during its circadian oscillation.

In *N. plumbaginifolia* leaves *Cat1* and *Cat2* (not similar to the maize *Cat1* and *Cat2* genes) transcript levels changed dramatically in response to UV-B stress; *Cat1* was repressed, whereas *Cat2* was induced four-fold after UV-B exposure. In addition, *Cat3* (also not similar to the maize *Cat3* gene) was induced by UV-B.[19] These data suggest a distinct role of each catalase in UV-light stressed *N. plumbaginifolia* leaves.

CIRCADIAN REGULATION OF PLANT CATALASES

Similarities and differences among different plant species

The *Cat3* gene of maize (a monocot C4 plant) was the first catalase gene reported to exhibit a transcriptionally regulated circadian rhythm.[12] Since then, three additional plant catalases (in dicot C3 plants), the *Arabidopsis Cat2*[20] and *Cat3*[21] (previously called *Cat1*),

and the *Cat1* gene of *N. plumbaginifolia*[22] have been shown to be transcriptionally regulated by the circadian clock; the most important characteristics of the circadian expression of catalase genes in different plants are summarized in Table 1. Among them, two different patterns of circadian regulation are observed. The maize *Cat3* and the *Arabidopsis Cat3* show maximal expression late in the light period, approximately 10 h after the light onset (CT-10, circadian time) and minimal transcript accumulation late in the dark period at CT-22. The *Arabidopsis Cat2* and the *N. plumbaginifolia Cat1* exhibit a circadian rhythm similar to the typical rhythm observed for the photosynthetic genes *cab* and *rbcS* with maximal transcript accumulation early after exposure to light, and minimal at the start of the dark period.

Additional differences between the opposite cycling catalases *Cat2* of *Arabidopsis* and *Cat3* of maize have been observed. The *Arabidopsis Cat2* mRNA reaches a peak of abundance 1 day after imbibition in continuous dark (DD) or continuous light (LL) grown seedlings.[20] A second peak of mRNA abundance appears 6 days after imbibition only in light grown seedlings and may be associated with the development of photosynthetic competence and induction of photorespiration. This second peak is regulated by light and is not seen in etiolated seedlings.[20] *Cat2* mRNA accumulation is induced by exposure to high-fluence blue or far-red light but not by red light. In addition, light induction is unaffected by mutations that block blue-light mediated inhibition of hypocotyl elongation (*blue1, blue2, blue3, hy4*), suggesting phytochrome involvement. Upon transfer of etiolated seedlings to constant white light, *Cat2* mRNA rapidly accumulates and its abundance undergoes robust oscillations with 24 h periodicity, indicating control by an endogenous circadian clock. The rhythm is also present in plants growing under dark-light cycles and persists for at least 5 circadian cycles when plants are transferred either to constant dark or to constant light, indicating the robustness of the circadian rhythm.[20] In contrast, the maize *Cat3* mRNA is present at constant levels in leaves of either DD or LL growing seedlings without an apparent oscillation.[13] The same is observed with the *Arabidopsis Cat3* as its expression is similar in seedlings germinated and growing either in continuous dark or in continuous light.[21]

Physiological role(s) relative to the circadian rhythms of the catalase genes

Considering that different patterns of circadian expression of catalase genes are present within the same (*Arabidopsis*) as well as between different plant species (*Arabidopsis*, *Zea mays*, *N. plumbaginifolia*), it is reasonable to assume that each gene fulfills different metabolic roles. In C3 plants like *Arabidopsis* and N. plumbaginifolia, the phase of accumulation of catalase transcripts early in the light period coincides with that of photosynthetic genes and is in good agreement with a potent physiological role of catalase in decomposing H_2O_2 generated during the photorespiratory oxidation of glycolate in the peroxisome.[25]

Table 1. Characteristics of the Circadian Regulation of Oscillating Catalases from Different Plants

Species	Gene	Max. Exp.	LL Cycling	Role
Zea mays (maize)	*Cat3*	CT 10	NO	Mitochondria?
Arabidopsis thaliana	*CAT2*	CT 4	YES	Photorespiration?
	CAT3	CT 10	NO	?
N. plumbaginifolia	*Cat1*	CT 4	?	Photorespiration?

Maximum expression (Max. exp) is the circadian time (CT) in hours after the onset of light when the catalase mRNA accumulation reaches the maximum. The circadian oscillation under constant light (LL) and the possible functional role of the gene are indicated.

Photorespiration in maize, a C4 plant, occurs to a lesser degree as compared to C3 plants, and the phasing of *Cat3* in maize with maximal expression late in the light and early in the dark period suggests that the role of this gene is likely not associated with photorespiration. The existence of a C3 plant catalase (*Arabidopsis Cat3*) exhibiting a similar circadian expression phase as *Cat3* of maize (C4) implies a common metabolic necessity in C3 and C4 plants for catalase during the dark period. The nature of such a metabolic requirement remains obscure. However, there is substantial evidence that the maize CAT-3 protein is associated with the maize mesophyll mitochondria.[9,26]

In C4 plants, malate oxidation in mesophyll mitochondria is sensitive to cyanide and shows strong respiratory control, as in mitochondria from leaves of C3 species and etiolated tissues. In bundle sheath mitochondria, however, malate oxidation is largely insensitive to cyanide and shows no respiratory control. On the other hand this oxidation is strongly inhibited by salicylhydroxamic acid (SHAM), showing that the alternative oxidase is involved.[27] Localization of CAT-3 in mesophyll mitochondria is in good agreement with ROS production during cyanide sensitive respiration. The need for the circadian oscillation of maize *Cat3* may be explained by two different hypotheses that converge to a fluctuation of ROS produced during the dark-light cycles. First, mitochondrial respiration can be higher late in the light period and in the early dark period when metabolites from photosynthesis are amply supplied. Later, during the dark period, the rate of respiration becomes lower as metabolites are depleted. That could result in a fluctuation of ROS produced at

a rate similar to that of respiration. Second, the engagement of the alternative oxidase in the maize mesophyll cells could be light dependent. Actually, differential engagement of the alternative oxidase during the dark-light cycle has been reported in plants with CAM metabolism.[28] And light dependent induction of the alternative oxidase pathway (AOP) has been reported in etiolated soybean cotyledons exposed to light.[29] The physiological role of the AOP is still uncertain (with the exception of a few cases as in *Arum lilies* wherein the AOP is apparently directly related to thermogenic metabolism). Several lines of evidence lead to the suggestion that the AOP may be related to prevention of oxidative stress.[30] An apparent induction of alternative oxidase by superoxide in the yeast *Hansenula anomala* has been shown.[31] It has also been suggested that oxidation of ubisemiquinones by the alternative oxidase would prevent them from reacting with molecular oxygen to generate superoxide.[32] Apparently diversion of the electron flow from the cytochrome pathway when this pathway is overloaded and the rate of free radical generation is high, could result in prevention of ROS production. If that is true, then CAT-3 and alternative oxidase could represent synergistic and/or complementary mitochondrial protective mechanisms for ROS scavenging.

Thus, our working hypothesis (currently under investigation in our laboratory) is that a diurnal fluctuation of ROS produced by mesophyll mitochondria, dependent on the metabolite accumulation-consumption rhythm and/or differential alternative oxidase engagement during the dark-light cycle, could account of the necessity for the circadian rhythm of *Cat3* whose product is associated with mitochondria.

Entrainment of the maize Cat3 *circadian rhythm*

The circadian expression of the maize *Cat3* gene requires the entraining signal of a light-dark cycle. This is a marked difference from what is observed with the *Arabidopsis Cat2*, or photosynthetic genes like *cab*,[33] which oscillate under continuous light. An effort was undertaken in our laboratory in order to define the necessary conditions for the entrainment of the maize *Cat3* circadian rhythm.[15] Our results demonstrate that the circadian rhythm of *Cat3* is inducible by transferring DD or LL growing plants to a cycling dark-light regime. A rhythm is induced by the first dark (D) to light (L) or L to D transition, but seems to be more stable and synchronized after a second transition to the initial condition. The photoperiod (12h D/12h L or 8h L/ 16h D) does not affect the appearance of the maximum and minimum in *Cat3* expression which is set at CT-10 and CT-22 respectively.

A different pattern of circadian induction, concerning the phase of the rhythm and related to the initial light conditions is observed, when LL or DD growing plants are transferred to the opposite continuous regime. When DD growing plants are transferred to LL the induction of the rhythm starts with an increase in mRNA abundance that reaches a maximum 10 h and a minimum 22 h after the transition, which represents the normal phase of an established rhythm in 12h D/12h L growing plants. The entrainment of the rhythm in plants transferred from LL to DD begins with a rapid decrease of *Cat3* mRNA accumulation reaching a minimum 10 h and a maximum 22 h after the transition. In this case although the phase of the rhythm is the opposite of what is observed in the DD to LL transition, it still represents the normal phase of an established rhythm in plants growing under a 12h D/12h L regime. Thus, the phase in the entrainment of the circadian expression of *Cat3* depends upon the nature of the transition and is in accordance with the phase of a normal rhythm that exhibit 12h D/12h L growing plants. These results indicate that the maize *Cat3* gene responds to light-on signals with induction and to light-off with repression of its expression. A diurnal oscillation in *Cat3* mRNA levels also occurs in roots.[14] However, the amplitude of the oscillation in roots is much less and the phase of the rhythm appears to lag behind that in leaves.

In a very interesting analysis of the UV light effects on the induction of the *Cat3* circadian expression, Boldt and Scandalios[55] demonstrated that single transitions of LL or DD growing plants to constant full-spectrum (240–400 nm) UV-light strongly induces the circadian expression of the *Cat3* gene, and significantly, in a manner similar to that observed in DD to LL or LL to DD transitions. Surprisingly, not only did the DD to UV transition (''dark'' to ''light'') induce the circadian *Cat3* expression, but in addition, the LL to UV transition (''light'' to ''light'') also induced a circadian rhythm similar to the one observed in the transition from constant light to constant dark. It is therefore tempting to speculate that the internal ''regulator'' of the rhythm reacts not only to light-on and light-off signals, but also to signals related with the quality of the light (wavelength), indicating the complex and sensitive nature of the oscillator.

In addition to dark-light transitions, short 15 min light pulses of different wavelength monochromatic or polychromatic light given to 8 days old etiolated seedlings can induce the circadian *Cat3* expression in a markedly uniform way, regardless of the wavelength of the light.[15] In doing so, light pulses of white light, red, far-red, red followed by far-red, UV-light (290–400 nm) or UV-light from which different portions of the spectrum (UV-C, UV-C and UV-B, or UV-C and

UV-B and UV-A) have been removed, using appropriate filters, can rapidly induce *Cat3* mRNA accumulation that reaches a maximum 4–8 hours after the pulse. The *Cat3* mRNA decreases thereafter reaching a minimum within 12–16 h and then peaks again 24–28 h after the pulse. Taken together these results suggest a very low fluence phytochrome response in the induction of the *Cat3* circadian expression in etiolated seedlings, along with the involvement of a blue-light/UV-A and a UV-B photoreceptor.[15]

The *Cat3* circadian rhythm damps to constant expression when 12h D/12h L growing plants are transferred to continuous light or darkness. Damping of the rhythm occurs rapidly and slight oscillations are detected three days after transfer to constant conditions,[14] in contrast to the observed robust oscillations of the *Arabidopsis Cat2* gene which persist for 5 days after transfer to constant conditions.[20] Because the *Cat3* gene is continually transcribed in the absence of a cycling light regime, the normally observed diurnal variation of *Cat3* expression has been proposed to be the result of a circadian-regulated transcriptional repressor.[13]

Regulatory elements of the Cat3 *promoter*

Studies with other plant genes have fortified the assumption that light and circadian responsive sequences are located in the 5′ flanking regions of structural genes.[33–43] The complete genomic sequence of the maize *Cat3* gene has been isolated and characterized.[3] Recent reports and knowledge on light and circadian regulation of more plant genes has prompted us to re-examine the *Cat3* 5′ upstream region for the presence of regulatory motifs.

Several transcription factor binding sites were recognized (Table 2, Fig. 1) and surprisingly enough, the presence of a transposable element in the *Cat3* promoter was identified. The transposable element located at −171 (Fig. 1, Fig. 2) belongs to a large family of small inverted repeat elements designated ''*Tourist*'',[53] first described in the *wx*-B2 mutation of maize. Members of this family of elements are highly repetitive in genomes of some and perhaps all members of the grasses, are associated with insertion mutations, and are also found in the introns and flanking sequences of wild-type genes.[54] Of all *Tourist* elements reported in 5' flanking sequences of wild-type genes to date, only the one found in the *Cat3* 5′ flanking region is proximal to the promoter. Moreover, the sequence (Fig. 2) of this element, termed *Zm13*,[54] revealed very interesting motifs that are not present in other members of the *Tourist* family. The terminal inverted repeats of the element are two oppositely oriented core motifs of the SV-40 enhancer,[52] located in a perfect palindrome with sequence CAATCCAT|ATGGATTG (the vertical axis denotes the symmetry center). The two CAAT boxes of each palindrome are two of the three CCAAT motifs located on the *Cat3* promoter. The third CCAAT motif is also present within the transposable element overlapping a GATA repeat present at −196.

The ''*Tourist*'' region of the maize *Cat3* promoter shares striking sequence similarities with the −111 to −38 region of the *Arabidopsis CAB2* promoter that has been shown to be sufficient for induction of a luciferase (*luc*) reporter gene by red light in etiolated tobacco plants, as well as, for rhythmic expression in green tissue.[37] The GATA repeat of the *Arabidopsis CAB2* promoter lies between −55 and −74 and serves as a binding site for the GATA-binding protein CGF-1 that is closely related to the GT-1 transcriptional factor and can play a role in light regulation.[39] *In vivo* analysis of *CAB2::luc* fusion constructs in transgenic *Arabidopsis* demonstrated that a circadian regulated element lies within a 36bp sequence immediately upstream the GATA repeat that overlaps a conserved CCAAT box and contains binding sites for three putative transcription factors.[40]

Table 2. Regulatory Elements Located on the *Cat3* 1kb 5′ Upstream Region

MOTIF	Position	Response (signal/factor)	Reference
GT-1	−174, −332, −556, −796	light	41,42
l-box	−428, −721, −842	light	43
GATA repeat	−196	light, circadian clock	37
ACGT core	−606	leucine zipper factors	43,44
ARE	−148	antioxidants, H_2O_2	45
AP-1 binding	−217	PMA, UV, H_2O_2	46
NFkB binding	−423	H_2O_2, radiation, infection, chemicals,	46,47
XRE	−622	Aryl-hydrocarbons (dioxin)	48
TGACG	−108	auxin, salicyclic acid	43
bHLH core	−16, −136, −180, −263, −328	basic helix-loop-helix proteins	49
RY motif	−386	gene expression in seed development,	50,51
SV40 enhan.	−179, −260	enhancer	52

Position is relative to the transcription initiation +1. Signals or factors that elicit responses through these elements are listed. Light responsive elements are in bold.

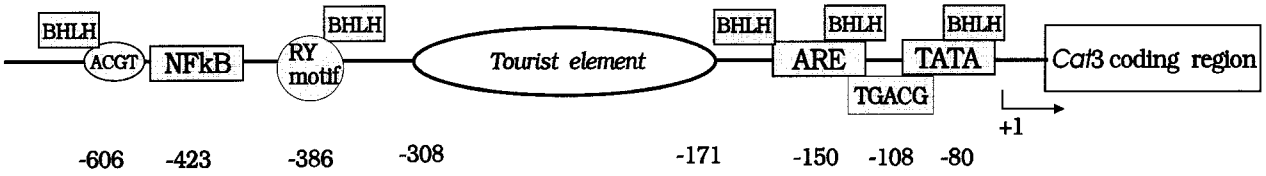

Fig. 1. Schematic representation of the *Cat3* promoter structure. Regulatory elements located in the promoter region of the maize *Cat3* and their position relative to the transcription initiation (+1) are shown. The elements are as listed in Table 1. The location of the *Tourist Zm13* transposable element in the *Cat3* promoter is also shown.

Based on the similarities between the ''*Tourist*'' region of the maize *Cat3* promoter and the *Arabidopsis CAB2* promoter, it is likely that the *Zm13* transposable element present in the maize *Cat3* promoter is a perfect candidate regulatory sequence directing the light inducible and circadian expression of the gene. If that is true, it is possible that we may be able to identify maize genotypes lacking the transposable element in the promoter of the *Cat3* gene and thus, do not exhibit a circadian rhythm. Alternatively, in genotypes exhibiting circadian regulation of the *Cat3* we should be able to identify the *Zm13* element in the *Cat3* promoter. Actually, limited data (obtained after analysis of three different genotypes) indicated that genetic background and allelic variation do not directly affect the temporal pattern of *Cat3* accumulation in leaves.[13] We have recently expanded this analysis examining several North and South American maize genotypes. Preliminary results indicate that *Cat3* is cycling in all of them. Interestingly, these results also show that there is variation in the amount of *Cat3* mRNA accumulation in each time point of the circadian cycle between the different inbred lines.[56] We are currently examining those genotypes for presence of the *Zm13* element in the promoter of the *Cat3* gene. And certainly the most efficient way to provide evidence for the regulatory role of the element is to use transcriptional fusions with a reporter gene and examine the pattern of the reporter's expression in transient assays and/or transgenic plants. Such approaches are currently being pursued in our laboratory in order to obtain thorough insights into the molecular basis of the maize *Cat3* circadian regulation of expression.

SUMMARY

Light is the environmental signal that triggers a major developmental transition in plants, initiating photosynthesis and autotrophic metabolism. Metabolic pathways such as photosynthesis and respiration contribute to ROS production and create the need for compensating antioxidant gene expression to balance the ROS levels. From this point of view, light response of maize catalases could represent a coordinated regulatory mechanism developed to cope with light induced oxidative stress. Differential response of the maize catalases to light signals implies different physiological roles for each gene. Two of the maize catalases, namely *Cat1* and *Cat2*, encode peroxisomal or cytosolic enzymes. *Cat1* gene expression in leaves is constitutive at low levels and is insensitive to light. *Cat2* response to light is positive at both the transcriptional and the translational levels. In C3 plants catalase induction by light is suggested to be a response to photorespiration and the consequent increase of H_2O_2. Low photorespiration rate in C4 plants along with the survival of CAT-2 null maize genotypes under normal environmental conditions denote that the *Cat2* gene is probably

Sequence of the *Zm13 Tourist* transposable element

TTAGGGCTTGTT CGG TTCTAC CCCAATCCATATGGATTGAGGGGGATTGAGGGGGT TTTA
AATCCCGAACAAGCCAAGATGGGGTTAGGTATACCTAACT CCC CCTAACTCC CCCAAAAT

ATCCCTAGTAAGT CAAAATCCCCTCCAATCCGTATCAATCCCCT CCAAT CCATATGGATT
TAGGGATCATTCAGTTTTAGGGGAGGTTAGGCATAGTTAGGGGAGGTTAGGTATACCTAA

GAAAATAACC GAACAAGCCC TTA
CT TT TATTGG CT TGT TCGGGAAT

Fig. 2. The sequence of the *Tourist Zm13* transposable element. The duplicated incorporation site TTA, the light responsive GATA repeat and the three CCAAT boxes are in shaded boxes.

not essential in degrading photorespiration generated H_2O_2, and may be important in conditions favoring oxidative stress. The CAT-3 catalase isozyme is associated with the mesophyll mitochondria and *Cat3* gene expression is regulated by a circadian rhythm. Maximum *Cat3* transcript accumulation is observed late in the light period which suggests that CAT-3 may play an important role during mitochondrial respiration in the dark. The need for the *Cat3* circadian rhythm could emerge from differential production of ROS in mesophyll mitochondria during the day-light cycle.

Many aspects of the catalase responses to light need still to be investigated. Recent work with other plants has shown that catalase genes respond to light in specific ways comparable with those described in this review for maize. Thus, light responses may represent evolutionary conserved mechanisms in the regulation of catalase gene expression in plants. Further studies are needed for understanding the underlying regulatory mechanisms from signal perception to specific gene response. Such knowledge will enable us to manipulate catalase gene expression in order to elicit effective antioxidant responses in severe oxidative stress conditions. For these genetic engineering manipulations light may prove to be a useful and effective switch.

Acknowledgments — We acknowledge the financial support, during the course of aspects of these studies in our laboratory, from the National Science Foundation, the U.S. Environmental Protection Agency, the U.S.D.A. and the N.I.H.

REFERENCES

1. Thompson, W. F.; White, M. J. Physiological and molecular studies of light regulated nuclear genes in higher plants. *Annu. Rev. Plant Physiol. Plant Mol. Biol.* **42:**423–466; 1991.
2. Scandalios, J. G. Regulation and properties of plant catalases. In: Foyer, C.H.; Mullineaux, P. M. eds. *Causes of Photooxidative Stress and Amelioration of Defense Systems in Plants*. Boca Raton, Ann Arbor, London, Tokyo. CRC Press; 1994:275–315.
3. Abler, M. L.; Scandalios, J. G. Isolation and characterization of a genomic sequence encoding the maize *Cat3* catalase gene. *Plant Mol. Biol.* **22:**1031–1038; 1993.
4. Guan, L.; Scandalios, J. G. Characterization of the catalase antioxidant defense gene *Cat1* of maize and its developmentally regulated expression in transgenic tobacco. *Plant J.* **3:**527–536; 1993.
5. Guan, L., Polidoros, A. N.; Scandalios, J. G. Isolation, characterization and expression of the maize *Cat2* catalase gene. *Plant Mol. Biol.* **30:**913–924; 1996.
6. Scandalios, J. G. Subunit dissociation and recombination of catalase isozymes. *Proc. Natl. Acad. Sci. USA* **53:**1035–1040; 1965.
7. Scandalios, J. G. Genetic control of multiple molecular forms of catalase in maize. *Ann. NY Acad. Sci. USA* **151:**274–293; 1968.
8. Scandalios, J. G. Control of gene expression and enzyme differentiation. In: *Physiological Genetics*. Scandalios, J. G. eds. New York. Academic Press. 1979:63–107.
9. Scandalios, J. G.; Tong, W.-F.; Roupakias, D. G. *Cat3*, a third gene locus coding for a tissue-specific catalase in maize: Genetics, intracellular location, and some biochemical properties. *Mol. Gen. Genet.* **179:**33–41; 1980.
10. Skadsen, R. W.; Scandalios, J. G. Translational control of photoinduced expression of the *Cat2* catalase gene during leaf development in maize. *Proc. Natl. Acad. Sci. USA* **84:**2785–2789; 1987.
11. Redinbaugh, M. G.; Sabre, M.; Scandalios, J. G. The distribution of catalase activity, isozyme protein, and transcript in the tissues of the developing maize seedling. *Plant Physiol.* **92:**375–380; 1990.
12. Redinbaugh, M. G.; Sabre, M.; Scandalios, J. G. Expression of the maize *Cat3* catalase gene is under the influence of a circadian rhythm. *Proc. Natl. Acad. Sci. USA* **87:**6853–6857; 1990.
13. Acevedo, A.; Williamson, J. D.; Scandalios, J. G. Photoregulation of the *Cat2* and *Cat3* catalase genes in pigmented and pigment-deficient maize: The circadian regulation of *Cat3* is superimposed on its quasi-constitutive expression in maize leaves. *Genetics* **127:**601–607; 1991.
14. Abler, M. L.; Scandalios, J. G. Regulation of the cyclic repression of the *Cat3* catalase gene in maize leaves and roots occurs via the dark/light transition. *Maydica* **39:**83–88; 1994.
15. Boldt, R.; Scandalios, J. G. Circadian regulation of the *Cat3* catalase gene in maize (*Zea mays L.*): Entrainment of the circadian rhythm of *Cat3* by different light treatments. *Plant J.* **7:**989–999; 1995.
16. Mitchell, R. L.; Anderson, I. C. Catalase photoinactivation. *Science*. **150:**74; 1965.
17. Feierabend, J.; Engel, S. Photoinactivation of catalase *in vitro* and in leaves. *Arch. Biochem. Biophys.* **251:**567–576; 1986.
18. Hertwig, B.; Streb, P.; Feierabend, J. Light dependence of catalase synthesis and degradation in leaves and the influence of interfering stress conditions. *Plant Physiol.* **100:**1547–1553; 1992.
19. Willekens, H.; Van Camp, W.; Van Montagu, M.; Sandermann, H., Jr.; Langebartels, C. Ozone, sulfur dioxide, and ultraviolet B have similar effects on mRNA accumulation of antioxidant genes in *Nicotiana plumbagifolia. Plant Physiol.* **106:**1007–1014; 1994.
20. Zhong, H. H.; Young, J. C.; Pease, E. A.; Hangarter, R. P.; McClung, R. C. Interactions between light and the circadian clock in the regulation of the *Cat2* expression in *Arabidopsis. Plant Physiol.* **104:**889–898; 1994.
21. Zhong, H. H.; McClung, R. C. The circadian clock gates expression of two *Arabidopsis* catalase genes to distinct and opposite circadian phases. *Mol. Gen. Genet.* **251:**196–203; 1996.
22. Willekens, H.; Langebartels, C.; Tire, C.; Van Montagu, M.; Inze, D.; Van Camp, W. Differential expression of catalase genes in *Nicotiana plumbaginifolia. Proc. Natl. Acad. Sci. USA* **91:**10450–10454; 1994.
23. Ni, W.; Trelease, R. N. Post-transcriptional regulation of catalase isozyme gene expression in cotton seeds. *Plant Cell.* **3:**737–744; 1991.
24. Acevedo, A.; Skadsen, R. W.; Scandalios, J. G. Two barley catalase genes respond differentially to light. *Physiol. Plant* **96:**369–374; 1996.
25. Ogren, W. L. Photorespiration: Pathways, regulation and modification. *Annu. Rev. Plant Physiol.* **35:**415–442; 1984.
26. Tsaftaris, A. S.; Bosabalidis, A. M.; Scandalios, J. G. Cell-type-specific gene expression and acatalasemic peroxisomes in a null *Cat2* catalase mutant of maize. *Proc. Natl. Acad. Sci. USA* **80:**4455–4459;1983.
27. Douce, R. Mitochondria in Higher Plants: Structure Function and Biogenesis. Orlando, FL. Academic Press; 1985.
28. Robinson, S. A.; Yakir, D.; Ribas-Carbo, M.; Giles, L.; Osmond, B. C.; Siedow, J. N.; Berry, J. A. Measurements of the engagement of cyanide-resistant respiration in the crassulacean acid metabolism plant *Kalanchoe daigermontiana* with the use of online oxygen isotope discrimination. *Plant Physiol.* **100:**1087–1091; 1992.
29. Robinson, S. A.; Ribas-Carbo, M.; Giles, L.; Yakir, D.; Berry, J. A.; Siedow, J. N. Partitioning of electrons between the alternative and cytochrome respiration pathways during development

of photosynthetic function in soybean cotyledons. Supplement to *Plant Physiol.* **108:**667; 1995.
30. Wagner, A. M.; Krab, K. The alternative respiration pathway in plants: Role and regulation. *Physiol. Plant* **95:**318–325; 1995.
31. Minagawa, N.; Koga, S.; Nakano, M.; Sakajo, S.; Yoshimoto, A. Possible involvement of superoxide anion in the induction of cyanide resistant respiration in *Hansenula anomala. FEBS Lett.* **302:**217–219; 1992.
32. Purvis, A. C.; Shewfelt, R. L. Does the alternative pathway ameliorate chilling injury in sensitive plant tissues? *Physiol. Plant* **88:**712–718; 1993.
33. Nagy, F.; Kay, S. A.; Chua, N.-H.. A circadian clock regulates transcription of the wheat Cab-1 gene. *Genes & Dev.* **2:**376–382; 1988.
34. Herrera-Estrella, L.; Simpson, J. Influence of environmental factors on photosynthetic genes. *Adv. Genet.* **28:**133–163; 1990.
35. Borello, U.; Ceccarelli, E.; Giuliano, G. Constitutive, light-responsive and circadian clock-responsive factors compete for the different l box elements in plant light-regulated promoters. *Plant J.* **4:**611–619; 1993.
36. Millar, A. J.; Kay, S. A. Circadian control of *cab* gene transcription and mRNA accumulation in *Arabidopsis. Plant Cell.* **3:**541–550; 1991.
37. Anderson, S. L.; Teakle, G. R.; Martino-Catt, S. A.; Kay, S. Circadian clock- and phytochrome-regulated transcription is conferred by a 78bp cis-acting domain of the *Arabidopsis* CAB2 promoter. *Plant J.* **6:**457–470; 1994.
38. Anderson, S. L.; Kay, S. A. Functional dissection of circadian clock- and phytochrome-regulated transcription of the *Arabidopsis* CAB2 gene *Proc. Natl. Acad. Sci. USA* **92:**1500–1504; 1995.
39. Teakle, G. R.; Kay, S. A. The GATA-binding protein CGF-1 is closely related to GT-1 *Plant Mol. Biol.* **29:**1253–1266; 1995.
40. Carre, I. A.; Kay, S. A. Multiple DNA-protein complexes at a circadian-regulated promoter element. *Plant Cell.* **7:**2039–2051; 1995.
41. Green, P. J.; Yong, M. H.; Cuozzo, M.; Kano-Murakami, Y.; Silverstein, P.; Chua, N. H. Binding site requirements for pea nuclear protein factor GT-1 correlate with sequences required for light-dependent transcriptional activation of the *rbcS*-3A gene. *EMBO J.* **7:**4035–4044; 1988.
42. Lam, E.; Chua, N. H. GT-1 binding site confers light responsive expression in transgenic tobacco. *Science* **248:**471–474; 1990.
43. Terzaghi, W. B.; Cashmore, A. R. Light regulated transcription. *Annu. Rev. Plant Physiol. Plant Mol. Biol.* **46:**445–474; 1995.
44. Armstrong, G. A.; Weisshaar, B.; Hahlbrock, K. Homodimeric and heterodimeric leucine zipper proteins and nuclear factors from parsley recognize diverse promoter elements with ACGT cores. *Plant cell.* **4:**525–537; 1992.
45. Rushmore, T. H.; Morton, M. R.; Pickett, C. B. The antioxidant responsive element. *J. Biol. Chem.* **266:**11632–11639; 1991.
46. Meyer, M.; Schreck, R.; Baeuerle, P. A. H_2O_2 and antioxidants have opposite effects on activation of NF-kB and AP-1 in intact cells: AP-1 as secondary antioxidant-responsive factor. *EMBO J.* **12:**2005–2015; 1993.
47. Siebenlist, U.; Brown, K.; Franzoso, G. NFkB: A mediator of pathogen and stress responses. In: Baeuerle, P. A., eds. *Inducible gene expression. Environmental Stress and Nutrients*. Boston. Birkhauser; 1995:93–141.
48. Poellinger, L. Mechanism of signal transduction by the basic helix-loop-helix dioxin receptor. In: Baeuerle, P. A., eds. *Inducible gene expression. Environmental Stress and Nutrients.* Boston. Birkhauser; 1995:177–205.
49. Pabo, C. O.; Sauer R. T. Transcription factors: Structural families and principles of DNA recognition. *Annu. Rev. Biochem.* **61:**1053–1095; 1992.
50. Baumlein, H.; Nagy, I.; Villarroel, R.; Inze, P.; Wobus, U. *Cis*-analysis of seed protein promoter: The conservative RY repeat CATGCATG within the legumin box is essential for tissue specific expression of a legumine gene. *Plant J.* **2:**233–239; 1992.
51. Lelievre, J. M.; Oliveira, L. O.; Nielsen, N. C. 5'-CATGCATG-3' elements modulate the expression of glycinin genes. *Plant Physiol.* **98:**387–391; 1992.
52. Hatzopoulos, A. K.; Schlokat, U.; Gruss, P. Enhancers and other cis-acting regulatory elements. In: Hames, B. D.; Glover, D. M. eds. ''Transcription and Splicing.'' Washington D.C. IRL Press. 1988:43–96.
53. Bureau, T. E.; Wessler, S. R. *Tourist*: A large family of small inverted repeat elements frequently associated with maize genes. *Plant Cell.* **4:**1283–1294; 1992.
54. Bureau, T. E.; Wessler, S. R. Mobile inverted-repeat elements of the *Tourist* family are associated with the genes of many cereal grasses. *Proc. Natl. Acad. Sci. USA* **91:**1411–1415; 1994.
55. Boldt, R.; Scandalios, J. G. Influence of UV-light on the expression of *Cat2* and *Cat3* catalase genes in maize. *Free Radic. Biol. Med.* **23:**505–514; 1997.
56. Polidoros, A. N.; Scandalios, J. G. Unpublished results.

ABBREVIATIONS

AOP—Alternative oxidase pathway
ROS—Reactive oxygen species
CAM—Crassulacean acid metabolism
CAT—Catalase protein; isozyme
Cat—Catalase gene; transcript
CT—Circadian time
D—Dark
DD—Constant dark
L—light
LL—Constant light
SHAM—Salicylhydroxamic acid

Copyright © 1998 by the Genetics Society of America

Circadian Expression of the Maize Catalase *Cat3* Gene Is Highly Conserved Among Diverse Maize Genotypes With Structurally Different Promoters

Alexios N. Polidoros and John G. Scandalios

Department of Genetics, North Carolina State University, Raleigh, North Carolina 27695-7614

Manuscript received September 19, 1997
Accepted for publication February 4, 1998

ABSTRACT

The *Cat3* gene of maize exhibits a transcriptionally regulated circadian rhythm. In the present study we examined the following: (1) the extent of the circadian *Cat3* expression between maize genotypes of diverse origin; (2) the functional significance of a *Tourist* transposable element located in the *Cat3* promoter of the inbred line W64A, which harbors putative regulatory elements (GATA repeat, CCAAT boxes) shown to be involved in the light induction and circadian regulation of the Arabidopsis *CAB2*, as well as other plant genes; and (3) aspects of the physiological role of CAT-3 in maize metabolism. Results confirm that the circadian *Cat3* expression is a general phenomenon in maize. Regulation of *Cat3* gene expression is not dependent on the presence of the *Tourist* element in the promoter of the gene nor on the presence of motifs similar to those found significant in the circadian expression of the Arabidopsis *CAB2* gene. Structural diversity was revealed in the *Cat3* promoters of maize genotypes of diverse origins. However, highly conserved regions with putative regulatory motifs were identified. Relevance of the conserved regions to the circadian regulation of the gene is discussed. Possible physiological roles of CAT-3 are suggested.

THE three maize catalase genes respond differentially to light in developing maize leaves. *Cat1* expression is light-independent (Redinbaugh *et al.* 1990), *Cat2* is positively regulated by light (Skadsen and Scandalios 1987; Acevedo *et al.* 1991), and *Cat3* is regulated by a circadian rhythm (Redinbaugh *et al.* 1990; Acevedo *et al.* 1991). Studies on several aspects of the *Cat3* circadian expression as well as indications of putative physiological role(s) of CAT-3 have been recently reviewed (Scandalios *et al.* 1997). Because studies with other plant genes have fortified the assumption that light and circadian responsive elements are located in the 5′ flanking regions of structural genes (Millar and Kay 1991; Anderson *et al.* 1994), we examined the *Cat3* 5′ upstream region for the presence of regulatory motifs. Several transcription factor binding sites and a transposable element were identified (Polidoros and Scandalios 1997). The transposable element located at −171 belongs to a large family of small inverted repeat elements designated "*Tourist*," first described in the *wx*-B2 mutation of maize. Members of this family of elements are highly repetitive in genomes of some and perhaps all members of the grasses, are associated with insertion mutations, and are also found in the introns and flanking sequences of wild-type genes (Bureau and Wessler 1994a).

Transposable elements can alter gene expression when inserted in or near genes. The most common effect is a null mutation when an element interrupts the coding region of a gene (McLaughlin and Walbot 1987; McCarty *et al.* 1989; Abler and Scandalios 1991). Insertion of an element in an intron may result in novel RNA-processing events, as in the maize *Adh1-S* gene (Luehrsen and Walbot 1990). The presence of an element in the promoter region can cause a spectrum of altered expression responses, as has been evident from paradigms in maize as well as in many other organisms. Low amounts of the *Bz* gene product (Schiefelbein *et al.* 1988), reduced levels of Wx enzymatic activity (Weil *et al.* 1992), and no detectable reporter activity of a PGT3 patatin promoter fusion to β-Glucuronidase in transgenic potato or tobacco plants (Koester-Toepfer *et al.* 1990) are some examples of negative regulation after incorporation of a transposable element in the 5′ flanking region of diverse genes. There are also examples where insertion of an element in the 5′ upstream region of the gene does not affect transcription. Comparison of the *Arabidopsis thaliana* meiosis-specific gene *AtDMC1* isolated from Landsberg erecta ecotype to its Columbia allele *ArLIM15*, revealed the presence of a 1874-bp transposon-like element within the promoter region of *ArLIM15*, located 219 bp upstream of the transcription initiation. Reverse transcription-polymerase chain reaction (RT-PCR) analysis showed that the expression levels of *AtDMC1* and *ArLIM15* are similar (Klimyuk and Jones 1997).

Rigorous control of gene expression by transposon element insertion in the promoter can be accomplished

Corresponding author: John G. Scandalios, Department of Genetics, North Carolina State University, Raleigh, NC 27695-7614.
E-mail: jgs@unity.ncsu.edu

when the element carries regulatory sequences. This has been described in several examples, including mouse (Stavenhagen and Robins 1988), human (Ting *et al.* 1992), and plant genes (White *et al.* 1994). In plants, *copia*-like retrotransposon sequences have been shown to contain *cis*-regulatory elements which, in several cases, control the expression of the recipient genes (White *et al.* 1994). Members of the *Stowaway* family of plant inverted repeat elements are frequently located in 5′ upstream regions of several genes and appear to contain previously identified *cis*-regulatory domains (Bureau and Wessler 1994b). *Stowaway* elements share many structural features with the *Tourist* elements but have no significant sequence similarity.

Careful examination of the *Tourist* element located in the maize *Cat3* promoter (termed *Zm13*) revealed motifs that share striking similarities to a 78-bp *cis*-acting domain of the Arabidopsis *CAB2* promoter (Polidoros and Scandalios 1997). This domain is sufficient to confer red-light induction of a luciferase (*luc*) reporter gene in etiolated tobacco plants and rhythmic expression in green tissue (Anderson *et al.* 1994). Based on these similarities, we hypothesized that the *Tourist Zm13* transposable element present in the *Cat3* promoter of the maize inbred line W64A might represent a *cis*-regulatory sequence directing the light-inducible and circadian expression of the gene (Polidoros and Scandalios 1997).

Considering that maize is a highly polymorphic species, we set up an experimental scheme to test the above hypothesis and determine whether *Cat3* expression is under circadian control in other maize lines and whether the circadian expression of the *Cat3* gene depends upon the presence of the *Tourist* element in the *Cat3* promoter. Results obtained from these studies could also provide information on the physiological role of CAT-3. More specifically, we examined whether among diverse maize genotypes (1) the circadian regulation of *Cat3* is conserved, (2) the structure of *Cat3* is conserved, (3) the *Tourist* element is present in the *Cat3* promoter, (4) the presence of the *Tourist* element or presence of the motifs it harbors are necessary for the circadian regulation of *Cat3*, and (5) the circadian regulation of *Cat3* is associated with a specific physiological role.

MATERIALS AND METHODS

Plant material: In this study we used the following: the North American maize inbred lines W64A, KYS, Tx303, and Oh51A; A16, a line of Yugoslavian origin that is CAT-2 null; five inbred lines developed from tropical germplasm of diverse background, namely, NC296, NC298, NC300, NC302, and NC304, kindly provided by M. Goodman (North Carolina State University); and the line Black Mexican Sweet (BMS). Seeds were surface sterilized in 10% hypochlorite, soaked in distilled water overnight, and planted in soil mix or germinated in plastic containers on several layers of germination paper moistened with distilled water.

Zymogram analysis: Seeds were germinated and grown in plastic containers in darkness at 25° for 10 days. Samples were prepared from coleoptile tissue in glycylglycine buffer, catalase activity and protein concentration were determined, and gel electrophoresis of CAT isozymes was performed according to Chandlee and Scandalios (1984).

Northern analysis: RNA was isolated from soil-grown plants. Germination and subsequent growth was at 25° for 10 days in 12-hr dark/12-hr light (12D/12L) photoperiod. Leaf material was harvested the 10th day at circadian times (CT) 2, 6, 10, 14, 18, and 22, using a green safety light during the dark period. All samples were frozen in liquid nitrogen and stored at −80° for analysis. Total RNA from leaf material was extracted according to Thompson *et al.* (1983) and separated on denaturing 1.2 or 1.6% agarose gels. It was then transferred onto nitrocellulose or nylon membranes and hybridized with a *Cat3* gene-specific probe (Redinbaugh *et al.* 1988). Hybridization buffers and conditions were modifications of protocols recommended by the manual of the S&S Nytran Plus membrane (Schleicher and Schuell, Keene, NH). Briefly, the prehybridization solution contained 50% formamide, 6× SSPE, 5× Denhardt's, 7% sodium dodecyl sulfate (SDS), 200 ug/ml salmon sperm DNA, and 1% dextran sulfate. After 4-hr prehybridization at 42°, the prehybridization solution was substituted with hybridization solution. This was the same as the prehybridization solution without 5× Denhardt's, to which probe was added. Hybridization proceeded at 42° for 24–36 hr, and washes were performed twice for 30 min with 0.1× SSC/0.1% SDS at 42°.

DNA isolation and Southern analysis: Genomic DNA from each maize line was isolated from 10-day-old light-grown leaves using the DNeasy Plant Mini Kit (Qiagen, Valencia, CA) according to instructions. For W64A and A16, genomic DNA was also isolated from 10-day-old light-grown leaves as described (Redinbaugh *et al.* 1988). Genomic DNA (10 μg) was digested with *Sst*I, electrophoresed through 1% agarose gel, and transferred onto S&S Nytran membranes using alkaline transfer according to the manufacturer. Hybridization and washes were as described for Northern analyses. A ^{32}P-labeled *Cat3* gene-specific probe (Redinbaugh *et al.* 1988) was used in order to examine the 3′ flanking region of the gene. A 185-bp *Apa*I-*Xho*I fragment of the *Cat3* promoter that includes the 143-bp *Tourist Zm13* transposable element was subcloned into pBluescript SK and used to detect the element in the different lines. The *Tourist* probe, prepared with PCR using the M13 reverse and M13 forward primers, was nonradioactively labeled using 1× Fluorescein-N^6-dATP and unlabeled nucleotide mix from the Random Primer Fluorescein Labeling Kit with Antifluorescein-AP (DuPont NEN, Wilmington, DE). The reaction started with 3 min denaturation at 95° followed by 29 cycles of 15-sec denaturation at 95°, 15-sec annealing at 55°, and 30-sec extension at 75°. The last extension step was for 5 min to ensure completion of the reaction. The *Tourist* probe was then hybridized and detected according to the Random Primer Fluorescein Labeling Kit with Antifluorescein-AP (DuPont NEN) instruction manual.

PCR amplification of the *Cat3* promoter, Southern analysis, subcloning, and sequencing: The structure of the promoter region of *Cat3* in the genotypes examined was analyzed with PCR and sequencing. The primers used in PCR were 5′-GGGCCCGACCATCAGACGAACAAC-3′ upper and 5′-GTG GCTGCTGGAACGGACGGAACT-3′ lower, amplifying a 556-bp fragment of the *Cat3* promoter in W64A (GenBank accession no. L05434), which includes the *Zm13* transposon element. The upper primer is located between nt 2172–2196 in the promoter and the lower at nt 2704–2727 at the junction

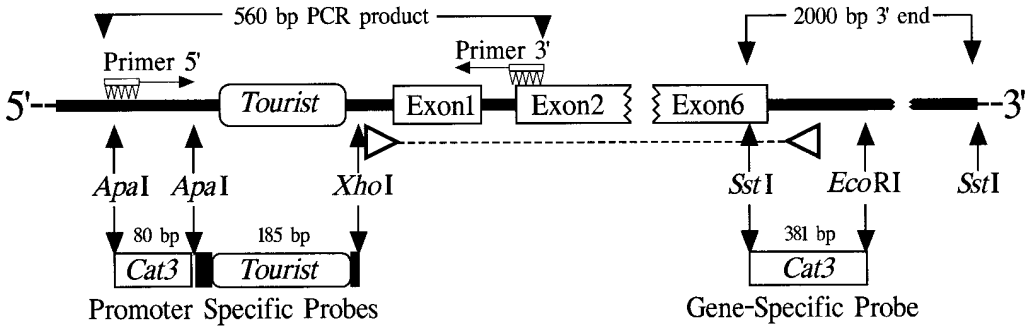

Figure 1.—Schematic of the known sequence of *Cat3* in the inbred line W64A showing features relative to this study. The combined PCR and hybridization strategy followed to detect the *Tourist* element and to determine the similarity with the *Cat3* promoter in the PCR products from the different maize genotypes is illustrated. Positions of the PCR primers and restriction enzyme borders of the promoter *Cat3*-specific, the *Tourist*-specific, and the *Cat3* gene-specific probes are shown. The illustration is not to scale, and the length (bp) of each probe or fragment is indicated.

of the first intron with the second exon of the gene. A second upper primer 5′-ATTACCGCGACGACAGGGACGATA-3′ located 54 bp 5′ of the first one was used to verify PCR results. An unrelated set of primers used to amplify the maize alternative oxidase gene (Polidoros *et al.* 1998) was also used to examine the purity of the DNA used as template in the PCR. The reactions started with 3-min denaturation at 95° followed by 35 cycles of 30 sec denaturation at 95°, 1-min annealing at 58°, and 1-min extension at 75°. The last extension step was for 5 min. The PCR products were analyzed on 1.5% agarose gels, visualized by staining with ethidium bromide, and either transferred onto nylon membranes or used for subcloning. Hybridization of the PCR products was performed with two probes: the 185-bp *Apa*I-*Xho*I fragment of the *Cat3* promoter that includes the 143-bp *Tourist Zm13* transposable element and the immediately upstream 80-bp *Apa*I fragment (Figure 1). Both probes were nonradioactively labeled and used as described for the *Tourist* probe above. To subclone the PCR products, the amplified band from each line was excised from the gel, and the DNA was isolated using the QIAquick Gel Extraction Kit (Qiagen) according to the instructions. It was then ligated to the PCR-Script SK(+) plasmid vector using the PCR-Script™ Amp SK(+) Cloning Kit (Stratagene, La Jolla, CA) according to instructions. Positive clones were identified with direct colony characterization by PCR (Gussow and Clackson 1989). PCR conditions were 3-min denaturation at 95° followed by 29 cycles of 15-sec denaturation at 95°, 15-sec annealing at 55°, and 30-sec extension at 75°, using the M13 reverse and M13 forward set of primers. The last extension step was 5 min. Plasmid DNA from positive clones was prepared for sequencing using the QIAprep Spin Miniprep Kit (Qiagen) according to instructions. Labeling and sequencing of the PCR-amplified *Cat3* promoter region of each genotype were performed using the ABI PRISM™ Dye Terminator Cycle Sequencing Ready Reaction Kit (Perkin Elmer, Norwalk, CT) and the ABI 377 automatic DNA sequencer (Perkin Elmer).

RESULTS

Extent of *Cat3* cycling: Our results indicate that *Cat3* diurnal cycling occurs in all genotypes examined (Figure 2). The only exception is the BMS line that is null for CAT-3, because no *Cat3* message is detectable at any time point examined and no CAT-3 activity is detectable in different tissues on zymograms (S. Ruzsa and J. G. Scandalios, unpublished data). The circadian nature of the *Cat3* cycling in all genotypes was confirmed by examining *Cat3* expression in a free-running cycle. Plants grown in 12D/12L photoperiod for 10 days were subjected to constant dark for 24 hr, and *Cat3* expression was examined at the time points corresponding to the expected maximum (10 hr in constant dark) and minimum (22 hr in constant dark). Transcript levels were identical with those observed at CT 10 and CT 22 (Figure 2), respectively. The circadian rhythm of *Cat3* in the North American lines is markedly similar with high levels of expression at CT 10 and lowest expression

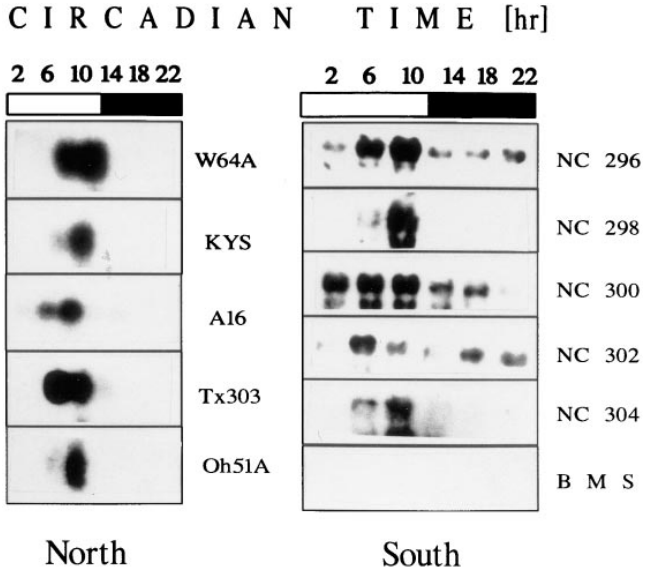

Figure 2.—Northern analysis of the circadian *Cat3* gene expression in maize genotypes of diverse origin. The left panel represents North American and the right South American genotypes. Hybridization was performed using the *Cat3* gene-specific probe. Note the similar expression pattern among the North American lines and the variant patterns among the South American lines. In all the lines *Cat3* transcripts increase during the light period and decrease during dark. No *Cat3* transcript can be detected in the CAT-3 null BMS line. Results are representative of three independent experiments.

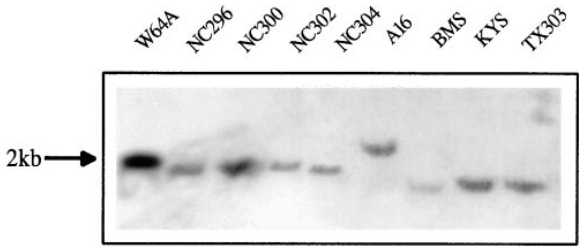

Figure 3.—Southern analysis representing restriction fragment length polymorphism (RFLP) at the 3′ end of the *Cat3* gene in diverse maize genotypes. Hybridization was performed using the *Cat3* gene-specific probe. An arrow indicates the W64A band, approximately 2 kb in length.

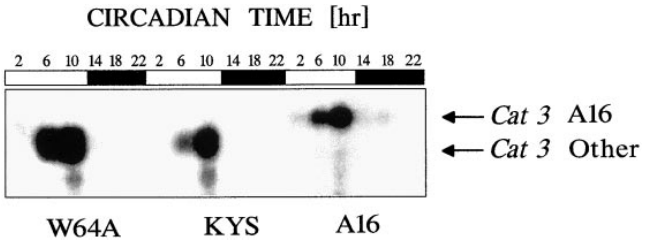

Figure 4.—Differences in transcript size for the *Cat3* mRNA among three maize lines. Northern hybridization was performed using the *Cat3* gene-specific probe. The A16 transcript is obviously longer than the transcripts of W64A and KYS, which are fairly similar.

at CT 22. A circadian expression is also present in all the NC lines, but the level of expression is quite diverse, resulting in variant patterns. Among the 5 NC lines, NC298 and NC304 display robust cycling with high levels of expression at CT 10. Lines NC296 and NC300 have a similar expression pattern with an increase in transcript very early after the onset of light, a maximum at CT 10, and lower amounts of transcript at the dark period. However, the early induction is much stronger in NC300. Line NC302 shows high expression at CT 6, slightly lower at CT 10, and constant lower expression during the dark period. In conclusion, our analysis indicates that a circadian expression of *Cat3* occurs among all the lines examined. However, differences exist with respect to the amplitude of the circadian rhythm, or the level of expression at specific times.

Modification of the 3′ end does not affect the *Cat3* circadian rhythm: We examined whether the structure of the *Cat3* gene is conserved among genetically diverse maize lines. First we examined the 3′ end of the gene using a *Cat3* gene-specific probe in Southern hybridizations of genomic DNA digested with SstI. Results indicate that extensive polymorphism exists at the 3′ end of the *Cat3* in the lines we analyzed (Figure 3). The reference line W64A gives a strong signal of the expected size at ~2 kb. In the rest of the examined lines the signal is weaker, indicating possible mismatches in the hybridization, as an equal amount of DNA was loaded on the gel (determined spectrophotometrically and after staining with ethidium bromide). One line, A16, shows a band of higher molecular weight, and the rest of the lines show variable lower MW bands than that of W64A. The higher MW of the A16 3′ end correlates to higher transcript size, whereas the lower MW of KYS does not (Figure 4). However, in all the lines, zymogram analysis indicated that the same CAT-3 isozyme (CAT-3A) is present (Figure 5). This strongly suggests that the modifications at the 3′ end are most probably located at the 3′ untranslated (for A16) and untranscribed (for the other lines) region.

These results indicate that extensive modifications in the gene structure occur at the 3′ end of the *Cat3* gene in maize genotypes of diverse origin. In connection with the conserved *Cat3* cycling in the same diverse genotypes, our results clearly indicate that modifications in the 3′ prime end of *Cat3* do not affect the cycling expression of the gene in these inbred lines.

The promoter region of *Cat3* is not conserved among different maize genotypes: To determine the presence of the *Zm13* transposon element, we used a PCR-based approach to identify the structure of the *Cat3* promoter in the genotypes examined. Results of the PCR were single band products of variable size for 10 out of the 11 lines examined, indicating that the promoter region of the gene has differences in length among these lines. In line Oh51A we failed to amplify any fragment after several attempts with different DNA isolates as templates, indicating strong sequence differences at the primer locations between W64A and Oh51A. Thus we omitted this line from further analyses. Three lines, BMS, KYS, and Tx303, had low amounts of PCR product (Figure 6). These results were identical when either of the two upper primers were used in PCR (see materials and methods). To ensure that the faint bands in BMS, KYS, and Tx303 were not because of template impurities, we used the same DNA templates in PCR with a set of test primers and under the same conditions to amplify a 500-bp fragment of the maize alternative oxidase gene (Polidoros *et al.* 1998). DNA templates from all the lines were sufficiently pure for successful amplification of the same fragment in equal quantity (Figure 6). Further analyses showed that these faint bands in BMS, KYS, and Tx303 were nonspecifically amplified

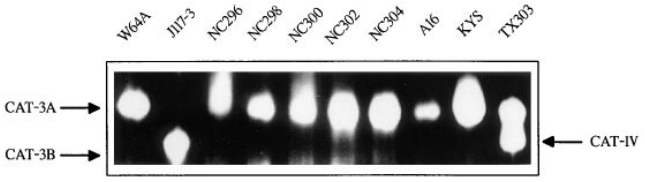

Figure 5.—Zymogram analysis indicating that the same *Cat3A* allele is present in all the lines examined in the present study. J117-3 is *Cat3B* control.

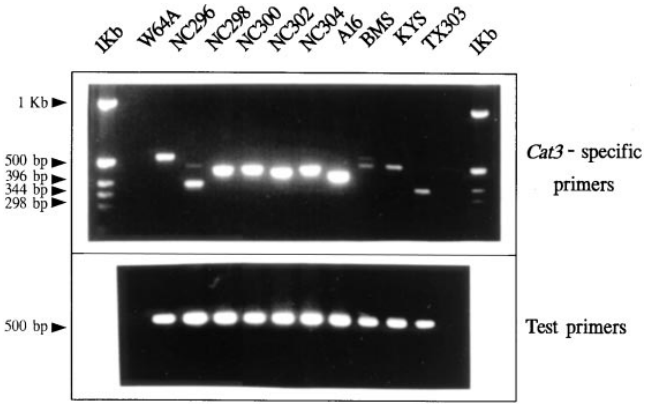

Figure 6.—Electrophoretic analysis of PCR products. Top: amplification of a promoter region of *Cat3* using DNA template from maize inbred lines of diverse origin. A single band of variable size can be detected, indicating that the promoter region of the gene differs in length among these lines. Intensity of the band is much lower in BMS, KYS, and Tx303, indicating that false product amplification likely occurred in these lines. Bottom: control PCR using a set of test primers that amplify part of the maize alternative oxidase gene and the same template DNA as in the top panel. A single band of similar size and intensity can be observed, indicating that the DNA template used in both PCRs is of sufficient purity to allow specific amplification.

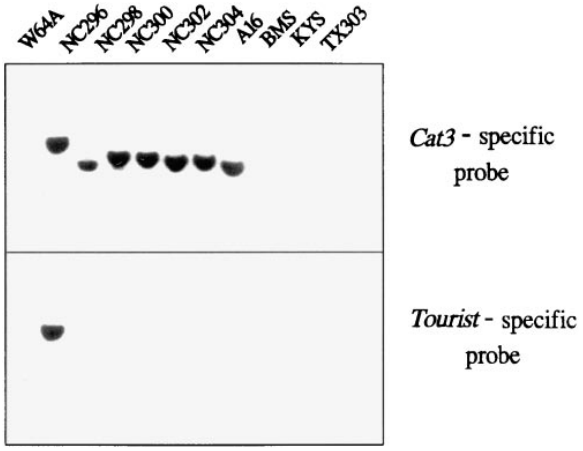

Figure 7.—Detection of similarity with the 5′ *Cat3* and the *Tourist* sequences in the PCR products from different lines. Top: hybridization of PCR bands from the different genotypes with the 80-bp *Cat3*-specific probe depicted in Figure 1. All NC lines and A16 show a strong hybridization signal. Bottom: hybridization of PCR bands from the different lines with the 185-bp *Tourist*-specific probe depicted in Figure 1. Only the W64A band hybridizes with this probe.

bands bearing no similarity to the *Cat3* promoter (see below).

The length of the PCR products in the rest of the lines was in all cases smaller than that of W64A. The difference in length is in the range of 80–100 bp except for NC296 and Tx303, where a difference of ~150 bp was detected. Because the size of the *Zm13* element is 145 bp, further analyses were required to determine the presence of the transposon element in the promoter of the *Cat3* gene in these genotypes. For this purpose we used a hybridization strategy depicted in Figure 1. Hybridization of the PCR products was performed with two probes. The 185-bp *Apa*I-*Xho*I fragment of the *Cat3* promoter that includes the 143-bp *Tourist Zm13* transposable element was used to determine the presence of the element in the different lines. The adjacent upstream 80-bp *Apa*I fragment was used to determine similarity with the *Cat3* promoter sequence of W64A. Our results indicate that, for all NC lines and A16, the amplified region is similar to the W64A *Cat3* promoter because strong hybridization signals were obtained with the 80-bp *Apa*I fragment (Figure 7, top). However, there was no detectable signal for the lines with weak PCR bands (BMS, KYS, and Tx303), indicating that possible modifications at the primer annealing sequences might cause mispriming and/or amplification of a false product. Hybridization of the same blot with the *Tourist* 185-bp *Apa*I-*Xho*I fragment of the *Cat3* promoter resulted in a strong signal only for W64A (Figure 7, bottom). This indicates that the element is missing in the *Cat3* promoter of the five NC lines and A16, whose PCR-amplified band hybridized with the *Cat3* promoter-specific 80-bp *Apa*I probe. However, multiple copies of *Tourist*-like sequences exist in the genomes of all the lines, as is evident from the multiple bands seen after hybridization of genomic DNA isolated from these lines with the *Tourist* probe (Figure 8).

Sequencing and multiple alignment of the PCR-amplified *Cat3* genomic fragments: The PCR products of the different genotypes were cloned and sequenced to determine the exact sequence of the *Cat3* promoter in these lines. Sequence analysis (Figure 9) confirmed the

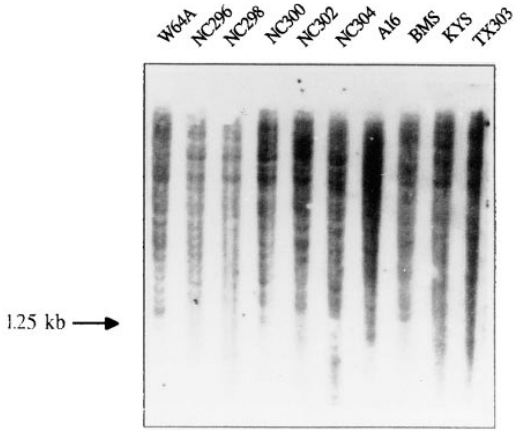

Figure 8.—Southern analysis indicating the presence of multiple copies of *Tourist*-like sequences in all the maize lines of diverse origin examined. Genomic DNA (10 μg) was digested with *Sst*I, electrophoresed through 1% agarose gel, and hybridized with the *Tourist*-specific probe. The position of the expected 1.25-kb hybridization band in W64A is indicated by an arrow.

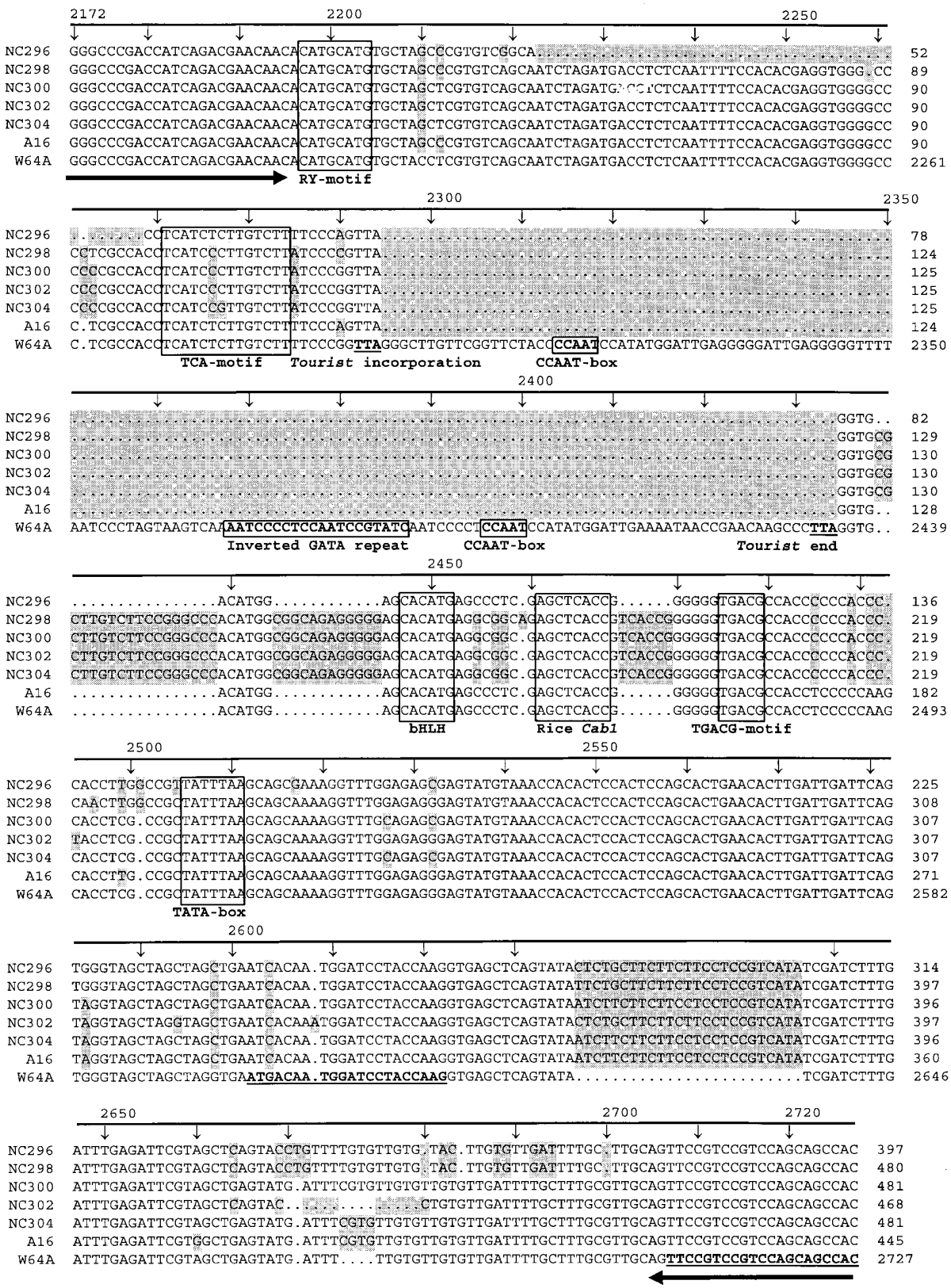
2172
2200
2250
NC296 GGGCCCGACCATCAGACGAACAACACATGCATGTGCTAGCCCGTGTCGGCA 52
NC298 GGGCCCGACCATCAGACGAACAACACATGCATGTGCTAGCCCGTGTCAGCAATCTAGATGACCTCTCAATTTTCCACACGAGGTGGG.CC 89
NC300 GGGCCCGACCATCAGACGAACAACACATGCATGTGCTAGCTCGTGTCAGCAATCTAGATG.CCTCTCAATTTTCCACACGAGGTGGGGCC 90
NC302 GGGCCCGACCATCAGACGAACAACACATGCATGTGCTAGCTCGTGTCAGCAATCTAGATGACCTCTCAATTTTCCACACGAGGTGGGGCC 90
NC304 GGGCCCGACCATCAGACGAACAACACATGCATGTGCTAGCTCGTGTCAGCAATCTAGATGACCTCTCAATTTTCCACACGAGGTGGGGCC 90
A16 GGGCCCGACCATCAGACGAACAACACATGCATGTGCTAGCCCGTGTCAGCAATCTAGATGACCTCTCAATTTTCCACACGAGGTGGGGCC 90
W64A GGGCCCGACCATCAGACGAACAACACATGCATGTGCTACCTCGTGTCAGCAATCTAGATGACCTCTCAATTTTCCACACGAGGTGGGGCC 2261
RY-motif
2300
2350
NC296 .....CCTCATCTCTTGTCTTTTCCCAGTTA 78
NC298 CCTCGCCACCTCATCCCTTGTCTTATCCCCGTTA 124
NC300 CCCCGCCACCTCATCCCTTGTCTTATCCCGGTTA 125
NC302 CCCCGCCACCTCATCCCTTGTCTTATCCCGGTTA 125
NC304 CCCCGCCACCTCATCCGTTGTCTTATCCCGGTTA 125
A16 C.TCGCCACCTCATCTCTTGTCTTTTCCCAGTTA 124
W64A C.TCGCCACCTCATCTCTTGTCTTTTCCCGGTTAGGGCTTGTTCGGTTCTACCCCAATCCATATGGATTGAGGGGGATTGAGGGGGTTTT 2350
TCA-motif Tourist incorporation CCAAT-box
2400
NC296 GGTG.. 82
NC298 GGTGCG 129
NC300 GGTGCG 130
NC302 GGTGCG 130
NC304 GGTGCG 130
A16 GGTG.. 128
W64A AATCCCTAGTAAGTCAAAATCCCCTCCAATCCGTATCAATCCCCTCCAATCCATATGGATTGAAAATAACCGAACAAGCCCTTAGGTG.. 2439
Inverted GATA repeat CCAAT-box Tourist end
2450
NC296 .....ACATGG.....AGCACATGAGCCCTC.GAGCTCACCG.....GGGGGTGACGCCACCCCCCACCC. 136
NC298 GTTGTCTTCCGGGCCCACATGGCGGCAGAGGGGGAGCACATGAGGCGGCAGAGCTCACCGTCACCGGGGGGTGACGCCACCCCCCACCC. 219
NC300 CTTGTCTTCCGGGCCCACATGGCGGCAGAGGGGGAGCACATGAGGCGGC.GAGCTCACCGTCACCGGGGGGTGACGCCACCCCCCACCC. 219
NC302 CTTGTCTTCCGGGCCCACATGGCGGCAGAGGGGGAGCACATGAGGCGGC.GAGCTCACCGTCACCGGGGGGTGACGCCACCCCCCACCC. 219
NC304 CTTGTCTTCCGGGCCCACATGGCGGCAGAGGGGGAGCACATGAGGCGGC.GAGCTCACCGTCACCGGGGGGTGACGCCACCCCCCACCC. 219
A16 .....ACATGG.....AGCACATGAGCCCTC.GAGCTCACCG.....GGGGGTGACGCCACCTCCCCCAAG 182
W64A .....ACATGG.....AGCACATGAGCCCTC.GAGCTCACCG.....GGGGGTGACGCCACCTCCCCCAAG 2493
bHLH Rice Cab1 TGACG-motif
2500
2550
NC296 CACCTTGGCCGTTATTTAAGCAGCGAAAGGTTTGGAGAGCGAGTATGTAAACCACACTCCACTCCAGCACTGAACACTTGATTGATTCAG 225
NC298 CAACTTGGCCGCTATTTAAGCAGCAAAAGGTTTGGAGAGGGAGTATGTAAACCACACTCCACTCCAGCACTGAACACTTGATTGATTCAG 308
NC300 CACCTCG.CCGCTATTTAAGCAGCAAAAGGTTTGCAGAGCGAGTATGTAAACCACACTCCACTCCAGCACTGAACACTTGATTGATTCAG 307
NC302 TACCTCG.CCGCTATTTAAGCAGCAAAAGGTTTGGAGAGGGAGTATGTAAACCACACTCCACTCCAGCACTGAACACTTGATTGATTCAG 307
NC304 CACCTCG.CCGCTATTTAAGCAGCAAAAGGTTTGCAGAGCGAGTATGTAAACCACACTCCACTCCAGCACTGAACACTTGATTGATTCAG 307
A16 CACCTTG.CCGCTATTTAAGCAGCAAAAGGTTTGGAGAGGGAGTATGTAAACCACACTCCACTCCAGCACTGAACACTTGATTGATTCAG 271
W64A CACCTCG.CCGCTATTTAAGCAGCAAAAGGTTTGGAGAGGGAGTATGTAAACCACACTCCACTCCAGCACTGAACACTTGATTGATTCAG 2582
TATA-box
2600
NC296 TGGGTAGCTAGCTAGCTGAATCACAA.TGGATCCTACCAAGGTGAGCTCAGTATACTCTGCTTCTTCTTCCTCCGTCATATCGATCTTTG 314
NC298 TGGGTAGCTAGCTAGCTGAATCACAA.TGGATCCTACCAAGGTGAGCTCAGTATATTCTGCTTCTTCTTCCTCCGTCATATCGATCTTTG 397
NC300 TAGGTAGCTAGCTAGCTGAATCACAA.TGGATCCTACCAAGGTGAGCTCAGTATAATCTTCTTCTTCCTCCTCCGTCATATCGATCTTTG 396
NC302 TAGGTAGCTAGGTAGCTGAATCACAAATGGATCCTACCAAGGTGAGCTCAGTATACTCTGCTTCTTCTTCCTCCGTCATATCGATCTTTG 397
NC304 TAGGTAGCTAGCTAGCTGAATCACAA.TGGATCCTACCAAGGTGAGCTCAGTATAATCTTCTTCTTCCTCCTCCGTCATATCGATCTTTG 396
A16 TAGGTAGCTAGCTAGCTGAATCACAA.TGGATCCTACCAAGGTGAGCTCAGTATAATCTTCTTCTTCCTCCTCCGTCATATCGATCTTTG 360
W64A TGGGTAGCTAGCTAGGTGAATGACAA.TGGATCCTACCAAGGTGAGCTCAGTATA.....TCGATCTTTG 2646
2650
2700
2720
NC296 ATTTGAGATTCGTAGCTCAGTACCTGTTTTGTGTTGTG.TAC.TTGTGTTGATTTTGC.TTGCAGTTCCGTCCGTCCAGCAGCCAC 397
NC298 ATTTGAGATTCGTAGCTCAGTACCTGTTTTGTGTTGTG.TAC.TTGTGTTGATTTTGC.TTGCAGTTCCGTCCGTCCAGCAGCCAC 480
NC300 ATTTGAGATTCGTAGCTGAGTATG.ATTTCGTGTTGTGTTGTGTTGATTTTGCTTTGCGTTGCAGTTCCGTCCGTCCAGCAGCCAC 481
NC302 ATTTGAGATTCGTAGCTCAGTAC.....CTGTGTTGATTTTGCTTTGCGTTGCAGTTCCGTCCGTCCAGCAGCCAC 468
NC304 ATTTGAGATTCGTAGCTGAGTATG.ATTTCGTGTTGTGTTGTGTTGATTTTGCTTTGCGTTGCAGTTCCGTCCGTCCAGCAGCCAC 481
A16 ATTTGAGATTCGTGGCTGAGTATG.ATTTCGTGTTGTGTTGTGTTGATTTTGCTTTGCGTTGCAGTTCCGTCCGTCCAGCAGCCAC 445
W64A ATTTGAGATTCGTAGCTGAGTATG.ATTT....TTGTGTTGTGTTGATTTTGCTTTGCGTTGCAGTTCCGTCCGTCCAGCAGCCAC 2727

conclusions drawn from the PCR hybridization experiments. The complete *Tourist* sequence is present only in the W64A maize line. The PCR bands amplified from BMS, KYS, and Tx303 do not resemble the W64A *Cat3* promoter sequence and are not presented below. The published *Cat3* sequence from W64A (Abler and Scandalios 1993) and the amplified sequence from W64A in this report are identical. Multiple alignment of the amplified sequences of the five NC lines, A16, and W64A was performed using the MegAlign program, which is part of the Lasergene Biocomputing Software Package (DNAStar, Madison, WI) and the PILEUP program, part of the GCG Wisconsin Package (GCG, Madison, WI). The resulting alignments using either program showed that short regions with similarities between the seven lines existed within the *Tourist* element and close to its 5′ end (alignments not shown). However, most of the *Tourist* sequence was present only in W64A. The alignment downstream of the *Tourist* element (located between nt 2291 and 2434) revealed several gaps, and the seven sequences regained high similarity at position 2465 and thereafter. One possible explanation for these results could be that a *Tourist*-like element was present in ancestors of these lines, but sometimes it transposed and left behind or carried along a few nucleotides after its excision. Such phenomena are not unusual in transposition of mobile elements. However, in multiple alignments of the sequences in different combinations (each time omitting one or more lines) we observed that the NC lines and A16 were aligned better without the W64A sequence, or with W64A after deleting the *Tourist* element. This alignment indicated that the sequences of NC298, NC300, NC302, and NC304 were almost identical in a 85-bp long region immediately downstream of the *Tourist* incorporation trinucleotide TTA at position 2291. The sequences of W64A, A16, and NC296 were also identical and differed from the other NC lines as they were interrupted by three short gaps 18 bp, 12 bp, and 6 bp long. The rest of the alignments upstream and downstream of the 85-bp region were identical with the alignments obtained before the *Tourist* element was deleted from W64A and were the same using either computer program.

Alignment of the PCR-amplified *Cat3* segments was different when the *Tourist* element was retained or excised from the W64A sequence. In order to give the same alignment in the presence and the absence of the element, the computer programs should have been forced to introduce a very long gap in the other sequences, where the element is incorporated in W64A. This is an unfavorable option even after adjusting the gap penalty parameters of the programs. Thus, we simply used the alignment of the seven lines in which the sequence of the *Tourist* element was deleted, then reinserted the element in its position in the W64A sequence, and aligned with gaps in the other lines (Figure 9). The *Cat3* promoter sequences in two lines, NC300 and NC304, are exactly the same, indicating that the *Cat3* gene in these lines derived from a common ancestor. Line NC296 is the only one that is missing about 45 bp of the 116-bp region immediately upstream of the *Tourist* element location. It is also the only South American line having exactly the same gaps as A16 and W64A downstream from the *Tourist* element. Similarity between A16 and W64A is high.

DISCUSSION

Implications of the presence of a transposable element in the *Cat3* promoter: In a previous study, we reported the presence of putative circadian- and light-regulatory motifs (GATA repeat, CCAAT boxes) within the region of a *Tourist* transposable element in the *Cat3* promoter (Polidoros and Scandalios 1997). Similar motifs have been shown to be involved in the light and circadian regulation of the Arabidopsis *CAB2* gene (Anderson *et al.* 1994). This raised the possibility that circadian regulation of *Cat3* may be dependent on the presence of the transposable element (or the motifs it harbors) in the promoter of the gene. Such an assumption could have significant implications on the necessity for circadian *Cat3* expression and the physiological role of the CAT-3 isozyme in cellular metabolism. For example, if the circadian *Cat3* expression is dependent upon the presence of the *Tourist* element, then it could be a random feature due to the incorporation of the element rather than to a specific biological necessity. Based on this assumption, maize genotypes might exist that do not harbor the *Tourist* element in their *Cat3* promoter and show no circadian *Cat3* expression. Alternatively, if the circadian *Cat3* expression is because of a specific biological necessity and is independent of the presence

Figure 9.—Multiple alignment of part of the *Cat3* gene sequences resulting from PCR amplification using DNA from the maize inbred lines NC296, NC298, NC300, NC302, NC304, A16, and W64A. The genotype is shown at the left of each sequence and the nucleotide count at the right. The first nucleotide in W64A is number 2172, following the numbering of the sequence in GenBank (accession number L05934). In the rest of the lines, nucleotide count starts with number one. The length of each sequence is shown at right except for W64A, which is 655 bp. Nucleotides or sequences in shaded boxes represent disagreement with the W64A sequence. The ruler on top of the sequences shows the nucleotide count in W64A in increments of 10. Conserved motifs are shown in open boxes, and their names are in bold below the boxes. The PCR primers are shown as bold arrows below the sequence of each primer. The two exons of the *Cat3* gene in W64A are in bold and underlined. The *Tourist* incorporation target site TTA and its end site (duplicated) TTA are in bold, underlined, and indicated underneath. Within the *Tourist* sequence the CCAAT boxes and the inverted GATA repeat (which includes one additional CCAAT box) are in bold, in open boxes, and indicated below.

of the *Tourist* element, then genotypes might exist that maintain circadian *Cat3* expression in the absence of the *Tourist* element in the *Cat3* promoter. It is obvious that proving either of the above possibilities would have significant implications on the evolutionary origin of the *Cat3* circadian expression, as well as for the biological significance of this regulation.

Examination for a circadian expression of *Cat3* in maize genotypes of diverse origin in relation to the presence/absence of the *Tourist* element in the *Cat3* promoter: To study the functional significance of the *Tourist* element in the *Cat3* promoter we sought to take advantage of the highly polymorphic maize genome and the availability of diverse maize genotypes. Among these we could likely identify genotypes that harbor no *Tourist* element in the *Cat3* promoter and/or genotypes in which the expression of *Cat3* is not circadian. In fact, after examining three additional maize inbreds, Acevedo *et al.* (1991) concluded that neither *Cat3* allelic variation nor genetic background alters the circadian pattern of *Cat3* mRNA accumulation in the leaves of these lines. However, at the time this study was conducted, it was not known that a transposable element, harboring putative circadian- and light-regulatory motifs, is present in the *Cat3* promoter of W64A. Accordingly, it was suggested that the circadian regulation of *Cat3* transcription in W64A (Redinbaugh *et al.* 1990) is likely a general phenomenon in maize. This situation was questioned when the *Tourist* element was discovered in the *Cat3* promoter and the putative circadian- and light-regulatory motifs were identified on the element (Polidoros and Scandalios 1997).

To further investigate the general nature of the *Cat3* circadian expression we expanded the analysis in 10 additional maize inbreds of diverse origin (see materials and methods). Northern hybridization analysis confirmed that the circadian *Cat3* expression is conserved and has the same pattern among all these diverse genotypes (Figure 2). Differences were present regarding the amplitude of the rhythm and the expression level at different time points, especially between the South American genotypes, but this could be the result of modifications at the 3′ end of the gene, where the *Cat3* gene-specific probe used in this study hybridized. However, the same general expression pattern with the transcript increasing during the light period, and decreasing during the dark, was obvious in all the lines. Significantly, we also demonstrated that modifications of the 3′ end of the gene in these genotypes (Figure 3) did not affect the circadian expression of the gene. These modifications did not result in CAT-3 allelic variation because the same *Cat-3A* allele was present in all the lines (Figure 5). However, the transcript size was affected in A16 (Figure 4). Taken together, the above results suggest that the circadian regulation of *Cat3* transcription is a general phenomenon in maize, validating our previous assumptions (Acevedo *et al.* 1991). After ensuring the *Cat3* circadian expression in these genotypes, we asked whether it correlates with the presence of the *Tourist* element in the promoter of the gene. Combined results from PCR amplification of a *Cat3* promoter region that includes the *Tourist* element in W64A and hybridization of the PCR products with *Cat3*-specific and *Tourist*-specific probes (Figures 6 and 7) proved that none of the South American lines nor A16 harbored the *Tourist* element in the *Cat3* promoter. Thus, we could safely conclude that the presence of the *Tourist* element was not necessary for regulating the *Cat3* circadian expression. We also observed PCR-product length variability, which could not be explained solely by the absence of the *Tourist* element in all the lines. Along with our inability to amplify a promoter region in some of the lines, this was strong evidence that the *Cat3* promoter had extensive differences in the genotypes examined. The conclusion from this analysis is that incorporation of the *Tourist* element in the *Cat3* promoter of W64A does not appear to affect the circadian regulation of the gene. However, we cannot rule out the possibility that motifs similar to those present in the *Tourist* element (GATA repeat, CCAAT boxes) in W64A are also present and important for the circadian regulation of *Cat3* gene expression, but located elsewhere in the promoter of the *Cat3* in the rest of the lines. To examine this possibility, as well as to determine the exact *Cat3* promoter structure, we sequenced the PCR-amplified *Cat3* promoter region in the South American lines, A16, and W64A.

Sequence analysis and *Cat3* promoter structure: The sequences of the *Cat3* promoter from each of the seven genotypes, derived by sequencing of the PCR fragments, were aligned as described in results and analyzed for the presence of regulatory motifs. The alignment (Figure 9) confirmed the following: The sequence of the *Cat3* promoter has highly conserved and highly variable regions among the seven diverse lines examined. Relative to the differences among these lines is the absence of a *Tourist* transposable element in lines other than W64A. Significantly, no motifs similar to those present in the *Tourist* element, and presumed to play a role in the circadian regulation of *Cat3* (GATA repeat, CCAAT boxes), were present in the promoter of any other line. This suggests that other regulatory elements are responsible for the circadian regulation of the maize *Cat3* gene and indicates that differences might exist between monocot (maize) and dicot (Arabidopsis) circadian regulatory components.

The first translatable ATG triplet in W64A (Redinbaugh *et al.* 1988) is not conserved in the rest of the lines. Instead, the ATG of the third amino acid in the first *Cat3* exon of W64A seems to be the first translatable ATG in all the other lines, as it is in 14 of the 15 other plant catalase transcripts reported (Guan and Scandalios 1996). There is a 24-bp sequence with CTT repeats and a 4-bp stretch absent in W64A in the first

intron and present in all other lines. Some single base mismatches can be observed sporadically and at very low frequency in pairwise alignments between W64A and the rest of the lines. The region upstream of the element is identical between W64A and A16. Most divergent is NC296 that is missing ~45 bp of the 116 bp of the region. The rest of the NC lines have a few random single base mismatches.

Among the similarities between the lines are several highly conserved regions and putative regulatory motifs in the *Cat3* promoter sequence (Figure 9). The region between the TATA-box and the first exon is almost identical in all the lines. Upstream of the TATA-box in a short 40-bp region, the following are conserved: a TGACG motif that is a component of the promoters of many plant, animal, and viral genes (Bouchez *et al.* 1989; Inoue *et al.* 1991), serving as a binding site for basic-leucine-zipper (bZIP) transcription factors and mediating responses to auxin and salicylic acid (SA) (Miao and Lam 1995; Rouster *et al.* 1997); the light-responsive element AGCTCACC of the rice *Cab1* gene (Luan and Bogorad 1992); and a basic helix-loop-helix (bHLH) transcription factor binding site (Pabo and Sauer 1992). This is the only conserved region, between the genotypes examined, that harbors a light-responsive element and may be important in the circadian regulation of *Cat3*. Upstream of the *Tourist* location there is one motif resembling the TCA element (TCATCTT CTT), which is the binding site of the salicylic acid-inducible TCA-1 regulatory protein (Goldsbrough *et al.* 1993). In moderate concentrations, SA can induce catalase genes, and a developmental stage-specific *Cat3* induction has been observed during germination of immature developing maize embryos treated with SA (Guan and Scandalios 1995). The TCA motif at nt 2270 has a conserved TCATC part and a variable (C/T) (C/G)TTGTCTT part and may mediate the SA responses in *Cat3* transcription. Further upstream (nt 2198) there is a conserved RY motif (CATGCATG) (Baumlein *et al.* 1992; Lelievre *et al.* 1992). This motif merits special attention. The RY motif CATGCATG is present in the 5′ upstream region of a large number of plant genes mostly expressed during seed development (Baumlein *et al.* 1992). It is also present as the *Sph*I element in the SV40 enhancer (Zenke *et al.* 1986) and at the promoter of the rice *CatA* catalase gene, a rice homologue of the maize *Cat3* (Higo and Higo 1996). Destruction of this motif by short internal deletions nearly abolishes the function of a C1 maize gene (Hattori *et al.* 1992) and the legumin B4 gene of *Vicia faba* (Baumlein *et al.* 1992). Strong positive effects have also been reported for glycinin (Lelievre *et al.* 1992) and β-conglycinin (Chamberland *et al.* 1992) expression in soybean. In contrast, in *Vicia faba* the RY motif of the *usp* gene promoter exerts a silencing effect because its destruction increases transcription (Fiedler *et al.* 1993). It has been hypothesized that positive or negative effects of the RY motif in transcription are controlled by the presence of enhancers or silencer-like elements upstream of the motif (Baumlein *et al.* 1992; Fiedler *et al.* 1993). In addition, the hypothesis is supported by a number of reported unsuccessful attempts to demonstrate binding of nuclear proteins to the RY motif (Riggs *et al.* 1989; Meakin and Gatehouse 1991). A role of the RY motif in repression of *Cat3* transcription could place it as a component of the circadian regulatory apparatus of the gene as the circadian *Cat3* expression has been proposed to be the result of a cyclic repression superimposed on a quasi-constitutive mode of expression in maize leaves (Acevedo *et al.* 1991).

Downstream of the RY motif there is a sequence between nt 2241 and 2276 that is present in the rice *CatA* gene promoter (*CatA* is a homologue to the maize *Cat3*) and proposed to be specific to the promoter of the gene encoding the CAT-3 type catalase of monocots (Higo and Higo 1996). This region of unknown function is almost totally missing from NC296 and is highly conserved in the rest of the lines.

Unraveling the structural variability of the *Cat3* promoter might have important implications. Even if the circadian expression of the gene is conserved among these genotypes with structurally different promoters, other aspects of the regulation of the gene remain unknown. The W64A *Cat3* gene has been shown to respond to diverse stress conditions and challenges like the fungal toxin cercosporin (Williamson and Scandalios 1992), salycilic acid (Guan and Scandalios 1995), diverse antioxidants, H_2O_2, and mitochondrial respiration pathway-specific inhibitors (A. N. Polidoros and J. G. Scandalios, unpublished results). It is currently unknown whether *Cat3* responds similarly in other genotypes.

Aspects of the physiological role of CAT-3: The existence of CAT-3 null maize lines with no major discernible physiological defects under normal growth conditions (Scandalios *et al.* 1997) suggests that CAT-3 is a dispensable catalase isozyme. However, this does not imply that it has no specific physiological role in cellular metabolism, or that it may not be critical under adverse environments. Results presented in this study make apparent that circadian *Cat3* expression is the rule in maize. The pattern of the *Cat3* circadian rhythm in all the lines examined, with maximal mRNA accumulation late in the light period and minimal mRNA accumulation late in the dark, suggests that there might be a high demand for CAT-3 during the early dark period of the plant's metabolism. This distinguishes maize *Cat3* from the *Arabidopsis thaliana CAT2* (Zhong *et al.* 1994) and *Nicotiana plumbaginifolia Cat1* (Willekens *et al.* 1994), in which the phase of accumulation of catalase transcripts early in the light period coincides with that of photosynthetic gene transcripts and is in good agreement with a potent physiological role of catalase in decomposing H_2O_2 generated during the photorespi-

ratory oxidation of glycolate in the peroxisome. The presence of a catalase in a C3 dicot plant (*A. thaliana CAT3*) exhibiting a circadian expression phase similar to *Cat3* of maize (a C4 monocot plant) (Zhong and McClung 1996) might imply a common metabolic necessity in C3 and C4 as well as in monocot and dicot plants for catalase during the late light and early dark period. However, Arabidopsis *CAT3* has a consensus peroxisomal targeting signal and is expected to be localized in peroxisomes (Frugoli *et al.* 1996), whereas maize CAT-3 is mitochondrial (Scandalios *et al.* 1980). Thus, the nature of such a common metabolic requirement remains speculative.

Basically, two hypotheses have been proposed to explain the physiological role of CAT-3. One considers the high peroxidatic activity of CAT-3 and the overlapping histological patterns of lignification and catalase distribution in maize stem cells (Acevedo and Scandalios 1991). This suggests that CAT-3 may play a role in the lignification process providing the required peroxidatic activity. Several enzymes of the general phenylpropanoid pathway, which is part of the lignin biosynthetic pathway, are light-inducible, both at the mRNA (Ohl *et al.* 1990; Feinbaum *et al.* 1991; Kubasek *et al.* 1992; Ohl *et al.* 1990) and the enzyme activity levels (Wilkinson and Butt 1992). The activity of these enzymes reportedly showed a 1–5-hr lag before increasing after illumination in etiolated pea epicotyls, reaching a maximum over a 12-hr period when lignification was more rapid and declining thereafter. This time frame is in good agreement with the increase of *Cat3* expression 4–6 hr after the onset of light reaching a maximum after 10 hr and declining thereafter.

The second hypothesis suggests that there might be increased demand for catalase late in the light period and early in the dark period, because of an excessive H_2O_2 buildup during this period of the plant's metabolism. The excessive H_2O_2 can be attributed to decreased ascorbate peroxidase activity (Abler and Scandalios 1994), or to a diurnal fluctuation in the production of reactive oxygen species in the mitochondria of mesophyll cells (Polidoros and Scandalios 1997). The circadian regulation of *Cat3* expression fits a model of excessive H_2O_2 formation during the late light-early dark period, but this has to be examined. Further investigations are underway to examine the above hypotheses on the physiological role of maize CAT-3, the necessity of which has been implied by the results presented in this study.

We thank Stephanie Ruzsa and Sheri Kernodle for expert technical assistance and B. Wiegmann and B. Cassel for help with sequencing. This work was supported by National Science Foundation research grant No. DCB-9101238 to J.G.S.

LITERATURE CITED

Abler, M. L., and J. G. Scandalios, 1991 The CAT-2 null phenotype in maize is likely due to a DNA insertion into the *Cat2* gene. Theor. Appl. Genet. **81:** 635–640.

Abler, M. L., and J. G. Scandalios, 1993 Isolation and characterization of a genomic sequence encoding the maize *Cat3* catalase gene. Plant Mol. Biol. **22:** 1031–1038.

Abler, M. L., and J. G. Scandalios, 1994 Regulation of the cyclic repression of the *Cat3* catalase gene in maize leaves and roots occurs via the dark/light transition. Maydica **39:** 83–88.

Acevedo, A., and J. G. Scandalios, 1991 Catalase and superoxide dismutase gene expression and distribution during stem development in maize. Dev. Genet. **12:** 423–430.

Acevedo, A., J. D. Williamson and J. G. Scandalios, 1991 Photoregulation of the *Cat2* and *Cat3* catalase genes in pigmented and pigment-deficient maize: the circadian regulation of *Cat3* is superimposed on its quasi-constitutive expression in maize leaves. Genetics **127:** 601–608.

Anderson, S. L., G. R. Teakle, S. J. Martino-Catt and S. A. Kay, 1994 Circadian clock- and phytochrome-regulated transcription is conferred by a 78 bp *cis*-acting domain of the Arabidopsis *CAB2* promoter. Plant J. **6:** 457–470.

Baumlein, H., I. Nagy, R. Villarroel, D. Inze and U. Wobus, 1992 Cis-analysis of a seed protein gene promoter: the conservative RY repeat CATGCATG within the legumin box is essential for tissue-specific expression of a legumin gene. Plant J. **2:** 233–239.

Bouchez, D., J. G. Tokuhisa, D. J. Llewellyn, E. S. Dennis and J. G. Ellis, 1989 The ocs-element is a component of the promoters of several T-DNA and plant viral genes. EMBO J. **8:** 4197–4204.

Bureau, T. E., and S. R. Wessler, 1994a Mobile inverted-repeat elements of the *Tourist* family are associated with the genes of many cereal grasses. Proc. Natl. Acad. Sci. USA **91:** 1411–1415.

Bureau, T. E., and S. R. Wessler, 1994b *Stowaway*: A new family of inverted repeat elements associated with the genes of both monocotyledonous and dicotyledonous plants. Plant Cell **6:** 907–916.

Chamberland, S., N. Daigle and F. Bernier, 1992 The legumin boxes and the 3′ part of a soybean beta-conglycinin promoter are involved in seed gene expression in transgenic tobacco plants. Plant Mol. Biol. **19:** 937–949.

Chandlee, J. M., and J. G. Scandalios, 1984 Analysis of variants affecting the catalase (EC 1.11.1.6) developmental program in maize (*Zea mays*) scutellum. Theor. Appl. Genet. **69:** 71–77.

Feinbaum, R. L., G. Storz and F. M. Ausubel, 1991 High intensity and blue light regulated expression of chimeric chalcone synthase genes in transgenic *Arabidopsis thaliana* plants. Mol. Gen. Genet. **226:** 449–456.

Fiedler, U., R. Filistein, U. Wobus and H. Baumlein, 1993 A complex ensemble of cis-regulatory elements controls the expression of a *Vicia faba* non-storage seed protein gene. Plant Mol. Biol. **22:** 669–679.

Frugoli, J. A., H. H. Zhong, M. L. Nuccio, P. McCourt, M. A. McPeek *et al.* 1996 Catalase is encoded by a multigene family in *Arabidopsis thaliana* (L.) Heynh. Plant Physiol. **112:** 327–336.

Goldsbrough, A. P., H. Albrecht and R. Stratford, 1993 Salicylic acid-inducible binding of a tobacco nuclear protein to a 10 bp sequence which is highly conserved amongst stress-inducible genes. Plant J. **3:** 563–571.

Guan, L., and J. G. Scandalios, 1995 Developmentally related responses of maize catalase genes to salicylic acid. Proc. Natl. Acad. Sci. USA **92:** 5930–5934.

Guan, L., and J. G. Scandalios, 1996 Molecular evolution of maize catalases and their relationship to other eukaryotic and prokaryotic catalases. J. Mol. Evol. **42:** 570–579.

Gussow, D., and T. Clackson, 1989 Direct clone characterization from plaques and colonies by the polymerase chain reaction. Nucleic Acids Res. **17:** 4000.

Hattori, T., V. Vasil, L. Rosenkrans, L. C. Hannah, D. R. McCarty *et al.* 1992 The Viviparous-1 gene and abscisic acid activate the C1 regulatory gene for anthocyanin biosynthesis during seed maturation in maize. Genes Dev. **6:** 609–618.

Higo, K., and H. Higo, 1996 Cloning and characterization of the rice *CatA* catalase gene, a homologue of the maize *Cat3* gene. Plant Mol. Biol. **30:** 505–521.

Inoue, H., N. Watanabe, Y. Higashi and Y. Fujii-Kuriyama, 1991 Structures of regulatory regions in the human cytochrome P-450scc (desmolase) gene. Eur. J. Biochem. **195:** 563–569.

Klimyuk, V. I., and J. D. G. Jones, 1997 *AtDMC1*, the Arabidopsis homologue of the yeast *DMC1* gene: characterization, transposon-induced allelic variation and meiosis-associated expression. Plant J. **11:** 1–14.

Koester-Toepfer, M., W. B. Frommer, M. Rocha Sosa and L. Willmitzer, 1990 Presence of a transposon-like element in the promoter region of an inactive patatin gene in *Solanum tuberosum* L. Plant Mol. Biol. **14:** 239–248.

Kubasek, W. L., B. W. Shirley, A. McKillop, H. M. Goodman, W. Briggs *et al.* 1992 Regulation of flavonoid biosynthetic genes in germinating Arabidopsis seedlings. Plant Cell **4:** 1229–1236.

Lelievre, J. M., L. O. Oliveira and N. C. Nielsen, 1992 5′-CATG CAT-3′ elements modulate the expression of glycinin genes. Plant Physiol. **98:** 387–391.

Luan, S., and L. Bogorad, 1992 A rice *cab* gene promoter contains separate cis-acting elements that regulate expression in dicot and monocot plants. Plant Cell **4:** 971–981.

Luehrsen, K. R., and V. Walbot, 1990 Insertion of *Mu1* elements in the first intron of the *Adh1-S* gene of maize results in novel RNA processing events. Plant Cell **2:** 1225–1238.

McCarty, D. R., C. B. Carson, M. Lazar and S. C. Simonds, 1989 Transposable element-induced mutations of the *viviparous-1* gene in maize. Dev. Genet. **10:** 473–481.

McLaughlin, M., and V. Walbot, 1987 Cloning of a mutable *bz2* allele of maize by transposon tagging and differential hybridization. Genetics **117:** 771–776.

Meakin, P. J., and J. A. Gatehouse, 1991 Interaction of seed nuclear proteins with transcriptionally-enhancing regions of the pea (*Pisum sativum* L.) *legA* gene promoter. Planta **183:** 471–477.

Miao, Z. H., and E. Lam, 1995 Construction of a trans-dominant inhibitor for members of the TGA family of transcription factors conserved in higher plants. Plant J. **7:** 887–896.

Millar, A. J., and S. A. Kay, 1991 Circadian control of *cab* gene transcription and messenger RNA accumulation in Arabidopsis. Plant Cell **3:** 541–550.

Ohl, S., S. A. Hedrick, J. Chory and C. J. Lamb, 1990 Functional properties of a phenylalanine ammonia-lyase promoter from Arabidopsis. Plant Cell **2:** 837–848.

Pabo, C. O., and R. T. Sauer, 1992 Transcription factors: structural families and principles of DNA recognition. Annu. Rev. Biochem. **61:** 1053–1095.

Polidoros, A., and J. G. Scandalios, 1997 Response of the maize catalases to light. Free Radic. Biol. Med. **23:** 497–504.

Polidoros, A. N., P. V. Mylona and J. G. Scandalios, 1998 Partial isolation and characterization of the maize alternative oxidase gene. Maize Gen. Cooper. Newsl. **72** (in press).

Redinbaugh, M. G., G. J. Wadsworth and J. G. Scandalios, 1988 Characterization of catalase transcripts and their differential expression in maize. Biochim. Biophys. Acta **951:** 104–116.

Redinbaugh, M. G., M. Sabre and J. G. Scandalios, 1990 Expression of the maize *Cat3* catalase gene is under the influence of a circadian rhythm. Proc. Natl. Acad. Sci. USA **87:** 6853–6857.

Riggs, C. D., T. A. Voelker and M. J. Chrispeels, 1989 Cotyledon nuclear proteins bind to DNA fragments harboring regulatory elements of phytohemagglutinin genes. Plant Cell **1:** 609–621.

Rouster, J., R. Leah, J. Mundy and V. Cameron Mills, 1997 Identification of a methyl jasmonate-responsive region in the promoter of a lipoxygenase 1 gene expressed in barley grain. Plant J. **11:** 513–523.

Scandalios, J. G., W. F. Tong and D. G. Roupakias, 1980 *Cat3*, a 3rd gene locus coding for a tissue-specific catalase in maize (*Zea mays*): genetics, intracellular location and some biochemical properties. Mol. Gen. Genet. **179:** 33–42.

Scandalios, J. G., L. Guan and A. N. Polidoros, 1997 Catalases in plants: gene structure, properties, regulation, and expression, pp. 343–406 in *Oxidative Stress and the Molecular Biology of Antioxidant Defenses*, edited by J. G. Scandalios. Cold Spring Harbor Laboratory Press, New York.

Schiefelbein, J. W., D. B. Furtek, H. K. Dooner and O. E. J. Nelson, 1988 Two mutations in a maize *bronze-1* allele caused by transposable elements of the Ac-Ds family alter the quantity and quality of the gene product. Genetics **120:** 767–778.

Skadsen, R. W., and J. G. Scandalios, 1987 Translational control of photo-induced expression of the *Cat2* catalase gene during leaf development in maize. Proc. Natl. Acad. Sci. USA **84:** 2785–2789.

Stavenhagen, J. B., and D. M. Robins, 1988 An ancient provirus has imposed androgen regulation on the adjacent mouse sex-limited protein gene. Cell **55:** 247–254.

Thompson, W. F., M. Everett, N. O. Polans, R. A. Jorgensen and J. D. Palmer, 1983 Phytochrome control of RNA levels in developing pea and mung bean leaves [*Pisum sativum*, *Vigna radiata*]. Planta **158:** 487–500.

Ting, C. N., M. P. Rosenberg, C. M. Snow, L. C. Samuelson and M. H. Meisler, 1992 Endogenous retroviral sequences are required for tissue-specific expression of a human salivary amylase gene. Genes Dev. **6:** 1457–1465.

Weil, C. F., S. Marillonnet, B. Burr and S. R. Wessler, 1992 Changes in state of the *Wx-m5* allele of maize are due to intragenic transposition of Ds. Genetics **130:** 175–186.

White, S. E., L. F. Habera and S. R. Wessler, 1994 Retrotransposons in the flanking regions of normal plant genes: a role for *copia*-like elements in the evolution of gene structure and expression. Proc. Natl. Acad. Sci. USA **91:** 11792–11796.

Wilkinson, E. M., and V. S. Butt, 1992 Enzyme changes during lignogenesis in pea shoots induced by illumination. J. Exp. Bot. **43:** 1259–1265.

Willekens, H., C. Langebartels, C. Tire, M. V. Montagu, D. Inze *et al.* 1994 Differential expression of catalase genes in *Nicotiana plumbaginifolia* (L.). Proc. Natl. Acad. Sci. USA **91:** 10450–10454.

Williamson, J. D., and J. G. Scandalios, 1992 Differential response of maize catalases and superoxide dismutases to the photoactivated fungal toxin cercosporin. Plant J. **2:** 351–358.

Zenke, M., T. Grundstrom, H. Matthes, M. Wintzerith, C. Schatz *et al.* 1986 Multiple sequence motifs are involved in SV40 enhancer function. EMBO J. **5:** 387–398.

Zhong, H. H., and C. R. McClung, 1996 The circadian clock gates expression of two Arabidopsis catalase genes to distinct and opposite circadian phases. Mol. Gen. Genet. **251:** 196–203.

Zhong, H. H., J. C. Young, E. A. Pease, R. P. Hangarter and C. R. McClung, 1994 Interactions between light and the circadian clock in the regulation of CAT2 expression in Arabidopsis. Plant Physiol. **104:** 889–898.

Communicating editor: S. L. Allen

Free Radical Biology & Medicine, Vol. 25, Nos. 4/5, pp. 576–585, 1998
Copyright © 1998 Elsevier Science Inc.
Printed in the USA. All rights reserved
0891-5849/98 $19.00 + .00

PII S0891-5849(98)00090-2

Original Contribution

MODULATION OF ANTIOXIDANT RESPONSES BY ARSENIC IN MAIZE

PHOTINI V. MYLONA, ALEXIOS N. POLIDOROS, and JOHN G. SCANDALIOS
Department of Genetics, North Carolina State University, Raleigh, NC, USA

(*Received* 19 *November* 1997; *Revised* 6 *April* 1998; *Accepted* 8 *April* 1998)

Abstract—The effects of arsenic on the expression of the antioxidant genes encoding superoxide dismutase, catalase, and glutathione *S*-transferase, as well as the activity of SOD and CAT enzymes, were examined at different developmental stages and in different tissues. Both CAT and SOD activities increased in response to low concentrations (0.01-0.1 mM) of arsenic in developing maize embryos. In germinating embryos both CAT and SOD activities increased in response to a wide range of arsenic concentrations (0.01-10 mM). *Cat1* transcript increased in response to arsenic in developing and germinating embryos and in young leaves. Conversely, *Cat2* increased at low concentrations of arsenic only in germinating embryos. *Cat3* transcript levels increased in response to low concentrations of arsenic only in developing embryos. *Sod3* transcript increased at low concentrations of arsenic in developing, germinating embryos and in leaves. The cytosolic *Sod4* and *Sod4A* increased in response to arsenic in germinating embryos, while only *Sod4* transcript increased in response to arsenic in leaves. Expression of *Gst1* was similar to that of *Cat1* in all tissues examined. These results indicate that arsenic triggers tissue and developmental stage specific defense responses of antioxidant and detoxification related genes in maize. © 1998 Elsevier Science Inc.

Keywords—Arsenite, Arsenate, Catalase, Superoxide dismutase, Glutathione *S*-transferase, Reactive oxygen species, Free radicals

INTRODUCTION

Arsenic compounds are naturally present in the environment, and are also used in agriculture and forestry as pesticide or insecticide components. The major anthropogenic sources of environmental pollution with arsenic are the burning of coal and industrial metal smelting, and more recently the semiconductor industry. According to epidemiological studies and clinical observations, arsenic is associated with increased risk of certain types of human cancer, including epidermoid carcinomas of skin, lung cancer and possibly liver cancer.

Arsenic is a toxic metalloid, whose trivalent arsenite, As(III), and pentavalent arsenate, As(V), ions can inhibit many biochemical processes.[1–4] The solubility of As(III) oxide in water is fairly low, but high in either acid or alkali. In water, arsenic is usually in the form of arsenate or arsenite. As(III) is systemically more poisonous than the As(V), and As(V) is reduced to the As(III) form without exerting any toxic effects. Organic arsenicals also exert their toxic effects in vivo in animals by first metabolizing to the trivalent arsenoxide form. Overall, it seems that in most organisms arsenic is more toxic in the trivalent form, as arsenite, than in the pentavalent form, as arsenate. Numerous reports describe the higher toxicity of arsenite to that of arsenate in plants.[5,6] In plants the toxicity of arsenate is known to be competitively affected by phosphate, whereas such a relation seems to be obscure between arsenite and phosphate.[6]

At present, the mechanisms for the effects of arsenic toxicity are unclear. It is known that low concentrations of arsenicals may initiate gene transcription by altering the phosphorylation state of signal transduction proteins. Arsenic affects phosphorylation by activating specific phosphatases, by inhibiting thiol-dependent phosphatases, or by interfering with phosphotransferase reactions.[3,4,7] The protective effects of thiols, such as glutathione and cysteine, against the toxic effects of arsenic, suggests that arsenic toxicity results from forming reversible bonds with thiol groups of regulatory proteins.

Recently, evidence suggesting that oxygen radicals can be produced during arsenic metabolism has been

Address correspondence to: John G. Scandalios, Dept. of Genetics, Box 7614, North Carolina State University, Raleigh, NC 27695-7614, USA; Tel: 919-515-7079; Fax: 919-515-3355; E-Mail: jgs@unity.ncsu.edu.

provided.[8,9] The reactive oxygen scavenging enzymes catalase (CAT) and /or superoxide dismutase (SOD) were shown to effectively reduce the frequency of arsenite-induced sister chromatid exchanges in human peripheral lymphocytes and X-ray sensitive cells.[10] It was also shown that hemolysis induced by gaseous arsine in mice mimics induction by oxidative damage.[11] These results clearly suggest that some of the damaging effects of arsenic may be mediated by oxygen radicals.

Generation of reactive oxygen species (ROS) is a common phenomenon in all aerobic organisms. Overproduction or accumulation of ROS in cells (i.e., oxidative stress) can damage DNA, proteins, lipids, and other biomolecules.[12] DNA damage induced by ROS has been hypothesized to play a key role in initiation, promotion, and progression of malignancies.[13] Recent studies have indicated that metal-induced mutagenesis is closely associated with the generation of ROS.[14,15] In this study we have examined the expression of the *Cat*, *Sod*, and *Gst1* (glutathione *S*-transferase) genes. Previous studies have shown that glutathione levels increase in response to arsenic in various cell systems.[8,9,16,17] It was demonstrated that glutathione plays a major role in protecting cells from arsenic. Specifically it was shown[8] that exposure of animal cells to low levels of electrophilic compounds, such as trivalent arsenic, oxidizable diphenols, quinones, and Michael reaction acceptors,[8] result in the elevation of glutathione levels and induction of Phase II detoxification enzymes such as glutathione *S*-transferases (GSTs), NAD(P)H oxidoreductase, epoxide hydrolase, and UDP-glucoronosyltransferase. Detoxification of xenobiotics in plants proceeds in two phases, Phase I and Phase II. In Phase I, xenobiotics are detoxified through a series of redox reactions catalyzed by cytochrome P450 monooxygenases.[18] Phase II detoxification proceeds through the conjugation of xenobiotics with glutathione (GSH) catalyzed by the enzyme glutathione *S*-transferase (GST). GSTs are a family of enzymes that catalyze the conjugation of glutathione via the sulfhydryl group to a variety of electrophilic centers of hydrophobic compounds.[19] This reaction renders the compound more soluble to H_2O and facilitates its transport to vacuole or apoplast (the continuous network of intracellular spaces in plants).

We hypothesize that arsenic induces the Phase II detoxification enzymes. This occurs because the arsenic exposure rapidly depletes the pool of reduced glutathione, leading to a rise in the steady state concentrations of ROS. The latter is enforced by the intraconversion of arsenic molecules from one ionic form to the other, and by inhibition of the mitochondrial electron transport chain. This results in changes in the equilibrium of ROS and antioxidant enzymes that lead to induction of the antioxidant defense system including a rise in total glutathione levels.[16] To date, the maize superoxide dismutase/catalase gene-enzyme systems and the glutathione *S*-transferase enzymes have been well characterized. In maize, three catalase isozymes are encoded by three unlinked structural genes *Cat1*, *Cat2*, and *Cat3*.[20] The expression of each catalase gene is tissue and developmental stage dependent.[20] In maize, superoxide dismutase exists as nine distinct isozymes encoded by the unlinked nuclear genes *Sod1*, *Sod2*, *Sod3.1*, *Sod3.2*, *Sod3.3*, *Sod3.4*, *Sod4*, *Sod4A*, and *Sod5*. SOD-2, SOD-4, SOD4A and SOD-5 are cytosolic enzymes; SOD-1 is a chloroplast-associated enzyme, while SOD-3.1, -3.2, -3.3 and -3.4 are mitochondria-associated.[21] Glutathione *S*-transferases exist as four distinct enzymes, GST I, GST II, GST III, and GST IV that are members of the Type I GSTs. Type I GSTs appear to function as defense genes or cellular protectant genes, producing proteins in response to pathogen attack, wounding, senescence, and the resulting lipid peroxidation which accompanies these processes.[1] Thus, we chose to investigate the responses of *Cat*, *Sod*, and *Gst* to arsenic, in this well-characterized defense system in maize.

MATERIALS AND METHODS

Plant materials and treatment conditions

Zea mays L. inbred line W64A, maintained by our laboratory, was used in these studies. For immature embryos maize ears were harvested in the morning from greenhouse-grown plants and whole embryos were excised from kernels on the same day. Embryos were dissected from kernels at 28 days postpollination (dpp). For germinating embryos, seeds were surface sterilized with 1% sodium hypochlorite for 10 min, and rinsed with deionized water. The seeds were then soaked with deionized water for 24 h and placed in germination trays at 25°C for 4 days postimbibition (dpi). Germinating embryos were then excised and treated with the appropriate concentrations of arsenic. With the term arsenic we refer to both forms of arsenic, the trivalent form, arsenite, and the pentavalent form, arsenate. Excised embryos were placed on Murashige-Skoog (MS) basic medium supplemented with sodium arsenate or sodium arsenite at 0.01, 0.1, 1, and 10 mM. Plates were incubated at 25°C for 24 h. At the end of each treatment, scutella were isolated and half the samples were used for catalase and superoxide dismutase activity assays and gel electrophoresis. The remaining samples were frozen in liquid nitrogen and stored at −70°C for RNA analyses. Ten-day-old, greenhouse-grown seedlings were treated by hydroponic uptake with different concentrations of sodium arsenate or sodium arsenite for 24 h in the light and total RNA was isolated from leaves for RNA analysis. In all exper-

iments controls were included. All experiments were repeated at least twice and representative results are shown.

Chemicals

All reagents were purchased from Sigma (St. Louis, MO). Purity of sodium arsenite was 92.5% (highest purity available). Sodium arsenate and the other reagents were ACS reagents of the highest available grade.

Catalase enzyme assay, zymogram analysis, and protein determination

Five to ten scutella from each arsenic treatment were selected for uniformity in size. Scutella from each treatment were homogenized in a mortar and pestle in 25 mM glycylglycine buffer, pH 7.4. The crude supernatant was used directly for protein and enzyme assay or zymogram analysis. Total catalase activity (treatment) was determined.[22] Catalase activity is expressed as the change in absorbance per min (unit) per mg of protein. Protein concentration was determined.[23] Zymogram analysis was performed with equal protein samples and the Tris/citrate buffer system for catalase analyses.[24] Western blot analysis was performed with monospecific maize catalase polyclonal antibodies.[25]

Superoxide dismutase enzyme assay

Total superoxide dismutase activity in equal protein samples pooled from each arsenic treatment was determined using the xanthine oxidase-cytochrome *c* method[26] at pH 10.0. Enzyme activity (Units/mg protein) was proportional to (V/v-1)/mg protein, where V equals the change in absorbance (550 nm) per minute in the absence of SOD and v equals the change in absorbance per minute (Unit) in the presence of SOD. Addition of KCN, to a final concentration 1 mM to the assay conditions, was used to inhibit Cu/Zn SOD and assay for mitochondrial, MnSOD-3 activity[26] at pH 7.8. Gel electrophoresis was performed using a previously described method.[27]

Statistical analysis

Means ± SD were derived from three independent experiments (two assays in each experiment). Results were analyzed using one-way analysis of variance (ANOVA) and statistically significant differences between treatments were determined with the *F*-test. Multiple range analysis of means was performed with 95% LSD intervals.

RNA analyses

Total RNA was isolated from control and arsenic treated samples as described.[28] For Northern analysis, total RNA (20 μg) from each sample was separated in denaturing 1.6% agarose gel and transferred onto Nylon membranes. The blots were sequentially hybridized with ^{32}P-labeled gene-specific probes (gsp) for *Cat1*, *Cat2*, *Cat3*, *Sod3*, *Sod4*, and *Sod4A*[29–32] in modified Church buffer[33] containing 7% SDS, 0.5 M EDTA, 0.5 M NaH_{2PO_4}, and 1% BSA. The full length *Sod3* gsp detects all four *Sod3* transcripts (i.e., *Sod3.1, 3.2, 3.3, and 3.4*). After each analysis, probes were removed from the filters by repeated washes in boiling 0.1% SDS/0.1X SSC (0.15M NaCl, 0.0015 M sodium citrate, pH 7.0) and reprobed with a DNA fragment from clone pHA2 containing an *18S* ribosomal sequence.[34]

PCR amplification and cloning of the Gst1 *fragment used as probe*

The *Gst1* probe was prepared with PCR. The set of primers used in PCR were phi080 forward 5′-CACCCGATGCAACTTGCGTAGA-3′ and phi080 reverse 5′-TCGTCACGTTCCACGACATCAC-3′ amplifying a 155 bp fragment of the *Gst1* first exon in W64A.[35] Genomic DNA (1 μg) isolated from leaves of 10-day old, light-grown seedlings was used as a template. The reaction started with 3 min denaturation at 95°C followed by 35 cycles of 30 s denaturation at 95°C, 1 min annealing at 58°C, and 1 min extension at 75°C. The last extension step was for 5 min to ensure completion of the reaction. The PCR product was analyzed on 1.5% agarose gel, visualized by staining with ethidium bromide, excised from the gel using a razor blade, and the DNA was isolated using the QIAquick Gel Extraction Kit (Qiagen, CA) according to the instructions. It was then ligated to the PCR-ScriptTM Amp SK(+) Cloning Kit (Stratagene, CA) according to the instructions. Positive clones were identified with a direct clone characterization method from colonies by PCR.[36]

RESULTS

Effects of increasing arsenic concentrations on catalase gene expression in developing embryos

The effect of arsenic on catalase and *Gst1* expression in developing embryos was examined. Two forms of arsenic ions were used, sodium arsenite, a trivalent form, and sodium arsenate, a pentavalent form. The former is considered to be more toxic than the latter, and it was of interest to examine whether this property has any effect on the expression and activity pattern of the genes ex-

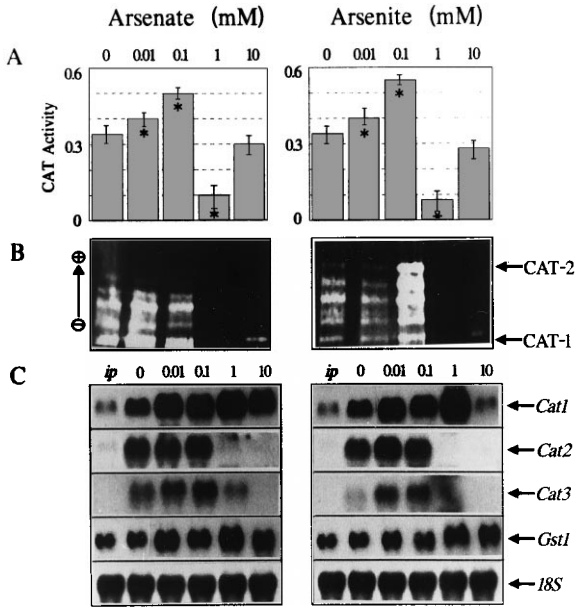

Fig. 1. Changes in catalase activity, isozyme protein, and transcripts of 28 dpp developing embryos in the presence of arsenate or arsenite. Embryos were isolated from 28 dpp kernels of greenhouse-grown W64A plants and incubated on MS medium supplemented with increasing concentrations of arsenate for 24 h in light. Scutella were isolated from treated embryos and equal amounts of protein were used. The in planta control is designated as ip. (A) Changes in total CAT activity in response to various concentrations of arsenate or arsenite. Total CAT activity is represented as changes in absorbance of 240 nm (Unit or U) per mg of protein after treatment. Values are the mean ± SD of three independent experiments. Asterisks indicate statistically significant differences between control and sodium arsenate ($F = 29.039$; $p < 0.001$) or sodium arsenite ($F = 48.814$, $p < 0.001$) treated embryos. (B) Zymogram pattern of 28 dpp scutella treated with arsenic. The two catalase homotetramers are indicated by arrows. The rest of the bands are CAT-1/CAT-2 heterotetramers. (C) Accumulation of *Cat* transcripts in scutella treated with arsenate or arsenite. Total RNA (20 μg) was separated by electrophoresis on denaturing 1.6% agarose gels and transferred onto nylon membranes. The same blot was sequentially hybridized with gene specific probe (gsp) of the maize *Cat1*, *Cat2*, *Cat3*, and *Gst1*. The 18S rRNA was used as a control to demonstrate equal RNA loading and transfer. Results are representative of at least three independent experiments.

amined. In 28 dpp scutella, total CAT activity increased at low doses of both arsenate and arsenite (0.01–0.1 mM) with the maximum of CAT activity observed at 0.1 mM and rebound at 10 mM (Fig. 1A). Zymogram analysis (Fig. 1B) indicated that with both treatments the observed increase of CAT activity at low concentrations was due to both CAT-1 and CAT-2 isozymes, while the increase of CAT activity at 10 mM was solely due to CAT-1. However, on comparing treatments with 0.1 mM of both forms of arsenic the contribution of CAT-2 in the observed increase of total CAT activity seems to be higher in the arsenite treatment.

The effects of arsenic on the accumulation of the three *Cat* and the *Gst1* transcripts in scutella of developing maize embryos were investigated. As is evident (Fig. 1C), all three maize *Cat* genes are induced when the embryo is excised from the scutellum and placed on an agar plate for 24 h. Comparing in planta control and the 24 h control we observed a high induction of *Cat1* and *Cat2*, a lower induction of *Cat3*, while *Gst1* transcript did not change. It is conceivable that the observed increase in *Cat* transcript levels is due to wounding and/or changes in endogenous hormone levels (Guan, L.; Scandalios, J. G., unpublished results). Differential responses of these genes were observed after treatment of the excised embryos with increasing concentrations of arsenic. *Cat1* transcript increased to high expression levels up to 1 mM of arsenic. This increase was followed by a sharp decrease at 10 mM arsenite while a lower decrease was observed at 10 mM arsenate. *Cat2* transcript remained high and/or increased slightly after treatment with arsenic up to 0.1 mM, and *Cat2* expression was totally inhibited at higher concentrations. The *Cat3* expression pattern was very similar to that of *Cat2* with an increase after treatment with up to 0.1 mM, and a drastic decrease at 1 mM and total inhibition at 10 mM arsenic. *Gst1* expression was higher than the control in all concentrations examined. The highest expression was observed at 1 mM arsenic (Fig. 1C).

Effects of arsenic on catalase gene expression in germinating embryos

The effects of arsenic on catalase and *Gst1* expression were also studied in mature germinating 5 dpi maize embryos. Total catalase activity increased with increasing arsenic concentrations, reaching a maximum at 10 mM arsenic (Fig. 2A). Zymogram analysis showed that the increase in total CAT activity is due to an increase in the activity of the CAT-2 isozyme after treatment with both forms of arsenic (Fig. 2B). However, western blot analyses using the CAT-2 antibody indicated that accumulation of CAT-2 protein increased only as the concentrations of arsenate increased from 1–10 mM (Fig. 2C). In arsenite-treated embryos CAT-2 protein appeared to increase at 0.01 to 0.1 mM concentration of arsenite, while it decreased to control levels at high doses of 1 mM and 10 mM arsenite (Fig. 2C).

Transcription of the three maize *Cat* and the *Gst1* genes was also examined. Upon excision of the germinating embryo and placement on an agar plate for 24 h, a slight induction of *Cat1*, *Cat3*, and *Gst1*, and a slight repression of *Cat2*, were observed (Fig. 2D). *Cat1* transcript increased in arsenate-treated embryos as the doses of arsenate increased from 0.01 mM to 1 mM, while it dropped to control levels at 10 mM arsenate. In arsenite-treated embryos *Cat1* transcript gradually increased with increasing doses of arsenite up to 0.1 mM, while it decreased at 1 mM and totally repressed at 10 mM (Fig.

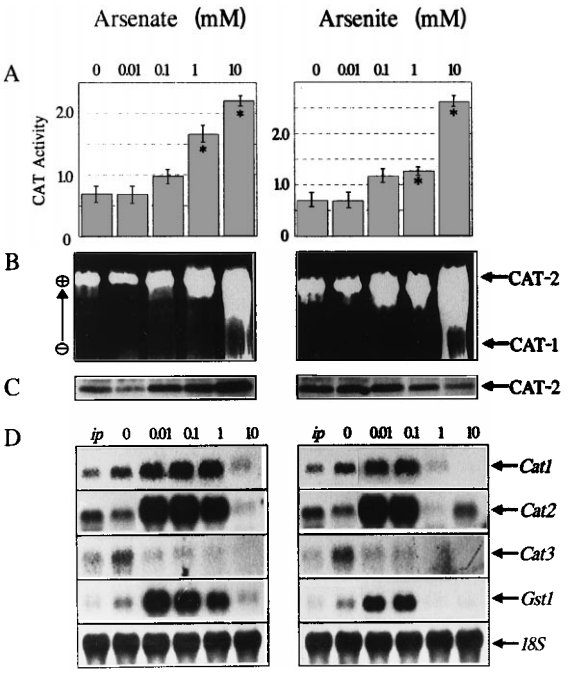

Fig. 2. Postgermination changes in catalase activity, isozymes, and transcripts in the presence of arsenate or arsenite. Embryos were excised from 5 dpi germinating W64A seeds and treated with increasing concentrations of sodium arsenate or sodium arsenite. Scutella were isolated from treated embryos and equal amounts of protein for each dose treatment were used for catalase activity assays, zymograms and Western blot analysis, using CAT-2 antibody. Changes in catalase activity (A). Values are the mean ± SD of three independent experiments. Asterisks indicate statistically significant differences between control and sodium arsenate ($F = 19.976$, $p < 0.001$) or sodium arsenite ($F = 105.681$, $p < 0.001$) treated embryos. Zymogram patterns (B), protein (C), and transcripts (D) in the presence of sodium arsenate or sodium arsenite. Total RNA (20 μg) was used for Northern blot and probed with each of the three *Cat* and *Gst1* gsps. The 18S rRNA was used as a loading control.

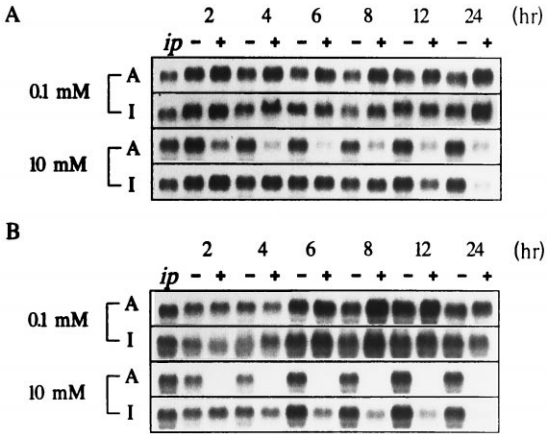

Fig. 3. Kinetics of changes in catalase transcripts in response to arsenate (A) or arsenite (I). Embryos were dissected from 5 dpi germinating seeds of W64A. (A) Excised embryos were incubated on MS medium in light for 2, 4, 6, 8, 12, and 24 h on MS medium supplemented with (+) and without (−) 0.1 mM arsenate (A) or arsenite (I). (B) Excised embryos were incubated on MS medium in light for 2, 4, 6, 8, 12, and 24 h with (+) and without (−) 10 mM arsenate (A) or arsenite (I). Embryos were collected and total RNA was isolated from each treated sample. Total RNA (15 μg) from each (+) and (−) treated time point was used for Northern blot analysis with *Cat1* (Panel A) and *Cat2* probes (Panel B). Results are representative of two independent experiments.

2D). *Cat2* gene expression was highly induced by arsenic at 0.01 and 0.1 mM (Fig. 2D). However, at 1 mM it was slightly decreased by arsenate while it was totally repressed by arsenite. At 10 mM a dramatic decrease was observed with arsenate, while with arsenite the *Cat2* transcript rebounds to a level comparable to that observed in planta. *Cat3* transcription was repressed to the in planta level by arsenic up to 1 mM, while it was totally inhibited at 10 mM. A high induction of the *Gst1* gene was observed after treatment with 0.01 mM arsenic followed by a gradual decrease in arsenate treatments, reaching the control levels at 10 mM, while with arsenite it remained unchanged at 0.1 mM and disappeared thereafter (Fig. 2D).

To further understand the accumulation pattern of *Cat1* and *Cat2* genes in response to low and high concentrations of arsenic, we conducted time course experiments using 0.1 and 10 mM of arsenate or arsenite. *Cat1* transcript increased in response to 0.1 mM arsenate or arsenite within 4 h, reaching highest levels by 24 h (Fig. 3A). In contrast, the *Cat2* transcript increased in response to 0.1 mM arsenate or arsenite starting at 6 h and reached highest levels by 12 h (Fig. 3B). Time course experiments with 10 mM arsenate showed that accumulation of *Cat1* transcript appears to be inhibited in response to this concentration of arsenate (Fig. 3A). Kinetics studies using 10 mM arsenite showed that accumulation of *Cat1* transcript initially increased at 2 h, and then at 8 h started to decrease gradually, reaching the lowest level at 24 h (Fig. 3A). A similar pattern was observed with the *Cat2* transcripts at 10 mM arsenate or arsenite (Fig. 3B).

Accumulation of Cat *transcripts in response to arsenic in young leaves*

Ten-day-old light-grown W64A seedlings were treated hydroponically with increasing concentrations of arsenic (see Materials and Methods). After treatment, leaves were collected and total RNA was isolated for Northern blot analysis. We observed that the arsenic-treated seedlings looked normal at low concentrations of 0.01–0.1 mM; however, as the concentrations increased from 1-10 mM, treated leaves showed signs of dehydration and wilting. Normal leaves showed a dramatic increase in *Cat1* transcript, reaching highest levels at 1 mM arsenate or arsenite (Fig. 4). At 10 mM arsenate or arsenite *Cat1*

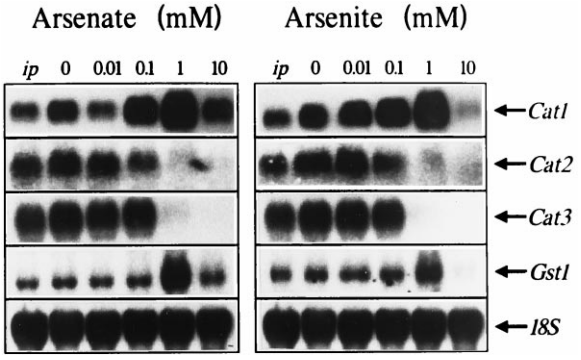

Fig. 4. Responses of catalase and glutathione-*S*-transferase genes to arsenate or arsenite in young seedlings. Ten-day-old light grown W64A seedlings were treated hydroponically with different concentrations of sodium arsenate or sodium arsenite. Leaves were collected and total RNA (20 μg) was separated on 1.6% denatured agarose gels and transferred onto nylon membranes. Blots were probed with maize *Cat* and Gst gsps. The 18S rRNA was used as a loading and transfer control. Results are representative of two independent experiments.

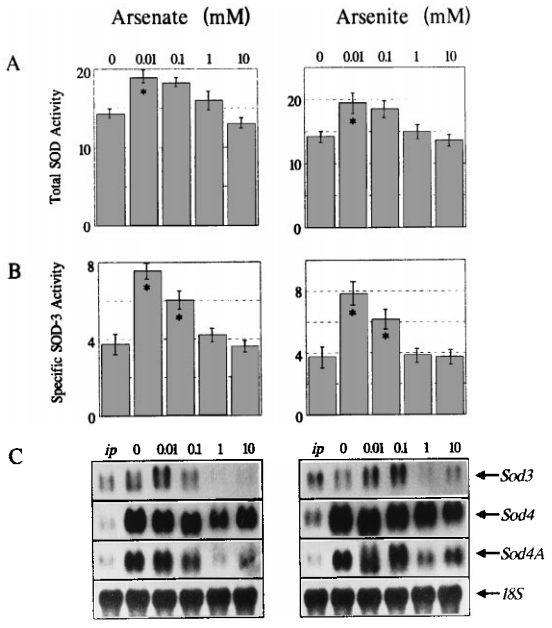

Fig. 5. Changes in SOD activity and transcripts in response to arsenate or arsenite in 28 dpp developing embryos. Embryos were isolated from 28 dpp kernels and treated with increasing concentrations of sodium arsenate, or sodium arsenite. (A) Changes in total SOD activity in response to arsenic. Values are the mean ± SD of three independent experiments. Asterisks indicate statistically significant differences between control and sodium arsenate ($F = 9.942$, $p = 0.0016$) or sodium arsenite ($F = 2.866$, $p = 0.0806$) treated embryos. SOD activity (Units/mg protein) was proportional to (V/v − 1)/mg protein, where V equals the change in absorbance (550 nm) per min in the absence of SOD and v equals the change in absorbance in the presence of SOD. (B) Changes in specific SOD-3 activity in response to arsenic. Values are the mean ± SD of three independent experiments. Asterisks indicate statistically significant differences between control and sodium arsenate ($F = 45.746$, $p < 0.001$) or sodium arsenite ($F = 42.287$, $p < 0.001$) treated embryos. (C) Total RNA (20 μg) was used for Northern blot and probed with each of the three *Sod* gsps. The 18S rRNA was used as a loading control. Results are representative of two independent experiments.

transcript decreased dramatically. The *Cat2* mRNA was not significantly affected by the presence of arsenic at 0.01–0.1 mM; however, *Cat2* mRNA decreased significantly at arsenic concentrations of 1 and 10 mM (Fig. 4). The *Cat3* transcript appeared to accumulate at control levels at low concentrations of 0.01–0.1 mM arsenate or arsenite, while it was undetectable at high concentrations of 1 and 10 mM arsenic (Fig. 4). Accumulation of *Gst1* transcript was at the control level at low concentrations of arsenic, and increased dramatically at 1 mM arsenic. *Gst1* transcript levels remained at the control level at 10 mM arsenate and decreased to nearly undetectable level with arsenite (Fig. 4).

Effects of arsenic on SOD gene expression in developing embryos

The effects of arsenate and arsenite on superoxide dismutase were investigated in developing embryos. Immature embryos (28 dpp) were isolated from W64A kernels and incubated on MS medium containing 0.01, 0.1, 1, and 10 mM arsenate or arsenite. After treatment, total protein was analyzed for changes in total superoxide dismutase (SOD) activity, and specific SOD-3 activity. In 28 dpp scutella, total SOD increased at low concentrations of arsenic, with a maximum of SOD activity observed at 0.01 mM (Fig. 5A). As the dose of arsenic increased, induction of total SOD activity gradually decreased to below control levels at 10 mM (Fig. 5A). A similar pattern of changes is observed for the specific SOD-3 activity in response to arsenate or arsenite (Fig. 5B).

The effects of arsenic on the accumulation of various *Sod* transcripts in scutella of developing maize embryos were also investigated. *Sod3* transcript levels appear to be upregulated in response to arsenic. *Sod3* transcripts increased from 0 to 0.01 mM arsenate and from 0 to 0.1 mM arsenite (Fig. 5C). At 1 mM concentration of arsenate, *Sod3* transcript levels decreased, while at 10 mM arsenate they were undetectable. On the other hand, at 1 mM arsenite concentration *Sod3* transcript levels were barely detectable, while at 10 mM concentration they were very low (Fig. 5C).

A high induction of *Sod4/4A* expression was observed in the excised embryos. Accumulation of *Sod4* transcript in response to arsenate appeared to be at control levels as the dose of arsenate increased to 0.01 and 0.1 mM, while it decreased slightly as the concentrations further increased (Fig. 5C). On the other hand, accumulation of *Sod4* transcript in response to arsenite appeared to accumulate at control levels as the concentrations of arsenite increased from 0.01 to 1 mM, while a slight decrease was

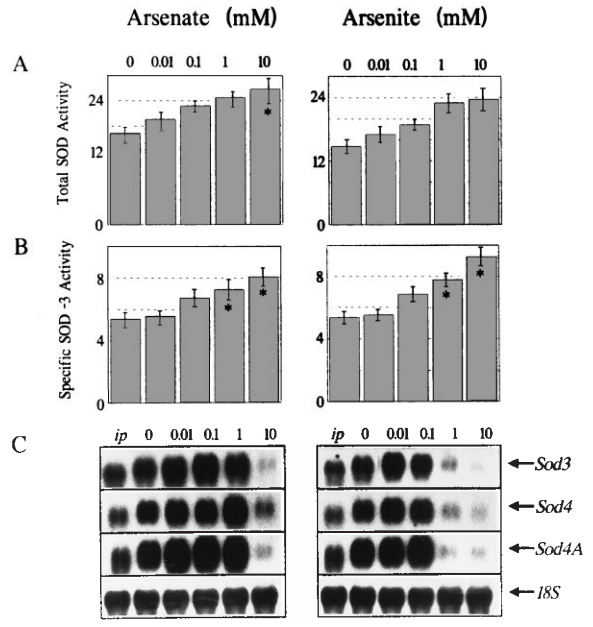

Fig. 6. Postgermination changes in SOD activity and transcripts in the presence of arsenate or arsenite. Embryos were excised from 5 dpi germinating W64A seeds and treated with increasing doses of sodium arsenate or sodium arsenite. (A) Changes in SOD activity. Values are the mean ± SD of three independent experiments. Asterisks indicate statistically significant differences between control and sodium arsenate ($F = 2.401$, $p = 0.1191$) or sodium arsenite ($F = 1.949$, $p = 0.1787$) treated embryos. (B) changes in specific SOD-3 activity. Values are the mean ± SD of three independent experiments. Asterisks indicate statistically significant differences between control and sodium arsenate ($F = 7.472$, $p = 0.0047$) or sodium arsenite ($F = 21.624$, $p < 0.001$) treated embryos. (C) transcripts in the presence of arsenate or arsenite. Total RNA (20 μg) was separated by electrophoresis on denaturing 1.6% agarose gels and transferred onto nylon membranes. The same blot was sequentially hybridized with each of the three maize *Sod* gsps. The 18S rRNA was used as a loading control.

observed at 10 mM arsenite (Fig. 5C). Accumulation of *Sod4A* transcript appeared to be at control levels at 0.01 mM arsenic while it decreased at 0.1 mM arsenate and increased at the same concentration of arsenite. However, with 1 mM of either arsenic forms *Sod4A* transcript decreased, while at 10 mM it increased in comparison to 1 mM, but was lower than the control (Fig. 5C).

Accumulation of SOD transcripts and isozyme activity in germinating embryos

The effects of arsenic on SOD expression were also studied in mature 5dpi germinating maize embryos. Total SOD activity increased with increasing doses of arsenic, with the maximum SOD activity observed at 10 mM arsenic (Fig. 6A). SOD-3 specific activity also increased with increasing concentrations of arsenate or arsenite (Fig. 6B). A very similar pattern of *Sod* gene responses to arsenic was observed with *Sod3*, *Sod4*, and *Sod4A*. Transcript levels increased as the dose of arsenate increased up to 1 mM, and arsenite up to 0.1 mM, while they decreased at higher concentrations of arsenic (Fig. 6C).

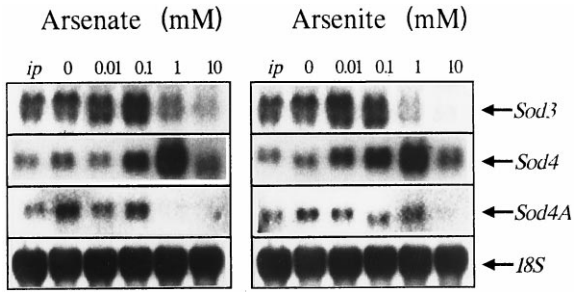

Fig. 7. Responses of SOD genes to arsenic in young seedlings. Ten-day-old light-grown W64A seedlings were treated hydroponically with different concentrations of sodium arsenate or sodium arsenite. Leaves were collected and total RNA (20 μg) was separated on 1.6% denatured agarose gels and transferred onto nylon membranes. Blots were probed with maize *Sod* gsps. The 18S rRNA was used as a loading and transfer control. Results are representative of two independent experiments.

Accumulation of Sod *transcripts in response to arsenic in young leaves*

To further understand the mechanisms of *Sod* gene responses to arsenic, we examined the effect of arsenate and arsenite on *Sod* expression in young leaves. Ten-day-old light-grown W64A seedlings were harvested and treated with arsenate or arsenite as described above. Northern blot analysis indicated that the *Sod3* transcripts increased in response to low doses of 0.01–0.1 mM arsenic and they decreased as the dose further increased (Fig. 7). *Sod4* transcript levels gradually increased at low concentrations of 0.01 and 0.1 mM arsenic, followed by an increase at 1 mM arsenic, and then decreased to control levels at 10 mM arsenic (Fig. 7). Slight variations from the control levels were observed in *Sod4A* responses to arsenate up to 0.1 mM and arsenite up to 1 mM, while no transcript could be observed at higher concentrations (Fig. 7).

DISCUSSION

Expression of Cat *genes in response to arsenic*

In this study we have demonstrated that total catalase activity increased in response to arsenic. Plants are particularly sensitive to arsenates in their avid quest for acquiring phosphate.[37] Growth of arsenate- or arsenite-treated maize embryos did not noticeably affect viability or germination. We have demonstrated that the increase in total catalase activity in developing embryos treated with arsenic was due to CAT-1 and CAT-2 at low concentrations (Fig. 1B). It is interesting to observe that

the increase in total CAT activity at 0.1 mM arsenite treatment was due primarily to CAT-2 and secondarily to CAT-1 (Fig. 1B). At this developmental stage both CAT-1 and CAT-2 isozymes are detected[20]; however, it is evident that the two ionic forms of arsenic have a distinct effect on induction of activity of specific CAT isozymes. The increase in CAT-1 and CAT-2 activities was paralleled with an increase of *Cat1* and *Cat2* mRNA levels (Fig. 1C). At this developmental stage *Cat3* mRNA or CAT-3 activity are not normally expressed[20]; however, arsenic induced accumulation of *Cat3* mRNA at low concentrations.

In germinating embryos total catalase activity is increased within a wide range of arsenic concentrations (from 0.01 to 10 mM). The observed increase in CAT activity is due to specific increase of CAT-2 activity (Fig. 2B). However, this increase in enzyme activity is accompanied with an increase of CAT-2 protein only in the arsenate treatments. Conversely, in treatments with arsenite the increase in enzyme activity is concurrent with decrease of the amount of CAT-2 (Fig. 2C). The apparent antithesis is probably due to differential posttranscriptional and/or posttranslational mechanisms affecting CAT-2 in arsenic-treated plants. The nature of these mechanisms is obscure. Treatment of germinating embryos of the CAT-2 null line (WA8B) with arsenic, showed that neither CAT-1 or CAT-3 isozymes compensated for the absence of CAT-2, suggesting the involvement of molecular mechanisms specific to the induction of the CAT-2 isozyme at this particular developmental stage (data not shown). Time-course experiments showed that at 10 mM arsenate, accumulation of *Cat1* and/or *Cat2* mRNA is inhibited after 2 h of treatment, while in arsenite treatment accumulation of *Cat1* and/or *Cat2* mRNA is decreased as a factor of time (Fig. 3B). Based on this observation, it is clear that at 10 mM concentration arsenate has a more severe effect on the accumulation of *Cat1* and *Cat2* transcript than arsenite. However, it is not clear whether the observed differences in mRNA levels are due to changes in mRNA turnover rate or to inhibition of gene transcription. In leaves, as with developing and germinating embryos, *Cat1* transcript levels increased in response to arsenate or arsenite. *Cat2* and *Cat3* mRNA levels were at steady-state levels at low concentrations of arsenic, while at high concentrations they were suppressed.

Overall, the data presented in this study suggest that the *Cat* genes in maize are regulated in a multilayered fashion in response to arsenic. Treatment with arsenic induces expression of the *Cat1* gene irrespective of the developmental stage of the tissue or tissue type. This suggests that the *Cat1* gene may represent a more direct response to stress induced by metal toxicity, than do *Cat2* and *Cat3*. It was reported that induction of Phase II detoxification enzymes is mediated by activation of an upstream electrophilic responsive element/antioxidant-responsive element (EpRE/ARE).[8] Studies in our laboratory[20] have shown the presence of an 11-bp element located at −470 in the promoter region of the *Cat1* gene. This element was identified to be homologous to the ARE element (5′-puGTGACNNNGC-3′) of the rat glutathione-*S*-transferase Ya subunit and the rat NAD(P)H quinone reductase gene.[38,39] The ARE of the rat glutathione *S*-transferase Ya subunit is highly activated by diverse inducers, including sodium arsenite and phenylarsine oxide.[8] It was concluded that activation of the EpRE/ARE by electrophile and antioxidant inducers is mediated by EpRE/ARE specific proteins. To date such protein complexes have not been identified. ARE elements have also been identified in the promoter region of the *Cat2* and *Cat3* genes.[20] In addition to the ARE motif, an MRE (metal responsive element) was identified at −480 in the *Cat2* promoter region. MRE motifs can be found in the promoter region of metalothionine proteins that bind heavy metal ions and has been functionally implicated in heavy metal detoxification.[40] Thus, the catalase gene enzyme system of maize provides us with an excellent opportunity to identify the EpRE/ARE specific proteins as well as other protein-complexes implicated in the regulation of these important defense genes (*Cat1*, *Cat2*, and *Cat3*) and their relationship with metal-mediated oxidative stress. Deletion analysis and gel-retardation studies on *Cat* gene promoter fragments are currently underway, and should enable us to identify *cis*- and *trans*-acting elements involved in metal-mediated stress.

Expression of Gst1 *in response to arsenic*

Previous studies[8,17] have shown that detoxification (Phase II) enzymes such as GSTs and NAD(P)H:(quinone acceptor)oxidoreductase are induced in animal cell systems in response to a variety of electrophilic compounds, including arsenic. Plants, like animals, possess a two-phase detoxification process that enables them to detoxify xenobiotics. In this study we have demonstrated that arsenic induces expression of *Gst1* in all tissues examined, and that its expression pattern appears to be identical to that of *Cat1*. This observation indicates a correlation in the function of *Gst1* with that of *Cat* genes. It is possible that both genes respond to the same regulatory mechanisms. The most likely possibility is that during detoxification of arsenic, expression of *Gst1* is induced to catalyze the conjugation of arsenic to glutathione (GSH). Previous reports[10,17] have shown that increased levels of glutathione correlated with arsenic resistance in animal systems. In addition, it is known that arsenic ions interact highly with sulfhydryl groups of

amino acids; therefore, it is likely that the conjugation of arsenic to GSH is promoted to prevent its interaction with other proteins or enzymes. Depletion of GSTI could lead to oxidative stress, resulting in the induction of antioxidant enzymes such as catalase.

Differential responses of cytosolic and mitochondrial SODs to arsenic

An equally important outcome of this study is the demonstration of changes in SOD activity and gene expression in response to arsenic. Total SOD activity and specific SOD-3 activity increased in response to low concentrations of arsenic in developing embryos. Previous studies have shown that arsenic uncouples the oxidative phosphorylation pathway in mitochondria by inhibiting the F_B factor of the H^+-ATPase[1], thus promoting generation of superoxide radicals. It has also been shown that treatment with arsenite can produce extensive oxidation of intramitochondrial NAD(P)H transhydrogenase.[41] NAD(P)H shortages may result in accumulation of oxidized glutathione and ROS.[41] Furthermore, it is known that arsenate is reduced rapidly to arsenite via cytochrome and cytochrome oxidase, using oxygen as a final electron acceptor,[37] a reaction that is catalyzed rapidly in plants such as corn, peas, melons, and tomatoes. During this reduction generation of superoxide radicals is possible through reduction of oxygen. Several reports (ref. 42 and references therein) indicate that superoxide radicals can be generated during the reaction of cytochrome oxidase with oxygen. Thus the observed increase in mitochondrial SOD-3 activity could be justified by the need for the removal of increased levels of superoxide radicals. Under such conditions, the observed increase in mitochondrial SOD activity is coupled with an increase in *Sod3* mRNA levels. Cytosolic *Sod4* and *Sod4A* mRNA are at steady-state levels while an increase in total SOD activity is evident, which could be largely attributed to the increase in specific SOD-3 activity.

In germinating embryos total SOD activity and specific SOD-3 activity increased gradually in response to arsenic. At this developmental stage, *Sod3*, *Sod4*, and *Sod4A* mRNA levels are upregulated in response to a wide range of arsenate concentrations (from 0.01 to 1 mM). A similar increase in *Sod* transcript levels is observed in arsenite treatment. However, at 1 and 10 mM concentrations of arsenite, transcripts are barely detectable. It appears that high concentrations of arsenite have an inhibitory effect on the accumulation of *Cat*, and *Sod* mRNAs, while this is observed only with 10 mM concentration of arsenate. It is known that the toxic effect of arsenic on various cellular processes is accomplished via its conversion to arsenite. Therefore, it is possible that higher concentrations of arsenate are required to establish a toxic intracellular level. The decreased mRNA levels of *Sod3*, *Sod4*, and *Sod4A* at 10 mM arsenate, 1 mM, and 10 mM arsenite do not mimic the increase of total SOD or SOD-3 activity. Likely, there is a posttranscriptional event that regulates the translational output, or possibly the turnover rate of the enzyme.

Expression of *Sod*s was also examined in leaves of light-grown seedlings. Induction of *Sod3* appears to be consistent in all tissues examined. Meanwhile in leaves, cytosolic *Sod*s respond differentially to arsenic, which appears to be tissue specific. Previous studies[21] showed that although *Sod4* and *Sod4A* share a high degree of homology in the coding region, they are different at the promoter regions. Accumulation of *Sod4* mRNA in response to arsenic in leaves followed a similar pattern to that of *Cat1* and *Gst1*. It is conceivable that induction of *Sod4* correlates with an increase in intracellular superoxide levels, a result of detoxification process.

Further experiments are designed to characterize the underlying mechanisms regulating induction of antioxidant genes in response to arsenic in maize.

Acknowledgements—This study was supported, in part, by research grants to J. G. S. from the U.S. Environmental Protection Agency (R-819360), and the N.R.I. competitive grants program, U.S.D.A. (37-100-0690). We thank Stephanie Ruzsa and Sheri Kernodle for expert technical assistance.

REFERENCES

1. Joshi, S.; Hughes, J. B. Inhibition of coupling factor B activity by cadmium ion, arsenite-2,3-dimercaptopropanol, and phenylarsine oxide, and preferential reactivation by dithiols. *J. Biol. Chem.* **256:**11112–11116; 1981.
2. Beeler, T. Oxidation of sulfhydryl groups and inhibition of the (Ca^{2+} + Mg^{2+})-ATPase by arsenazo III. *Biochim. Biophys. Acta* **1027:**264–267; 1990.
3. Landry, J.; Lambert, H.; Zhou, M.; Lavoie, J. N.; Hickey, E.; Weber, L. A.; Anderson, C. W. Human HSP27 is phosphorylated at serines 78 and 82 by heat shock and mitogen-activated kinases that recognize the same amino acid motif as S6 kinase II. *J. Biol. Chem.* **267:**794–803; 1992.
4. Guy, G. R.; Cairns, J.; Ng, S. B.; Tan, Y. H. Inactivation of a redox-sensitive protein phosphatase during the early events of tumor necrosis factor/interleukin-1 signal transduction. *J. Biol. Chem.* **268:**2141–2148; 1993.
5. Madhusudana, R. I.; Anderson, L. E. Light and stomatal metabolism. *Plant Physiol.* **71:**456–459; 1983.
6. Tsutsumi, M. Comparative toxicity of arsenite and arsenate to rice seedling under various levels of phosphate supply. *Soil Sci. Plant Nutr.* **29:**63–69; 1983.
7. Bencko, V. *Arsenic. Adv. Mod. Environ. Toxicol.* **11:**1–30; 1987.
8. Prestera, T.; Talalay, P. Electrophile and antioxidant regulation of enzymes that detoxify carcinogens. *Proc. Natl. Acad. Sci. USA* **92:**8965–8969; 1995.
9. Lee, T. C.; Ho, I. C. Modulation of cellular antioxidant defense activities by sodium arsenite in human fibroblasts. *Arch. Toxicol.* **69:**498–504; 1995.
10. Guzzo, A.; Karatzios, C.; Diorio, C.; DuBow, M. S. Metallothionein-II and ferritin H mRNA levels are increased in arsenite-exposed HeLa cells. *Biochem. Biophys. Res. Commun.* **205:**590–595; 1994.

11. Blair, P. C.; Thompson, M. B.; Bechtold, M.; Wilson, R. E.; Moorman, M. P.; Fowler, B. A. Evidence for oxidative damage to red blood cells in mice induced by arsine gas. *Toxicology* **63:**25–34; 1990.
12. Cerutti, P. A. Prooxidant states and tumor promotion. *Science* **227:**375–381; 1985.
13. Ames, B. N.; Gold, L. S. Endogenous mutagens and the causes of aging and cancer. *Mutat. Res.* **250:**3–16; 1991.
14. Klein, C. B.; Frenkel, K.; Costa, M. The role of oxidative processes in metal carcinogenesis. *Chem. Res. Toxicol.* **4:**592–604; 1991.
15. Stohs, S. J.; Bagchi, D. Oxidative mechanisms in the toxicity of metal ions. *Free Radic. Biol. Med.* **18:**321–336; 1995.
16. Bannai, S.; Sato, H.; Ishii, T.; Taketani, S. Enhancement of glutathione levels in mouse peritoneal macrophages by sodium arsenite, cadmium chloride and glucose/glucose oxidase. *Biochim. Biophys. Acta* **1092:**175–179; 1991.
17. Zaman, K.; MacGill, R. S.; Johnson, J. E.; Ahman, S.; Pardini, R. S. An insect model for assessing oxidative stress related to arsenic toxicity. *Arch. Insect. Biochem. Physiol.* **29:**199–209; 1995.
18. Kreuz, K.; Tommasini, R.; Martinoia, E. Old enzymes for a new job: Herbicide detoxification in plants. *Plant Physiol.* **111:**349–353; 1996.
19. Marrs, K. A. The functions and regulation of glutathione S-transferases in plants. *Annu. Rev. Plant Physiol. Plant Mol. Biol.* **47:**127–158; 1996.
20. Scandalios, J. G.; Guan, L.; Polidoros, A. N. Catalases in plants: Gene structure, properties, regulation, and expression. In: Scandalios, J. G., ed. Oxidative stress and the molecular biology of antioxidant defenses. New York: Cold Spring Harbor Laboratory Press; 1997:343–406.
21. Scandalios, J. G. Molecular genetics of superoxide dismutase in plants. In: Scandalios, J. G., ed. Oxidative stress and the molecular biology of antioxidant defenses. New York: Cold Spring Harbor Laboratory Press; 1997:527–568.
22. Beers, P. F.; Sizer, I. W. A spectrophotometric assay measuring the breakdown of hydrogen peroxide by catalase. *J. Biol. Chem.* **195:** 133–138; 1952.
23. Lowry, O. H.; Rosebrough, N. J.; Farr, A. L.; Randall, R. J. Protein measurment with folin phenol reagent. *J. Biol. Chem.* **193:**265–275; 1951.
24. Scandalios, J. G. Genetic control of multiple molecular forms of catalase in maize. *Ann. NY Acad. Sci.* **151:**274–293; 1968.
25. Skadsen, R. W.; Scandalios, J. G. Translational control of photoinduced expression of the *Cat2* catalase gene during leaf development in maize. *Proc. Natl. Acad. Sci. USA* **84:**2785–2789; 1987.
26. Baum, J. A.; Scandalios, J. G. Isolation and characterization of the cytosolic and mitochondrial superoxide dismutases of maize. *Arch. Biochem. Biophys.* **206:**249–264; 1981.
27. Beauchamp, C.; Fridovich, I. Superoxide dismutase: Improved assays and an assay applicable to acrylamide gels. *Anal. Biochem.* **44:**276–287; 1971.
28. Thompson, W. F.; Everett, M.; Polans, N. O.; Jorgensen, R. A.; Palmer, J. D. Phytochrome control of RNA levels in developing pea and mung bean leaves [*Pisum sativum, Vigna radiata*]. *Planta* **158:**487–500; 1983.
29. Bethards, L. A.; Skadsen, R. W.; Scandalios, J. G. Isolation and characterization of a complementary DNA clone for the *Cat2* gene in maize and its homology with other catalases. *Proc. Natl. Acad. Sci. USA* **84:**6830–6834; 1987.
30. Cannon, R. E.; White, J. A.; Scandalios, J. G. Cloning of complementary DNA for maize superoxide dismutase 2 (SOD2). *Proc. Natl. Acad. Sci. USA* **84:**179–183; 1987.
31. Redinbaugh, M. G.; Wadsworth, G. J.; Scandalios, J. G. Characterization of catalase transcripts and their differential expression in maize. *Biochim. Biophys. Acta* **951:**104–116; 1988.
32. White, J. A.; Scandalios, J. G. Isolation and characterization of a complementary DNA for mitochondrial manganese superoxide dismutase (SOD-3) of maize and its relation to other manganese superoxide dismutases. *Biochim. Biophys. Acta* **951:**61–70; 1988.
33. Church, G. M.; Gilbert, W. Genomic sequencing. *Proc. Natl. Acad. Sci. USA* **81:**1991–1995; 1984.
34. Jorgensen, R. A.; Cuellar, R. E.; Thompson, W. F.; Kavanagh, T. A. Structure and variation in the ribosomal RNA gene of pea. Characterization of a cloned rDNA repeat and chromosomal rDNA variants. *Plant Mol. Biol.* **8:**3–12; 1987.
35. Senior, M. L.; Chin, E. C. L.; Lee, M.; Smith, J. S. C.; Stuber, C. W. Simple sequence repeat markers developed from maize sequences found in the GENBANK database: Map construction. *Crop Sci.* **36:**1676–1683; 1996.
36. Gussow, D.; Clackson, T. Direct clone characterization from plaques and colonies by the polymerase chain reaction. *Nucleic Acids Res.* **17:**4000; 1989.
37. Tamaki, S.; Frankenberger, W. T., Jr. Environmental biochemistry of arsenic. *Rev. Environ. Contam. Toxicol.* **124:**79–110; 1992.
38. Favreau, L. V.; Pickett, C. B. Transcriptional regulation of the rat NAD(P)H:quinone reductase gene. Identification of regulatory elements controlling basal level expression and inducible expression by planar aromatic compounds and phenolic antioxidants. *J. Biol. Chem.* **266:**4556–4561; 1991.
39. Rushmore, T. H.; Morton, M. R.; Pickett, C. B. The antioxidant responsive element. Activation by oxidative stress and identification of the DNA consensus sequence required for functional activity. *J. Biol. Chem.* **266:**11632–11639; 1991.
40. Westin, G.; Schaffner, W. A zinc-responsive factor interacts with a metal-regulated enhancer element (MRE) of the mouse metallothionein-I gene. *EMBO J.* **7:**3763–3770; 1988.
41. Lenartowicz, E. A complex effect of arsenite on the formation of alpha-ketoglutarate in rat liver mitochondria. *Arch. Biochem. Biophys.* **283:**388–396; 1990.
42. Naqui, A.; Chance, B.; Cadenas, E. Reactive oxygen intermediates in biochemistry. *Ann. Rev. Biochem.* **55:**137–166; 1986.

ABBREVIATIONS

CAT—catalase protein and isozymes
Cat—catalase genes and transcripts
SOD—superoxide dismutase protein and isozymes
Sod—superoxide dismutase genes and transcripts
GST—glutathione *S*-transferase
Gst1—glutathione *S*-transferase I gene and transcript
GSH—reduced glutathione
ROS—reactive oxygen species

PHYSIOLOGIA PLANTARUM 106: 112–120. 1999
Printed in Ireland—all rights reserved
Copyright © Physiologia Plantarum 1999
ISSN 0031-9317

Role of hydrogen peroxide and different classes of antioxidants in the regulation of catalase and glutathione S-transferase gene expression in maize (*Zea mays* L.)

Alexios N. Polidoros and John G. Scandalios*

Department of Genetics, North Carolina State University, Raleigh, NC 27695-7614, USA
**Corresponding author, e-mail: jgs@unity.ncsu.edu*

Received 3 February 1999

The role of hydrogen peroxide (H_2O_2) and various antioxidants in the regulation of expression of the three *Cat* and *Gst1* genes of maize (*Zea mays* L.) has been investigated. Low concentrations of H_2O_2 appeared to inhibit *Cat1*, *Cat3*, and *Gst1* gene expression, while higher doses strongly induced these genes. Time course experiments indicated that high concentrations of H_2O_2 induced *Cat1*, *Cat2*, and *Gst1* gene expression to higher levels, and in less time, than lower H_2O_2 concentrations. Induction of *Cat3* was superimposed on the circadian regulation of the gene. These results demonstrate a direct signaling action of H_2O_2 in the regulation of antioxidant gene responses in maize.

The effects of the antioxidant compounds N-acetylcysteine, pyrrolidine dithiocarbamate, hydroquinone, and the electrophile antioxidant responsive element (ARE)-inducer β-naphthoflavone were quite different and specific for each gene/compound/concentration combination examined. The response of each gene to each antioxidant compound tested was unique, suggesting that the ability of these compounds to affect expression of the maize *Cat* and *Gst1* genes may not be the result of a common (antioxidant) mode of action. A putative regulatory ARE motif involved in the regulation of antioxidant and oxidative stress gene responses in mammalian systems is present in the promoter of all three maize catalase genes and we tested its ability to interact with nuclear extracts prepared from 10 days post-imbibition senescing scutella. Protein-DNA interactions in the ARE motif and the U2 snRNA homologous regions of the *Cat1* promoter were observed, suggesting that ARE may play a role in the high induction of *Cat1* in a tissue which, due to senescence, is under oxidative stress.

Introduction

Aerobic organisms depend on oxygen (O_2) as the electron acceptor in controlled electron transfer reactions. However, during the stepwise one-electron reduction of O_2, cells continuously produce the stable O_2 intermediates superoxide radical ($O_2^{\bullet -}$), hydrogen peroxide (H_2O_2), and hydroxyl radical ($^{\bullet}OH$), commonly known as reactive oxygen species (ROS), and can cause damage to the cell (Scandalios 1993). To minimize the adverse effects of ROS, aerobic organisms evolved numerous antioxidant defenses, including catalases (CAT) and glutathione S-transferases (GST). Antioxidant defenses are activated in response to unbalanced increases of ROS that cause oxidative stress. The mechanisms by which cells sense H_2O_2 and $O_2^{\bullet -}$ are not very well understood, but a number of transcriptional factors that regulate the expression of antioxidant genes, or genes whose activities are modulated by oxidation and reduction, are known. In *Escherichia coli* and other prokaryotes the transcription factor OxyR activates a battery of genes inducible by H_2O_2, while the transcription factors SoxR/SoxS mediate responses to $O_2^{\bullet -}$. Similarly, in the yeast *Saccharomyces cerevisiae*, a lower eukaryote, there are two distinct adaptive stress responses, one towards H_2O_2 and one towards $O_2^{\bullet -}$ (Jamieson and Storz 1997).

In higher eukaryotes, oxidative stress responses are more complex and modulated by several different regulators. There is increasing evidence suggesting that eukaryotic re-

Abbreviations – AP-1: activator protein-1; ARE: antioxidant responsive element; β-NF: β-naphthoflavone; Cat/CAT: catalase gene/enzyme; Gst/GST: glutathione S-transferase gene/enzyme; HQ: hydroquinone; NAC: N-aceltylcysteine; NF-κB: nuclear factor-κB; PDTC: pyrrolidine dithiocarbamate; ROS: reactive oxygen species.

sponses to different kinds of stress, including starvation, heat shock, osmotic stress, and heavy metal intoxication, overlap oxidative stress responses. In mammalian systems, many studies point to the significance of two classes of transcription factors, nuclear factor κB (NF-κb) and activator protein-1 (AP-1), in the regulation of oxidative stress response (Angel and Karin 1991, Schreck et al. 1991, Meyer et al. 1993). However, AP-1 responds strongly to the antioxidants N-acetylcysteine (NAC) and pyrrolidine dithiocarbamate (PDTC), and only weakly to H_2O_2. This led to the suggestion that AP-1 is a secondary antioxidant-responsive factor (Meyer et al. 1993). Antioxidant-specific gene induction has also been reported for a number of enzymes involved in phase II xenobiotic metabolism, which is mediated by a regulatory motif common in the promoter region of these genes. This motif, named 'antioxidant responsive element' (ARE), 'electrophile responsive element' (EpRE), or GPE1, is present in the promoter of mammalian GST, NADPH-quinone oxidoreductase (NQOR), γ-glutamylcysteine synthetase, metalothioneine-I (MT-1), and manganese superoxide dismutase (MnSOD) genes (Kahl 1997). The signal transduction pathway leading to gene induction through the ARE has not yet been elucidated. The significance of the antioxidant properties of many of the inducers has been questioned, as compounds with no antioxidant activity are also potent inducers. In contrast, many of the inducers are Michael reaction acceptors (electrophilic), and their potency parallels their efficiency in Michael reactions (Talalay et al. 1988). ROS can also activate the ARE, as H_2O_2 itself is a capable inducer (Rushmore et al. 1991). An ARE motif has not yet been identified in any plant *Gst* gene (Marrs 1996). However, ARE-like motifs are present in the promoter region of the three maize *Cat* genes (Scandalios et al. 1997), but the effects of antioxidants on the expression of these plant genes are unknown.

In plants, ROS have been implicated in damaging effects of various environmental stress conditions including UV light and other forms of radiation, xenobiotics (herbicides), ozone, temperature extremes, especially in relation with high light, drought, and pathogen attack (Scandalios 1993). Many plant defense genes are activated in response to these conditions. H_2O_2 appears to be a signaling intermediate in plant defense, activating gene expression (Bi et al. 1995, Levine et al. 1994, Neuenschwander et al. 1995), hypersensitive cell death (Levine et al. 1994), and promoting programs leading to immunity (Wu et al. 1995). H_2O_2 scavengers like catalase can modulate H_2O_2 homeostasis and consequently its signaling capacity. However, information on the effects of H_2O_2 on the expression of catalase genes is limited. Similarly, there are a few reports on H_2O_2-induced *Gst* gene expression (Levine et al. 1994, Tenhaken et al. 1995). The maize *Cat* and *Gst* antioxidant defense genes provide an excellent system for investigation of antioxidant gene responses to antioxidants and oxidants. Catalases catalyze the dismutation of H_2O_2 into O_2 and H_2O, preventing the damaging effects of H_2O_2 accumulation and protecting cells from oxidative stress. Presence of ARE-like motifs in the maize *Cat* genes renders them suitable tools for characterization of their potential regulatory roles in plants (Scandalios et al. 1997). Glutathione S-transferases are a family of enzymes that catalyze the conjugation of glutathione via the sulfhydryl group to a variety of electrophilic centers of hydrophobic compounds. This reaction renders the compound more soluble to H_2O and facilitates its transport to vacuole or apoplast. Among the substrates of GSTs are many plant secondary metabolites like phenolic antioxidants and anthocyanins (Marrs et al. 1995), and many xenobiotics (Kreuz et al. 1996). Importantly, GSTs are also responsible for detoxification of the strongly electrophilic and highly cytotoxic lipid peroxidation products such as 4-hydroxyalkenals, which are generated when lipid membranes are damaged by oxidative stress (Marrs 1996).

In the present study, we examined the responses of the *Cat* and *Gst1* genes of maize to different classes of antioxidants and to H_2O_2-induced oxidative stress. We also examined potential involvement of promoter regions of *Cat1*, including a sequence harboring an ARE-like motif, in the regulation of *Cat1* expression in scutella at 10 days post-imbibition (dpi), when the tissue is under senescence-induced oxidative stress.

Materials and methods

Plant material

The maize inbred line W64A was used in this study. Seeds were surface sterilized by soaking in 1% hypochlorite for 10 min and then washed 5–6 times with deionized water. Seeds were then soaked in distilled water for 24 h and planted in soil mix. Germination occurred in controlled environment with 12 h/12 h D/L photoperiod and constant 25°C temperature.

Treatments

After 9 days dpi, seedlings were removed from the soil with the root, the root was rinsed in tap water and placed in open 50-ml tubes (four plants per tube) containing 20 ml of each compound's solution. The compounds NAC, PDTC, and hydroquinone (HQ) were applied to study antioxidant responses, β-naphthoflavone (β-NF) to study response to an electrophile ARE-inducer, and H_2O_2 to study responses under oxidative stress. Control plants were placed in tubes containing water or the appropriate concentration of the compound's solvent in water. The plants were then placed in the growth chamber for 24 h.

Northern analysis

Leaf material was harvested after a 24-h treatment with each compound. All samples were frozen in liquid nitrogen and stored at -80°C for analysis. Total RNA from leaf material was extracted (Thompson et al. 1983), separated on denaturing 1.2 or 1.6% agarose gels, and stained with ethidium bromide to ensure equal loading. It was then transferred onto nylon membranes and hybridized with ^{32}P-labeled *Cat* (Bethards et al. 1990, Redinbaugh et al. 1988) or *Gst1* gene-specific probes. The *Gst1* gene-specific

probe was prepared with polymerase chain reaction (PCR) using the phi080 set of primers (Senior et al. 1996). Hybridization buffers and conditions were as follows: the pre-hybridization solution contained 6 × SSPE, 5 × Denhardt's, 7% SDS, 200 μg ml^{-1} salmon sperm DNA, and 1% dextran sulfate. After 4 h pre-hybridization at 65°C, the pre-hybridization solution was substituted with hybridization solution that was the same as the pre-hybridization solution without 5 × Denhardt's, and probe was added. Hybridization proceeded at 65°C for 24–36 h, and washes were twice for 30 min with 0.1 × SSC/0.1% SDS at 65°C.

Isolation of nuclei and preparation of nuclear extracts

Nuclei were isolated from post-germination scutella (Hall and Spiker 1994). Scutella were ground to a fine powder with mortar and pestle using liquid nitrogen, and transferred to a beaker sitting on ice. All subsequent manipulations were carried out at 4°C. Nuclei isolation buffer 1 (NIB1: 0.5 *M* hexylene glycol, 0.5% Triton X-100, 20 m*M* HEPES pH 7.4, 20 m*M* Thiodiglycol, 1 m*M* PMSF, 0.5 m*M* EDTA pH 7.4, 2 μg ml^{-1} aprotinin, 50 m*M* spermine, 125 m*M* spermidine) was added in a volume of 10 ml g^{-1} of scutella. The slurry was homogenized with a Polytron homogenizer at low setting for 30 s. Nuclei were filtered away from cell debris through a tiered setup of 300, 200, 100, 50, and 30 μm nylon mesh screens. Aliquots of 25-ml filtrate were layered above a 30–50% Percoll/NIB1 gradient and centrifuged at 900 *g* for 20 min. The supernatant above the Percoll cushion was removed by aspiration. The nuclei were extracted from the 30–50% Percoll interface using a glass pipette and pelleted by centrifugation at 3000 *g* for 15 min. The pellet was resuspended and washed twice with 20 ml cold NIB2 (NIB2: as NIB1 without Triton X-100). The final pellet was resuspended in 1 ml nuclei suspension buffer (NSB: 50% glycerol, 50% 2 × NIB2) and stored at −80°C until use.

Nuclear protein preparation was essentially as described in Holdsworth and Laties (1989), with minor modifications. Nuclei were recovered from NSB with a brief centrifugation, and resuspended in nuclear protein isolation buffer (NPIB: 40 m*M* KCl, 20 m*M* HEPES pH 7.7, 0.5 m*M* EDTA pH 7.7, 5 m*M* $MgCl_2$, 2 m*M* dithiothreitol, 1m*M* PMSF, and 2 μg ml^{-1} aprotinin). Nuclei were lysed with the addition of 1/10 vol saturated ammonium sulfate pH 7.6 on ice for 30 min. Debris was removed by centrifugation at 15000 *g* for 15 min. Nuclear proteins were precipitated from the supernatant with the addition of solid powdered ammonium sulfate to a 65% saturation (337 mg ml^{-1} in the 10% saturated solution), and collected by centrifugation at 15000 *g* for 15 min. Pelleted nuclear proteins were resuspended in dialysis buffer (NPDB: 40 m*M* KCl, 20 m*M* HEPES pH 7.7, 0.5 m*M* EDTA pH 7.7, 2 m*M* dithiothreitol, 1 m*M* PMSF, 20% glycerol) containing 2 μg ml^{-1} aprotinin and dialyzed against two changes of 1000 ml dialysis buffer for 2 h, using Spectapore membrane tubing (Amicon, Beverly, MA, USA) with 3500 MW cutoff. The dialysate was aliquoted, frozen in liquid nitrogen, and stored at −80°C. Protein concentration was determined using the Bio-Rad protein assay kit and BSA as a standard.

Electrophoretic mobility shift assays

Probes for electrophoretic mobilibty shift assay probes (EMSAs) (Fig. 5) were prepared as follows: a 0.8 kb *Xba*I fragment from the *Cat1* promoter (Guan and Scandalios 1993) was digested with *Sau*3A, generating a 90 bp *Xba*I-*Sau*3A fragment containing the U2 snRNA homologous region, which was subcloned into an *Xba*I-*Bam*HI digested pBluescript vector, and a 158 bp *Sau*3A fragment containing the ARE motif, which was subcloned into the *Bam*HI site of the pBluescript. The two probes were labeled by fill-in 5′ overhangs with α-^{32}P-dCTP using Klenow polymerase. Binding reactions were performed using the Bandshift kit (Pharmacia, Piscataway, NJ) according to instructions. Briefly, the reaction mixture contained 10000–40000 cpm-labeled target DNA (0.1–1 ng DNA) in 10 m*M* Tris-HCl pH 7.5, 50 m*M* NaCl, 0.5 m*M* dithiothreitol, 10% glycerol, 0.05% NP-40, and 0.25 μg poly(dI-dC). Nuclear proteins in a range of 0.1–0.25 μg were added and the mixture incubated at room temperature for 20 min. DNA-protein complexes were separated from unbound DNA probe by electrophoresis on native 4% polyacrylamide gels in Tris-acetate-EDTA buffer (7 m*M* Tris-HCl pH 7.5, 3 m*M* sodium acetate, 1 m*M* EDTA). Gels were vacuum dried and autoradiographed at −70°C for 0.5–2 h.

Results

Responses of the maize *Cat* and *Gst1* genes to antioxidants, electrophilic compounds, and H_2O_2

Specific responses of the maize *Cat* and *Gst1* genes were observed upon treatment with antioxidants, electrophilic compounds, and H_2O_2. The responses were not uniform with the different compounds used. Thus, each gene-compound combination resulted in a different response.

Responses of Cat1

In young maize leaves, *Cat1* is normally expressed at a constant low level and is not affected by light (Scandalios et al. 1997). *Cat1* expression was decreased in response to low concentrations of NAC up to 5 m*M* (Fig. 1A), and increased at 10 m*M*. Treatment with PDTC did not affect *Cat1* expression, while treatment with HQ resulted in gradually increasing *Cat1* expression with increasing (1–10 m*M*) HQ concentrations (Fig. 1A). *Cat1* expression was not affected by ethanol, which was used as solvent for β-NF (Fig. 1B). β-NF resulted in a slight decrease at 0.25 m*M*, followed by an increase at 1 m*M*, and the expression was similar to the control at higher concentrations (Fig. 1B). Treatment with low (0.5 m*M*) concentration of H_2O_2 decreased transcript level. At 1 m*M* H_2O_2, *Cat1* expression was slightly lower than the control, while it was comparable with the control at higher concentrations (Fig. 1C). It is known that in other tissues like scutellum, *Cat1* is induced when the scutellum is excised from the kernel and incubated in control agar plates for 24 h (L. Guan and J. G. Scandalios, unpublished results). This induction was explained as a result of wounding and/or hormone imbalance. In this experiment, *Cat1* expression in leaves is significantly induced

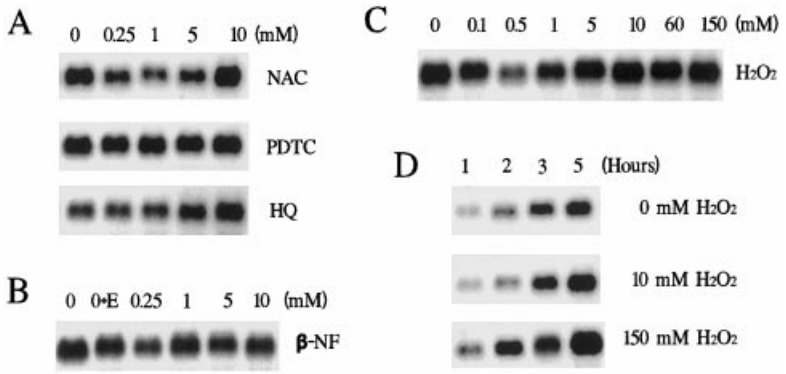

Fig. 1. Response of the maize *Cat1* gene to antioxidants, electrophiles, and H_2O_2. Seedlings (10 dpi) were treated hydroponically with increasing concentrations of the indicated compounds, and *Cat1* transcript in leaves was detected after hybridization with ^{32}P-labeled *Cat1* gene-specific probe. Equal loading of the gels was confirmed by ethidium bromide staining prior to transfer. A. Responses to 24-h treatments with the antioxidants NAC, PDTC, and HQ. B. Responses to 24-h treatments with the electrophile ARE-inducer β-NF. The 0 + E lane is control with the β-NF solvent ethanol. C. Responses to 24-h treatments with H_2O_2. D. Time course responses to 10 and 150 m*M* H_2O_2. Abbreviations are: NAC, N-acetylcysteine; PDTC, pyrrolidine dithiocarbamate; HQ, hydroquinone; β-NF, beta-naphthoflavone; E, ethanol; H_2O_2, hydrogen peroxide.

within 1 h after submersion of the roots in water, and gradually increases during the next 5 h (Fig. 1D). Induction continues for 24 h, as is evident comparing the 5-h control (0 m*M*) in Fig. 1D with the 24-h control (0 m*M*) in Fig. 1C. The observed induction is enhanced by H_2O_2. Addition of 10 m*M* H_2O_2 in the solution results in enhanced induction after 3–5 h. Addition of 150 m*M* H_2O_2 enhances *Cat1* induction after 1 h of treatment and results in higher induction after 5 h. However, enhancement of the induction by H_2O_2 is not observed after 24 h of treatment, indicating that elevated *Cat1* expression due to submersion of the roots in water is reaching a maximum that is not affected by addition of H_2O_2.

Responses of Cat2

Expression of *Cat2* in young maize leaves is constant at low levels (Scandalios et al. 1997). Thus, we investigated *Cat2* responses examining a sample of antioxidant and H_2O_2 treatments. There was no significant induction upon submersion of the roots in water as is evident by comparison of the 24-h control in Fig. 2A with the 0-h control in Fig. 2B. NAC caused a decrease of *Cat2* transcript at 0.25–2.5 m*M*, followed by an increase at 5 m*M* (Fig. 2A). A similar response was observed for HQ, but the decrease was at 0.1–0.25 m*M* and the level of *Cat2* transcript was similar to the control at 0.5–1 m*M*. A high induction was evident at 2.5–5 m*M* HQ (Fig. 2A). *Cat2* was induced by H_2O_2 (60–150 m*M*) within 1 h after submersion of the roots in H_2O_2 solution, and was even stronger 24 h later (Fig. 2B). It was also evident that 150 m*M* H_2O_2 induced *Cat2* to higher expression levels than 60 m*M* H_2O_2 at both 1 and 24 h.

Responses of Cat3

Expression of *Cat3* in young maize leaves is regulated by a circadian rhythm (Scandalios et al. 1997). Thus, analyses regarding *Cat3* responses should be in the context of the circadian expression of the gene. In the present experiments a normal circadian *Cat3* expression was observed in seedlings with roots submerged in water for 24 h, as long as the light regime was maintained at 12 h/12 h L/D photoperiod. NAC increased the *Cat3* transcript in all the concentrations applied (Fig. 3A). PDTC caused a strong induction at 0.25 m*M* that declined at higher concentrations, and expression was inhibited at 10 m*M* (Fig. 3A). HQ caused a high induction between 0.25–5 m*M*, while at 10 m*M* induction was lower (Fig. 3A). With β-NF, a high induction was observed at 0.25–1 m*M* and complete inhibition at higher concentrations (Fig. 3B). Ethanol also inhibited *Cat3* gene expression (Fig. 3B). The effects of H_2O_2 on *Cat3* transcription were examined at two different time points: circadian time 10 (CT-10: 10 h after the onset of light), which represents the time point of the highest *Cat3* expression, and CT-4, which represents a time point with low and increasing *Cat3* transcription. Results were similar and those obtained at CT-4 are shown in Fig. 3C. Low doses (0.1–0.5 m*M*) of H_2O_2 caused a significant decrease on *Cat3* transcript levels. Transcription was similar with the control at 1 m*M* H_2O_2 and significantly increased at 5–60 m*M*. The transcript at 150 m*M* was lower than that of 60 m*M*, but still higher than that of the control.

Responses of Gst1

Expression of *Gst1* in maize is constitutive in young seedling roots, but can be enhanced by herbicide safeners (Jepson et

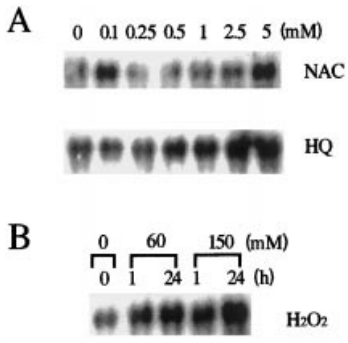

Fig. 2. Response of the maize *Cat2* gene to antioxidants and H_2O_2. Transcripts in leaves of 10 dpi seedlings treated hydroponicaly were detected after hybridization with ^{32}P-labeled *Cat2* gene-specific probe. Equal loading of the gels was confirmed by ethidium bromide staining prior to transfer. A. Responses to 24-h treatments with NAC and HQ. B. Responses to treatments with 60 and 150 m*M* H_2O_2 for 1 and 24 h. Abbreviations are as in Fig. 1.

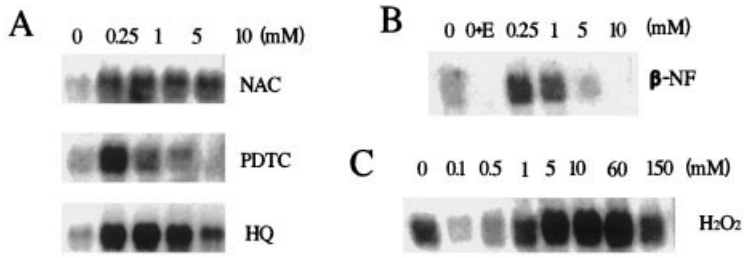

Fig. 3. Response of the maize *Cat3* gene to antioxidants, electrophiles, and H_2O_2. Seedlings (10 dpi) were treated hydroponically for 24 h with increasing concentrations of the indicated compounds, and *Cat3* transcript in leaves was detected after hybridization with ^{32}P-labeled *Cat3* gene-specific probe. Equal loading of the gels was confirmed by ethidium bromide staining prior to transfer. Treatment began 4 h after the onset (CT-4) of light and the plants were maintained at 12 h/12 h L/D photoperiod in order to examine the effects of the compounds in the context of the *Cat3* circadian rhythm. A. Responses to the antioxidants NAC, PDTC, and HQ. B. Responses to the electrophile ARE-inducer β-NF. The 0 + E lane is control with the β-NF solvent ethanol. C. Responses to H_2O_2. Abbreviations are as in Fig. 1.

al. 1994). *Gst1* responses (Fig. 4) were very similar with those of *Cat3* (Fig. 3). NAC increased the *Gst1* transcript, and the highest induction was observed at 10 m*M* (Fig. 4A). PDTC caused a strong *Gst1* induction at 0.25 m*M* that declined at higher concentrations (Fig. 4A). HQ caused a stronger induction at 0.25, 5, and 10 m*M*, while at 1 m*M* the response was weaker (Fig. 4A). β-NF caused a high induction between 0.25 and 1 m*M* and expression was at the levels of the control at 10 m*M* (Fig. 4B). Ethanol also repressed *Gst1* gene expression (Fig. 4B). With H_2O_2 treatments, the *Gst1* transcript decreased at low (0.1 m*M*) concentrations and was comparable with that of the control at 0.5–1 m*M* (Fig. 4C). Significantly higher transcription was evident at higher (5–150 m*M*) H_2O_2 concentrations (Fig. 4C). *Gst1* expression is not affected by submersion of the roots in water, as no difference in transcript was observed between the 24 h control in Fig. 4C and the controls at different time points in Fig. 4D. However, H_2O_2 treatments induced *Gst1* expression within 3–5 h at 10 m*M* and as early as 1 h at 150 m*M* (Fig. 4D).

Protein-DNA interactions in specific *Cat1* promoter regions

Interactions of nuclear proteins, isolated from 10-day-old germinating scutella, with promoter regions of *Cat1* have been examined by electrophoretic mobility shift assays. Results indicated that a 158-bp fragment containing the ARE core sequence as well as a 90-bp fragment highly homologous with the U2 snRNA gene of maize (Guan and Scandalios 1993), located 5′ and in continuous sequence with the 158-bp fragment (Fig. 5), were strongly interacting with nuclear proteins. A very strong interaction was observed for the ARE-harboring fragment as almost the total amount of the probe was shifted on the gel (Fig. 6). Specificity of the observed binding was further analyzed with the addition of 30 × cold probe in a binding reaction. Results (Fig. 6) suggest that the observed binding is highly specific, as with the addition of cold probe the shifted band disappears. A similar strong and specific interaction was observed with the U2 snRNA homologous fragment (Fig. 7). In both experiments, specificity was also examined with the addition of salmon sperm DNA as non-specific competitor in the binding reaction and the binding was maintained (data not shown).

Discussion

Regulatory role of antioxidants in the expression of antioxidant genes

The effects of antioxidants on *Cat* and *Gst1* gene expression were different and specific for each compound and concentration examined. Even compounds whose antioxidant activity is the result of similar chemical properties, like the –SH-containing compounds NAC and PDTC, affected the same genes in different ways. Thus, the responses do not seem to be due solely to the antioxidant properties of the compounds.

There are studies indicating that compounds that exhibit antioxidant activity in vitro can be metabolically transformed, or act as oxidants in vivo (Pinkus et al. 1996). The possibility exists that the observed responses might, in part, result from such conversions. Consistent with this hypothesis, NAC can produce thiyl and other sulfur-containing radicals (Aruoma et al. 1989), which can oxidize glutathione and weaken the antioxidant defenses of the cell. In our experiments, 10 m*M* NAC induced all the genes examined. This concentration is much lower than the 30 m*M* reported to be effective in inhibition of NF-κB in mammalian cell cultures (Meyer et al. 1993). However, 100 m*M* NAC in hydroponic treatments resulted in severe stress of the plants from which they could not recover, high induction of *Cat1*, and complete inhibition of *Cat3* (data not shown). These results suggest that a mechanism of NAC-induced stress could be responsible for the observed responses. PDTC, due to its metal-chelating properties, can inhibit Cu/Zn superoxide dismutase activity, potentiate oxygen toxicity in animal tissues, and cause a decrease in glutathione peroxidase activity and thiol levels (Goldstein et al. 1979). In the present study, PDTC was a very potent inducer of *Cat3* and *Gst1* at low concentrations (0.25 m*M*), while it exhibited inhibitory effects at higher concentrations. However, it did not affect *Cat1* expression. In this study, HQ, which can undergo reversible oxidation-reduction generating ROS, was a potent inducer of all genes examined. *Cat3* exhibited a strong induction at low concentrations, which was gradually decreased as the concentration increased. The other genes examined (*Cat1*, *Cat2*, and *Gst1*) exhibited weaker but persistent induction at the higher concentrations.

The data presented suggest that diverse antioxidants are potent inducers of antioxidant gene expression in maize.

This apparently paradoxical situation is not unique, as both antioxidants and H_2O_2 have been reported to serve as signals inducing oxidative stress responsive factors in animal cells (Bergelson et al. 1994, Meyer et al. 1993). However, the possibility exists that oxidative mechanisms are responsible for the apparent effects of antioxidants in *Cat* and *Gst1* gene expression in maize.

Regulatory role of H_2O_2 in the expression of antioxidant genes

Plants, like other living organisms, sense increased levels of ROS and react with antioxidant mechanisms, finely coordinated and expressed, to effectively protect the organism from oxidative stress. In the progress of these events, H_2O_2, a well-established second messenger in animal systems (Ramasarma 1982), appears to be a significant signaling intermediate in plants as well (Alvarez and Lamb 1997). In the present study, we investigated the role of H_2O_2 in the expression of the *Cat* and *Gst1* genes of maize. Catalases are among the primary H_2O_2 scavenger enzymes and could play a central role in the control of H_2O_2 homeostasis and consequently in the H_2O_2-dependent signaling pathway. This has been indirectly established in several experimental systems by addition of catalase, or the catalase inhibitor aminotriazole, demonstrating differential effects on H_2O_2-induced gene expression (Alvarez and Lamb 1997, Chen et al. 1993, Levine et al. 1994). However, the role of H_2O_2 in the regulation of *Cat* gene expression has not yet been thoroughly investigated. Thus, we examined the effects of exogenously applied H_2O_2 in the regulation of *Cat* and *Gst1* gene expression in maize. We used a wide range of H_2O_2 concentrations (100 μM–150 mM) in hydroponic treatments of whole plants, and examined the transcript level of each gene in leaves 24 h later. With this experimental scheme, the actual concentration of H_2O_2 was changing throughout the treatment period. Developing roots of young maize seedling are known to secrete catalase in the incubation medium as well as in the root apoplast (Salguero and Boettger 1995). As soon as the seedling roots were submerged in the H_2O_2 solution, bubbles appeared on the surface of the roots, indicating very active H_2O_2 decomposition. Depletion of H_2O_2 from the culture medium has also been reported in rat hepatocyte cultures with H_2O_2 half-life between 2.5 and 8 min, depending on the initial H_2O_2 concentration (1–2.5 mM) and the age of the culture (Rohrdanz and Kahl 1998). This rapid decomposition probably caused an early depletion of H_2O_2 at low concentrations, while it decreased the actual concentration of H_2O_2 at the higher concentrations applied.

Low doses of H_2O_2 appeared to reduce *Cat1*, *Cat3*, and *Gst1* steady-state mRNA levels, while higher doses enhanced the amount of the *Cat2*, *Cat3*, and *Gst1* mRNA. Induction of *Cat2* and *Gst1* increased as the concentration of H_2O_2 increased up to 150 mM (the highest concentration used), while the induction of *Cat3* reached a maximum at 60 mM and declined at 150 mM. Time course experiments indicated that a high concentration of H_2O_2 induced *Cat1*, *Cat2*, and *Gst1* gene expression at higher levels and in less time than a lower concentration. *Cat1* expression was affected by the control treatment as it was induced by submersion of the roots into water. However, addition of H_2O_2 enhanced *Cat1* induction within 1 h of treatment, and increased expression over the control level could be observed for the next 5 h. At 24 h, the level of *Cat1* expression in samples treated with high H_2O_2 concentrations (5–150 mM) was similar with the control, indicating that there is a time point where high H_2O_2 concentrations can no longer enhance *Cat1* expression. Taken together, these results demonstrate that responses of the *Cat* and *Gst1* genes are specific for the concentration and the duration of treatment, suggesting a regulatory role for H_2O_2 in the expression of these antioxidant genes.

As mentioned above, very rapid decomposition of H_2O_2 near the roots of the seedlings occurred immediately after submersion in the H_2O_2-containing solution. This could lead to a rapid depletion of the lower concentrations of H_2O_2 used. Thus, treatment with low H_2O_2 concentrations could represent a short transient oxidative burst. The effects of this transient exposure to H_2O_2 could be distinct from those observed for prolonged exposures to higher concentrations. The transient exposure to increased concentrations of H_2O_2 is reminiscent of the oxidative burst in the hypersensitive response of plants to pathogen attack. This localized oxidative burst at the root caused systemic inhibition of *Cat* gene expression observable 24 h later in the leaf. Thus, systemic H_2O_2 accumulation could be accomplished by inhibition of *Cat* gene expression. It has been suggested that H_2O_2 accumulation and initiation of the signaling pathway leading to systemic acquired resistance (SAR) are due to specific inhi-

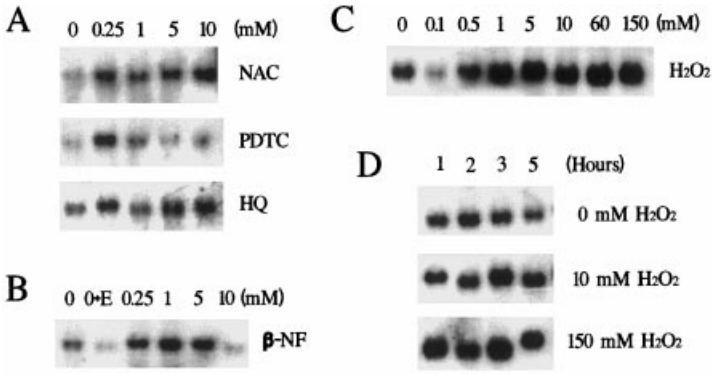

Fig. 4. Response of the maize *Gst1* gene to antioxidants, electrophiles, and H_2O_2. Seedlings (10 dpi) were treated hydroponically with increasing concentrations of the indicated compounds, and *Gst1* transcript in leaves was detected after hybridization with ^{32}P-labeled *Gst1* gene-specific probe. Equal loading of the gels was confirmed by ethidium bromide staining prior to transfer. A. Responses to 24-h treatments with the antioxidants NAC, PDTC, and HQ. B. Responses to 24-h treatments with the electrophile ARE-inducer β-NF. The 0 + E lane is control with the β-NF solvent ethanol. C. Responses to 24-h treatments with H_2O_2. D. Time course responses to 10 and 150 mM H_2O_2. Abbreviations are as in Fig. 1.

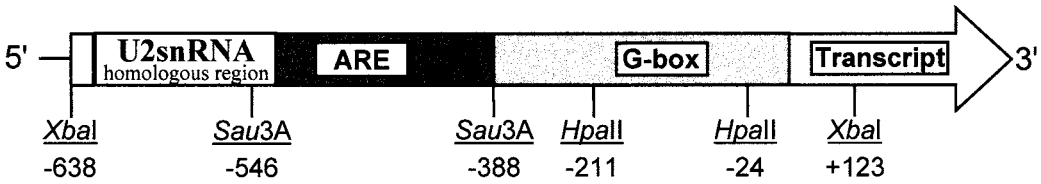

Fig. 5. Schematic of the *Xba*I fragment of the *Cat1* promoter that was used in preparation of electrophoretic mobility shift assay probes. The restriction enzyme sites and their distance from the initiation of transcription + 1 are shown. Transcript is represented as an arrow. The putative regulatory motifs are boxed. ARE is the antioxidant responsive element, and G-box is the ABA responsive element. The U2 snRNA homologous region is also shown.

bition of catalase activity by salicylic acid (SA) (Chen et al. 1993), which allows accumulation of systemic H_2O_2. However, there is also evidence that the H_2O_2 signal does not act downstream of SA in the development of SAR, as *NahG* transgenic plants that cannot accumulate SA do not induce PR-1 expression upon treatment with H_2O_2 and do not develop SAR (Bi et al. 1995, Neuenschwander et al. 1995). Involvement of H_2O_2 in disease resistance has been demonstrated in transgenic plants expressing the H_2O_2-generating glucose oxidase enzyme, and increased resistance of the transgenics could be counteracted with addition of catalase (Wu et al. 1995). Our results, in addition to the reported ability of H_2O_2 to induce SA accumulation (Bi et al. 1995, Neuenschwander et al. 1995), could provide a mechanism for H_2O_2 signaling in the induction of SAR, in which catalase inhibition and H_2O_2 act before SA accumulation (upstream of SA).

High concentrations of H_2O_2 rapidly induced *Cat* and *Gst1* gene expression, indicating that oxidative stress directly induces antioxidant responses. Particularly for *Cat3*, which is regulated by a circadian rhythm (Redinbaugh et al. 1990), its induction overrode the default circadian expression. Our data demonstrate that at CT-4, when *Cat3* transcript is very low, H_2O_2 treatment overrides the circadian regulation and induces high expression with high H_2O_2 concentration (Fig. 3C). Induction over the normal levels was also observed at CT-10, when the *Cat3* transcript reaches maximal expression (data not shown). This suggests that H_2O_2 can induce *Cat3* expression at different time points of the circadian cycle. However, the two time points we examined represent times in the circadian cycle where *Cat3* expression is increasing (CT-4) or is at its maximum (CT-10). Whether induction can also be observed at time points of declining expression, and whether the induced expression is still circadian, remains to be investigated.

Regulatory sequences in the *Cat1* promoter

The maize *Cat* genes harbor the ARE regulatory motif, which has a well-characterized role in induction of mammalian gene expression in response to oxidative stress. In order to investigate the role of ARE in maize *Cat* gene expression, we examined protein-DNA interactions in the ARE region of the *Cat1* promoter. The *Cat1* promoter has been sequenced revealing several regulatory elements, and has been used for the construction of promoter-reporter gene fusions that can drive the expression of the reporter gene GUS in transgenic tobacco plants (Guan and Scandalios 1993). A minimal 800 bp promoter fragment is sufficient for the regulation of GUS expression with a pattern similar to the *Cat1* expression observed in maize (Guan and Scandalios 1993). An ABA response element, located − 110 relative to the transcription start site, displays differential binding of nuclear proteins isolated from germinated and developing embryos, as well as from embryos grown in the presence and absence of absisic acid; this indicates that ABA up-regulates *Cat1* transcript accumulation in the scutellum during embryogenesis, but not during germination (Williamson and Scandalios 1994). However, *Cat1* transcript accumulates to high levels in the scutellum of germinating maize seeds. The promoter regions responsible for the control of *Cat1* expression during germination were not identified. The increase of *Cat1* transcript in the scutellum during germination could be an antioxidant response to oxidative stress. Active oxidative metabolism is well characterized in germinating seeds. During germination of oilseeds,

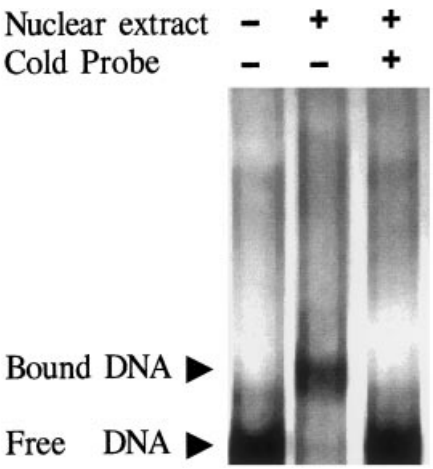

Fig. 6. Protein-DNA interactions in the *Cat1* promoter region harboring the ARE motif. Electrophoretic mobility shift assay was probed with a 158 bp *Sau3*A *Cat1* promoter fragment containing the ARE motif. The probe (0.1 ng ^{32}P-labeled DNA) in binding buffer containing 100 ng poly(dI-dC) non-specific competitor was incubated with 0.1 μg nuclear extract prepared from 10 dpi germinating scutella of maize. The free and bound probes were separated on 4% native acrylamide gel, vacuum dried, and autoradiographed. Specificity of the interaction was determined by addition of 30 × cold probe as specific competitor in the assay. Lanes are: Probe alone control (−, −), probe with nuclear extract and no specific competitor (+, −), and probe with nuclear extract and 30 × cold probe as specific competitor (+, +). Arrowheads indicate the bands of free and bound probe. Note the very strong interaction (+, −) revealed by the retardation of the whole amount of probe used in the assay.

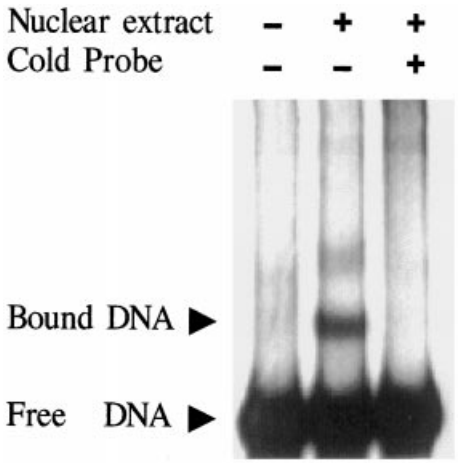

Fig. 7. Protein-DNA interactions in the U2 snRNA homologous region of the *Cat1* promoter. Electrophoretic mobility shift assay was probed with a 90 bp *Xba*I-*Sau3*A *Cat1* promoter fragment containing the U2 snRNA homologous region. The probe (1 ng ^{32}P-labeled DNA) in binding buffer containing 100 ng poly(dI-dC) non-specific competitor was incubated with 0.1 μg nuclear extract prepared from 10 dpi germinating scutella of maize. The free and bound probes were separated on 4% native acrylamide gel, vacuum dried, and autoradiographed. Specificity of the interaction was determined by addition of 30 × cold probe as specific competitor in the assay. Lanes are: probe alone control (−, −), probe with nuclear extract and no specific competitor (+, −), and probe with nuclear extract and 30 × cold probe as specific competitor (+, +). Arrowheads indicate the bands of free and bound probe.

fatty acids are converted into carbohydrates by hydrolysis of stored triglycerides, followed by the β-oxidation of fatty acids in specialized peroxisomes called glyoxysomes (Olsen and Harada 1995). Glyoxysomal catalase plays a vital role decomposing the H_2O_2 generated during β-oxidation. In addition, at the late stages of germination in maize, the scutellum, a terminally differentiated tissue is senescing. Senescence of plant organs and tissues is associated with formation of free radicals and oxidative stress (Thompson 1988). Thus, we examined the regulatory role of nuclear proteins isolated from 10 dpi scutella, when the tissue is under oxidative stress due to senescence. We assume that these nuclear factors may play a role in activation of the gene under oxidative stress conditions.

The 158 bp fragment that harbors the putative regulatory element ARE displayed a strong specific interaction with nuclear extracts prepared from 10 dpi germinating scutella. Specificity of the interaction was confirmed by the addition of 30 × cold probe, which resulted in elimination of the interacting band. These results indicate that regulatory element(s) are present on the 158 bp *Cat1* promoter fragment, and are strongly interacting with transcription factor(s) present in the 10 dpi germinating scutellum. In this region of the *Cat1* promoter, the only putative regulatory element recognized after computer searches for similarities with published regulatory sequences was the ARE motif. Numerous studies in animal systems demonstrate that the ARE motif is necessary and sufficient for regulation of gene responses to H_2O_2 via specific protein-DNA interactions in the region of ARE (Kahl 1997). Our data suggest a similar role of ARE in plants, and further experiments are designed to demonstrate its role in oxidative stress-induced gene expression.

Interestingly, the 90 bp *Cat1* promoter fragment upstream of the ARE motif also interacts with nuclear proteins prepared from 10 dpi scutella in a specific manner. Sequence comparisons of this fragment with published regulatory motifs show that no known regulatory element is present. However, most of the fragment contains a region 80% homologous to the first 100 bp of the coding region of the U2 snRNA gene of maize and other organisms. The major function reported for U2 products is in the formation of a ribonucleoprotein complex for intron splicing (Steitz et al. 1988). Thus, interaction of U2 snRNA homologous fragments with nuclear extracts could be expected. Our results raise the possibility that this fragment could also have a regulatory function in *Cat1* expression.

Acknowledgements – This work was supported, in part, by Research Grants from the US EPA (No. R819360 and No. R822546) and the NRI/CGP/USDA (No. 94371) to J.G.S. We thank Stephanie Ruzsa and Sheri Kernodle for expert technical assistance.

References

Alvarez A, Lamb C (1997) The oxidative burst of plant-pathogen interactions. In: Scandalios JG (ed.) Oxidative Stress and the Molecular Biology of Antioxidant Defenses. Cold Spring Harbor Laboratory Press, New York, pp 567–568. ISBN 0-87969-502-1

Angel P, Karin M (1991) The role of Jun, Fos and the AP-1 complex in cell-proliferation and transformation. Biochim Biophys Acta 1072: 129–157

Aruoma OI, Halliwell B, Hoey BM, Butler J (1989) The antioxidant action of N-acetylcysteine: Its reaction with hydrogen peroxide, hydroxyl radical, superoxide, and hypochlorous acid. Free Radic Biol Med 6: 593–598

Bergelson S, Pinkus R, Daniel V (1994) Intracellular glutathione levels regulate Fos/Jun induction and activation of glutathione-S-transferase gene expression. Cancer Res 54: 36–40

Bethards LA, Skadsen RW, Scandalios JG (1990) Isolation and characterization of a cDNA clone for the *Cat2* gene in maize and its homology with other catalases. Proc Natl Acad Sci USA 87: 6927

Bi YM, Kenton P, Mur L, Darby R, Draper J (1995) Hydrogen peroxide does not function downstream of salicylic acid in the induction of PR protein expression. Plant J 8: 235–245

Chen Z, Silva H, Klessig DF (1993) Active oxygen species in the induction of plant systemic acquired resistance by salicylic acid. Science 262: 1883–1886

Goldstein BD, Rozen MG, Quintavalla JC, Amoruso MA (1979) Decrease in mouse lung and liver glutathion peroxidase activity and potentiation of the lethal effects of ozone and paraquat by the superoxide dismutase inhibitor diethyldithiocarbamate. Biochem Pharmacol 28: 27–30

Guan L, Scandalios JG (1993) Characterization of the catalase antioxidant defense gene *Cat1* of maize, and its developmentally regulated expression in transgenic tobacco. Plant J 3: 527–536

Hall GEJ, Spiker S (1994) Isolation and characterization of nuclear scaffolds. In: Gelvin SB Schilperoort RA (eds) Plant Molecular Biology Manual. Kluwer Academic Publisher, Dordrecht, Boston, pp 1–12. ISBN 0-79232-858-2

Holdsworth MJ, Laties GG (1989) Site-specific binding of a nuclear factor to the carrot extensin gene is influenced by both ethylene and wounding. Planta 179: 17–23

Jamieson DJ, Storz G (1997) Transcriptional regulators of oxidative stress responses. In: Scandalios JG (ed.) Oxidative Stress and the Molecular Biology of Antioxidant Defenses. Cold Spring Harbor Laboratory Press, New York, pp 91–115. ISBN 0-87969-502-1

Jepson I, Lay VJ, Holt DC, Bright SWJ, Greenland AJ (1994) Cloning and characterization of maize herbicide safener-induced cDNAs encoding subunits of glutathione S-transferase isoforms I, II and IV. Plant Mol Biol 26: 1855–1866

Kahl R (1997) Phenolic antioxidants: Physiological and toxicological aspects. In: Packer L, Cadenas E (eds) Handbook of Synthetic Antioxidants. Marcel Dekker, Inc., New York, pp 177–224. ISBN 0-82479-810-4

Kreuz K, Tommasini R, Martinoia E (1996) Old enzymes for a new job: Herbicide detoxification in plants. Plant Physiol 111: 349–353

Levine A, Tenhaken R, Dixon R, Lamb C (1994) H_2O_2 from the oxidative burst orchestrates the plant hypersensitive disease resistance response. Cell 79: 583–593

Marrs KA (1996) The functions and regulation of glutathione S-transferases in plants. Annu Rev Plant Physiol Plant Mol Biol 47: 127–158

Marrs KA, Alfenito MR, Lloyd AM, Walbot V (1995) A glutathione S-transferase involved in vacuolar transfer encoded by the maize gene *Bronze-2*. Nature 375: 397–400

Meyer M, Schreck R, Baeuerle PA (1993) Hydrogen peroxide and antioxidants have opposite effects on activation of NF-kappa-B and AP-1 in intact cells: AP-1 as secondary antioxidant-responsive factor. EMBO J 12: 2005–2015

Neuenschwander U, Vernooij B, Friedrich L, Uknes S, Kessmann H, Ryals J (1995) Is hydrogen peroxide a second messenger of salicylic acid in systemic acquired resistance? Plant J 8: 227–233

Olsen LJ, Harada JJ (1995) Peroxisomes and their assembly in higher plants. Annu Rev Plant Physiol Plant Mol Biol 46: 123–146

Pinkus R, Weiner LM, Daniel V (1996) Role of oxidants and antioxidants in the induction of AP-1, NF-kappaB, and glutathione S-transferase gene expression. J Biol Chem 271: 13422–13429

Ramasarma T (1982) Generation of H_2O in biomembranes. Biochim Biophys Acta 694: 69–93

Redinbaugh MG, Wadsworth GJ, Scandalios JG (1988) Characterization of catalase transcripts and their differential expression in maize. Biochim Biophys Acta 951: 104–116

Redinbaugh MG, Sabre M, Scandalios JG (1990) Expression of the maize *Cat3* catalase gene is under the influence of a circadian rhythm. Proc Natl Acad Sci USA 87: 6853–6857

Rohrdanz E, Kahl R (1998) Alterations of antioxidant enzyme expression in response to hydrogen peroxide. Free Rad Biol Med 24: 27–38

Rushmore TH, Morton MR, Pickett CB (1991) The antioxidant responsive element. Activation by oxidative stress and identification of the DNA consensus sequence required for functional activity. J Biol Chem 266: 11632–11639

Salguero J, Boettger (1995) Secreted catalase activity from rrots of developing maize (*Zea mays* L.) seedlings. Protoplasma 184: 72–78

Scandalios JG (1993) Oxygen stress and superoxide dismutases. Plant Physiol 101: 7–12

Scandalios JG, Guan L, Polidoros AN, (1997) Catalases in plants: gene structure, properties, regulation, and expression. In: Scandalios JG (ed.) Oxidative Stress and the Molecular Biology of Antioxidant Defenses. Cold Spring Harbor Laboratory Press, New York, pp 343–406. ISBN 0-87969-502-1

Schreck R, Rieber P, Baeuerle PA (1991) Reactive oxygen intermediates as apparently widely used messengers in the activation of the NF-kappa B transcription factor and HIV-1. EMBO J 10: 2247–2258

Senior ML, Chin ECL, Lee M, Smith JSC, Stuber CW (1996) Simple sequence repeat markers developed from maize sequences found in the GENBANK database: map construction. Crop Sci 36: 1676–1683

Steitz PA, Black DL, Gerke V, Parke KA, Kramer A, Frendeway D, Keller W (1988) Small nuclear ribonucleoprotein particles. In: Birnstiel ML (ed.) Structure and Function of Major and Minor Small Nuclear Ribonucleoprotein Particles. Springer-Verlag, New York, pp 115–154. ISBN 0-38718-410-4

Talalay P, DeLong MJ, Prochaska HJ (1988) Identification of a common chemical signal regulating the induction of enzymes that protect against chemical carcinogenesis. Proc Natl Acad Sci USA 85: 8261–8265

Tenhaken R, Levine A, Brisson LF, Dixon RA, Lamb C (1995) Function of the oxidative burst in hypersensitive disease resistance. Proc Natl Acad Sci USA 92: 4158–4163

Thompson JE (1988) The molecular basis for membrane deterioration during senescence. In: Nooden LD, Leopold AC (eds) Senescence and Aging in Plants. Academic Press, New York, pp 51–83. ISBN 0-12520-920-7

Thompson WF, Everett M, Polans NO, Jorgensen RA, Palmer JD (1983) Phytochrome control of RNA levels in developing pea and mung bean leaves (*Pisum sativum*, *Vigna radiata*). Planta 158: 487–500

Williamson JD, Scandalios JG (1994) The maize (*Zea mays* L.) *Cat1* catalase promoter displays differential binding of nuclear proteins isolated from germinated and developing embryos and from embryos grown in the presence and absence of abscisic acid. Plant Physiol 106: 1373–1380

Wu GS, Shortt BJ, Lawrence EB, Levine EB, Fitzsimmons KC, Shah DM (1995) Disease resistance conferred by expression of a gene encoding H_2O_2-generating glucose oxidase in transgenic potato plants. Plant Cell 7: 1357–1368

Edited by L. McIntosh

Transgenic Research **10:** 555–569, 2001.
© 2001 *Kluwer Academic Publishers. Printed in the Netherlands.*

Transgenic tobacco plants expressing the maize *Cat2* gene have altered catalase levels that affect plant-pathogen interactions and resistance to oxidative stress

A.N. Polidoros, P.V. Mylona & J.G. Scandalios*
Department of Genetics, North Carolina State University Raleigh, NC 27695-7614, USA

Received 8 January 2001; revised 28 March 2001; accepted 2 April 2001

Key words: catalase, disease resistance, gene silencing, plant-pathogen interactions, reactive oxygen

Abstract

Transgenic tobacco genotypes expressing the maize *Cat2* gene were developed with altered catalase (CAT) levels that resulted in a moderate increase of CAT activity in two transgenic lines. Bacterial infection, with a pathogen that does not share homology with the transgene, caused local and systemic down-regulation of the steady state mRNA levels of the 35S-driven transgene in a manner resembling post-transcriptional gene silencing (PTGS). Phenotypic symptoms of hypersensitive response (HR) and systemic acquired resistance (SAR) were similar in control SR1 and the transgenic genotypes. Induction of *hin1*, used as a molecular marker of plant responses to invading bacteria, displayed a similar pattern between control and transgenic lines, but some variation in the levels of expression was observed. The major difference was recorded in the ability of the plants to restrict bacterial growth during HR. All transgenic lines were more sensitive than control SR1, with two lines exhibiting a significantly reduced capacity to inhibit bacterial growth. This is consistent with the putative enhanced capacity of transgenic lines containing the maize *Cat2* gene to more effectively remove H_2O_2, which may act as a direct antimicrobial agent. Steady state mRNA levels of *PR-1* and *PR-5* varied among the genotypes, possibly indicating differences in strength of the SAR signal. Transgenic line 2, which was the most sensitive during HR, was most effective in restricting bacterial growth during SAR. This indicates that a reverse correlation might exist between the severity of infection during HR and the ability to inhibit bacterial growth during SAR. Growth under high light conditions affected plant-pathogen interactions in control SR1, as well as in transgenic line 8. Early induction and higher expression of *PR-1* and *PR-5* was detected in both SR1 and line 8 in high light-grown plants as compared with their low light-grown counterparts. Our data indicate that growth under high light conditions can predispose plants to better resist pathogen attack, and may amplify local and systemic defense signals. Finally, one transgenic line, which exhibited 1.3-fold higher average CAT activity in comparison with the untransformed SR1 control, suffered significantly less methyl viologen (MV) damage than untransformed control plants at moderate and high MV concentrations.

Abbreviations: PTGS–post-transcriptional gene silencing; HR–hypersensitive response; SAR–systemic acquired resistance; MV–methyl viologen; ROS–reactive oxygen species; SA–salicylic acid; SOD–superoxide dismutase; CAT–catalase protein/isozyme; *Cat*–catalase gene/transcript; HDGS–homology-dependent gene silencing.

Introduction

Aerobic organisms gain significant energetic advantage by using molecular oxygen as the terminal oxidant in respiration. However, they can be severely damaged by partially reduced oxygen species, which are produced through normal or aberrant metabolic processes, as well as a consequence of various environmental stresses. The toxic effects of reactive oxygen species (ROS), termed oxidative stress, are circumvented by a combination of enzymatic and non-enzymatic mechanisms that can reduce oxidative stress by con-

* Author for correspondence: *E-mail:* jgs@unity.ncsu.edu

verting ROS to harmless compounds. Among the enzymes involved in the defense against oxidative stress, catalase plays a key role by converting H_2O_2, at an extremely rapid rate, to oxygen and water (Scandalios, 1993).

Many plants subjected to a variety of environmental stresses respond by increasing the levels of mRNA and/or enzyme activity of antioxidant defense enzymes including catalase (Scandalios et al., 1997). Effective antioxidant defenses are crucial for survival, and understanding how they function is of great importance. Several recent studies have been aimed at enhancing protection by the constitutive overexpression of antioxidant defense enzymes in transgenic plants, including superoxide dismutases (SOD), which catalyze the dismutation of superoxide anion radicals to H_2O_2 and molecular oxygen, as well as glutathione reductase, which regenerates the antioxidant peptide glutathione, and ascorbate peroxidase, which scavenges H_2O_2 in chloroplasts and cytosol (Allen, 1995). Results from such studies confirm the important role antioxidant defense enzymes play in protecting plants from oxidative stress and point to the significance of transgenic plants as tools for the study of oxidative stress protective mechanisms *in vivo*.

The role of catalase has also been investigated using transgenic plants. Photosynthesis of transgenic plants expressing a bacterial catalase in the chloroplasts was found to be tolerant to high irradiance under drought conditions (Shikanai et al., 1998). Altered photosynthesis was also reported in transgenic tobacco plants expressing sense and antisense constructs of tobacco and cotton catalase (Brisson et al., 1998). Most studies focused on inhibition of specific catalase alleles using antisense constructs, or co-suppression mechanisms involved in transgene and endogenous homologous gene(s) inactivation by using sense constructs for transformation. Transgenic tobacco with reduced CAT activity developed necrotic lesions, and induced pathogenesis-related gene expression when grown under high light (Chamnongpol et al., 1996; Takahashi et al., 1997). Ion leakage from *Cat1*-deficient transgenic tobacco leaf disks was increased after 3 h of methyl viologen (MV; paraquat) treatment and was twice the levels of the control after 6 h (Willekens et al., 1997). A significant temperature-dependent increase of the CO_2 compensation point was observed in catalase-deficient transgenics, while the opposite was detected for overexpressing genotypes (Brisson et al., 1998). These studies point to the significance of catalase as a sink for photorespiratory H_2O_2, and its indispensable role for stress defense in C_3 plants.

Transgenic plants with altered catalase levels can be useful in examining the roles of catalase and H_2O_2 in HR and SAR. Microbial elicitors or attempted infection with avirulent strains of a pathogen cause the sudden rapid production of ROS (i.e., 'oxidative burst'), leading to the induction of HR, a rapid collapse of the challenged host cells, and the deployment of a battery of inducible defenses in both the challenged and the surrounding cells (Lamb et al., 1989). The result of hypersensitive cell death is the formation of necrotic lesions and the restriction of the pathogen to a small zone around the site of infection. An important consequence of HR is that the remaining uninfected tissues of the plant develop enhanced resistance against a second attack of the same, or even an unrelated pathogen, that can be long-lasting ('systemic acquired resistance'; SAR).

During the HR oxidative burst, a rapid accumulation of H_2O_2 at the plant cell surface is observed (Mehdy, 1994). In soybean cells, H_2O_2 accumulates within 2–3 min after delivery of the elicitor. The oxidative burst is transient, and begins to decline after 40–50 min. A dual role for the H_2O_2 burst in HR has been proposed (Levine et al., 1994): as a localized trigger of cell death, and as a diffusible signal for the induction of cellular protectant genes that function in blocking oxidant-mediated programmed cell death. The catalase inhibitor 3-amino-1, 2, 4 triazole enhanced cell death in soybean cells inoculated with an avirulent strain, but not in uninoculated cells, or in cells inoculated with the isogenic compatible strain of the pathogen *Pseudomonas syringae*. Transgenic tobacco plants constitutively expressing an antisense cDNA copy of the *Cat* gene exhibited reduced CAT levels and constitutively synthesized one class of pathogenesis-related proteins (Dempsey & Klessig, 1994). Thus, H_2O_2 has been proposed to serve as second messenger inducing plant defense gene expression.

A mechanism based on catalase inhibition by salicylic acid (SA) has been proposed as the cause for elevated H_2O_2 levels during HR and SAR, (Chen et al., 1993). However, it is unlikely that SA inhibition of catalase is responsible for all defense responses, since H_2O_2 accumulation is a rapid process, while SA accumulates within 8–24 h after inoculation (Dempsey & Klessig, 1994). SA involvement in the SAR response has been shown in transgenic tobacco expressing the bacterial salicylate hydroxylase (*nahG*) gene. These plants cannot accumulate SA; the

consequence is an inability to acquire SAR (Delaney et al., 1994). However, an untransformed top, grafted to a transformed rootstock expressing the *nahG* gene (unable to accumulate SA), did develop SAR when the rootstock was infected with TMV, even though it could not accumulate SA (Vernooij et al., 1994). Therefore, a mobile signal, other than SA, is required to act as second messenger for SAR development. Recent data show that H_2O_2-induction of SAR genes is dependent on SA accumulation (Neuenschwander et al., 1995) and that H_2O_2 does not function downstream of SA in the induction of *PR* protein expression (Bi et al., 1995). These data do not support a role for H_2O_2 in SAR signaling. The interplay of catalase and salycylic acid has also been investigated in crosses of transgenic plants that are catalase-deficient, with *nahG* transgenic plants that do not accumulate salicylic acid. In contrast with the parental catalase-deficient plants, the progeny do not constitutively express the *PR-1* gene or develop enhanced resistance, indicating that salicylic acid is required for the induction of defense responses in the catalase-deficient plants (Du & Klessig, 1997). However, SA-independent spontaneous lesion formation could be observed in several progeny genotypes under high light. These investigators conclude that there seems to be an SA-independent pathway for the formation of necrosis which is related to catalase deficiency and strong light, and an SA-dependent pathway leading to the induction of *PR* genes and enhanced resistance.

In order to further investigate the possible involvement and role of catalase in such important physiological phenomena as HR and SAR, as well as in protection against oxidative stress, we examined the effects of catalase over-expression in relation to HR and SAR. Accordingly, we developed transgenic tobacco genotypes, expressing the maize *Cat2* gene, with altered catalase levels. *Cat2* is not inhibited by SA, and is induced in SA-treated maize scutella (Guan & Scandalios, 1995). Herein we report results from experiments conducted to provide information on the effects of the additional catalase copies in transgenic genotypes in plant-pathogen interactions and in oxidative stress.

Materials and methods

Gene constructs

Cat2 cDNA was excised from the plasmid clone po*Cat2*.1c (GenBank accession J02976) as a 1570-bp *Eco*RI-*Sst*I fragment, containing part of the 5′ and the 3′ untranslated regions, and including the whole coding sequence of the *Cat2* cDNA. The 5′ *Eco*RI site was first filled in by Klenow polymerase, and the fragment then isolated by agarose gel electrophoresis.

The plasmid vector pBI.121 (Clontech) was reconstructed to transfer the *Cat2* cDNA into tobacco. pBI.121 derived from the binary vector pBIN19 (Bevan, 1984), contains an 800-bp CaMV 35S promoter fused to a 1.87-kb *gusA* gene with a 260-bp *Sst*I-*Eco*RI fragment containing the nopaline synthase (NOS) polyadenylation signal from the *Agrobacterium tumefaciens* Ti plasmid. The *gusA* gene was excised from pBI.121 as a *Sma*I-*Sst*I fragment, and the linear plasmid was isolated by agarose gel electrophoresis. The *Cat2* cDNA was then ligated into the plasmid vector in 5′-3′ orientation. The *Sma*I site of the vector was ligated to the *Eco*RI filled-in site of the *Cat2* cDNA and the *Sst*I site of the vector with the *Sst*I site of the *Cat2* cDNA. As a result, *Cat2* cDNA was properly inserted into the vector for the CaMV 35S promoter to drive its expression and NOS-terminator to add the polyadenylation signal. Orientation of the insert was confirmed by sequencing. The reconstructed vector was designated pBI.*Cat2*.

Tobacco leaf disk transformation

pBI.*Cat2* DNA was used to transform competent *E. coli* DH5αF' cells. The construct was then mobilized into *Agrobacterium* strain LBA4404 by the method of triparental mating (Bevan, 1984). Leaf disks of *Nicotiana tabacum* cv. SR1 were transformed as described (Horsch et al., 1985), except that a higher BAP/NAA ratio was used in the shoot regeneration medium. Transformed plants were selected on MS medium (Murashige & Skoog, 1962) containing 100 μg/ml kanamycin and 500 μg/ml carbenicillin. After rooting, plants were transferred to soil and grown in the greenhouse. Primary transgenics (R_0) were self-fertilized to produce R_1 seeds. R_1 seeds were germinated on kanamycin-containing agar plates and resistant plants grown to maturity in the greenhouse. R_1 plants were self-fertilized to produce R_2 seeds. Kanamycin resistant R_2 plants were selected on agar plates, transferred to soil, and grown under controlled conditions in the NCSU Phytotron. These plants served as the material for this study.

DNA isolation and Southern analysis

Genomic DNA from primary transformed tobacco plants and control, untransformed, SR1 plants was isolated (Dellaporta et al., 1983), digested with the appropriate enzymes, electrophoresed through 1% agarose gels and transferred onto nylon membranes. Presence of the transgene was detected by hybridization with a ^{32}P-labeled maize *Cat2* cDNA probe in Church buffer (Church & Gilbert, 1984), at 65°C overnight, and two washes for 30 min with 0.1X SSC/0.1% SDS at 65°C.

RNA isolation and analysis

Leaf material was harvested at the indicated stages, frozen in liquid nitrogen, and stored at -80°C for analysis. Total RNA from leaf material was extracted (Thompson et al., 1983), and separated on denaturing 1.6% agarose gels. Equal loading was confirmed by ethidium bromide staining. RNA was then transferred to nylon membranes and hybridized with ^{32}P-labeled probes. Probes used were the maize *Cat2* full length cDNA, *hin1* (Gopalan et al., 1996), *PR-1* and *PR-5* (Ward et al., 1991), and *pHA2* (Jorgensen et al., 1987), containing an 18*S* ribosomal sequence as loading control. Hybridization was done in modified Church buffer (Church & Gilbert, 1984), containing 7% SDS, 0.5 M EDTA, 0.5 M NaH_2PO_4, and 1% BSA, at 65°C for 24–36 h. Filters were washed twice for 30 min with 0.1X SSC/0.1% SDS at 65°C. Duplicate northerns for each probe were prepared.

Catalase activity, protein determination, and western blot analysis

Leaf samples were homogenized in cold 25 mM glycylglycine buffer, pH 7.4. The crude supernatant was used for protein determination (Lowry et al., 1951) and catalase activity assay (Beers & Sizer, 1952). Catalase activity (reduction in absorbance at 240 nm/min/mg protein) was determined spectrophotometricaly. Western blotting was performed using maize CAT-2 specific polyclonal antibodies (Skadsen & Scandalios, 1987).

Plant material and growth conditions

The primary transformed lines (R_0) and the first transgenic generation (R_1) were grown to maturity in a greenhouse. R_2 plants were germinated and selected for 3–4 weeks on kanamycin plates, transferred to soil and grown in a controlled environment at the NCSU-Phytotron. The growing conditions were 12 h dark / 12 h light photoperiod at 25°C, 100 mol m^{-2} s^{-1} photosynthetic photon fluence rate, and 70% relative humidity. High light conditions were 500 mol m^{-2} s^{-1} photosynthetic photon fluence rate. Standard Phytotron nutrient solution was provided daily. Plants had 5–7 true leaves 30 days after transfer to soil. All treatments and analyses were at this stage, unless otherwise stated.

Pathogen infection and analysis

All experiments were conducted in two repetitions with five plants per genotype in each repetition. Bacteria used were *Pseudomonas syringae* pv. *syringae* isolate B728a and *P. syringae* pv. *tabaci* (ATCC 11528). Bacteria were grown in King's B medium (pH 7.0, 10 mg/ml protease peptone, 15 mg/ml glycerol, 1.5 mg/ml K_2HPO_4, and 4 mM $MgSO_4$). *P. syringae* pv. *syringae* was grown overnight in nutrient broth, centrifuged, and resuspended to an approximate concentration of 1×10^8 cfu/ml in distilled water. Leaves were infected with *P. syringae* pv. *syringae* by injection of leaf intracellular spaces using a 1 ml syringe without the needle. Each infiltration covered an area approximately 2 cm^2 and typically resulted in the application of approximately 100 µl bacterial suspension.

At 72 h after bacterial infiltration, the leaves were surface sterilized with 20% NaOCl, 0.1% Tween 20 for 1 min, and washed three times in sterile, distilled water. Leaf discs of 12 mm diameter were taken from the infection site, homogenized and plated. Two repetitions consisting of three plants per repetition (six leaf disks per genotype) were examined. Results were expressed as average number of colonies per leaf disk area at the appropriate dilution. Statistical significance of differences was examined by analysis of variance. No bacterial growth was observed on leaf discs obtained from mock-inoculated plants that were infiltrated with sterile water.

Seven days after initial treatment, SAR was induced by infecting the upper leaves of tobacco plants with *P. syringae* pv *tabaci* (ATCC 11528). Seventy-two hours after infiltration of leaves, bacterial growth was assessed as described above.

MV treatment and cell leakage analysis

MV belongs to the bipyridilium herbicide family. MV, as well as other amphiphilic viologens, can bind to

the thylakoid and mitochondrial membranes by hydrophobic interactions, and serve as an artificial electron carrier. During illumination, MV preferentially accepts electrons from photosystem I and donates them to molecular oxygen, generating the superoxide radical within the chloroplasts (Halliwell, 1984). Leaf disks (1.5 cm^2 each) were collected from transgenic and untransformed tobacco plants. Six leaf disks from each genotype were transferred to 35 mm Petri dishes containing 3 ml of MV solution of the following concentrations: 0.6, 1.2 or 2.4 μM. Control dishes contained distilled water. Each treatment was conducted in triplicate for each MV concentration and each genotype. Samples were vacuum infiltrated for 5 min and incubated at 21°C for 16 h in darkness. Leaf disks were then illuminated (500 μmol m^{-2} s^{-1}) for 2 h, and incubated in darkness at 30°C for an additional 16 h.

For cell leakage analysis, the solution on which the leaf disks had been floating was collected, made up to 3 ml (to correct for evaporation) and conductance was measured with a Markson model 1096 conductivity meter. The leaf disks were again floated on the MV solution, and incubated for 1 h at 65°C to release all solutes and the conductivity of the solution was measured again. The electrolyte leakage attributable to control and MV treatment was determined by dividing the conductivity value of the test sample by the conductivity of the sample after 1 h at 65°C.

Results

Introduction and expression of the maize Cat2 *gene in tobacco*

Transgenic tobacco plants expressing the maize *Cat2* gene were produced by introduction of a catalase cassette from the reconstructed vector pBI.*Cat2* (Figure 1A). Eight primary transformed kanamycin-resistant lines were analyzed for copy number of the transgene and found to contain 1–5 copies; one line (# 5) had no signal, indicating that the transferred *Cat2* gene was lost (Figure 1B). Expression of the maize *Cat2* in three transgenic lines was confirmed by slot-blot hybridization (Figure 1C). The RNA level produced in transgenic leaves under the control of 35S was comparable with that of maize leaves and epicotyls, but much lower than that of maize scutella at 4 d post-imbibition, when the highest level of *Cat2* transcript can be detected. No transcript was detected in the untransformed control, indicating that, under the hybridization conditions employed, no cross-hybridization of the maize *Cat2* cDNA with tobacco catalase transcripts occurred. Post-transcriptional processing of the maize *Cat2* transcript in tobacco leaves was confirmed by western blotting with the CAT-2-specific Ab. Immunodetection of CAT-2 protein in the transgenic lines indicated that six of the lines had similar CAT-2 content, which was slightly lower than that normally found in line W64A (Figure 1D). Line # 4 had significantly lower CAT-2 protein and line # 5, in which the introduced gene could not be detected, produced no CAT-2 protein. Line 5 was excluded from further experiments. No signal was detected in the untransformed control (SR1), confirming the specificity of the assay.

Variable levels of CAT activity were present in the transgenic lines depending on the generation (Table 1). CAT activity was determined from leaves of greenhouse-grown plants, and represents the mean of two experiments. The 5th leaf from the top of the plant, 30 days after transfer to the greenhouse (just before anthesis), was used for CAT activity. In the R_0 plants, lines 1 and 7 had higher CAT activity than that of the untransformed SR1, while the rest of the transgenics had lower CAT activity. The next transgenic generation (R_1) had significantly elevated CAT activity, and only one line (line 4) had lower activity than the control. This line had significantly lower CAT-2 protein in the primary transformants, as well. However, the generally higher CAT activity in the R_1 plants was not stable in the next generation (R_2), as only lines 7 and 8 had significantly higher CAT activity than the control SR1. Extended analysis of CAT activity in transgenic and wild type tobacco indicated that activity can vary widely depending on the age, type of tissue, light conditions, and nutrient supply (data not shown).

Plant-pathogen interaction relative to the expression of the maize Cat2 *in transgenic tobacco*

Physiological and molecular parameters of plant-pathogen interactions were examined in order to determine the role of the introduced *Cat* allele in the hypersensitive response (HR) and in systemic acquired resistance (SAR).

Hypersensitive response

Catalase transgenics and control SR1 plants were infected with *P. syringae* pv. *syringae* and progress of

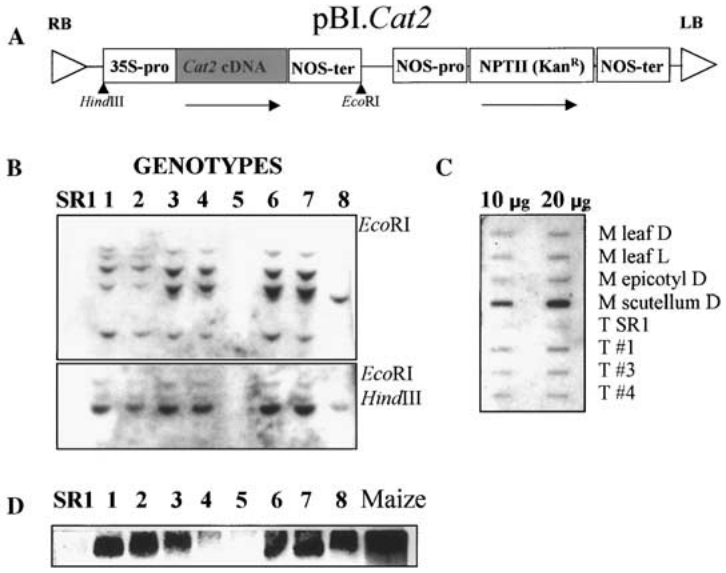

Figure 1. Transformation and expression of the maize *Cat2* cDNA in transgenic tobacco lines. **A**. The transformation vector pBI.*Cat2*. Arrows show the direction of transcription **B**. Southern hybridization with the maize *Cat2* cDNA probe of DNA isolated from control and transformed tobacco lines. Restriction only with *Eco*RI produced multiple bands in all but one line (#8), indicating incorporation of multiple copies of the transgene. Line #8 has a single copy. Double digestion with *Hind*III and *Eco*RI produced one band of the expected size in all lines. Line #5 did not produce a signal, indicating that it may have been a false positive and was excluded from further analysis. No signal is present in the control untransformed SR1. **C**. Slot-blot hybridization with the maize *Cat2* cDNA probe of total RNA from various maize (M) tissues grown under constant dark (D) or constant light (L) conditions, transgenic tobacco (T) lines, and untransformed control SR1. **D**. Immunodetection of the maize CAT-2 protein in the transgenic lines. No signal was observed in line #5, which did not hybridize with the *Cat2* cDNA in the Southern analysis, nor in the untransformed control line SR1. The maize band is included for comparisons.

Table 1. Leaf catalase (CAT) specific activity in transgenic tobacco lines transformed with the maize *Cat2* gene

	R_0		R_1		R_2	
Genotype	CAT activity	Samples	CAT activity	Plants	CAT activity	Plants
SR1	0.61 ± 0.24	4	0.58 ± 0.26	4	0.51 ± 0.23	11
1	0.94 ± 0.17	4	1.83 ± 0.31	4	0.58 ± 0.28	11
2	0.42 ± 0.16	4	1.38 ± 0.24	4	0.43 ± 0.13	11
3	0.18 ± 0.09	4	1.57 ± 0.12	4	0.46 ± 0.12	11
4	0.02 ± 0.00	4	0.42 ± 0.04	4	0.54 ± 0.21	11
6	0.32 ± 0.11	4	1.17 ± 0.19	4	0.54 ± 0.22	11
7	1.06 ± 0.32	4	1.51 ± 0.25	4	$0.71 \pm 0.23^*$	11
8	0.41 ± 0.15	4	1.36 ± 0.11	4	$0.68 \pm 0.32^*$	11

CAT specific activities ($\pm$ SD), expressed as units per milligram soluble protein, in three consecutive generations of seven families of transgenic tobacco plants and the untransformed control line, SR1. R_0, primary transformants; 4 samples per plant, grown in the greenhouse, were assayed just before anthesis, in duplicate experiments. In the selfed primary transformants (R_1) selected for kanamycin resistance, CAT activity was significantly higher, ranging from 2- to 3-fold that of SR1 in 6 lines; only line 4 was lower. Assays (with duplicate measurements) were performed in 4 greenhouse-grown plants (2 samples per plant) just before anthesis. In the next transgenic generation (R_2), derived from selfing of R_1 plants, CAT activity was determined in a wide range of developmental stages and conditions. Samples were taken from leaves of 45 days post-transplantation seedlings (2 plants @ 2 samples per plant), greenhouse-grown plants before anthesis (3 plants @ 2 samples per plant), and plants grown in controlled conditions (Phytotron) under low light ($100\,\mathrm{mol\,m^{-2}\,s^{-1}}$) (3 plants @ 2 samples per plant), or high light ($500\,\mathrm{mol\,m^{-2}\,s^{-1}}$) before anthesis (3 plants @ 2 samples per plant). CAT activity was determined in duplicate measurements as an average of 11 plants and 22 samples per genotype. Asterisks indicate statistically significant LSD from SR1 ($F = 1.98$, $p = 0.067$).

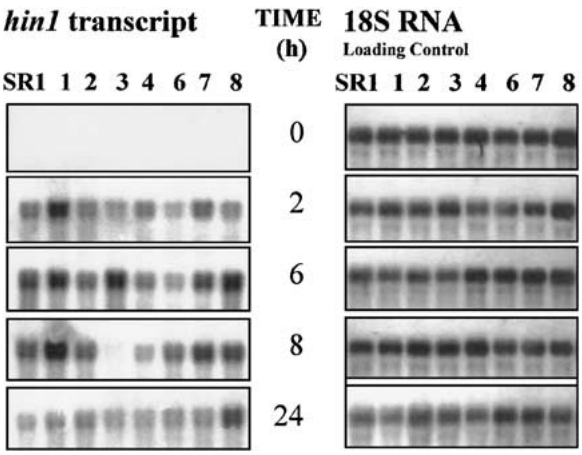

Figure 2. Expression of *hin1* in leaves of transgenic lines and in the untransformed control SR1 infected with the incompatible strain *P. syringae* pv. *syringae* at different time points during the progression of HR. Hybridization of the same filters with the *pHA2* probe containing an 18S ribosomal sequence was performed to ensure equal loading.

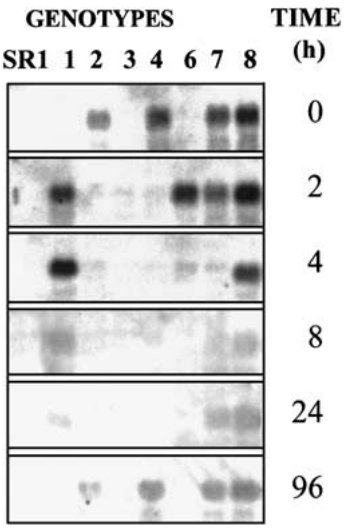

Figure 3. Expression of the introduced *Cat2* gene in transgenic tobacco lines during the progression of HR. Samples at time points 0 and 96 h are from uninfected leaves, while the rest of the samples are from infected leaves. No transcript is present in the untransformed SR1. The same set of filters was used also for hybridization with the *hin1* probe (time points 0–24 h) shown in Figure 2, and the *PR-1* probe (time point 96 h) shown in Figure 4 (*PR-1* d6). Equal loading was shown in Figure 2.

the HR was observed visually. Formation of necrotic lesions started ~8 h after infection; symptoms were indistinguishable between untransformed control and transgenic plants throughout the progression of HR. To determine if differences were present in the molecular events of HR, we monitored the induction of *hin1*, a plant gene activated rapidly by harpins and *avrPto* gene-mediated signals (Gopalan et al., 1996). The *hin1* transcript was not present in uninfected plants. Rapid induction of *hin1* was noted upon infection in wild type SR1, as well as in all the transgenic lines examined (Figure 2). The transcript was present at variable levels in all genotypes between 2–24 h after infection. The untransformed SR1 control displayed a typical *hin1* induction during the time course of the experiment, while the transformed genotypes displayed altered *hin1* expression, but with no unique pattern. Expression of the gene in line 1 was higher than the control SR1 at all time points and was the highest among all genotypes at 2 and 8 h post-infection. In line 2, expression was similar to the control SR1 at 2 h, slightly lower at 6 h, similar again at 8 h, and slightly higher at 24 h. In line 3 the *hin1* transcript was similar to the control SR1 at 2 h, higher at 6 h, significantly lower at 8 h, and similar at 24 h. Line 4 had similar transcript levels to the control SR1 at 2 h and 24 h, and lower at 6 h and 8 h. Line 6 had less transcript at 2 h, 6 h, 8 h, and slightly higher than the control at 24 h. Line 7 had a slightly higher transcript level at 2 h, similar at 6 h, and slightly higher than the control SR1 at 8 and 24 h. Line 8 had similar transcript levels to the control SR1 at 2 h, and higher thereafter.

In order to determine if expression of the introduced gene was affected, we monitored *Cat2* expression during the time course of HR using the same filter, after stripping off the *hin1* probe. We used the maize *Cat2* cDNA as probe, which specifically detected this transcript and detected nothing in the SR1 control (Figure 3). Expression of the gene was detected in uninfected plants in lines 2, 4, 7, and 8. In lines 1, 3, and 6 no transcript could be detected. Upon infection (2 h), the result was induction of the gene in lines 1 and 6, and in marked contrast, inhibition in line 4. At 4 h, the induction in line 1 was enhanced while in line 6 it was repressed. Expression in line 7 was also repressed, while in line 8 it declined slightly. Thus, 4 h after infection, only lines 1 and 8 were expressing the transgene. A significant reduction of transcript in lines 1 and 8 was evident at 8 h; this time point represents a stage in the progression of HR where the overall lowest level of expression of the introduced gene is detected. Very low transgene transcripts can be detected in genotypes 1, 7 and 8 at 24 h post-infection. We also examined the expression of the transgene in uninfected upper leaves 96 h post-infection. The expression pattern is similar to the one observed in uninfected plants, but at significantly lower level.

To determine if any relationship could be observed between this pattern of transgenic expression and bacterial survival in the infected tissue, we examined the number of bacterial-infected areas 72 h after infection. The lowest bacterial number was observed in the untransformed control SR1 (Table 2). Lines 1, 3, 6, and 8 had higher numbers of viable bacteria but the difference with the control was not statistically significant. Lines 2 and 7 had the highest numbers of viable bacteria, and differed significantly from the control SR1, but not from the other transgenic lines. These data indicate that killing of bacteria is more effective in the wild type SR1 plants than in the transgenic lines.

Table 2. Inhibition of bacterial growth during hypersensitive response (HR)

Genotype	Number of plates	Average colonies	Standard error
SR1	5	56.8	13.5
3	6	97.3	11.1
8	5	97.4	12.5
6	6	97.6	24.3
4	6	103.8	26.4
1	3	112.3	31.5
7	6	144.3*	10.8
2	5	168.6*	26.1

The average number of colonies of the incompatible strain *P. syringae* pv. *syringae* from leaf disk extracts of infected tissues 72 h after infection for each transgenic line and the untransformed control SR1. Asterisks indicate statistically significant differences from the control genotype SR1 ($F = 2.772$, $p = 0.0216$). Extracts were plated in a dilution of 10^{-6} on replicate plates.

Systemic acquired resistance

The ability of catalase transgenic plants to exhibit systemic acquired resistance was examined by monitoring the expression of *PR* genes in uninfected tissue at 4 days and 6 days after the primary infection with *P. syringae*. Results indicate that there are significant differences in the expression of *PR-1* and *PR-5* among all the genotypes examined (Figure 4). Expression of both *PR* genes is typical in the control SR1, with increasing transcript levels between day 4 and day 6 post-infection in systemic tissue. Transgenic lines display differences that are maximized at day 6, when lines 1 2, 4, and 7 have transcript levels lower than the control and lines 6 and 8 accumulate very high

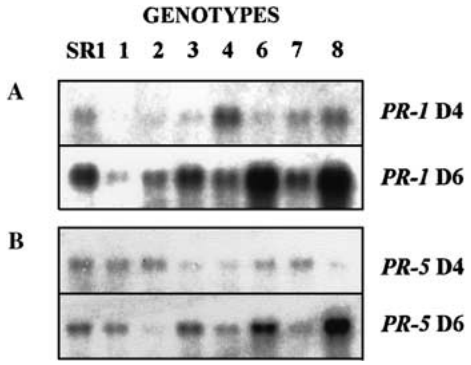

Figure 4. Expression of pathogenesis-related genes *PR-1* (**A**) and *PR-5* (**B**), four (D4) and six (D6) days post-infection with *P. syringae* pv. *syringae* used to induce HR, in transgenic lines and untransformed SR1. Samples were prepared from upper uninfected leaves. Equal loading was confirmed by hybridization of the same filters with the *pHA2* probe containing an 18S ribosomal sequence, with results similar to those displayed in Figure 2.

PR-1 and *PR-5* transcript, significantly higher than the control. Line 3 is at the level of the control.

The ability of the transgenic genotypes to express SAR as resistance to a second infection by a compatible pathogen was also estimated. Upper healthy leaves of plants previously infected with *P. syringae* pv. *syringae* were infected with the pathogenic strain of *P. syringae* pv. *tabaci* 7 days after the first infection. All genotypes were able to restrict the infection to the infiltrated area, exhibiting resistance to the pathogen. Symptoms were visually indistinguishable between control SR1 and transgenic plants. Bacterial survival was examined in the infected tissue 72 h post-infection (Table 3). The lowest bacterial count was observed in line 2 which had very high bacterial survival in HR. Lines 3, and 8 had the highest number of viable bacteria, and differed significantly from line 2. The other lines were intermediate and none differed significantly from the control.

Effect of light on pathogenesis-related gene expression in catalase transgenic plants

Catalase deficiency was shown to induce *PR-1* protein accumulation without pathogenic challenge in tobacco, but only after exposure to high light intensities (250–1000 $\mathrm{mol\,m^{-2}\,s^{-1}}$) which was accompanied by visible damage (Chamnongpol et al., 1996). To determine whether light has any effect on molecular events associated with SAR in our system, we examined *hin1* and *PR* gene expression in control SR1

Table 3. Inhibition of bacterial growth during systemic acquired resistance (SAR)

Genotype	Number of plates	Average colonies	Standard error
2	6	22.6	4.1
1	6	59.0	13.6
7	6	63.1	14.5
4	6	68.3	5.2
SR1	6	69.8	17.9
6	6	73.1	13.3
3	6	88.5*	21.1
8	6	99.3*	19.5

The second infection with the compatible strain *P. syringae* pv. *tabacci* was done 7 days after the primary infection with the incompatible *P. syringae* pv. *syringae*. The average number of colonies formed from leaf disk extract of infected tissue 72 h after the second infection for each transgenic line and the untransformed control SR1. Asterisks indicate statistically significant differences from genotype 2 ($F = 2.098$, $p = 0.0661$). Extracts were plated in a dilution of 10^{-5} on replicate plates.

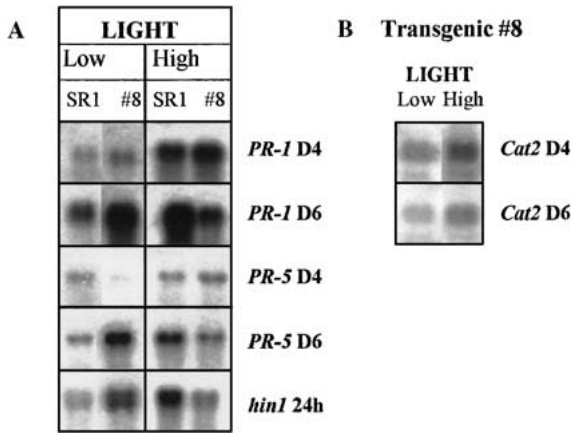

Figure 5. Effects of low and high light in expression of *PR-1*, *PR-5*, and *hin1* in SR1 and transgenic line #8, and *Cat2* in transgenic line #8 **A**. Effect of light on the expression of pathogenesis-related genes *PR-1* and *PR-5* four (D4) and six (D6) days post-infection with *P. syringae* pv. *syringae*, and the HR-specific *hin1* 24 h post-infection, in transgenic line #8 and untransformed SR1. **B**. Expression of the *Cat2* transgene in line #8 under low and high light conditions, four and six days post-infection. Equal loading was confirmed by hybridization of the same filters with the *pHA2* probe containing an 18S ribosomal sequence, with results similar to those displayed in Figure 2.

plants and transgenic line 8, which contains a single copy of the *Cat2* transgene, and showed the highest number of viable bacteria during SAR (Table 3). Plants grown under low ($100\,\mathrm{mol\,m^{-2}\,s^{-1}}$) or high ($500\,\mathrm{mol\,m^{-2}\,s^{-1}}$) light were infected with *P. syringae* pv. *syringae*, transferred to low light. The expression of *hin1* was examined in infected leaves 24 h later, while expression of *PR-1* and *PR-5* was examined in upper, uninfected leaves, 4 days and 6 days post-infection. In plants initially grown under low light, *PR-1* was detectable at low levels in both SR1 and line 8, at 4 days post-infection. At day 6 steady-state mRNA of *PR-1* increased in SR1, and greatly enhanced in line 8. The same pattern was observed for expression of *PR-5* in line 8. However, the difference in *PR-5* expression between day 4 and day 6 in SR1 was not significant (Figure 5A).

A different pattern was observed for plants grown under high light prior to infection. *PR-1* levels in both SR1 and line 8 were much higher than those observed under low light at day 4. Steady-state mRNA increased in SR1, while it slightly decreased in line 8 at day 6. This was in marked contrast with the *PR-1* expression observed under low light. At day 4, *PR-5* expression was no different in high light-grown plants than in their low light-grown counterparts. An increase in *PR-5* mRNA was detected under high light in SR1 at day 6, while there was no difference in line 8.

We also examined *hin1* expression in infected leaves 24 h post-infection. In plants grown under low light, *hin1* mRNA in SR1 was lower than that of line 8, while in plants grown under high light the reverse was true. In contrast, *hin1* mRNA in SR1 was much higher in plants grown under high light, while in line 8 it was higher in plants grown under low light.

In order to determine whether the patterns of *PR-1*, *PR-5*, and *hin1* expression in line 8, under low and high light, were related with any change in the *Cat2* transgene expression, we examined *Cat2* mRNA levels under the respective conditions. The *Cat2* transgene expression in line 8 was slightly higher under high than that under low light in the same upper uninfected leaves examined for *PR-1* and *PR-5* expression 4 and 6 days post-infection (Figure 5B).

The differences observed in molecular events in transgenic line 8 under low and high light were reflected in the ability of the plants to restrict bacterial growth after a second infection with the pathogenic *P. syringae* pv. *tabaci*. While this transgenic line harbored the highest number of viable bacteria under low light (average colonies 99.3, SE $\pm$ 19.5, Table 3), the number of surviving bacteria was significantly lower under high light (average colonies 49.5, SE $\pm$ 12.8).

MV resistance in catalase-overexpressing transgenic tobacco

Resistance of transgenic line 7 (exhibiting enhanced CAT activity in all experiments) to MV was determined by estimating electrolyte leakage as a measure of membrane damage. Leaf discs from the untransformed control SR1 showed increased sensitivity to the herbicide at 0–1.2 M, when membranes were almost completely disrupted. Leaf disks from the transgenic plants were significantly more resistant to the herbicide (Figure 6), showing 30% less damage than SR1 at 0.6 M, 45% less damage at 1.2 M and 25% less damage at 2.4 M. Similar experiments with the remaining transgenic lines revealed that increased resistance could be detected only at 1.2 M MV, and was of lower magnitude (20–30%) in comparison with 45% less damage in line 7 (data not shown).

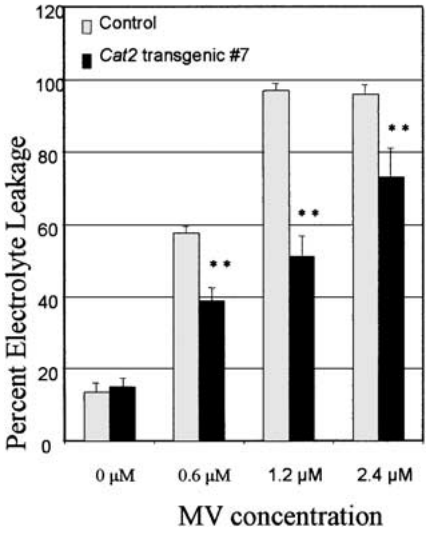

Figure 6. Percent electrolyte leakage (± SE) in leaf disks from the untransformed control SR1 and the transformed line #7 after treatment with the indicated concentration of MV. Six leaf disks of 1.5 cm^2 area from each genotype were assayed in triplicate experiments for each MV concentration. Samples were vacuum-infiltrated for 5 min and incubated at 21°C for 16 h in darkness. Leaf disks were then illuminated (500 $\mu mol\, m^{-2}\, s^{-1}$) for 2 h, and incubated in darkness for an additional 16 h at 30°C. The electrolyte leakage attributable to control and MV treatment was determined by dividing the conductivity value of the test sample by the conductivity of the sample after 1 h at 65°C. Double asterisks indicate statistically significant differences from the untransformed control ($F = 9.979$, $p = 0.0009$).

Discussion

Catalase expression in transgenic plants and their progeny

Catalase activity was enhanced in two primary transformed lines (1 and 7) and severely reduced in lines 3 and 4. In the remainder of the R_0 lines a moderate reduction in CAT activity was observed. Similar results have been reported in cotton (Chamnongpol et al., 1996), and tobacco (Brisson et al., 1998). These results might be explained by the action of a co-suppression mechanism (Matzke & Matzke, 1995). In R_1 six out of the seven transgenic lines exhibited CAT activity that was 2-3 fold higher than the untransformed control. Line 4, which had the most severe repression in R_0, was still lower in activity, but not as low as in the parental plants. In R_2 plants, CAT activity was comparable to that of the control SR1 and was higher in only two lines (7 and 8). This unstable inheritance of CAT activity in the transgenic lines strongly indicates the involvement of transgene inactivation, which is supported by the fact that most of the transgenic lines contained multiple copies of the transgene, while line 8 contained a single copy. It has been suggested that inactivation of gene expression in plants can result as a consequence of sequence duplications (Flavel, 1994). Northern analysis (Figure 3, time 0 h) revealed that there was no steady state *Cat2* mRNA in lines 1, 3, and 6, though it could be induced in lines 1 and 6, by pathogen attack. Thus, only line 3 showed no detectable steady state mRNA level of the *Cat2* transgene in our experiments, indicating a permanent inactivation of the transgene in this line. Lines 7 and 8 exhibited transgene expression and elevated CAT activity in the transgenic generation of our experiments (Table 1, R_2) and were considered as overexpressing lines. However, it must be noted that catalase activity and steady state mRNA levels are not always correlated. There are examples in maize (Redinbaugh et al., 1990) and cotton (Ni & Trelease, 1991) development where steady state mRNA levels do not reflect CAT activity or protein levels of different subunits, implying that post-transcriptional regulation is occuring. Our data are in accordance with previous results (Brisson et al., 1998) reporting a 1.3 to 1.5-fold increase in CAT activity over untransformed controls in transgenic tobacco transformed with a 35S-driven cotton and tobacco catalase cassettes, respectively. They also observed a lack of correlation between levels of RNA transcripts and

CAT specific activities in transformants overexpressing CAT.

Pathogen attack affects expression of the Cat2 *transgene*

In the course of our infection experiments we observed that in three transgenic R_2 lines (1, 3, and 6), a steady state *Cat2* mRNA could not be detected (Figure 3, time 0 h). However, while in line 3 transgene inactivation was permanent, in lines 1 and 6 there was an immediate induction of *Cat2* mRNA upon *P. syringae* infection, which declined during HR in infected leaves, and could not be observed 4 days post-infection in uninfected systemic leaves. The opposite pattern was observed in lines 2 and 4 where an immediate inactivation was detected upon infection, but a low level steady state *Cat2* mRNA was then present in systemic leaves 4 days post-infection. A similar but delayed inactivation was detected in lines 7 and 8, where very low steady state *Cat2* mRNA was observed 4 h post-infection in infected leaves, and 4 days post-infection in uninfected leaves. The above data derived from examination of four infected leaves in the same plants for the different time points, excluding random variation of transgene expression. Thus, we can identify at least four different transgene expression responses to invading bacteria among the seven transgenic genotypes examined:

(a) Immediate induction of steady state mRNA in silenced transgenes, followed by gradual silencing during the first 8 h post-infection (lines 1, 6);
(b) immediate silencing of previously active transgenes (lines 2, 4);
(c) gradual silencing of previously active transgenes during the first 8 h post-infection (lines 7, 8);
(d) no response of a silenced transgene (line 3). *Cat2* mRNA transcript could be detected 4 days post-infection in systemic uninfected leaves only in the genotypes that accumulated this transcript prior to infection, but at significantly reduced levels. These data indicate that transgene expression is affected by bacterial infection and its transcript is reduced 8–24 h post-infection.

Viral infection can cause stimulatory effects on a NOS promoter-regulated transgene and suppression on a 35S promoter-regulated transgene (Al-Kaff et al., 2000), suggesting that host responses to pathogen invasion may both up- and down-regulate transgenes. In transgenic plants where a transgene construct shares homology with the pathogen, the transgene can be silenced via a post-transcriptional gene silencing (PTGS) mechanism (Covey et al., 1997; Al-Kaff et al., 1998; Al-Kaff et al., 2000).

Although PTGS is a well-documented defense response to viral pathogens (Matzke & Matzke, 1995; Covey et al., 1997; Al-Kaff et al., 1998; Kooter et al., 1999) this is the first report providing evidence that bacterial infection (with a pathogen that does not share homologies with the transgene) causes local and systemic down-regulation of the steady state mRNA level of a 35S-driven transgene in a manner resembling PTGS.

Effects of altered catalase activity in plant-pathogen interactions

Catalase inactivation has been suggested as a primary step in SAR signaling during plant-pathogen interactions. The model suggests that CAT inactivation by SA enables the elevation of H_2O_2 levels and/or H_2O_2-derived ROS, which then serve as second messengers in the SAR signal transduction pathway (Chen et al., 1993). Thus, catalase should play a central role, serving as both receptor and transducer of the SA signal during plant-pathogen interactions. Consistent with this model are results from several studies indicating that H_2O_2 acts as a signal in *PR* gene induction (Conrath et al., 1995; Wu et al., 1995, 1997). However, this model has been questioned as results obtained by other investigators indicated that H_2O_2 acts upstream of SA in *PR* signaling (Bi et al., 1995; Leon et al., 1995; Neunschwander et al., 1995).

If catalase inactivation by SA is involved in HR induction, our transgenic plants expressing an SA-resistant CAT isoform should have shown altered HR responses. However, the phenotypic progression of HR was indistinguishable in untransformed control and transgenic lines. The induction of *hin1*, which is used as a molecular marker of plant responses to invading bacteria, displayed some variation between control and transgenic lines, but a similar pattern was observed. The major difference observed was in the ability of the plants to restrict bacterial growth. All transgenic lines were more sensitive than control SR1, with two lines (2 and 7) exhibiting a significantly reduced capacity to inhibit bacterial growth. This is consistent with the putative enhanced capacity of transgenic lines containing the maize *Cat2* gene to more effectively remove H_2O_2, which may act as a direct antimicrobial agent (Peng & Kuc, 1992), although

this finding is not consistent with the average CAT activity levels of these lines. Our findings are in agreement with the report that transgenic tobacco plants transformed with an antisense tobacco *Cat1* construct had significantly lower CAT activity, and were more effective in preventing growth of the incompatible *P. syringae* pv. *syringae* than the untransformed controls (Chamnongpol et al., 1996).

Regarding the effects of altered catalase expression in SAR signaling, we examined younger, uninfected tissue from inoculated plants for *PR-1* and *PR-5* expression. Detectable *PR* transcripts are produced in the younger uninfected leaves of tobacco between 3 and 6 days post-inoculation with TMV (Ward et al., 1991). *PR* activation was detected in control as well as in catalase transgenic plants in our study, indicating that the SAR signal transduction pathway was not disrupted by the expression of the *Cat2* transgene.

Steady state mRNA levels of *PR-1* and *PR-5* were variable among the different genotypes, possibly indicating differences in the strength of the SAR signal. It has been suggested that HR induces secondary oxidative bursts in discrete cells in distant tissues, leading to low-frequency systemic micro-HRs required for systemic immunity. In this way, H_2O_2 mediates a reiterative signaling network underlying systemic, as well as local, resistance responses (Alvarez et al., 1998). If the strength of the H_2O_2 signaling capacity is analogous to the H_2O_2 accumulation during the micro-HR oxidative burst, it is possible that even moderate changes in catalase activity might compromise the progression of SAR. This could explain the variable *PR* gene expression in the transgenic lines. Our data support a role of H_2O_2 in the signal cascade leading to SAR, as altered catalase gene expression, and consequent induction or suppression of CAT activity in the various transgenic lines, leads to variable *PR* gene expression.

Phenotypic expression of SAR involving the ability of plants inoculated with an incompatible pathogen to restrict a second infection with a compatible pathogen was also examined. Control SR1, as well as the seven transgenic lines, exhibited similar symptoms and ability to restrict the compatible pathogen *Pseudomonas syringae* pv. *tabaci*, at the inoculated area of upper leaves 7 days after the first infection with *Pseudomonas syringae* pv. *syringae.* However, bacterial growth estimated 72 h post-infection was significantly variable among the genotypes. The most effective in restricting bacterial growth was line 2, which was the most sensitive line during HR. This result indicates that a reverse correlation might exist between severity of infection during HR and bacterial growth inhibition during SAR. In support of this view is the fact that at the low end of bacterial growth were lines 2, 1, 7, and 4, which displayed lower steady state *PR*-gene transcript accumulation, and higher levels of bacterial growth during HR. At the high end were lines SR1, 6, 3, and 8, which displayed higher *PR*-gene mRNA levels, and lower levels of bacterial growth during HR. These data point to a possible relationship between severity of the primary infection and early induction of systemic responses.

In several studies light has been proven as a signal capable of inducing defense responses, as well as *PR-1* gene expression in CAT-deficient transgenic tobacco plants (Chamnongpol et al., 1996; Takahashi et al., 1997). We sought to examine the effects of light in our system, as well. Growth under high light conditions affected plant-pathogen interactions in control SR1, as well as in transgenic line 8 plants. At 24 h after inoculation with *Pseudomonas syringae* pv. *syringae*, the HR marker gene *hin1* was expressed at higher levels in control SR1, and lower levels in line 8, plants grown in high light, as compared to plants grown under low light. Early induction and higher expression of *PR-1* was detected in both SR1 and line 8 in high light-grown plants as compared with their low light-grown counterparts. Higher expression continued for SR1 at day 6, but for line 8 was lower than in the low light plants. The effects of light in *PR-5* expression were similar, but less pronounced, than those observed for *PR-1*. It should be noted that the effects concern plants grown first under high light and then transferred to low light for inoculation and further growth. Thus, our data indicate that growth under high light conditions can predispose plants to better resist pathogen attack, and may amplify the local and systemic defense signals. This is supported by the finding that the number of viable bacteria in transgenic line 8 plants grown under low light were significantly greater (average colonies 99.3, SE $\pm$ 19.5), than the number of surviving bacteria in plants grown under high light (average colonies 49.5, SE $\pm$ 12.8), during SAR inoculation with *P. syringae* pv. *tabaci*.

The inhibitory effect of pathogen inoculation on the 35S-driven *Cat2* transgene expression detected under low light can also be observed under high light. Steady state *Cat2* mRNA is lower at day 6 than that detected at day 4 under both light conditions. However, in plants grown under high light mRNA levels are slightly higher.

Resistance to oxidative stress

The ability of maize *Cat2*-expressing transgenic tobacco plants to resist oxidative stress was assessed in treatments with the redox-cycling herbicide MV, which intercepts electrons from various electron transport chains and transfers them to oxygen-generating superoxide. Most of this superoxide is subsequently converted to oxygen and H_2O_2 by the enzymatic action of superoxide dismutases. Attempts have been made to enhance MV tolerance by generating transgenic plants that overexpress different forms of SODs, and targeting them to various cellular compartments (Bowler et al., 1991; Sen Gupta et al., 1993; Slooten et al., 1995). However, these efforts have not always been successful (Tepperman & Dunsmuir, 1990). Also, efforts have been targeted at overexpression and elevation of levels of antioxidant enzymes responsible for reduction of H_2O_2. Again results have not been consistent, and have depend upon the gene used and the subcellular compartment to which the enzyme is targeted (Aono et al., 1991; Broadbent et al., 1995).

After examining the effects of MV on transgenic tobacco expressing the maize *Cat2* gene, our data are consistent with the hypothesis that this highly effective enzyme confers increased resistance to MV induced oxidative stress. Transgenic line 7 suffered significantly lower MV damage than untransformed control plants at moderate and high MV concentrations. This finding is consistent with results reporting enhanced MV-resistance in transgenic tobacco plants expressing the *E. coli katE* catalase gene, under control of the tomato *rbcS3C* promoter, targeted to the chloroplast (Shikanai et al., 1998). The rest of the transgenic lines were resistant only at low MV concentrations (data not shown). This was attributed to weak enhancement of catalase activity and/or transgene inactivation in several of these lines. Enhanced MV resistance of line 7 was detected with moderate elevation of mean CAT activity, supporting the significance of CAT as a cellular sink for H_2O_2 (Willekens et al., 1997). Catalase activity is likely regulated in multiple steps, one of which is the rate of transcription, but several post-transcriptional steps are also involved (Skadsen & Scandalios 1987; Scandalios et al., 1997). Increasing the rate of transcription is likely to speed up protein accumulation and to elevate CAT activity. Use of transgenes driven by the 35S promoter resulted in a small enhancement of CAT activity, as observed in this study and by others (Brisson et al., 1998). Perhaps the use of even stronger promoters will be necessary to attain high and stable CAT activity, in order to determine the magnitude of protection conferred by this enzyme under oxidative stress.

Acknowledgements

We thank P. Lindgren for the *P. syringae* pv. *syringae* isolate B728a and *P. syringae* pv. *tabaci* (ATCC 11528), and for valuable suggestions on infection techniques, S.Y. He for the *hin1* probe, and Novartis for the *PR-1* and *PR-5* probes. Much appreciation is expressed to Stephanie Ruzsa and Sheri Kernodle for expert technical assistance. Research was supported by Grants from USEPA, USDA, and NSF to J.G.S.

References

Al-Kaff NS, Covey SN, Kreike MM, Page AM, Pinder R and Dale PJ (1998) Transcriptional and posttranscriptional gene silencing in response to a pathogen. *Science* **279**: 2113–2115.

Al-Kaff NS, Kreike MM, Covey SN, Pitcher R, Page AM and Dale PJ (2000) Plants rendered herbicide-susceptible by cauliflower mosaic virus-elicited suppression of a 35S promoter-regulated transgene. *Nature Biotech* **18**: 995–999.

Allen R (1995) Dissection of oxidative stress tolerance using transgenic plants. *Plant Physiol* **107**: 1049–1054.

Alvarez ME, Pennell RI, Meijer P-J, Ishikawa A, Dixon RA and Lamb C (1998) Reactive oxygen intermediates mediate a systemic signal network in the establishment of plant immunity. *Cell* **92**: 773–784.

Aono M, Kubo A, Saj H, Natori T, Tanaka K and Kondo N (1991) Resistance to active oxygen toxicity of transgenic *Nicotiana tabacum* that express the gene for glutathione reductase from *Escherichia coli. Plant Cell Physiol* **32**: 691–697.

Beers PF and Sizer IW (1952) A spectrophotometric assay measuring the breakdown of hydrogen peroxide by catalase. *J Biol Chem* **195**: 133–138.

Bevan M (1984) Binary *Agrobacterium* vectors for plant transformation. *Nucl Acids Res* **12**: 8711–8721.

Bi YM, Kenton P, Mur L, Darby R and Draper J (1995) Hydrogen peroxide does not function downstream of salicylic acid in the induction of *PR* protein expression. *Plant J* **8**: 235–245.

Bowler C, Slooten L, Vandenbranden S, Rycke Rd, Botterman J, Sybesma C, Montagu Mv and Inze D (1991) Manganese superoxide dismutase can reduce cellular damage mediated by oxygen radicals in transgenic plants. *EMBO J* **10**: 1723–1732.

Brisson LF, Zelitch I and Havir EA (1998) Manipulation of catalase levels produces altered photosynthesis in transgenic tobacco plants. *Plant Physiol* **116**: 259–269.

Broadbent P, Creissen GP, Kular B, Wellburn AR and Mullineaux PM (1995) Oxidative stress responses in transgenic tobacco containing altered levels of glutathione reductase activity. *Plant J* **8**: 247–255.

Chamnongpol S, Willekens H, Langebartels C, Van Montagu M, Inze D and Van Camp W (1996) Transgenic tobacco with reduced catalase activity develops necrotic lesions and induces pathogenesis-related expression under high light. *Plant J* **10**: 491–503.

Chen Z, Silva H and Klessig DF (1993) Active oxygen species in the induction of plant systemic acquired resistance by salicylic acid. *Science* **262**: 1883–1886.

Church GM and Gilbert W (1984) Genomic sequencing. *Proc Natl Acad Sci USA* **81**: 1991–1995.

Conrath U, Chen ZX, Ricigliano JR and Klessig DF (1995) Two inducers of plant defense responses, 2,6-dichloroisonicotinic acid and salicylic acid, inhibit catalase activity in tobacco. *Proc Natl Acad Sci USA* **92**: 7143–7147.

Covey SN, Al-Kaff NS, Langara A and Turner DS (1997) Plant combat infection by gene silencing. *Nature* **385**: 781–782.

Delaney TP, Uknes S, Vernooij B, Friedrich L, Weymann K, Negrotto D, Gaffney T, Gut Rella M, Kessmann H, Ward E and Ryals J (1994) A central role of salicylic acid in plant disease resistance. *Science* **266**: 1247–1250.

Dellaporta SL, Wood J and Hicks JB (1983) A plant DNA minipreparation: version 2. *Plant Mol Biol Rep* **1**: 19–22.

Dempsey DA and Klessig DF (1994) Salicylic acid, active oxygen species and systemic acquired resistance in plants. *Trends Cell Biol* **4**: 334–338.

Du H and Klessig DF (1997) Role for salicylic acid in the activation of defense responses in catalase-deficient transgenic tobacco. *Mol Plant Microbe Interact* **10**: 922–925.

Flavell RB (1994) Inactivation of gene expression in plants as a consequence of novel sequence duplications. *Proc Nat Acad Sci USA* **91**: 3490–3496.

Gopalan S, Wei W and He SY (1996) *hrp* gene-dependent induction of *hin1*: a plant gene activated rapidly by both harpins and the *avrPto* gene-mediated signal. *Plant J* **10**: 591–600.

Guan L and Scandalios JG (1995) Developmentally related responses of maize catalase genes to salicylic acid. *Proc Natl Acad Sci USA* **92**: 5930–5934.

Halliwell B (1984) *Chloroplast Metabolism – The Structure and Function of Chloroplasts in Green Leaf Cells*. Clarendon Press, Oxford.

Horsch RB, Fry JE, Hoffmann NL, Eichholtz D, Rogers SG and Fraley RT (1985) A simple and general method for transferring genes into plants. *Science* **227**: 1229–1232.

Jorgensen RA, Cuellar RE, Kavanagh TA and Thompson WE (1987) Structure and variation in ribosomal-RNA genes of pea – characterization of a cloned rDNA repeat and chromosomal rDNA variants. *Plant Mol Biol* **8**: 3–12.

Kooter JM, Matzke MA and Meyer P (1999) Listening to the silent genes: transgene silencing, gene regulation and pathogen control. *Trends Plant Sci* **4**: 340–347.

Lamb CJ, Lawton MA, Dron M and Dixon RA (1989) Signals and transduction mechanisms for activation of plant defenses against microbial attack. *Cell* **56**: 215–224.

Leon J, Lawton MA and Raskin I (1995) Hydrogen peroxide stimulates salicylic acid biosynthesis in tobacco. *Plant physiol* **108**: 1673–1678.

Levine A, Tenhaken R, Dixon R and Lamb C (1994) H_2O_2 from the oxidative burst orchestrates the plant hypersensitive disease resistance response. *Cell* **79**: 583–593.

Lowry OH, Rosebrough NJ, Farr AL and Randall RJ (1951) Protein measurment with folin phenol reagent. *J Biol Chem* **193**: 265–275.

Matzke MA and Matzke AJM (1995) How and why do plants inactivate homologous (trans)genes? *Plant Physiol* **107**: 679–685.

Mehdy MC (1994) Active oxygen species in plant defense against pathogens. *Plant Physiol* **105**: 467–472.

Murashige T and Skoog F (1962) A revised medium for rapid growth and bioassays with tobacco tissue cultures. *Physiol Plant* **15**: 473–497.

Neuenschwander U, Vernooij B, Friedrich L, Uknes S, Kessmann H and Ryals J (1995) Is hydrogen peroxide a second messenger of salicylic acid in systemic acquired resistance? *Plant J* **8**: 227–233.

Ni W and Trelease RN (1991) Post-transcriptional regulation of catalase isozyme expression in cotton seeds. *Plant Cell* **3**: 737–744.

Peng M and Kuc J (1992) Peroxidase-generated hydrogen peroxide as a source of antifungal activity *in vitro* and on tobacco leaf disks. *Phytopathology* **82**: 696–699

Redinbaugh MG, Sabre M and Scandalios JG (1990) The distribution of catalase activity, isozyme protein, and transcript in the tissues of the developing maize seedling. *Plant Physiol* **92**: 375-380.

Scandalios JG (1993) Oxygen stress and superoxide dismutases. *Plant Physiol* **101**: 7–12.

Scandalios JG, Guan L and Polidoros AN (1997) Catalases in plants: gene structure, properties, regulation, and expression. In: Scandalios JG (ed.), *Oxidative Stress and the Molecular Biology of Antioxidant Defenses*. (pp. 343–406) Cold Spring Harbor Laboratory Press, New York.

Sen Gupta A, Heinen JL, Holaday AS, Burke JJ and Allen RD (1993) Increased resistance to oxidative stress in transgenic plants that overexpress chloroplastic Cu/Zn superoxide dismutase. *Proc Natl Acad Sci USA* **90**: 1629–1633.

Shikanai T, Takeda T, Yamauchi H, Sano S, Tomizawa K-I, Yokota A and Shigoeka S (1998) Inhibition of ascorbate peroxidase under oxidative stress in tobacco having bacterial catalase in chloroplasts. *FEBS Lett* **428**: 47–51.

Skadsen RW and Scandalios JG (1987) Translational control of photo-induced expression of the *Cat2* catalase gene during leaf development in maize. *Proc Natl Acad Sci USA* **84**: 2785–2789.

Slooten L, Capiau C, Van Camp W, Van Montagu M, Sybesma C and Inze D (1995) Factors affecting the enhancement of oxidative stress tolerance in transgenic tobaco overexpressing manganese superoxide dismutase in the chloroplasts. *Plant Physiol* **107**: 737–750.

Takahashi H, Chen Z, Du H, Liu Y and Klessig DF (1997) Development of necrosis and activation of disease resistance in transgenic tobacco plants with severely reduced catalase levels. *Plant J* **11**: 993–1005.

Tepperman JM and Dunsmuir P (1990) Transformed plants with elevated levels of chloroplastic SOD are not more resistant to superoxide toxicity. *Plant Mol Biol* **14**: 501–511.

Thompson WF, Everett M, Polans NO, Jorgensen RA and Palmer JD (1983) Phytochrome control of RNA levels in developing pea and mung bean leaves [*Pisum sativum*, *Vigna radiata*]. *Planta* **158**: 487–500.

Vernooij B, Friedrich L, Morse A, Reist R, Kolditz Jawhar R, Ward E, et al. (1994) Salicylic acid is not the translocated signal responsible for inducing systemic acquired resistance but is required in signal transduction. *Plant Cell* **6**: 959–965.

Ward ER, Uknes SJ, Williams SC, Dincher SS, Wiederhold DL, Alexander DC, et al. (1991) Coordinate gene activity in response to agents that induce systemic acquired resistance. *Plant Cell* **3**: 1085–1094.

Willekens H, Chamnongpol S, Davey M, Schraudner M, Langebartels C, Van Montagu M, et al. (1997) Catalase is a sink for H_2O_2 and is indispensable for stress defense in C3 plants. *EMBO J* **16**: 4806–4816.

Wu G, Shortt BJ, Lawrence EB, Levine EB, Fitzsimmons KC and Shah DM (1995) Disease resistance conferred by expression of a gene encoding H_2O_2-generating glucose oxidase in transgenic potato plants. *Plant Cell* **7**: 1357–1368.

Wu G, Short BJ, Lawrence EB, Leon J, Fitzsimmons KC, Levine EB, et al. (1997) Activation of host defense mechanisms by elevated production of H_2O_2 in transgenic plants. *Plant Physiol* **115**: 427–435.

Available online at www.sciencedirect.com
SCIENCE DIRECT®
Plant Science 166 (2004) 1235–1243
PLANT SCIENCE
www.elsevier.com/locate/plantsci

Isolation of three homologous *AP1*-like MADS-box genes in crocus (*Crocus sativus* L.) and characterization of their expression

Athanasios S. Tsaftaris [a,b,*], Konstantinos Pasentsis [a], Ioannis Iliopoulos [a], Alexios N. Polidoros [a]

[a] *Institute of Agrobiotechnology, CERTH, 6m km Charilaou-Thermis Road, P.O. Box 361, Thermi GR-57001, Greece*
[b] *Department of Genetics and Plant Breeding, AUTh, Thessaloniki GR-54006, Greece*

Received 11 July 2003; received in revised form 30 December 2003; accepted 30 December 2003

Abstract

We have cloned and characterized the expression of three homologous Apetala1-like (*AP1*-like) genes from a crocus variety (*Crocus sativus* L) cultivated exclusively in Kozani, at northern Greece. The three different homologous genes were designated *CsAP1* (*C. sativus AP*ETALA*1*) and each one was named *CsAP1a*, *CsAP1b*, and *CsAP1c*. They are the first reported MADS-box genes isolated from this important monocot species cultivated for its flowers.

The deduced amino acid sequence of the three genes indicated high homology with members of the MADS-box family of transcription factors, and particularly with other members of the AP1-like family of MADS-box proteins that control floral-meristem and floral-organ identity. All the isolated sequences lack the typical CaaX-motif that is present in dicot AP1 functional proteins but absent in the monocot homologues thus far examined. CsAP1a and CsAP1b are more similar having 88.2% identical amino acids while CsAP1c is more divergent having 70.9% similarity with CsAP1a, and 64.5% similarity with CsAP1b. Phylogenetic analysis of the isolated genes at the amino acid level indicated that they form a clade with other monocot AP1-like genes from maize (ZmM28), barley (BM3), and rice (OsMADS18). Southern experiments indicated the presence of additional AP1-like homologues in crocus.

Expression analysis indicated the presence of different amount of steady-state mRNAs for all the three homologous genes in leaves, as well as, in the three mature flower parts, namely: tepals, stamen and carpels. Similar expression pattern display many monocot AP1-like MADS-box genes, which comprise a distinct phylogenetic clade of monocot class A MADS-box genes and may reflect a novel, yet unidentified role of their corresponding proteins in these species.
© 2004 Elsevier Ireland Ltd. All rights reserved.

Keywords: MADS-box genes; *Crocus sativus* L.; Floral-organ; AP1-like

1. Introduction

Crocus (*C. Sativus* L.), a monocot triploid species belonging to the Iridaceae family, is cultivated for its red stigmatic lobes that constitute saffron, mainly in southern Europe, Iran, and India. It is popular because of its delicate aroma and attractive color and can be used as a food additive, as well as in medicine and the coloring industry. Saffron has three main chemical components that confer the bright yellow color (crocein), a bitter taste (picrocrocein), and a spicy aroma (saffronal). The flowers of crocus are bisexual. Perianth has no distinct sepals and it only consists of six petaloid tepals in two whorls. Androecium consists of three distinct stamens and the gynoecium consists of a single compound pistil of three carpels, a single three-branched style, and an inferior ovary. The flower is sterile.

Crocus blooms only once a year and its collection period in southern Europe is very short (3–4 weeks in October–November). The method of crocus cultivation contributes greatly to its high price. *C. Sativus* requires a strict agroclimatic condition for growth, which has an influence on its quality. To produce high quality saffron, each flower is harvested by hand, and after mechanical separation of tepals, the stigmas are separated by hand from stamens, sorted, and dried. The size of individual stigmas and the amount of style collected from each flower influence total yield and quality of saffron. Between 70,000 and 200,000 flowers are needed to produce 1 kg of dried saffron threads, which equates to

* Corresponding author. Tel.: +30-2310-498271; fax: +30-2310-498270.
E-mail address: tsaft@certh.gr (A.S. Tsaftaris).

0168-9452/$ – see front matter © 2004 Elsevier Ireland Ltd. All rights reserved.
doi:10.1016/j.plantsci.2003.12.037

around 370–470 h of work. Consequently, the cultivation of this crop for its flowers and particularly the separation of its stigmas is very labor intensive leading to very high costs.

Among a number of genes controlling flower development, the floral-organ identity genes, including the so called A, B, and C class homeotic genes, determine the fate of floral-organ primordia. In arabidopsis and other angiosperms, the class A genes lead to the formation of sepals in whorl 1, class A and B genes together lead to the formation of petals in whorl two, the class B and C genes specify the formation of stamens in whorl three, and the class C genes are required for the formation of carpels [1–3]. In this ABC model, A and C genes interact in a mutually antagonistic manner.

Many of the A, B, and C class homeotic genes are members of the MADS-box multigene family encoding putative transcription factors which are characterized by a conserved DNA-binding/dimerization domain. Most of plant MADS proteins initially described, consist of a stereotypic organization of conserved domains. The highly conserved MADS domain is located at the amino-terminal end of the protein spanning 60 amino acids, and is involved in promoter DNA-binding and protein–protein interactions. A second conserved domain of about 70 amino acids, the K-box, is located in the central region of the protein and is able to form coiled-coil structures that may promote dimerization [4]. Two other domains, the I and C-domains are less conserved. Evidence suggests that the C-domain is necessary for the formation of higher order MADS multimers [5]. Recent phylogenetic analysis in *Arabidospis* has led to the proposal of two evolutionary lineages represented by type I and type II MADS-box genes, which differ both in the amino acid sequence of the MADS-box as well as in the domain structure of the predicted protein (for review see [6]). Type I factors lack the K-box, conforming a structure with a MADS-box followed by a rather undefined and length-variable domain, while most of type II factors exhibit the typical MIKC structure [6]. Further fine analysis of phylogenetic relationships among the members of the *Arabidospis* MADS-box transcription factors suggested the presence of five subfamilies one of which is the MIKC (type II) subfamily and the others named Mδ (type II) and Mα, Mβ, Mγ (type I) subfamilies [7].

In angiosperm plants, most of the MADS genes are expressed in reproductive tissue, where they control floral-meristem and floral-organ development, but are also important regulators of flowering time and cell-type specificity in floral organs [8]. Some MADS genes, particularly in monocot species, are expressed in non-floral tissues, suggesting that their role may not only be restricted to the control of flower development [9–13]. Until now MADS genes have been cloned from *Arabidopsis*, which contain 107 genes encoding MADS-box proteins, 84% of which are of unknown function [7], and a variety of mostly dicot plant species, few monocots, as well as, non-flowering plants such as gymnosperms and ferns.

Understanding flower development in crocus could reveal ways to increase yield and lower production costs since flower and more specifically isolated stigmas comprise the valuable commercial part of the plant. Despite the high industrial and medicinal importance and value of crocus flowers, there are no reports on MADS genes and their control in flower development in this plant. Therefore, in order to uncover and understand the molecular mechanisms that control flower development and possible homeotic changes in crocus, we made an effort to clone and characterize crocus MADS-box genes. Here, we describe the cloning and characterization of three different homologous *CsAP1* genes, namely *CsAP1a*, *CsAP1b*, and *CsAP1c*, the first reported MADS-box genes isolated from flowers and leaves of cultivated crocus.

2. Materials and methods

2.1. Plant material

C. sativus var. Kozani field growing plants were collected from Kozani, Greece. Sampling was during the late flowering season in October, and samples were flowers and leaves. As the flower of crocus has not distinct sepals and petals, we treated separately the three tepals of the outer whorl and designated them as sepals, while the three tepals of the inner whorl were designated petals. Tissues were separated and immediately frozen in liquid nitrogen and stored at −80 °C until used.

2.2. DNA Isolation, PCR amplification, and sequencing

Genomic DNA was isolated from leaves using the DNeasy Plant Mini Kit (Qiagen) according to the manufacturer's protocol. For amplification of the MADS-box sequences, two degenerate primers were used. Primer MADS-F, 5′-ATCSAGATMAARAGRATHGARAA-3′, corresponding to the MADS-box conserved amino acid sequence: I(E/Q) IKRIE(N/K) and primer MADS-R, 5′-CATCTTGCCAGWRYTAGMRAARAT-3′ corresponding to the conserved amino acid sequence: IF(A/S)(N/S)(S/T)GKM of the MADS genes [14].

PCR was performed as previously described [15]. A 150 bp PCR product was subcloned into the pGEM T easy Vector (Promega) according to the manufacturer's protocol. Sequencing was performed using a LiCor 4200 sequencer. Using the cloned MADS-box fragment as template a digoxigenin labeled DNA probe was synthesized (MADS-probe) using the PCR DIG Probe Synthesis Kit (Roche). This probe was used to monitor the specificity of the PCR products obtained by different primer combinations and to screen individual clones in Southern blots after hybridization using standard techniques.

2.3. Inverse PCR

We used inverse PCR to amplify the flanking sequences of the isolated MADS-box clone. One microgram genomic DNA was digested with *Eco*RI, *Hind*III, and a combination of *Bam*HI and *Bgl*II in a total volume of 25 μl. The reactions were incubated at 80 °C for 10 min to inactivate the restriction enzymes, diluted to 500 μl with 1 × ligation buffer and supplemented with two Weiss units T4 DNA ligase (NEB). After 2 h incubation at 25 °C the DNA was precipitated with ethanol, resuspended in 10 μl sterile water and used as template in PCR experiments. Two sequence specific primers based on the sequence of the previously isolated MADS clone were designed for PCR. These were: Inv1: 5′-GCGCTTCGAGAAGGTGACCTG-3′ and Inv2: 5′-GGCGGCCTCCTCAAGAAAGC-3′. The PCR was performed using 2 μl of the digested and ligated genomic DNA as template, 0.2 μM of the primers Inv1 and Inv2, 0.2 mM dNTPs and 1.25 U Platinum Taq Polymerase (Invitrogen). The thermocycler program was: 2 min at 94 °C, 35 cycles of 1 min at 94 °C, 30 s at 59 °C, 3.5 min and 10 s per cycle at 72 °C and a final extension step of 10 min at 72 °C.

The PCR products were separated on an agarose gel, but were not visible after EtBr staining. Therefore, the gel was blotted on Nylon membrane and hybridized with the digoxigenin labeled MADS-box probe. After development, one hybridized band of about 500 bp derived from the *Hind* III digest could be identified. In order to obtain sufficient DNA for cloning, a reamplification experiment was performed using 1 μl of the initial PCR as template. The rest of the conditions were the same except that the annealing was at 57 °C and the DyNAzyme II DNA polymerase (Finnzymes) was used. Several strong bands could be observed. A Southern blot was performed as described above and only the 500 bp band of the *Hind* III digest gave a strong hybridization signal with the MADS-probe. This band was cut out from the gel, purified with the Qiaex Purification Kit (Qiagen), cloned in the pGEM T easy vector and sequenced.

2.4. RNA Isolation, cDNA synthesis, and cloning

Total RNA from leaves, closed flowers (3 cm in length), sepals, petals, stamens, and carpels was extracted using the RNeasy Plant Mini Kit (Qiagen). On-column digestion of DNA during RNA purification was performed using the RNase-Free DNase Set (Qiagen). The 3′ end of the cloned fragments was isolated by 3′ RACE. First strand cDNA synthesis was performed using 2 μg total RNA, 1 μg 3′ RACE Adapter Primer 5-GGCCACGCGTCGACTAGTAC$(T)_{17}$-3, (Gibco-BRL), 1 mM dNTPs and 200 U M-MuLV reverse transcriptase (NEB) in 50 μl total volume. Specific forward primers were MADS-A: 5′-CCTTACTGCACACAGCGAATC-3′ (designed from the sequence of the PCR product obtained by the Inv1–Inv2 primer pair) for *CsAP1a*, Inv2 for *CsAP1b*, and MADS-F for *CsAP1c*. Ten percent of the synthesized cDNA from closed flowers (*CsAP1a*) or leaves (*CsAP1b* and *CsAP1c*) was used as template in a PCR reaction with 0.2 pmol forward primer, 0.2 pmol Abridged Universal Amplification primer (AUA) 5′-GGCCACGCGTCGACTAGTAC-3′ (Gibco-BRL), 0.2 mM dNTPs and 1 U DyNAzyme II DNA polymerase (Finnzymes). The thermocycler program was: 1 min at 94 °C, 35 cycles of 30 s at 94 °C, 30 s at 56 °C, 1.5 min at 72 °C and a final extension step of 10 min at 72 °C. PCR products were subcloned into a pGEM T easy vector according to the manufacturer's protocol.

To obtain the cDNA's 5′ end, an RNA ligase-mediated rapid amplification reaction was performed, starting with 3.5 μg total RNA pooled from leaves and closed flowers, using the GeneRacer Kit (Invitrogen) according to the manufacturer's instructions. PCR was then performed using the specific primers *CsAP1a* R (5′-AGTCCGAAATGCCATACAACG-3′) for *CsAP1a*, *CsAP1b* R (5′-CATCAGAAGCTTAGCAGATGTA-3′) for *CsAP1b*, and *CsAP1c* R (5′-GATAGAAATCCCCAAGTACACT-3′) for *CsAP1c*. Amplified fragments were then cloned into pCR 4-TOPO vector using the TOPO TA cloning Kit (Invitrogen).

2.5. Southern hybridization

Ten microgram genomic DNA was digested with *Eco*RI, *Hind* III, and *Bam*HI, (enzymes from NEB) and transferred to a positive charged Nylon membrane. The filter was hybridized with the MADS-box probe described in Section 2.2, stripped with 0.2 M NaOH/0.1% SDS for 10 min at 37 °C (twice), and reprobed with a *CsAP1a* gene-specific 401 bp fragment (708–1109 bp). The digoxigenin labeled *CsAP1a* gene-specific probe was prepared with PCR using the cloned *CsAP1a* cDNA as template with the primers *CsAP1a* F (5′-AATGGCACAGCAGGGACACTG-3′) and *CsAP1a* R, and the PCR DIG Probe Synthesis Kit. Hybridization was performed with DIG Easy Hyb buffer at 42 °C according to the manufacturer and stringent washes at 68 °C in 0.5 × SSC/0.1% SDS (twice). Detection was performed using the DIG Luminescent Detection Kit according the instructions and chemiluminescense was detected using the GeneGnome Bio Imaging System (Syngene).

2.6. Comparison and phylogenetic analysis

The nucleotide and deduced amino acid sequence of the *CsAP1a*, *CsAP1b*, and *CsAP1c* cDNAs were used for BLAST searches on the GenBank/EMBL/DDBJ databases, and among the best BLAST hits, 19 class A floral identity genes for which there are published reports, were selected for comparison. Sequence names were changed to include initials of the species where needed. The sequences were: *Betula pendula* BpMADS5 (X99655) and BpMADS3 (X99653) [16]; *Eucalyptus globulus* EgAP1 (AF305076) [17]; *Capsicum annuum* CanMADS6 (AF130118) [18]; *Pisum sativum* PsPEAM4 (AJ279089) [19]; *Arabidopsis*

lyrata AlAP1 (AF143379) [20]; *Arabidopsis thaliana* AtAP1 (Z16421) [21]; *Sinapis alba* SaAP1 (X81480) [22]; *Brassica oleracea* BoAP1 (Z37968) [23]; *Lolium temulentum* LtMADS1 (AF035378) and LtMADS2 (AF035379) [13]; *Oryza sativa* OsAP1-L (AB041020) [24], OsMADS14 (AF058697) [25], OsMADS15 (AF058698) [25], OsMADS28 (CAB56800) and OsMADS18 (AAF04972) [25]; *Hordeum vulgare* HvMADS3 (originally BM3, CAB97351) [26]; *Zea mays* ZmM28 (AJ430695) [27] and ZmMADS3 (AF112150) [27,28]. The deduced amino acid sequences of the genes together with CsAP1 were aligned using the multiple sequence alignment program Clustal W [29]. Phylogenetic relationships of the sequences were performed using the Neighbor-Joining Method with p-distance correction [30]. The tree was constructed using the MEGA 2.1 software [31].

2.7. Expression analysis

Total RNA (1 μg) extracted from sepals, petals, stamens, and carpels was used in a reverse transcription reaction as previously described. PCR was performed in 1 × PCR buffer, 0.2 mM dNTPs, 0.4 pmol forward primer, 0.4 pmol reverse primer, and 1 U of the DyNAzyme II DNA polymerase (Finnzymes) having as template 1/10 of the synthesized cDNA. Primers were *CsAP1a* F and *CsAP1a* R for *CsAP1a*, *CsAP1b* F (5′-GAATTATTTGAGCAGCATCATAT-3′) and *CsAP1b* R for *CsAP1b*, *CsAP1c* F (5′-CGCTCTGTTAATGGATAGTATCC-3′) and *CsAP1c* R for *CsAP1c*, and: actin2-F (5′-CCGGTGTCATGGTTGGTAT-3′) and actin2-R (5′-GCAGGCACATTGAAGGTCT-3′) amplifying a fragment of the actin-beta gene as a control. The cycling parameters were incubation at 94 °C for 1 min, followed by 35 cycles of incubation at 94 °C for 30 s, 50 °C (*CsAP1b* and *CsAP1c*) or 54 °C (*CsAP1a* and actin-beta) for 30 s, 72 °C for 30 s and a final extension step of 5 min at 72 °C. A control RT-PCR was included for each sample using as template total RNA without reverse transcriptase at the same dilution as the cDNA template. The PCR products were separated on a 1.8% agarose gel and amplification products of the expected size could be observed.

Quantitative expression analysis of the isolated *CsAP1a* gene was performed with real-time RT-PCR using an Opticon (MJ Research) real-time PCR system. PCR was performed in 1 × PCR buffer, 0.2 mM dNTPs, 0.4 pmol *CsAP1a* F primer, 0.4 pmol *CsAP1a* R primer, 0.2 × Sybr-Green (Sigma) and 1 U of the DyNAzyme II DNA polymerase (Finnzymes) having as template 1/10 of cDNA synthesized from 2.5 μg of total RNA extracted from leaves and closed flowers. Actin-beta was used as a control for relative gene expression quantification. The cycling parameters were incubation at 95 °C for 1 min, followed by 33 cycles of incubation at 95 °C for 15 s, 52 °C for 30 s, 72 °C for 30 s, plate read at 80 °C and a final extension step of 5 min at 72 °C. For identification of the PCR products a melting curve was performed from 65 to 95 °C with read every 0.2 °C and 10 s hold between reads. A control RT-PCR was included for each sample using as template total RNA without reverse transcriptase at the same dilution as the cDNA template. The reactions were performed in triplicate. Relative quantification was performed using the Q-Gene software for estimation of the normalized gene expression [32].

3. Results

3.1. Cloning of three MADS-box Apetala1-like cDNAs from C. sativus

Three homologous MADS-box Apetala1-like cDNAs designated *CsAP1a*, *CsAP1b*, and *CsAP1c*, were isolated from *C. sativus* using a combination of PCR techniques. *CsAP1a* (1281 bp, GenBank accession number AY337928) was isolated from flowers and contain a 750 bp ORF, which encodes for a 250 amino acid predicted polypeptide. *CsAP1b* (1164 bp, GenBank accession number AY337929) and *CsAP1c* (1257 bp, GenBank accession number AY337930) were isolated from leaves and contain a 735 bp ORF, which encodes for a 244 amino acid predicted polypeptide, and a 741 bp ORF, which encodes for a 246 amino acid predicted polypeptide, respectively. The sequences of the three *CsAP1* cDNAs were more homologous in the coding region spanning the MADS, I and K domains while were more divergent at the C terminal domain and the 5′ and 3′ untranslated regions. A microsatellite locus was revealed at the 5′ untranslated region of *CsAP1a* and *CsAP1b* consisting of a $(GA)_5$ and a $(GA)_{19}$ repeat, respectively.

3.2. Amino acid sequence comparisons, phylogenetic analysis, and copy number of AP1-like genes in crocus

Based on the amino acid sequence similarity of the entire coding region, the three CsAP1 homologous deduced protein sequences can be grouped into Apetala1-like family of proteins [33]. Published genes that belong to the Apetala1 family of proteins and showed high degree of homology to the three CsAP1 were selected for the multiple alignment process (Fig. 1). The MADS domain of the aligned proteins is highly conserved and conserved regions are also observed in the I and K domains, while the C terminal domain is more divergent. In this comparison the three CsAP1 homologues -a, -b, and -c present 87, 82, and 84% identity, 92, 92, and 91% similarity to the consensus AP1-like proteins MADS-box domain and 64, 59, 51% identity, 79, 77, 76% similarity to the consensus K-box of the AP1-like proteins, respectively. The three CsAP1 proteins lack at the C-terminus the CFAA motif, a typical CaaX box recognition motif for farnesyltransferase (FTase). CaaX-boxes (where C is Cys, a is an aliphatic amino acid, and X is Cys, Met, Ser, Ala or Glu) are present in many AP1-like dicot proteins (Fig. 1).

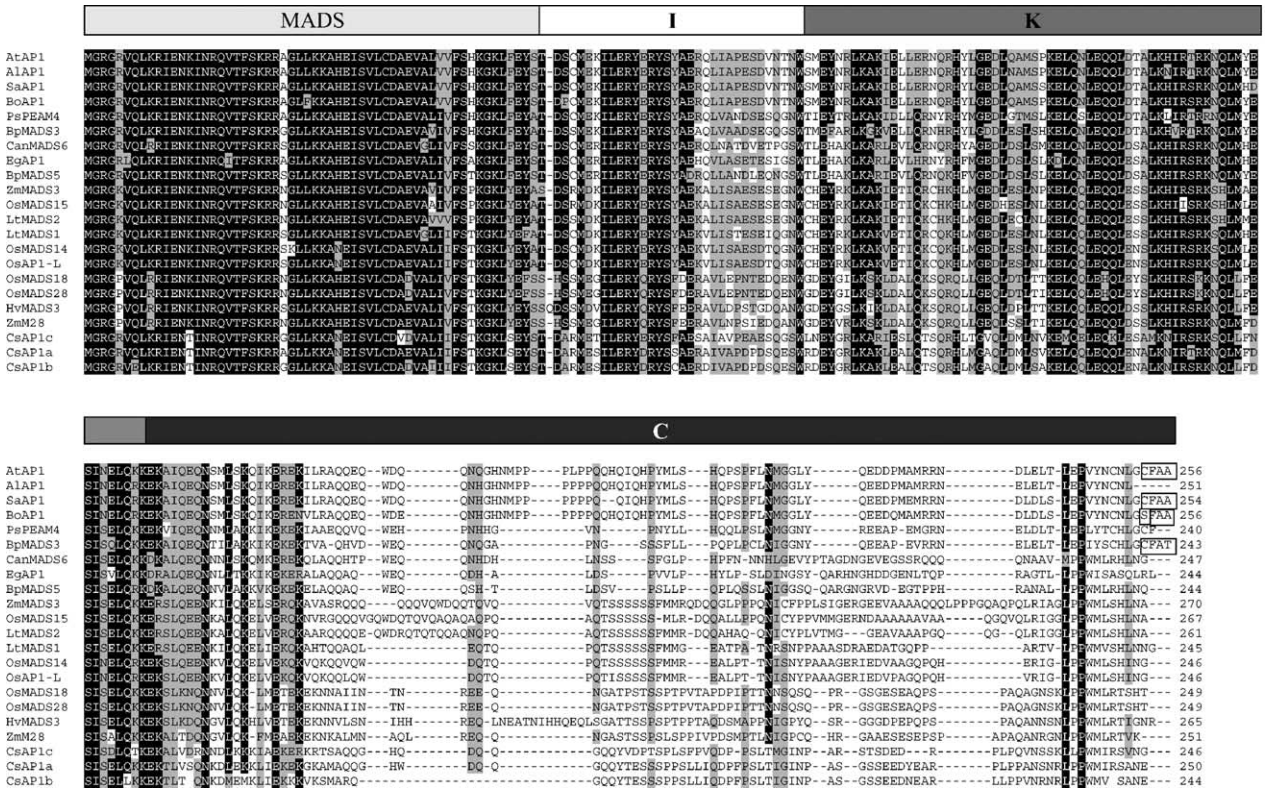

Fig. 1. Alignment of the predicted amino acid sequences of the three CsAP1 proteins and members of the AP1 family in other plants. The CaaX box motif at the C-terminus of BpMADS3, AtAP1, and SaAP1 that is conserved between AP1 and functional homologues from distantly related plant species is boxed, and the substituted cysteine of this box in BoAP1 is boxed separately. Identical amino acids in all proteins are in white letters highlighted by black background, while identical amino acids in more than 75% of the sequences are highlighted by grey background. Dashes indicate gaps to maximize alignment. The MADS-box, I , K, and C-domains are shown by boxes on top of the alignment. The alignments were generated using ClustalW.

The higher BLAST similarity scores between each of the three homologues CsAP1 crocus proteins and sequences in the GenBank were recorded for MADS-box proteins of plants belonging to the class of Liliopsida (monocots). The highest score was for a monocot orchid hybrid (*Dendrobium grex* Madame Thong-In) MADS-box protein DOMADS2 (AAF13261.1) [34] with 61% identity and 74% similarity for CsAP1a, 57% identity and 71% similarity for CsAP1b, and 58% identity and 72% similarity for CsAP1c. Next higher scores for CsAP1a and CsAP1b were for the maize ZmM28 (CAD23441) and the rice OsMADS28 (CAB56800) and OsMADS18 (AAF04972) proteins. For CsAP1c next higher scores were for the chrysanthemum MADS-box transcription factor CDM8 (AAO22981), the *B. pendula* BpMADS3 (CAA67967), and a carrot MADS-box transcription factor (CAC81068).

A phylogenetic tree was calculated for the full length amino acid sequence of the three CsAP1 proteins and the selected Apetala1-like proteins using the Neighbor-Joining Method (Fig. 2). The three CsAP1 proteins fall in a group with the maize ZmM28 MADS-box protein, the barley BM3 (HvMADS3), and the rice OsMADS18 and OsMADS28.

Southern blot experiments revealed the presence of additional putative *AP1*-like orthologs in crocus (Fig. 3). Multiple bands were observed with the MADS-box probe indicating the large number of MADS-box genes in crocus many of which may be *AP1*-like homologues. The *CsAP1a* gene-specific probe revealed three high molecular weight bands after *Bam*HI digestion (there is no *Bam*HI restriction site within the three *CsAP1* mRNA sequences), six after *Hind* III digestion (in *CsAP1a* and *CsAP1b* there is a *Hind* III internal site) and six bands after *Eco*RI digestion (in *CsAP1a-c* no *EcoR*I site exist within the mRNA of the genes, however, there is an *Eco*RI site within an intron of the *CsAP1a* gene (data not shown)). Since no further genomic information is currently available we concluded, based on the results from the *Bam*HI digest, that three homologous genes were hybridized to our probe. With *CsAP1a,b,c* being homologous to each other it is reasonable to predict that these three genes were detected on the membrane.

3.3. Expression analysis

Initial experiments on cDNAs derived from leaves and closed flowers revealed the presence of the *CsAP1a* transcript in both tissues. A real-time PCR experiment was performed to provide quantitative estimation of *CsAP1a* expression. The results indicated that the normalized expression level of the *CsAP1a* transcript is almost double in leaves than that in flowers (Fig. 4).

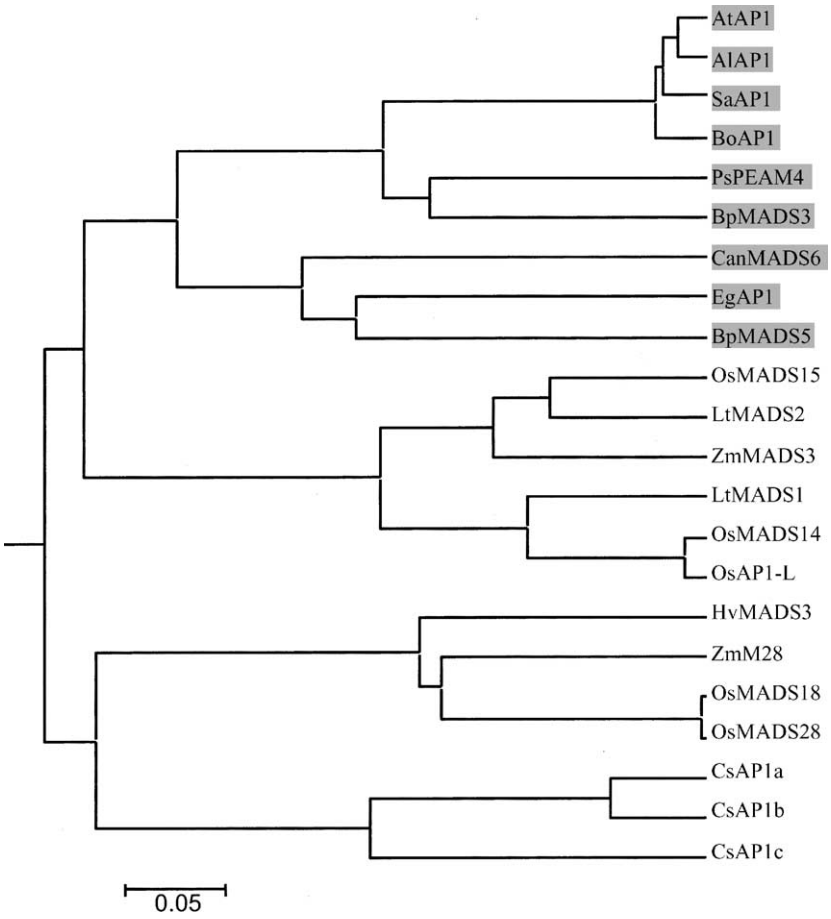

Fig. 2. Phylogenetic relationships of the protein sequences aligned in figure 1. The tree was generated by the Neighbor-Joining method using the p-distance correction. Dicot genes are highlighted in gray. The three CsAP1 sequences are grouped with the maize ZmM28, the barley HvMADS3, and the rice OsMADS18, and OsMADS28.

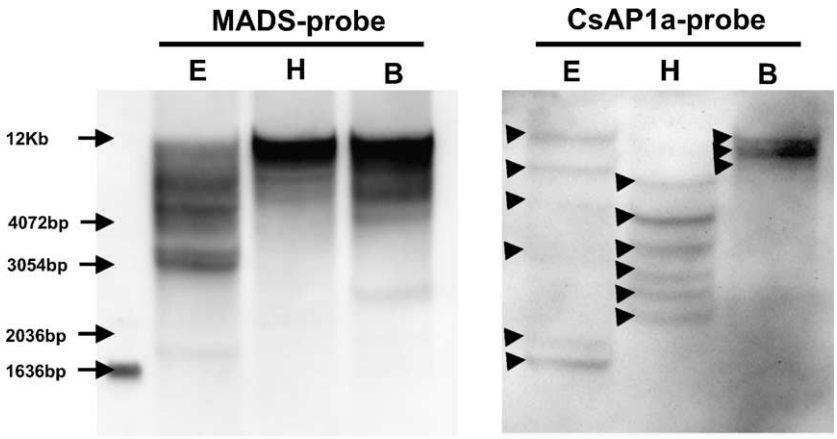

Fig. 3. Southern blot revealing the presence of additional putative AP1 orthologs in crocus. Ten microgram crocus genomic DNA digested with *EcoR*I (E), *Hind* III (H) and *Bam*HI (B), was hybridized with the MADS-box probe described in Section 2.2, stripped and reprobed with a CsAP1a gene-specific 401 bp fragment (708–1109 bp). Multiple bands were observed with the MADS-box probe indicating the large number of MADS-box genes in crocus many of which may be AP1-like homologues. The CsAP1a gene-specific probe hybridized with three high molecular weight bands after BamHI digestion, six after Hind III digestion and six bands after *Eco*RI digestion. Since no further genomic information is currently available the *Bam*HI digestion hybridization pattern suggests that three homologous genes were hybridized to our probe. With *CsAP1a,b,c* being homologous to each other it is reasonable to predict that these three genes were detected on the membrane.

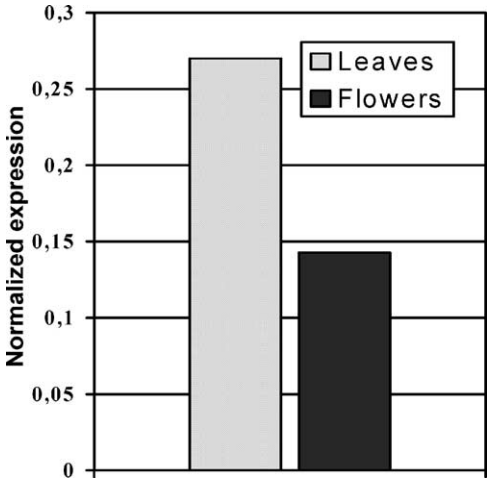

Fig. 4. The mean normalized CsAP1a expression in crocus leaves and flowers as determined by real-time PCR and analyzed using the Q-Gene software.

The expression pattern of all the three homologous genes in leaves and flowers was compared by RT-PCR (Fig. 5). Results show that transcripts of each gene are present in leaves, as well as, in flowers of crocus. The expression pattern of the three genes was also examined in different flower tissues (Fig. 5A). The RT-PCR experiment performed with cDNA synthesized from sepals, petals, stamens, and carpels resulted in the identification of the *CsAP1a*, *CsAP1b*, and *CsAP1c* transcripts in all tissues examined (Fig. 5B). In all the expression experiments the actin-beta gene (Fig. 5C) was used as an RT-PCR positive control. In addition, all the experiments included a negative RT-PCR control using a template that was prepared in a similar manner except that reverse transcriptase was omitted in cDNA synthesis. No amplification could be observed in the negative controls (data not shown).

4. Discussion

In our effort to isolate MADS-box transcription factor genes and assess their involvement in flower development in *C. sativus*, we followed a PCR-based approach and we were able to isolate and examine the expression of three homologous MIKC-type (type II) Apetala1-like MADS-box cDNAs.

AP1 of *Arabidopsis* and its homologue *SQUAMOSA* (*SQUA*) in *Antirrhinum* are MADS-box genes belonging to the SQUA subfamily (also termed AP1/AGL9 clade) which includes MADS-box genes from many other plant species [35]. *AP1* and *SQUA* are key regulatory genes specifying floral-meristem identity in both *Arabidopsis* and *Antirrhinum*. Despite many similarities in their sequence, expression, and functions, only *AP1* appears to have the additional role of class A floral identity gene specifying sepal and petal identity in *Arabidopsis*. There is scarce evidence regarding how the different functions of *AP1*-like genes are conserved between different species. Analysis of the *PEAM4* pea *AP1* functional homologue, from a plant with different floral morphology and inflorescence architecture than that of *Arabidopsis* and *Antirrhinum*, suggested that the *AP1*-like gene dual role in the control of both

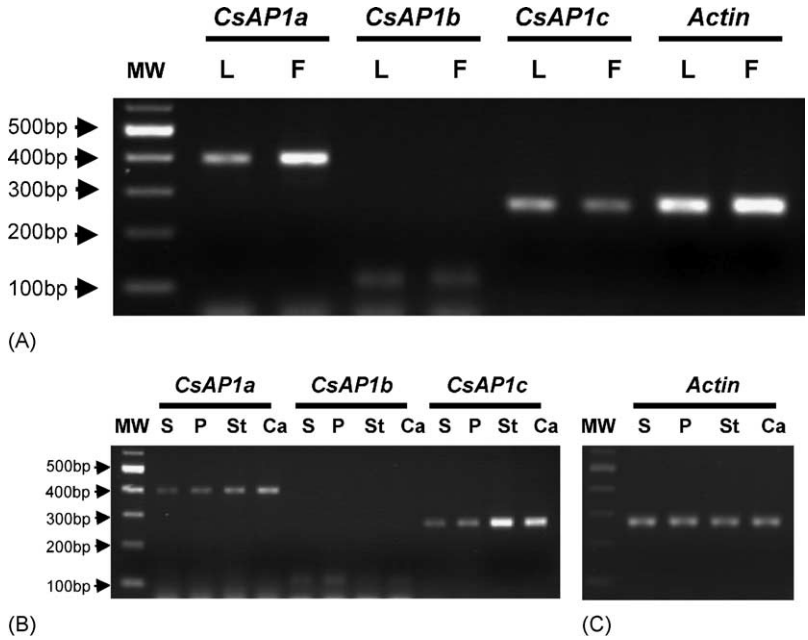

Fig. 5. (A) RT-PCR analysis of the three homologous genes *CsAP1a*, *CsAP1b*, *CsAP1c*, expression in crocus leaves and flowers, (B) different crocus flower tissues and (C) the actin control. Lanes are: MW, 100 bp size marker; L, Leaves; F, Flower; S, Sepals (the three tepals of the outer whorl); P, Petals (the three tepals of the inner whorl); St, Stamens; Ca, Carpels. Amplicons of the expected size are observed. The PCR bands for *CsAP1b* are faint due to the small size of the product and possibly to low target amount or efficiency of amplification.

floral-meristem and floral-organ identity is not restricted to *Arabidopsis*, but can be conserved in species with diverse floral morphologies, such as pea [36]. The *CsAP1* sequence similarity with *AP1*-like genes is not adequate to infer a functional role of these genes in crocus. There are several differences between *AP1* and the three *CsAP1* genes that have to be considered. In *Arabidopsis*, expression of *AP1* occurs specifically in the tissues and at the developmental stage in which floral fate is assumed. In the flower, expression of *AP1* is restricted to petals and sepals. In contrast, RT-PCR experiments revealed that the three *CsAP1* genes are expressed in leaves, as well as in all the flower organs examined. The amino acid sequence of *AP1* and many of its dicot homologues terminates in CFAA (Fig. 1), a typical CaaX box recognition motif for farnesyltransferase (FTase). AP1 is a target of FTase and farnesylation alters the function and perhaps specificity of the transcription factor [37]. The three *CsAP1* genes lack a CaaX-box at the C-terminus, and this, additional to the above mentioned differences, probably suggest divergence from the typical arabidopsis *AP1*-function. Other genes with structural similarity to *AP1* have different expression patterns and function, as for example the *FRUITFULL* (*FUL*) gene (previously called *AGL*8) that is weakly expressed in rosette leaves during vegetative development and is subsequently strongly upregulated in the shoot apex upon the transition to flowering. Experimental evidence suggests that *FUL* regulates the transcription of genes required for cellular differentiation during fruit and leaf development [38].

The three isolated *CsAP1* genes from crocus, are *AP1*-like MADS-box genes expressed in vegetative as well as in all floral tissues of the plant. There are also several examples of MADS-box genes belonging to different homeotic classes that are expressed in vegetative tissues and have different functional roles [9–13]. It is conceivable that despite the high level of sequence similarity between *AP1*-like MADS-box genes their expression profile can be quite different. Functional analysis will have to show whether these genes have AP1 function in inflorescence development.

Sequence similarities between the three *CsAP1* genes were higher in the MADS, I and K domains, while the C-domain was more divergent. This is consistent with other studies reporting similar results. Experimental data based on southern hybridization after digestion with different restriction enzymes indicated that multiple MADS-box genes (and possibly more *AP1*-homologues) were present in this species. However, the three isolated homologous *AP1*-like crocus genes were the only with enough similarities at the C-terminus domain to be detected after hybridization with a probe specific for one of them (Fig. 3). Phylogenetic analyses along with 19 class A floral identity genes showed that the three CsAP1 proteins fell in a group with ZmM28, a typical apetala1-like MADS-box representative of maize. This clade also comprise OSMADS18 from rice and BM3 from barley [27]. There are no published data on the expression pattern of ZMM28. OsMADS18 (previously known as FDRMADS 7) is expressed in all rice plant tissues with higher level in the inflorescence. Initially, it is detected in the spikelet apical meristem, and at a later stage, when flower organ primordia differentiate, it is abundantly detectable throughout the organ primordia. When the spikelet reaches maturity its expression is not detected in the lodicules (which are considered as a reduced perianth in rice) or the sterile glumes. OsMADS18 shares considerable sequence similarity with OsMADS14 (previously known as FDRMADS 6) but its expression pattern is quite distinct. OsMADS14 expression is detectable only in flowers and when all organ primordia have developed, its expression appear to be specifically localized in developing stamens and pistil [39]. BM3 is abundantly expressed in all organ primordia and the vascular tissue of the barley floret throughout inflorescence development. Its expression can also be detected in vegetative tissues (nodes and leaves) [26]. The similarities in expression pattern of many monocot *AP1*-like MADS-box genes, including the rice *OsMADS*18, the barley *BM3*, the three isolated in this study crocus *CsAP1* genes, as well as other such genes with floral and vegetative expression may indicate a novel class of MADS-box genes in monocots, and possibly reflect a novel, yet unidentified role of the corresponding proteins as transcriptional regulators in these species.

The three isolated class A crocus MADS-box genes constitute a start point for our studies of flower development in crocus. We have recently isolated several class B and class C MADS-box genes of crocus and characterized their expression (manuscripts in preparation). Experiments are underway to further characterize the possible specific role(s) of each gene in crocus that will enable us to infer a flower development model of this plant, to understand the formation of a number of mutant flowers observed in the field, and define ways to enhance its productivity exploiting molecular genetic techniques.

Acknowledgements

We thank Yiannis Patsios for his help in collecting plant material in the field.

References

[1] V.F. Irish, Patterning the flower, Dev. Biol. 15 (1999) 211–220.
[2] H. Ma, C. dePamphilis, The ABCs of floral evolution, Cell 101 (2000) 5–8.
[3] G. Theissen, Development of floral-organ identity: stories from the MADS house, Curr. Opin. Plant Biol. 4 (2001) 75–85.
[4] Y. Yang, L. Fanning, T. Jack, The K domain mediates heterodimerization of the *Arabidopsis* floral-organ identity proteins, APETALA3 and PISTILLATA, Plant J. 33 (2003) 47–59.
[5] T. Honma, K. Goto, Complexes of MADS-box proteins are sufficient to convert leaves into floral-organs, Nature 409 (2001) 525–529.
[6] F. Garcia-Maroto, M.-J. Carmona, J.-A. Garrido, M. Vilches-Ferron, J. Rodrigez-Ruiz, D. Lopez Alonso, New roles for MADS-box genes in higher plants, Biol. Plant 46 (2003) 321–330.

[7] L. Parenicova, S. de Folter, M. Kieffer, D.S. Horner, C. Favalli, J. Busscher, H.E. Cook, R.M. Ingram, M.M. Kater, B. Davies, G.C. Angenent, L. Colombo, Molecular and phylogenetic analyses of the complete MADS-box transcription factor family in Arabidopsis: new openings to the MADS world, Plant Cell 15 (2003) 1538–1551.
[8] T. Jack, Plant development going MADS, Plant Mol. Biol. 46 (2001) 515–520.
[9] E.R. Alvarez-Buylla, S.J. Liljegren, S. Pelaz, S.E. Gold, C. Burgeff, G.S. Ditta, F. Vergara-Silva, M.F. Yanofsky, MADS-box gene evolution beyond flowers: expression in pollen, endosperm, guard cells, roots and trichomes, Plant J. 24 (2000) 457–466.
[10] H. Zhang, B.G. Forde, An Arabidopsis MADS-box gene that controls nutrient-induced changes in root architecture, Science 279 (1998) 407–409.
[11] M. Skipper, Genes from the APETALA3 and PISTILLATA lineages are expressed in developing vascular bundles of the tuberous rhizome, flowering stem and flower Primordia of *Eranthis hyemalis*, Ann. Bot. (Lond.) 89 (2002) 83–88.
[12] C.G. van der Linden, B. Vosman, M.J. Smulders, Cloning and characterization of four apple MADS-box genes isolated from vegetative tissue, J. Exp. Bot. 53 (2002) 1025–1036.
[13] G.F. Gocal, R.W. King, C.A. Blundell, O.M. Schwartz, C.H. Andersen, D. Weigel, Evolution of Floral-meristem Identity Genes. Analysis of Lolium temulentum Genes Related to APETALA1 and LEAFY of Arabidopsis, Plant Physiol. 125 (2001) 1788–1801.
[14] K. Kitahara, S. Hirai, H. Fukui, S. Matsumoto, Rose MADS-box genes 'MASAKO BP and B3' homologous to class B floral identity genes, Plant Sci. 161 (2001) 549–557.
[15] K. Kitahara, S. Matsumoto, Rose MADS-box genes 'MASAKO C1 and D1' homologous to class C floral identity genes, Plant Sci. 151 (2000) 121–134.
[16] A. Elo, J. Lemmetyinen, M.L. Turunen, L. Tikka, T. Sopanen, Three MADS-box genes similar to APETALA1 and FRUITFULL from silver birch (*Betula pendula*), Physiol. Plant 112 (2001) 95–103.
[17] J. Kyozuka, R. Harcourt, W.J. Peacock, E.S. Dennis, Eucalyptus has functional equivalents of the Arabidopsis AP1 gene, Plant Mol. Biol. 35 (1997) 573–584.
[18] S.-K. Sung, Y.-H. Moon, J.-E. Chung, S.-Y. Lee, H.G. Park, G. An, Characterization of MADS-box genes from hot pepper, Mol. Cells 11 (2001) 352–359.
[19] A. Berbel, C. Navarro, C. Ferrandiz, L.A. Canas, F. Madueno, J.P. Beltran, Analysis of PEAM4, the pea AP1 functional homologue, supports a model for AP1-like genes controlling both floral-meristem and floral-organ identity in different plant species, Plant J. 25 (2001) 441–451.
[20] A.L. Lawton-Rauh, E.S. Buckler IV, M.D. Purugganan, Patterns of molecular evolution among paralogous floral homeotic genes, Mol. Biol. Evol. 16 (1999) 1037–1045.
[21] M.A. Mandel, C. Gustafson-Brown, B. Savidge, M.F. Yanofsky, Molecular characterization of the Arabidopsis floral homeotic gene APETALA1, Nature 360 (1992) 273–277.
[22] G. Menzel, K. Apel, S. Melzer, Isolation and analysis of SaMADS C, the APETALA 1 cDNA homolog from mustard, Plant Physiol. 108 (1995) 853–854.
[23] R.G. Anthony, P.E. James, B.R. Jordan, The cDNA sequence of a cauliflower apetala-1/squamosa Homolg, Plant Physiol. 108 (1995) 441–442.
[24] J. Kyozuka, T. Kobayashi, M. Morita, K. Shimamoto, Spatially and temporally regulated expression of rice MADS-box genes with similarity to Arabidopsis class A, B and C genes, Plant Cell Physiol. 41 (2000) 710–718.
[25] Y.H. Moon, H.G. Kang, J.Y. Jung, J.S. Jeon, S.K. Sung, G. An, Determination of the motif responsible for interaction between the rice APETALA1/AGAMOUS - LIKE9 family proteins using a yeast two-hybrid system, Plant Physiol. 120 (1999) 1193–1204.
[26] J. Schmitz, R. Franzen, T.H. Ngyuen, F. Garcia-Maroto, C. Pozzi, F. Salamini, W. Rohde, Cloning, mapping and expression analysis of barley MADS-box genes, Plant Mol. Biol. 42 (2000) 899–913.
[27] T. Münster, W. Deleu, L.U. Wingen, M. Ouzunova, J. Cacharrón, W. Faigl, S. Werth, J.T.T. Kim, H. Saedler, G. Theißen, Maize MADS-box genes galore, Maydica 47 (2002) 287–301.
[28] S. Heuer, S. Hansen, J. Bantin, R. Brettschneider, E. Kranz, H. Lorz, T. Dresselhaus, The maize MADS-box gene *ZmMADS3* affects node number and spikelet development and is co-expressed with *ZmMADS1* during flower development, in egg cells, and early embryogenesis, Plant Physiol. 127 (2001) 33–45.
[29] J.D. Thompson, D.G. Higgins, T.J. Gibson, CLUSTAL W: improving the sensitivity of progressive multiple sequence alignment through sequence weighting, positions-specific gap penalties and weight matrix choice, Nucleic Acids Res. 22 (1994) 4673–4680.
[30] N. Saitou, M. Nei, Neighbor-joining Method, Mol. Biol. Evol. 4 (1987) 406–425.
[31] S. Kumar, K. Tamura, I.B. Jakobsen, M. Nei, MEGA2: molecular evolutionary genetics analysis software, Bioinformatics 17 (2001) 1244–1245.
[32] P.Y. Muller, H. Janovjak, A.R. Miserez, Z. Dobbie, Processing of gene expression data generated by quantitative real-time RT-PCR, BioTechniques 32 (2002) 1372–1378.
[33] J.L. Riechmann, E.M. Meyerowitz, MADS domain proteins in plant development, Biol. Chem. 378 (1997) 1079–1101.
[34] H. Yu, C.J. Goh, Identification and characterization of three orchid MADS-box genes of the AP1/AGL9 subfamily during floral transition, Plant Physiol. 123 (2000) 1325–1336.
[35] G. Theissen, A. Becker, A. Di Rosa, A. Kanno, J.T. Kim, T. Munster, K.-U. Winter, H. Saedler, A short history of MADS-box genes in plants, Plant Mol. Biol. 42 (2000) 115–149.
[36] A. Berbel, C. Navarro, C. Ferrandiz, L.A. Canas, F. Madueno, J.-P. Beltran, Analysis of PEAM4, the pea AP1 functional homologue, supports a model for AP1-like genes controlling both floral-meristem and floral-organ identity in different plant species, Plant J. 25 (2001) 441–451.
[37] S. Yalovsky, M. Rodríguez-Concepcion, K. Bracha, G. Toledo-Ortiz, W. Gruissem, Prenylation of the floral transcription factor APETALA1 modulates its function, Plant Cell 12 (2000) 1257–1266.
[38] Q. Gu, C. Ferrándiz, M.F. Yanofsky, R. Martienssen, The *FRUITFULL* MADS-box gene mediates cell differentiation during *Arabidopsis* fruit development, Development 125 (1998) 1509–1517.
[39] H.W. Jia, R. Chen, B. Cong, K.M. Cao, C.R. Sun, D. Luo, Characterization and transcriptional profiles of two rice MADS-box genes, Plant Sci. 155 (2000) 115–122.

Research article

The maize alternative oxidase 1a (*Aox1a*) gene is regulated by signals related to oxidative stress

Alexios N. Polidoros[1], Photini V. Mylona[2], Konstantinos Pasentsis[1], John G. Scandalios[3], Athanasios S. Tsaftaris[1,4]

[1]*Institute of Agrobiotechnology, Center for Research and Technology Hellas, Thermi, Greece*
[2]*Agricultural Research Center of Macedonia-Thrace, NAGREF, Thermi, Greece*
[3]*Department of Genetics, North Carolina State University, Raleigh, North Carolina, USA*
[4]*Department of Genetics and Plant Breeding, Aristotle University of Thessaloniki, Thessaloniki, Greece*

We isolated and characterized the expression of *Aox1a*, a member of the maize alternative oxidase (*Aox*) small multigene family. *Aox1a* consists of four exons interrupted by three introns and its promoter harbors diverse stress-specific putative regulatory motifs pointing to complex regulation and response to multiple signals. Responses of *Aox1a* to such signals were examined and compared with those of maize glutathione S-transferase I (*GstI*), a typical oxidative stress inducible gene. Potassium cyanide (KCN) and hydrogen peroxide (H_2O_2) induced a rapid increase of the *Aox1a* and *GstI* transcripts, which was persisted in prolonged treatment at high H_2O_2 concentration only for *Aox1a*. High concentration of salicylic acid (SA) and salicyl hydroxamic acid (SHAM) induced *Aox1a* mRNA only after prolonged exposure, while *GstI* displayed an early strong induction, which declined thereafter. Nitric oxide (NO) induced a high increase of *Aox1a* after prolonged exposure at high concentration, while *GstI* displayed a weak response. Our results show that multiple signaling pathways, involved in stress responses, also participate and differentially regulate *Aox1a* and *GstI* in maize. A ROS-depended signaling event may be involved, suggesting an essential role of *Aox1a* under oxidative stress in maize.

Keywords: Alternative oxidase, glutathione S-transferase, reactive oxygen species, nitric oxide, salicylic acid, mitochondrial respiration

Introduction

Plant mitochondria are different from those of animals as their electron transport chain contains a number of components that enable non-coupled respiration. Among them, the best characterized is the cyanide-resistant alternative terminal oxidase (AOX), a homodimeric di-iron protein, which transfers electrons via an alternative pathway from the ubiquinone pool directly to oxygen.[1] Because the alternative pathway branches in electron transport at the ubiquinone pool, its contribution to energy balance is one-third that of the cytochrome pathway. The physiological role of such a 'wasteful' respiratory pathway has been linked to thermogenesis during anthesis in arum lilies,[2] and has been suggested to operate as a passive overflow mechanism under conditions where the cytochrome chain is restricted,[3] or function to prevent reactive oxygen species (ROS) formation produced as a result of impaired or restricted respiratory activity.[3,4]

Received 31 August 2004
Revised 24 January 2005
Accepted 26 January 2005

Correspondence to: Alexios N. Polidoros PhD, Institute of Agrobiotechnology, Center for Research and Technology Hellas, 6th km. Charilaou-Thermis Rd, 57001 Thermi, Greece
Tel: +30 2310498273; Fax: +30 2310498270;
E-mail: alexios@certh.gr

Abbreviations: Aox, alternative oxidase; Gst, glutathione S-transferase; H_2O_2, hydrogen peroxide; KCN, potassium cyanide; NO, nitric oxide; ROS, reactive oxygen species; SHAM, salicyl hydroxamic acid; SNP, sodium nitroprusside

DOI 10.1179/135100005X21688
© W. S. Maney & Son Ltd

Table 1. The primers used in this study

Abbreviation	Description	Sequence	Synthesis
3RAP	3′-RACE adapter primer	5′-GGCCACGCGTCGACTAGTAC$(T)_{17}$-3′	Gibco-BRL
SAoxF	Short AoxF	5′-GCTGCGGTGCCGGGAATGGT-3′	Custom
SAoxR	Short AoxR	5′-CGGCGCGGACGACGGTGACTA-3′	Custom
AUP	Abridged universal amplification primer	5′-GGCCACGCGTCGACTAGTAC-3′	Gibco-BRL
LAoxF	Long AoxF	5′-GATCGGAATTCGCAACTT-3′	Custom
LAoxR	long AoxR	5′-AGCACCTCTCGCACTTAG-3′	Custom
InvF	Inverse forward	5′-CGAGTGGAAGTGGACTTGCT-3′	Custom
InvR	Inverse reverse	5′-TGGACATAAGCCGTAGCATG-3′	Custom

The alternative oxidase protein is found in every plant species examined thus far, and in almost every plant organ. It is encoded by a small gene family that exhibits highly conserved regions.[5–8] This family is divided in two discrete gene subfamilies. *Aox1* is most widely known for its induction by stress stimuli in many tissues and is present in both monocot and dicot plant species. *Aox2*, on the other hand, is usually constitutive or developmentally expressed in eudicot species but is absent from the genomes of all monocot species examined to date.[9] Differential tissue and developmental regulation of *Aox* genes has been reported in *Arabidopsis*,[10] soybean[9,11,12] and rice.[13]

Aox genes also respond differentially to various biotic and abiotic stresses,[7,14,15] pathway-specific mitochondrial electron transport chain inhibitors,[8,12,15] hormones and signaling molecules, particularly ROS,[3,14,15] salicylic acid[2,12] and nitric oxide.[16,17] Overall, the above studies are in good agreement with the proposed AOX function as a means to prevent ROS formation during aberrant or restricted respiratory activity.[3,4,15]

In maize, limited data are available on the *Aox* gene family, gene structure, role, and regulation of expression. Preliminary studies suggested that a maize *Aox* sequence (GenBank accession no: AF040566) could be induced in maize seedlings by salicylic acid (SA) treatment.[18] Three full-length maize *Aox* cDNAs were then detected that were specifically expressed at high levels in maize mitochondrial mutants.[19] Data on the gene structure and regulation of expression of the *Aox* gene family of maize are largely missing.

To study the maize *Aox* gene family further, we isolated and investigated structural and regulatory aspects of the maize *Aox1a* gene. We examined the *Aox1a* responses after treatment with mitochondrial inhibitors, and the signaling molecules NO, SA and H_2O_2. The responses were compared with those of *GstI*, a typical oxidative stress inducible maize gene and a hypothesis for the role of oxidative signaling in *Aox1a* expression is suggested.

Materials and Methods

Plant material and treatments

The maize inbred line B73 was used in this study. Seeds were surface sterilized, planted in soil mix, and grown in a chamber under a 16-h light/8-h dark cycle at 22°C and 70% relative humidity for 2 weeks. Fifteen days post imbibition (15 dpi) seedlings were derooted and the shoot was submerged in 50-ml tubes containing the mitochondrial respiratory inhibitors KCN and SHAM, the NO releasing compound SNP, or SA at the concentrations indicated in each experiment. Control plants were placed in tubes containing water. The plants were then placed back in the growth chamber for the indicated duration in each experiment. Treatments with H_2O_2 were on detached leaves submerged in the appropriate concentration of H_2O_2 in water, vacuum infiltrated for 2.5 min and incubated for the indicated duration in the growth chamber. Controls were prepared from leaves submerged in water.

Primers

The primers used in this study are presented in Table 1.

RNA isolation, cDNA synthesis and 3′-RACE

Total RNA was extracted using the RNeasy plant mini kit (Qiagen, Hilden, Germany) with on-column digestion of DNA with the RNase-Free DNase Set (Qiagen). First strand cDNA synthesis was performed using 2 μg total RNA, 1 μg 3′-RAP primer, 1 mM dNTPs and 200 units M-MuLV reverse transcriptase (NEB, Beverly, USA) in 50 μl total volume.

An *Aox1a*-specific probe was synthesized by PCR using cDNA template with the SAoxF and SAoxR primer pair and subcloned into a pGEM T easy vector (Promega, Madison, WI, USA).

The 3′-end of the transcript was isolated by 3′-RACE using either SAoxF or LAoxF as forward and the AUP reverse primer and the DyNAzyme II DNA polymerase (Finnzymes, Espoo, Finland). PCR products were subcloned into a pGEM T easy vector (Promega) according to the manufacturer's protocol.

DNA isolation, PCR amplification and sequencing

Genomic DNA was isolated from leaves using the DNeasy plant mini kit (Qiagen) according to the manufacturer's protocol. PCR was performed with the LAoxF and LaoxR primer pair, and the products were subcloned and sequenced. Inverse PCR[20] was used to amplify the 5′-flanking sequence of the isolated *Aox1a* fragment. Genomic DNA (1 μg) was digested with *Nco*I, *Pst*I, *Spe*I, and *Sph*I, the enzymes were heat inactivated, the DNA fragments were self-ligated with 2 Weiss units T4 DNA Ligase (NEB) for 2 h at 25°C and used as template in PCR with the primers InvF and InvR. The PCR products were separated on an agarose gel, blotted on Nylon membrane and hybridized with a 190-bp digoxigenin labeled probe prepared using the LAoxF and InvR primer pair and the PCR DIG Probe Synthesis Kit (Roche, Mannheim, Germany). A band derived from the *Nco*I digest could be identified and was re-amplified, cut out from the gel, purified with the Qiaex purification kit (Qiagen), cloned in the pGEM T easy vector and sequenced.

Expression analysis

Leaf material was harvested after treatment with each compound. All samples were frozen in liquid nitrogen and stored at –80°C for analysis. Total RNA from leaf material was extracted as previously described,[21] separated on denaturing 1.6% agarose gels, stained with ethidium bromide to ensure equal loading, and transferred to nylon membranes. Digoxigenin-labeled DNA probes were synthesized using the PCR DIG Probe Synthesis Kit (Roche).

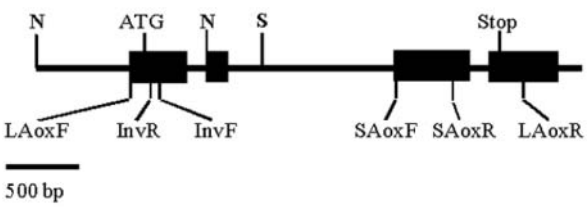

Fig. 1. Schematic representation of the *Aox1a* genomic sequence. The filled boxes indicate coding regions. The translation start ATG and the stop positions, as well as the restriction sites for *Nco*I (N) and *Spe*I (S) are indicated above the scheme. The positions and the labels of the PCR primers used to isolate the gene are indicated below the scheme.

An *Aox* probe was prepared using the SAoxF–SAoxR primer pair and a *GstI* probe was prepared as previously described.[21] Hybridization was performed with DIG Easy Hyb buffer (Roche) at 50°C according to the manufacturer and washes were at 68°C in 0.5x SSC/0.1% SDS. Detection was performed using the DIG Luminescent Detection Kit (Roche) according the instructions and chemiluminescence was detected using the GeneGnome Bio Imaging System (Syngene, Cambridge, UK). Duplicate expression analysis experiments were performed and representative results are presented.

RESULTS

The Aox1a *transcript has alternative polyadenylation sites*

The 3′-end of the *Aox1a* cDNA was isolated by 3′-RACE using the SAoxF primer. This fragment was almost identical to an EST sequence (GenBank accession no. AY059647) which encoded a full-length maize alternative oxidase open reading frame[19] and probably represented the *Aox1a* mRNA. To confirm this, we performed 3′-RACE with a new primer (LAoxF) that was designed from the AY059647 sequence and located upstream of the transcription start codon. Eight clones derived from the LAoxF and 5 clones from the SAoxF primers were sequenced. The sequence of these clones was identical to the AY059647 for the overlapping regions as expected, because in both cases the same maize inbred line B73 was used as nucleic acid source. Sequencing revealed alternate polyadenylation in the *Aox1a* mRNA. The length of the 3-untranslated region in bases, the number and the percentage of clones detected for each UTR size are shown in Table 2. A majority of the clones (40%) had the same UTR length with the previously deposited AY059647 sequence, but several clones were shorter and one clone was 31 nucleotides longer. The sequence of the 31 additional bases can be found at the 3′-end of the genomic *Aox1a* sequence (GenBank accession no. AY485264).

Isolation of the Aox1a *gene*

In order to isolate a genomic *Aox1a* clone, we designed an LAoxR primer based on the sequence of the 3′-UTR of the cDNA and used it in combination with the LAoxF primer in PCR having genomic maize DNA as template. The reaction amplified a 2500-bp gene fragment encompassing 1219-bp coding sequence and suggesting that it was interrupted by 1281-bp intron(s). Complete sequencing of the fragment revealed that the maize *Aox1a* gene consists of 4 exons interrupted by 3 introns

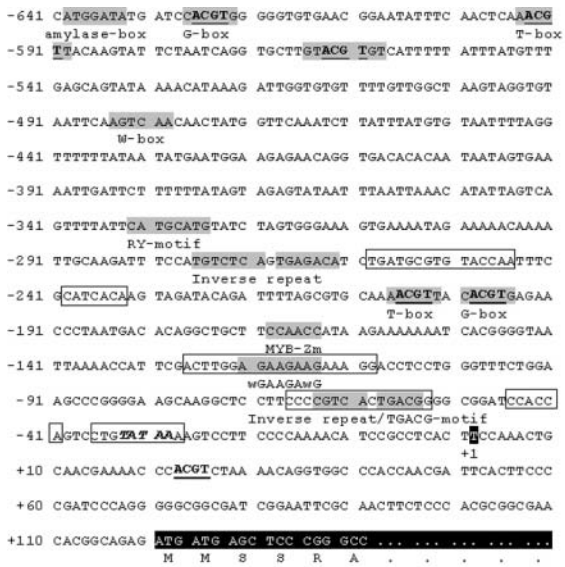

Fig. 2. Nucleotide sequence of the maize *Aox1a* promoter. The promoter spans 641 nucleotides upstream of the transcription initiation +1 (white letter over black background). Promoter motifs are shaded gray and positions of G-box, T-box, W-box, MYC, RY, MYB-Zm, the inverse repeat, the TGACG motif, and the *Aox*-specific wGAAGAwG motif, are shown. The ACGT-core sequence is bold and underlined. The TATA-box is shown in bold italics. Sequences identical between rice and maize *Aox1a* genes are boxed. Translated sequence is shown with white letters over black background for orientation.

(Fig. 1). The exact intron insertion positions were predicted using the Spidey software at NCBI (<http://www.ncbi.nlm.nih.gov/IEB/Research/Ostell/Spidey/>). All introns are typical in structural characteristics of plant introns, being A+T rich (50% for intron 1, 60% for intron 2, and 55% for intron 3) and containing 5′-splice donor GT and 3′-splice acceptor AG signals.[22] The relative intron–exon positions are conserved between the maize *Aox1a* gene and its rice homologue.

A 653-bp promoter sequence of the *Aox1a* gene was isolated using an inverse PCR approach[20] and was searched for plant-specific *cis*-acting regulatory elements that serve as binding sites for transcription factor using the PLACE[23] and the PlantCARE[24] databases. Numerous motifs were recognized indicating the complex nature of *Aox1a* regulation in maize, and the most relevant are highlighted in Figure 2. These include a perfect TATA box at –34 relative to the transcription start site (+1), and the motifs TGACG, ACGT core sequence, W-box (TTGAC), CCAACC (MYB-Zm), which are present in numerous stress-activated plant gene promoters.[25–27]

The maize *Aox1a* promoter was compared with its rice counterpart and several highly homologous regions were observed (identical regions are shown in boxes in Fig. 2). Particularly, the immediate upstream the TATA-box region between –40 and –130 was 73.4% homologous, and the TGACG-motif (as inverse repeat) within this region was conserved between the two promoters. The TGACG motif is conserved in the promoters of soybean *GmAox2b* and *Arabidopsis AtAox1a* and *AtAox1b* genes, and in addition a wGAAGAwG motif is conserved in soybean *GmAox2a* and *Arabidopsis AtAox1c*.[28]

With the sequences of all the cloned fragments we compiled the *Aox1a* gene contig. All clones were sequenced from both ends and no ambiguities remained after the compilation of the contig. The sequence of the *Aox1a* gene can be found at the GenBank under the accession number AY485264.

Expression analysis

Expression analysis demonstrated different patterns of early and late responses of *Aox1a* and *GstI* in hydroponically treated seedlings to mitochondrial respiration inhibitors (KCN, SHAM) and signaling molecules (SA, NO). In short (1–5 h) treatments, *Aox1a* was effectively induced only by KCN (after 2.5 h) and declined thereafter (Fig. 3A). All other compounds caused negligible effects. In contrast, *GstI* transcript could be detected in each treatment within 1 h, and increased with SA, KCN, and SHAM after 2.5 h. The highest accumulation was observed at 5 mM SA followed by 0.5 mM KCN and 5 mM SHAM, while NO had no effect. *GstI* transcript was still higher than the control for the above-mentioned treatments at 5 h, although at lower magnitude than that observed at 2.5 h. Prolonged (28 h) exposure to the tested compounds caused a high increase of *Aox1a* transcript at 7.5 mM SNP and a moderate increase at 5 mM SA and 5 mM SHAM, while KCN had no effect (Fig. 3B). In contrast, *GstI* transcript accumulation was slightly higher than the control level at the higher concentration of each compound tested.

Finally, the effect of H_2O_2, a ROS, metabolic by-product, and signaling molecule in plants[29] was examined in vacuum infiltrated leaves (Fig. 4). Our results revealed that *Aox1a* responded rapidly to H_2O_2 and the steady-state mRNA level of the gene increased as soon as within 30 min exposure at all the applied concentrations. Increased accumulation of *Aox1a* transcript was detected thereafter only at high (100 mM) H_2O_2 concentration, reaching a maximum at 5 h. Interestingly, the H_2O_2 concentration-dependent *Aox1a* transcript accumulation did not display a linear increase as 10 mM H_2O_2 solution was not as effective as 1 and 100 mM H_2O_2 between 1 and 2.5 h of exposure, something that has also been observed with other genes in maize.[21] *GstI* mRNA accumulation followed a similar induction pattern with the sharp difference that it was barely detectable after 5 h at 100 mM H_2O_2, when the highest induction of *Aox1a*

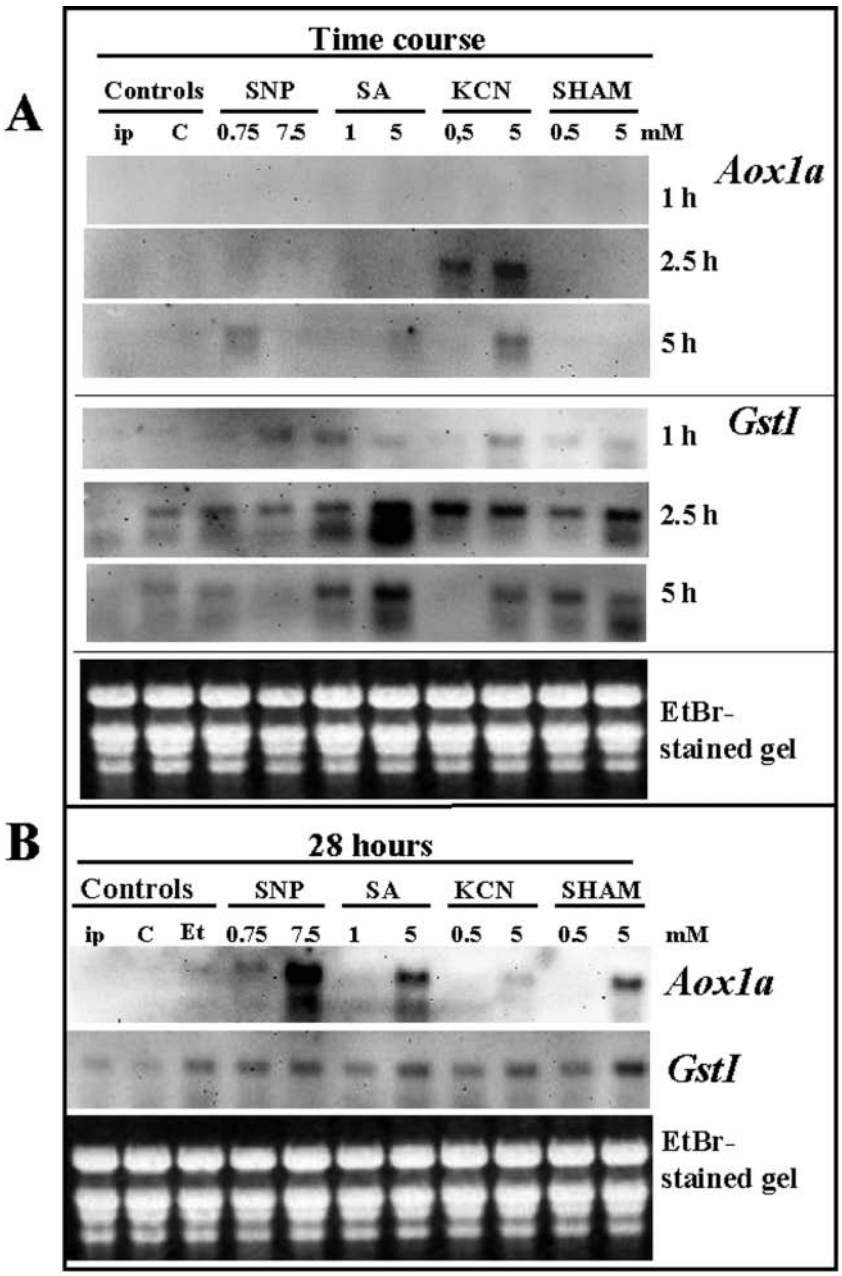

Fig. 3. Effects of mitochondrial pathway-specific inhibitors and signaling molecules on the *Aox1*a and *GstI* gene expression in maize. The cytochrome c pathway inhibitor KCN, the AOX inhibitor SHAM, and the signaling molecules NO (released from SNP) and SA were applied in two concentrations (low and high) and their effects on *Aox1a* and *GstI* gene expression were tested at different time points after short 1–5 h (A) or prolonged 28 h (B) treatment of derooted 2-week old maize seedlings. Northern hybridization was performed with *Aox1a* and *GstI* digoxigenin-labeled gene-specific probes and chemiluminescence was detected using the GeneGnome Bio Imaging System (Syngene). The ethidium bromide stained gel is included as loading control.

occurred. Another important observation was made comparing the 0 mM H_2O_2 controls at the four consecutive time points. Results showed that *Aox1a* as well as *GstI* transcript levels increased within 1 h after submersion of the leaf tissue in distilled water, which reportedly induces hypoxia. *Aox1a* transcript declined thereafter while *GstI* transcript continued to increase at 2.5 h and declined thereafter.

Discussion

The maize *Aox1a* gene consists of four exons and three introns (Fig. 1) like other plant *Aox* genes[6,8,11] pointing to an evolutionary conservation of *Aox* gene structure in diverse plant species. Numerous putative transcription factor-binding sites were detected in the *Aox1a* promoter (Fig. 2). Most of these are stress responsive factor bind-

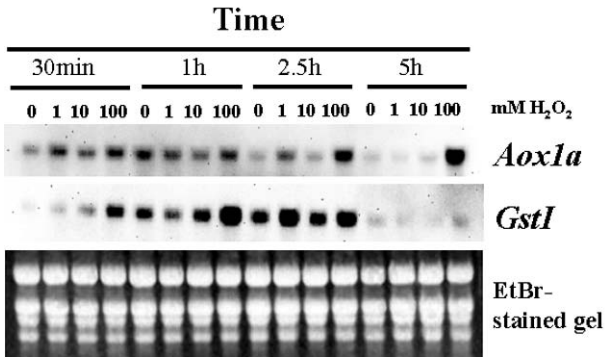

Fig. 4. Effects of H_2O_2 on the *Aox1a* and *GstI* gene expression in maize. Transcript accumulation was determined after 30 min, 1 h, 2.5 h, and 5 h incubation of vacuum-infiltrated leaves with different concentrations of H_2O_2. Northern hybridization was performed with *Aox1a* and *GstI* digoxigenin-labeled gene-specific probes and chemiluminescence was detected using the GeneGnome Bio Imaging System (Syngene). The ethidium bromide stained gel is included as loading control.

ing sites and show significant over-representation in the promoters of stress and defense inducible *Arabidopsis* genes.[25–27] The TGACG motif and a wGAAGAwG motif present in the maize *Aox1a* are conserved in the promoters of soybean and *Arabidopsis Aox* genes[28] and may be critical for specific *Aox* responses in different plant species. The presence of stress-related promoter motifs suggests that the gene is at least partly regulated by stress signals, and its expression is involved in the plant's stress defense responses.

Transcription of *Aox1a* resulted in transcripts with variable length due to alternate polyadenylation that affects a large number of higher eukaryote mRNAs, producing mature transcripts with 3′-ends of variable length. The role of alternate polyadenylation is not very well understood, although it has been suggested to be regulated in a tissue- or disease-specific manner in humans and mouse.[30] The *Aox1a* mRNA used as reverse-transcriptase template derived from 100 mM H_2O_2 treated tissue, and this may indicate stress-specific regulation of polyadenylation. However, preliminary experiments (unpublished results) indicated that both, control and H_2O_2 treated tissues contained the two major mRNA classes shown in Table 2.

Table 2. Alternative polyadenylation of the *Aox1a* transcripts detected by 3′-RACE experiments. The length of the 3-untranslated region in bases, the number, and the percentage of clones detected for each UTR size are shown

3′-UTR size (bp)	Number of clones	%
313	1	6.6
277	6	40.0
252	1	6.6
228	1	6.6
195–201	2	26.6
160	1	6.6
111	1	6.6

Regulation of *Aox* gene expression seems to involve the same signals in different species. However, different *Aox* orthologs may respond variously to these signals. In maize, specific induction of the *Aox1b* transcript was observed in roots of 10 mM KCN-treated seedlings, while *Aox1a* did not respond between 4 and 24 h.[19] Nevertheless, our results clearly showed a transient *Aox1a* transcript induction after KCN application within 2.5 h. The difference between the two studies could be due to the different tissue, and/or different time-points of sampling. It is also possible that *Aox1a* represents an early and *Aox1b* a late response to KCN-induced inhibition of mitochondrial electron transport. Induction of *GstI* transcript accumulation by KCN was very similar with the pattern of *Aox1a*, suggesting that a common mechanism may be underlying.

SHAM is an inhibitor of alternative respiration as it inhibits specifically the alternative and not the cytochrome respiratory pathway.[1] Our data show that SHAM caused an increase in *Aox1a* transcript only after prolonged treatment. We are not aware of other studies examining SHAM effects on *Aox* gene expression. However, SHAM effects may be indirect as it may inhibit other enzymes and also stimulate H_2O_2 production,[31] which could in turn induce *Aox1a* transcription. Unlike the similar effects of KCN on *Aox1a* and *GstI* expression, SHAM caused a rapid induction of *GstI* expression, which may be due to participation of *GstI* in SHAM detoxification processes in plant cells. The rest of the compounds examined, H_2O_2, SA, and NO, are well-characterized signaling molecules that can induce *Aox* responses,[3,17,32] and effectively induced *Aox1a* after short (H_2O_2) or prolonged (SA, NO) exposure. This induction is presumably correlated with increase of the AOX1a protein level since previous reports in several plant species show that increased *Aox* gene expression is correlated with elevated AOX protein.[7,12,33] Particularly in non-chromosomal stripe (NCS) mutant lines of maize, overexpression of *Aox1a* is accompanied with high levels of AOX1a protein in the examined tissues.[19]

Differences between the *Aox1a* hybridization signals with those of *GstI* were observed. Although ROS signaling is involved in the regulation of both genes, different ROS can induce different gene-specific responses. Additionally, there are probably other signaling events that contribute to gene-specific induction. The rapid response of *GstI* to SA could be due to a SA-dependent pathway, as could be the NO response of *Aox1a* due to a NO-dependent pathway. Individual *Gst* genes have been shown to be SA-inducible in *Arabidopsis* as well as in

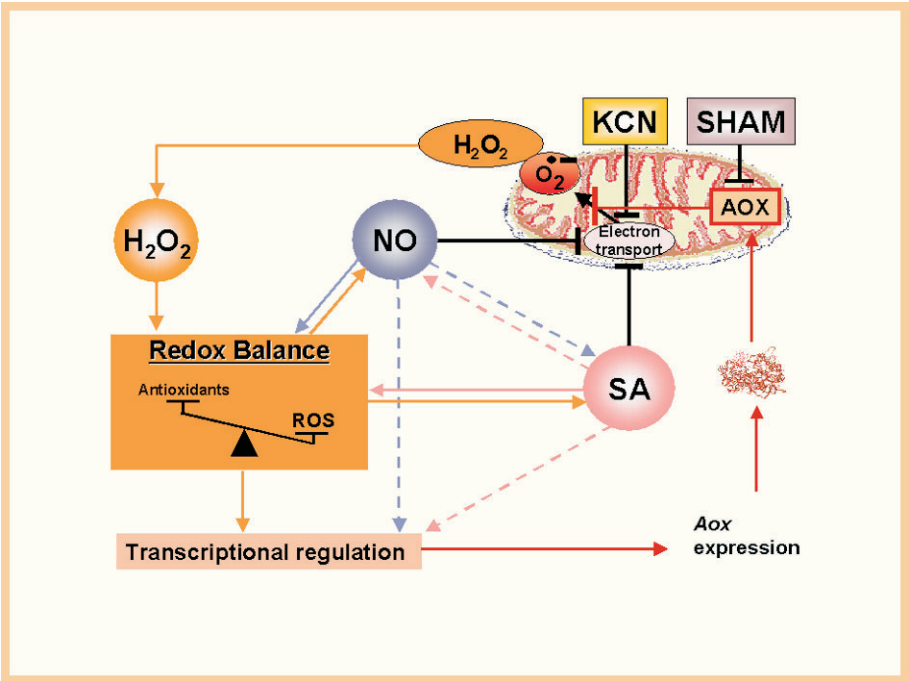

Fig. 5. Simple schematic depiction of the hypothetical central role of ROS in the regulation of *Aox1a* expression after treatments with SHAM, KCN, H_2O_2, NO, and SA. In the suggested model, mitochondria integrate and relay signaling via a ROS-specific pathway. KCN,[1] NO,[16] and SA[33,35] block the mitochondrial electron transport leading to an increase of H_2O_2 and other ROS, which disturb the redox balance of the cell and may activate signal transduction pathways and transcriptional activation of target genes. ROS-induced redox balance changes also lead to an increase of intracellular NO and SA levels that amplify the mitochondrial signaling circuit. NO- and SA-specific signaling pathways and their cross-talk may also contribute to *Aox1a* induction. After translation, the accumulated AOX protein can prevent mitochondrial ROS formation and restore redox balance enabling cell survival. Specific signaling events, transcription factors, and their binding sites in the promoter of the gene remain to be determined. Solid-line arrows depict ROS-dependent and broken-line arrows depict ROS-independent signaling.

other plants.[36] Also, *Aox1a* is a NO-inducible gene in *Arabidopsis*.[17] In addition, the observed responses could be due to synergistic effects of different signaling pathways on specific gene induction, which have been frequently reported.[29] Particularly, accumulation of ROS after prolonged treatments with NO and SA could lead to multiplication of the effects of the initial stressor and enhanced responses as observed with both compounds in *Aox1a* expression.

It has been reported that a potent increase of intracellular ROS, possibly of mitochondrial origin, may occur after exposure of the plant to the examined compounds KCN,[1] NO,[16] and SA,[33–35] due to restriction of the electron transport chain, which can be at least partially offset by high levels of AOX.[15] SHAM also can stimulate H_2O_2 production.[31] These data suggest that direct ROS signaling may be involved in *Aox1a* induction after treatment with the compounds examined in this study. In addition, SA-dependent signaling during plant pathogen interactions involves indirect redox regulation since the transcription factor NPR1 (non-expressor of pathogenesis related 1) undergoes activation from an inactive oligomer to the active monomer as a result of cellular redox changes induced by SA.[37] NPR1 interacts with members of the TGA class of transcription factors that recognize and bind to the TGACG motif (that is also present in many plant *Aox* genes including *Aox1a* of maize), and regulates their DNA binding activity in a redox-dependent manner. NO also affects the ROS-antioxidant balance of the cell and can act either by enhancing or suppressing the damaging effects of ROS depending on their respective concentrations.[38] Based on these data, we present a testable model (Fig. 5) suggesting that changes in redox balance of the cells induced after exposure to the examined compounds may represent a common signal in *Aox1a* induction in maize, which in turn may protect mitochondria from oxidative stress.

Acknowledgement

The authors thank Konstantinos Alexiou for his assistance to the isolation of the *Aox1a* promoter.

References

1. Siedow JN, Umbach AL. The mitochondrial cyanide-resistant oxidase: structural conservation amid regulatory diversity.

Biochim Biophys Acta 2000; **1459**: 432–439.
2. Rhoads DM, McIntosh L. Salicylic acid regulation of respiration in higher plants: alternative oxidase expression. *Plant Cell* 1992; **4**: 1131–1139.
3. Wagner AM. A role for active oxygen species as second messengers in the induction of alternative oxidase gene expression in *Petunia hybrida* cells. *FEBS Lett* 1995; **368**: 339–342.
4. Purvis AC, Shewfelt RL. Does the alternative pathway ameliorate chilling injury in sensitive plant-tissues. *Physiol Plant* 1993; **88**: 712–718.
5. Whelan J, Millar AH, Day DA. The alternative oxidase is encoded in a multigene family in soybean. *Planta* 1996; **198**: 197–201.
6. Ito Y, Saisho D, Nakazono M, Tsutsumi N, Hirai A. Transcript levels of tandem-arranged alternative oxidase genes in rice are increased by low temperature. *Gene* 1997; **203**: 121–129.
7. Vanlerberghe GC, McIntosh L. Alternative oxidase: from gene to function. *Annu Rev Plant Physiol Plant Mol Biol* 1997; **48**: 703–734.
8. Saisho D, Nambara E, Naito S, Tsutsumi N, Hirai A, Nakazono M. Characterization of the gene family for alternative oxidase from *Arabidopsis thaliana*. *Plant Mol Biol* 1997; **35**: 585–596.
9. Considine MJ, Holtzapffel RC, Day DA, Whelan J, Millar AH. Molecular distinction between alternative oxidase from monocots and dicots. *Plant Physiol* 2002; **129**: 949–953.
10. Saisho D, Nakazono M, Lee KH, Tsutsumi N, Akita S, Hirai A. The gene for alternative oxidase-2 (AOX2) from *Arabidopsis thaliana* consists of five exons unlike other AOX genes and is transcribed at an early stage during germination. *Genes Genet Syst* 2001; **76**: 89–97.
11. Finnegan PM, Whelan J, Millar AH *et al*. Differential expression of the multigene family encoding the soybean mitochondrial alternative oxidase. *Plant Physiol* 1997; **114**: 455–466.
12. Djajanegara I, Finnegan PM, Mathieu C, McCabe T, Whelan J, Day DA. Regulation of alternative oxidase gene expression in soybean. *Plant Mol Biol* 2002; **50**: 735–742.
13. Saika H, Ohtsu K, Hamanaka S, Nakazono M, Tsutsumi N, Hirai A. AOX1c, a novel rice gene for alternative oxidase; comparison with rice AOX1a and AOX1b. *Genes Genet Syst* 2002; **77**: 31–38.
14. McIntosh L, Eichler T, Gray G, Maxwell D, Nickels R, Wang Y. Biochemical and genetic controls exerted by plant mitochondria. *Biochim Biophys Acta* 1998; **1365**: 278–284.
15. Maxwell DP, Wang Y, McIntosh L. The alternative oxidase lowers mitochondrial reactive oxygen production in plant cells. *Proc Natl Acad Sci USA* 1999; **96**: 8271–8276.
16. Millar AH, Day DA. Nitric oxide inhibits the cytochrome oxidase but not the alternative oxidase of plant mitochondria. *FEBS Lett* 1996; **398**: 155–158.
17. Huang X, von Rad U, Durner J. Nitric oxide induces transcriptional activation of the nitric oxide-tolerant alternative oxidase in *Arabidopsis* suspension cells. *Planta* 2002; **215**: 914–923.
18. Polidoros AN, Mylona PV, Scandalios JG. Partial isolation and characterization of the maize alternative oxidase gene. *Maize Gen Coop Newsletter* 1998; **72**: 68–70.
19. Karpova OV, Kuzmin EV, Elthon TE, Newton KJ. Differential expression of alternative oxidase genes in maize mitochondrial mutants. *Plant Cell* 2002; **14**: 3271–3284.
20. Triglia T, Peterson MG, Kemp DJ. A procedure for *in vitro* amplification of DNA segments that lie outside the boundaries of known sequences. *Nucleic Acids Res* 1988; **16**: 81–86.
21. Polidoros AN, Scandalios JG. Role of hydrogen peroxide and different classes of antioxidants in the regulation of catalase and glutathione S-transferase gene expression in maize (*Zea mays* L.). *Physiol Plant* 1999; **106**: 112–120.
22. Lorkovic ZJ, Wieczorek Kirk DA, Lambermon MH, Filipowicz W. Pre-mRNA splicing in higher plants. *Trends Plant Sci* 2000; **5**: 160–167.
23. Higo K, Ugawa Y, Iwamoto M, Korenaga T. Plant *cis*-acting regulatory DNA elements (PLACE) database: 1999. *Nucleic Acids Res* 1999; **27**: 297–300.
24. Lescot M, Dehais P, Thijs G *et al*. PlantCARE, a database of plant *cis*-acting regulatory elements and a portal to tools for *in silico* analysis of promoter sequences. *Nucleic Acids Res* 2002; **30**: 325–327.
25. Desikan R, AH-Mackerness S, Hancock JT, Neill SJ. Regulation of the *Arabidopsis* transcriptome by oxidative stress. *Plant Physiol* 2001; **127**: 159–172.
26. Mahalingam R, Gomez-Buitrago A, Eckardt N *et al*. Characterizing the stress/defense transcriptome of *Arabidopsis*. *Genome Biol* 2003; **4**: R20.
27. Chen W, Provart NJ, Glazebrook J *et al*. Expression profile matrix of *Arabidopsis* transcription factor genes suggests their putative functions in response to environmental stresses. *Plant Cell* 2002; **14**: 559–574.
28. Thirkettle-Watts D, McCabe TC, Clifton R *et al*. Analysis of the alternative oxidase promoters from soybean. *Plant Physiol* 2003; **133**: 1158–1169.
29. Neill SJ, Desikan R, Clarke A, Hurst RD, Hancock JT. Hydrogen peroxide and nitric oxide as signalling molecules in plants. *J Exp Bot* 2002; **53**: 1237–1247.
30. Beaudoing E, Gautheret D. Identification of alternate polyadenylation sites and analysis of their tissue distribution using EST data. *Genome Res* 2001; **11**: 1520–1526.
31. Popov VN, Simonian RA, Skulachev VP, Starkov AA. Inhibition of the alternative oxidase stimulates H_2O_2 production in plant mitochondria. *FEBS Lett* 1997; **415**: 87–90.
32. Lieberherr D, Wagner U, Dubuis PH, Metraux JP, Mauch F. The rapid induction of glutathione S-transferases AtGSTF2 and AtGSTF6 by avirulent *Pseudomonas syringae* is the result of combined salicylic acid and ethylene signaling. *Plant Cell Physiol* 2003; **44**: 750–757.
33. Norman C, Howell KA, Millar AH, Whelan JM, Day DA. Salicylic acid is an uncoupler and inhibitor of mitochondrial electron transport. *Plant Physiol* 2004; **134**: 492–501.
34. Van Camp W, Van Montagu M, Inze D. H_2O_2 and NO redox signals in disease resistance. *Trends Plant Sci* 1998; **3**: 330–334.
35. Xie Z, Chen Z. Salicylic acid induces rapid inhibition of mitochondrial electron transport and oxidative phosphorylation in tobacco cells. *Plant Physiol* 1999; **120**: 217–226.
36. Murphy AM, Chivasa S, Singh DP, Carr JP. Salicylic acid-induced resistance to viruses and other pathogens: a parting of the ways? *Trends Plant Sci* 1999; **4**: 155–160.
37. Mou Z, Fan W, Dong X. Inducers of plant systemic acquired resistance regulate NPR1 function through redox changes. *Cell* 2003; **113**: 935–944.
38. Wendehenne D, Pugin A, Klessig DF, Durner J. Nitric oxide: comparative synthesis and signaling in animal and plant cells. *Trends Plant Sci* 2001; **6**: 177–183.

Isolation of a differentially spliced C-type flower specific *AG*-like MADS-box gene from *Crocus sativus* and characterization of its expression

A.S. TSAFTARIS*,**,[1], K. PASENTSIS* and A.N. POLIDOROS*

*Institute of Agrobiotechnology, CERTH, Thermi, GR-57001, Greece**
*Department of Genetics and Plant Breeding, AUTH, Thessaloniki, GR-54006, Greece***

Abstract

We have cloned and characterized the expression of *Crocus sativus AGAMOUS1* (*CsAG1*), a putative C-type MADS-box gene homologous to *AGAMOUS* (*AG*) from a triploid monocot species crocus (*Crocus sativus* L.). The typical domain structure of MIKC-type plant MADS proteins was identified. Phylogenetic analysis of the deduced amino acid sequence indicated that the isolated gene forms a clade with the *AGAMOUS* homologs from the monocots *Hyacinthus orientalis* and *Phalaenopsis equestris*. A differential splicing event altering the amino acid sequence at the C terminus was identified, leading to the formation of two mRNAs differing ten nucleotides in size. The presence of both differentially spliced transcripts was restricted only to mature crocus flowers and particularly to stamens and carpels.

Additional key words: *AGAMOUS*, monocot, saffron, phylogeny.

Introduction

MADS-box genes encode transcription factors present in several eukaryotic organisms and contain a highly conserved sequence encoding the MADS-domain that is responsible for nuclear localization, DNA binding, dimerization and accessory factor binding (Theissen *et al.* 2000, Immink *et al.* 2002). The first isolated plant MADS-box genes were *DEFICIENS* (*DEF*) from *Antirrhinum* and *AGAMOUS* (*AG*) from *Arabidopsis.* Although initially found in floral tissues where they regulate floral organ identity, it was later established that MADS-box genes also act as regulators of various other aspects of plant development (Rounsley *et al.* 1995, Kim *et al.* 2002). It has been proposed that there are at least two lineages (type I and type II) of MADS-box genes in plants, animals and fungi (Alvarez-Buylla *et al.* 2000). Most of the plant MADS-box genes belong to type II and encode proteins with a stereotypic organization of four domains: the conserved ~55 amino acid (aa) MADS-domain (M), followed by the intervening (I) domain (~30 aa), the keratin-like coiled-coil (K) domain (~70 aa) and the variable C-terminal (C) domain that provides functional specificity. Therefore genes displaying this organization are called MIKC-type and are plant-specific transcriptional regulators. Subsequent work revealed in plants the existence of a large family with at least nine classes of MADS-box genes based on function and expression patterns (Nam *et al.* 2003). In angiosperms, at least five classes of MADS-box genes are involved in control of flower development. Particularly, the ABC model of flower development (Weigel and Meyerowitz 1994) predicts that three classes of floral MADS-box genes, encoding the A, B and C functions, act alone or in combination to specify floral organ identity. Since its initial proposal, the ABC model has been refined to include D- and E-class genes (Ferrario *et al.* 2004) and has been followed by the 'quartet model', which predicts that the identity of the different floral organs – sepals, petals, stamens and carpels – is determined by four combinations of floral homeotic MADS-box proteins (Theissen 2001). Regardless the model, AG-homologous genes are required for stamen, and carpel development and are known as the C-function genes. The class C function of floral organ development has been conserved during the 300 million years of evolution after the divergence of gymnosperms and angiosperms (Zhang *et al.* 2004).

Received 11 March 2004, *accepted* 14 April 2005.
Abbreviations: BLAST - basic local alignment search tool; MADS - minichromosomal maintenance *1 Agamous deficiens* serum response factor; MEGA - molecular evolutionary genetics analysis; MIKC - MADS-box intermediate keratin-like C-terminal domain structure; PAGE - polyacrylamide gel electrophoresis.
Acknowledgements: We thank Yiannis Patsios for his help in collecting plant material in the field, and the anonymous reviewers for their help to improve the manuscript.
[1] Corresponding author; fax:(+30) 2310 498270, e-mail: tsaft@certh.gr

We are interested in characterizing the expression of genes involved in flower development in crocus, a monocot triploid species belonging to the *Iridaceae* family, since its stigmas constitute the expensive food additive saffron. The flowers of crocus are bisexual. The outer two whorls (the perianth) consists of 6 tepals. The next two whorls form sequentially stamens and carpels. Removal of stamens and separation of stigmas by hand is very labour intensive leading to high costs (see also Tsaftaris *et al.* 2004). It would be desirable to have mutants without stamen formation in crocus flowers or even to transform stamens to carpels, which should double saffron production in a single flower while lowering the cost of production and improving saffron quality. In order to understand and exploit the molecular mechanisms that control flower development in crocus, we started to clone and characterize the expression of MADS-box genes in crocus flowers (Tsaftaris *et al.* 2004). As C-class MADS-box gene function is essential for both stamen and carpel formation we report here the isolation and characterization of *CsAG1*, a C-class *AG*-like gene that is differentially spliced in two products and its expression is restricted to flowers and particularly in stamens and carpels.

Materials and methods

Plants: *Crocus sativus* L. cv. Kozani field growing plants were collected during the late flowering season in October from Kozani, Greece. As the crocus perianth has not distinct sepals and petals we treated separately the three tepals of the outer whorl and the three tepals of the inner whorl. Tissues were separated and immediately frozen in liquid nitrogen and stored at -80 °C until used.

RNA isolation, cDNA synthesis and gene expression analysis: Total RNA from flowers was extracted using the RNeasy plant mini kit (*Qiagen*, Hilden, Germany). On-column digestion of DNA during RNA purification was performed using the RNase-Free DNase Set (*Qiagen*). Isolation of *CsAG1* was accomplished by RT-PCR using standard protocols, essentially as described previously (Tsaftaris *et al.* 2004). First strand cDNA synthesis was performed using 0.5 μg total RNA from closed flowers, 0.25 μg 3′RACE Adapter Primer 5′-GGCCACGCGTCGACTAGTAC$(T)_{17}$-3′ (*Gibco-BRL*, Paisley, UK), 1 mM dNTPs and 200 units M-MuLV reverse transcriptase (*NEB*, Beverly, USA) in 0.05 cm^3 total volume. MADS-box cDNAs were amplified in PCR using the degenerate MADS-F primer 5′-ATCSAGATMAARAGRATHGARAA-3′ and the Abridged Universal Amplification primer (AUA) 5′-GGCCACGCGTCGACTAGTAC-3′ (*Gibco-BRL*). Nested PCR on the amplification products was performed using the primer MADS-2F, 5′-GTKCTYTGYGAYGCYGAGGT-3′ (Van der Linden *et al.* 2002) and the primer AUA. PCR reactions were performed using 0.2 pmoles of each primer, 0.2 mM dNTPs and 1 unit DyNAzyme II DNA polymerase (*Finnzymes*, Espoo, Finland). The thermocycler's program was: 1 min at 94 °C, 30 cycles of 30 s at 94 °C, 30 s at 50 °C, 90 s at 72 °C and a final extension step of 10 min at 72 °C. Several products between 300 and 1100 bp were cloned into the pGEM T easy vector (*Promega*, Madison, USA). Sequencing was performed using a *LiCor 4200* sequencer. BLAST searches identified one clone of 806 bp with homology to *AGAMOUS* genes from other plant species. Based on this sequence, the gene specific primer AGAM-R (5′-ATAGCAATAAGGTACCCAGTCAC-3′) was designed from the 3-UTR and used to isolate the cDNA's 5′end, using the GeneRacer kit (*Invitrogen*, Paisley, UK) according the instructions. A PCR fragment of 1100 bp was purified from the gel and cloned into the pGEM T easy vector (*Promega*) according to the manufacturer's protocol.

Gene expression analysis was performed with RT-PCR. Total RNA (1 μg) extracted from leaves, flowers, tepals, stamens and carpels was used in a reverse transcription reaction as previously described. PCR was performed using primer AGAM-R and primer AG1F (5′-AAGCTTCCTTCAAGCGAACTTG-3′) on 1/50 of the synthesized cDNA as template. The primers were designed to amplify a 263 bp fragment containing the deletion observed in the isolated genes. Primers actin 2-F (5′-CCGGTGTCATGGTTGGTAT-3′) and actin 2-R (5′-GCAGGCACATTGAAGGTCT-3′), amplifying a fragment of the actin-beta gene, were used as control for successful cDNA syntesis. A control RT-PCR was included for each sample using as template total RNA without reverse transcriptase at the same dilution as the cDNA template. The PCR products were separated on a 1.8 % agarose gel and amplification products of the expected size could be observed.

DNA isolation and Southern hybridization: Genomic DNA was isolated from leaves using the DNeasy plant mini kit (*Qiagen*) according to the manufacturer's protocol. 10 μg genomic DNA was digested with *Eco*RI, *Hind*III and *Bam*HI, restriction enzymes (*NEB*), transferred onto a nylon membrane (*Roche*, Mannheim, Germany) and hybridized with an AG-specific digoxigenin labeled probe prepared with the PCR DIG Probe Synthesis Kit (*Roche*) using the primers AG1F and AGAM-R. Hybridization was performed in DIG Easy Hyb buffer (*Roche*) at 42 °C according to the manufacturer and stringent washes were at 68 °C in 0.5 X SSC / 0.1 % SDS (twice). Detection was performed using the DIG Luminescent Detection Kit (*Roche*) according the instructions and chemiluminescense was detected using the Gene-Gnome Bio Imaging System (*Syngene*, Cambridge, UK).

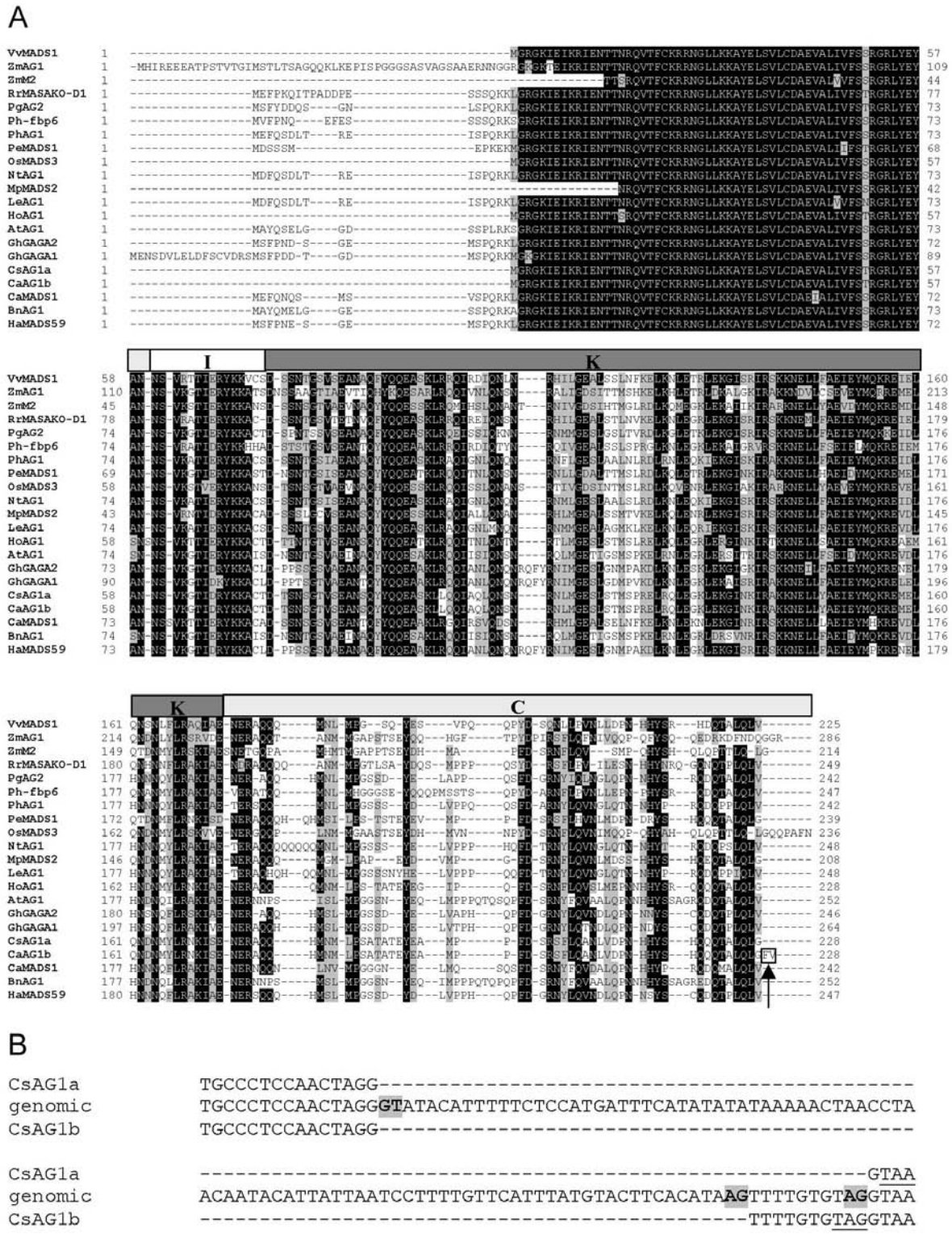

Fig. 1. *A* - Alignment of the deduced amino acid (aa) sequences of *CsAG1a* and *CsAG1b* and other homologous plant AG-like proteins using *Clustal W* (Thompson *et al.* 1994). Identical aa in all the sequences are highlighted in black and in 70 % of the sequences in gray. The 2 aa difference of the alternatively spliced products of *CsAG1*is boxed and indicated by an arrow. Highlighted on top of the alignment are the four domains of the MIKC-type proteins. *B* - Partial alignment of cDNA fragments from *CsAG1a*, *CsAG1b*, and the corresponding genomic fragment, showing the position of the intron. In bold and highlighted are the 5-splice donor element GT and the two alternative 3 splice acceptor elements AG of the intron. Underlined are the stop codons TAA for CsAG1a and TAG for CsAG1b.

Comparison and phylogenetic analysis: The deduced CsAG1 amino acid sequences were used in *BLAST* searches and the best hits were for AG-like genes from *Hyacinthus orientalis* (HoAG1, AAD19360), *Phalaenopsis equestris* (PeMADS1, AAL76415), and *Magnolia praecocissima* (MpMADS2, BAB70737). These, and 16 additional *AGAMOUS* genes were selected for phylogenetic analysis. The sequences were from: *Nicotiana tabacum* (NtAG1, Q43585) (Kempin *et al.* 1993); *Lycopersicon esculentum* (LeAG1, Q40168) (Pnueli *et al.* 1994); *Petunia hybrida* (PhMADS3, Q40885) (Tsuchimoto *et al.* 1993) and (Ph-fbp6, CAA48635) (Angenent *et al.* 1993); *Panax ginseng* (PgAG2, Q40872); *Gerbera hybrida* (GhGAGA1, CAA08800 and GhGAGA2, CAA08801) (Yu *et al.* 1999), *Corylus avellana* (CaMADS1, AAD03486) (Rigola *et al.* 1998); *Arabidopsis thaliana* (AtAG1, P17839) (Yanofsky *et al.* 1990); *Brassica napus* (BnAG1, Q01540) (Mandel *et al.* 1992); *Rosa rugosa* (RrMASAKO-D1, BAA90743) (Kitahara and Matsumoto 2000); *Zea mays* (ZmAG1, JQ2289) (Schmidt *et al.* 1993) and (ZmM2, CAA57074) (Theissen *et al.* 1995); *Helianthus annuus* (HaMADS59, AAO18229); *Oryza sativa* (OsMADS3, S59480) (Kang *et al.* 1995) and *Vitis vinifera* (VvMADS1, AAK58564) (Boss *et al.* 2001). The deduced amino acid sequences of the above genes together with CsAG1a and CsAG1b were aligned using the multiple sequence alignment program *Clustal W* (Thompson *et al.* 1994). Phylogenetic relationships of the sequences were examined using the Neighbor-Joining method with p-distance correction (Saitou and Nei 1987). The tree was constructed using the *MEGA 2.1* software (Kumar *et al.* 2001).

Results and discussion

Isolation and characterization of *CsAG1*: In this study we describe the isolation of *CsAG1* a putative C-type MADS-box gene homologous to *AGAMOUS* (AG) from crocus. Sequencing revealed the presence of two transcripts designated *CsAG1a* (GenBank accession number AY555579) and *CsAG1b* (GenBank accession number AY555580), which are different since *CsAG1a* is missing 10 bp from 890 to 899 in comparison with *CsAG1b*. This deletion alters the coding ORF of *CsAG1* in such a way that the deduced protein sequence of *CsAG1a* is two aa shorter at the C terminus from the deduced protein sequence of *CsAG1b* (Fig. 1*A*). To investigate if the phenomenon is due to differential splicing, we amplified the corresponding genomic DNA fragment by PCR using the primers AGAM-R and AG1F. PCR yielded only one distinct 360 bp band as determined by 5 % polyacrylamide electrophoresis (data not shown). Further, this genomic DNA fragment was sequenced (GenBank accession number AY555581) and revealed the presence of an 100-110 bp intron beginning with the typical plant intron 5' splice donor GT and ending at two nearby 3' splice acceptor AG signals (Lorkovic *et al.* 2000) being 10 bp apart and matching the observed deletion in the two isolated transcripts (Fig. 1*B*). This intron in crocus is located exactly at the conserved position of the 8th intron in plant *AGAMOUS* genes (Zhang *et al.* 2004). Southern hybridization analysis using a probe prepared by PCR with the primers AG1F and AGAM-R revealed that three copies of the *AGAMOUS* gene are present in the genome of crocus (Fig. 2) that is in agreement with the triploid nature of the crop.

Phylogenetic analysis of *CsAG1*: The deduced amino acid sequences were used in *BLAST* searches and the best hits were for AG-like genes from *Hyacinthus orientalis* (HoAG1, AAD19360), *Phalaenopsis equestris* (PeMADS1, AAL76415), and *Magnolia praecocissima* (MpMADS2, BAB70737). These, and several additional *AGAMOUS* genes for which there are published reports were aligned using *Clustal W* (Fig. 1*A*), and their phylogenetic relationships were examined using the Neighbor-Joining method with p-distance correction (Saitou and Nei 1987). The tree was constructed using the *MEGA 2.1* software (Kumar *et al.* 2001). The crocus sequences fall in a group with the *AGAMOUS* genes from a hyacinth (*Hyacinthus orientalis)* and an orchid plant (*Phalaenopsis equestris*), which both similarly to crocus have tepals in the perianth (Fig. 3).

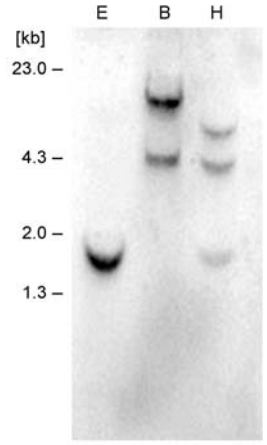

Fig. 2. Southern blot of genomic DNA from *Crocus* digested with: *Eco*RI (E), *Bam*HI (B) and *Hind*III (H) using as probe a PCR fragment of the cloned *CsAG1* genomic DNA. The profile of the *Hind*III digestion indicates that 3 copies of the gene are present in the crocus genome.

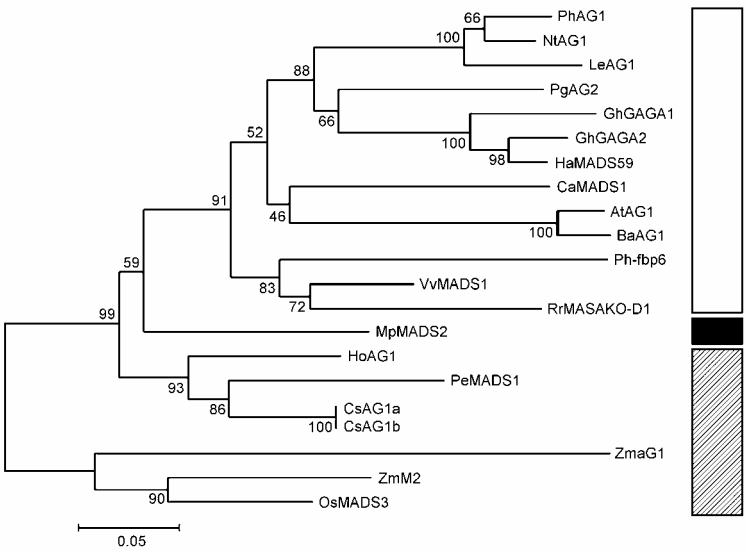

Fig. 3. Phylogenetic relationships of amino acid *AGAMOUS* sequences (alignment in Fig. 1*A*) estimated using the Neighbor-Joining method with p-distance correction. The tree was constructed using the *MEGA 2.1* software. Bootstrap values (1000 replications) are shown at the cross of clades and sequence distances are shown at the bottom of the tree. The crocus sequences are grouped with *AGAMOUS* genes from a hyacinth (*Hyacinthus orientalis)* and an orchid plant (*Phalaenopsis equestris*). *White bar* - eudicot plants, *black bar* - Magnoliids, *stripped bar* - monocot plants.

Expression analysis of *CsAG1* in crocus tissues: Expression analysis of *CsAG1* was performed with RT-PCR using the primer pair AGAM-R and AG1F. Primers actin2-F and actin2-R (Tsaftaris *et al.* 2004) amplifying a fragment of the actin-beta gene were used as a cDNA syntesis control, and all the experiments included a negative RT-PCR control. No amplification could be observed in the negative controls (data not shown).

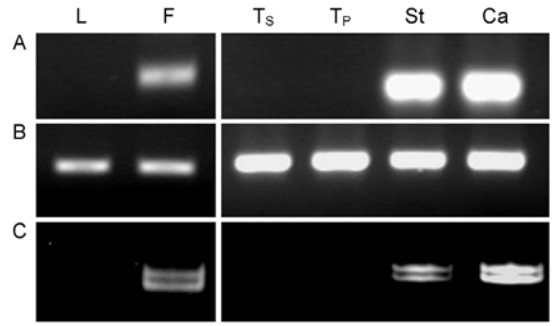

Fig. 4. *CsAG1* expression in leaves and flowers of crocus detected with RT-PCR. cDNA from leaves (L) , flowers (F), tepals of the outer whorl that forms sepals in other plants (T_S), tepals of the inner whorl that forms petals in other plants (T_P), stamens (St) and carpels (Ca) was amplified using: *A* - *CsAG1* gene specific primers, *B* - actin primers, *C* - fine resolution of PCR products from Fig. 3*A* on 5 % native PAGE.

Experiments revealed the presence of the transcript only in flowers and more specifically restricted in stamens and carpels (Fig. 4*A*). This expression pattern is in agreement with the expected according the ABC model of floral organ development and provides the basis for classification of *CsAG1* in the C-class MADS-box genes. A 5 % nondenaturing polyacrylamide gel was loaded with the same PCR products to investigate whether both isolated transcripts were expressed. The fine resolution through native PAGE revealed that both transcripts were present in stamens as well as in carpels (Fig. 4*C*).

Experiments are underway to isolate the complete set of flower-specific MADS-box genes in crocus. Towards this goal we have identified the *APETALA 3* (*AP3*) and *SEPALLATA* (*SEP*) homologs, which we are currently characterizing. Expression of the B-class *AP3* gene normally restricted to the second and third whorl is extended to the first whorl in crocus (data not shown). This could explain the homeotic transformation of sepals to petals in crocus flowers. Isolation and functional analysis of all the classes of MADS-box flower-specific genes will enable us not only to understand homeotic transformations in crocus flowers, but will also help to characterize and possibly exploit the numerous flower mutants (multiple flower organs, lack of stamens, *etc*.) frequently observed in fields cultivated with this asexually propagated crop.

References

Alvarez-Buylla, E.R., Pelaz, S., Liljegren, S.J., Gold, S.E., Burgeff, C., Ditta, G.S., Ribas de Pouplana, L., Martinez-Castilla, L., Yanofsky, M.F.: An ancestral MADS-box gene duplication occurred before the divergence of plants and

animals. - Proc. nat. Acad. Sci. USA **97**: 5328-5333, 2000.

Angenent, G.C., Franken, J., Busscher, M., Colombo, L., Van Tunen, A.J.: Petal and stamen formation in petunia is regulated by the homeotic gene fbp1. - Plant J. **4**: 101-112, 1993.

Boss, P.K., Vivier, M., Matsumoto, S., Dry, I.B., Thomas, M.R.: A cDNA from grapevine (*Vitis vinifera* L.), which shows homology to AGAMOUS and SHATTERPROOF, is not only expressed in flowers but also throughout berry development. - Plant mol. Biol. **45**: 541-553, 2001.

Ferrario, S., Immink, R.G., Angenent, G.C.: Conservation and diversity in flower land. - Curr. Opinion Plant Biol. **7**: 84-91, 2004.

Immink, R.G., Gadella, T.W., Jr., Ferrario, S., Busscher, M., Angenent, G.C.: Analysis of MADS box protein-protein interactions in living plant cells. - Proc. nat. Acad. Sci. USA **99**: 2416-2421, 2002.

Kang, H.G., Noh, Y.S., Chung, Y.Y., Costa, M.A., An, K., An, G.: Phenotypic alterations of petal and sepal by ectopic expression of a rice MADS box gene in tobacco. - Plant mol. Biol. **29**: 1-10, 1995.

Kempin, S.A., Mandel, M.A., Yanofsky, M.F.: Conversion of perianth into reproductive organs by ectopic expression of the tobacco floral homeotic gene NAG1. - Plant Physiol. **103**: 1041-1046, 1993.

Kim, S.H., Mizuno, K., Fujimura, T.: Isolation of MADS-box genes from sweet potato (*Ipomoea batatas* (L.) Lam.) expressed specifically in vegetative tissues. - Plant Cell Physiol. **43**: 314-322, 2002.

Kitahara, K., Matsumoto, S.: Rose MADS-box genes 'MASAKO C1 and D1' homologous to class C floral identity genes. - Plant Sci. **151**: 121-134, 2000.

Kumar, S., Tamura, K., Jakobsen, I.B., Nei, M.: MEGA2: molecular evolutionary genetics analysis software. - Bioinformatics **17**: 1244-1245, 2001.

Lorkovic, Z.J., Wieczorek, Kirk, D.A., Lambermon, M.H., Filipowicz, W.: Pre-mRNA splicing in higher plants. - Trends Plant Sci. **5**: 160-167, 2000.

Mandel, M.A., Bowman, J.L., Kempin, S.A., Ma, H., Meyerowitz, E.M., Yanofsky, M.F.: Manipulation of flower structure in transgenic tobacco. - Cell **71**: 133-143, 1992.

Nam, J., dePamphilis, C.W., Ma, H., Nei, M.: Antiquity and evolution of the MADS-box gene family controlling flower development in plants. - Mol. Biol. Evol. **20**: 1435-1447, 2003.

Pnueli, L., Hareven, D., Rounsley, S.D., Yanofsky, M.F., Lifschitz, E.: Isolation of the tomato *AGAMOUS* gene *TAG1* and analysis of its homeotic role in transgenic plants. - Plant Cell **6**: 163-173, 1994.

Rigola, D., Pe, M.E., Fabrizio, C., Me, G., Sari-Gorla, M.: CaMADS1, a MADS box gene expressed in the carpel of hazelnut. - Plant mol. Biol. **38**: 1147-1160, 1998.

Rounsley, S.D., Ditta, G.S., Yanofsky, M.F.: Diverse roles for MADS box genes in *Arabidopsis* development. - Plant Cell **7**: 1259-1269, 1995.

Saitou, N., Nei, M.: The neighbor-joining method: a new method for reconstructing phylogenetic trees. - Mol. Biol. Evol. **4**: 406-425, 1987.

Schmidt, R.J., Veit, B., Mandel, M.A., Mena, M., Hake, S., Yanofsky, M.F.: Identification and molecular characterization of *ZAG1*, the maize homolog of the *Arabidopsis* floral homeotic gene *AGAMOUS*. - Plant Cell **5**: 729-737, 1993.

Theissen, G.: Development of floral organ identity: stories from the MADS house. - Curr. Opinion Plant Biol. **4**: 75-85, 2001.

Theissen, G., Becker, A., Di Rosa, A., Kanno, A., Kim, J.T., Munster, T., Winter, K.U., Saedler, H.: A short history of MADS-box genes in plants. - Plant mol. Biol. **42**: 115-149, 2000.

Theissen, G., Strater, T., Fischer, A. and Saedler, H.: Structural characterization, chromosomal localization and phylogenetic evaluation of two pairs of AGAMOUS-like MADS-box genes from maize. - Gene **156**: 155-166, 1995.

Thompson, J.D., Higgins, D.G., Gibson, T.J.: CLUSTAL W: improving the sensitivity of progressive multiple sequence alignment through sequence weighting, position-specific gap penalties and weight matrix choice. - Nucl. Acids Res. **22**: 4673-4680, 1994.

Tsaftaris, A.S., Pasentsis, K., Iliopoulos, I., Polidoros, A.N.: Isolation of three homologous AP1-like MADS-box genes in crocus (*Crocus sativus* L.) and characterization of their expression. - Plant Sci. **166**: 1235-1243, 2004.

Tsuchimoto, S., Van der Krol, A.R., Chua, N.H.: Ectopic expression of pMADS3 in transgenic petunia phenocopies the petunia blind mutant. - Plant Cell **5**: 843-853, 1993.

Van der Linden, C.G., Vosman, B., Smulders, M.J.: Cloning and characterization of four apple MADS box genes isolated from vegetative tissue. - J. exp. Bot. **53**: 1025-1036, 2002.

Weigel, D., Meyerowitz, E.M.: The ABCs of floral homeotic genes. - Cell **78**: 203-209, 1994.

Yanofsky, M.F., Ma, H., Bowman, J.L., Drews, G.N., Feldmann, K.A., Meyerowitz, E.M.: The protein encoded by the *Arabidopsis* homeotic gene agamous resembles transcription factors. - Nature **346**: 35-39, 1990.

Yu, D., Kotilainen, M., Pollanen, E., Mehto, M., Elomaa, P., Helariutta, Y., Albert, V.A., Teeri, T.H.: Organ identity genes and modified patterns of flower development in *Gerbera hybrida* (*Asteraceae*). - Plant J. **17**: 51-62, 1999.

Zhang, P., Tan, H.T., Pwee, K.H., Kumar, P.P.: Conservation of class C function of floral organ development during 300 million years of evolution from gymnosperms to angiosperms. - Plant J. **37**: 566-577, 2004.

Maydica 50 (2005): 19-23

DNA METHYLATION PATTERNS ARE DIFFERENTLY AFFECTED BY PLANTING DENSITY IN MAIZE INBREDS AND THEIR HYBRIDS

E. Tani[1], A.N. Polidoros[1], I. Nianiou-Obeidat[2], A.S. Tsaftaris[1,2,*]

[1] Institute of Agrobiotechnology, CERTH, 6th km. Charilaou-Thermis Rd., 57001 Thermi, Greece
[2] Department of Genetics and Plant Breeding, Aristotelian University of Thessaloniki, 54006 Thessaloniki, Greece

Received July 14, 2004

ABSTRACT - Hybrid vigor or heterosis refers to the superiority in one or more characters of crossbred organisms relative to their inbred parents. This superiority can be related to increase in size or growth rate and increase in yield. While the biological basis of heterosis remains unknown, accumulated data clearly suggest the significance of quantitative regulation of gene expression in heterotic phenomena. DNA methylation is an epigenetic, genome-wide general regulatory mechanism that affects the expression of many genes important for the manifestation of heterosis. According to previous studies DNA methylation in maize varies among different genotypes (parental inbred lines and hybrids) and developmental stages. Our recent studies indicate that growth conditions affect the level and pattern of DNA methylation. Parental inbred lines and hybrids were grown under two different plant densities: 1.5m (spread) and 0.25m (dense) distance between individual plants with a density of 0.513 plants/m^2 and 18.5 plants/m^2, respectively. The effect of density-induced stress on the pattern of methylation in certain sites of DNA was examined using the Coupled Restriction Enzyme Digestion and Random Amplification (CRED-RA) technique. The results suggested that hybrids are more resistant to density-related methylation alterations in comparison to their parental inbreds.

KEY WORDS: Heterosis; Methylation; Stress; CRED-RA.

INTRODUCTION

Heterosis is a genetic phenomenon, in which hybrids manifest superiority over the inbred parental genotypes for several quantitative characters including yield. While plant breeders and agronomists achieved an impressive increase in maize yield utilizing heterosis, the biological basis of the phenomenon remains unknown. Previous attempts to understand physiological and biochemical aspects of heterosis demonstrated that maize hybrids possess superior physiological and biochemical properties than those of the parental lines (for review see TSAFTARIS, 1995). Farmers prefer F1 hybrids for their high and stable yield while growing in different fields and in different years. Genetic stability (homeostasis) refers to reduced genotype X environment interaction, particularly under stress conditions. The selection of adapted single crosses with high yield and high stability in high planting density has been responsible for the consistent increase in maize yields in USA since their introduction in the early 1960s (DUVICK, 1997; FASOULA and FASOULA, 1997; JANICK, 1998; TSAFTARIS and POLIDOROS, 2000). High planting density is considered as a stress condition and it is worthy to examine the parameters involved in hybrid resistance to density-induced stress.

Research performed in different laboratories clearly suggests the significance of regulation of gene expression in manifestation of complicated phenomena such as heterosis (TSAFTARIS and POLIDOROS, 1993; DE VIENNE *et al.*, 1996; TSAFTARIS and KAFKA, 1998; SONG and MESSING, 2003; WU *et al.*, 2003). One mechanism involved in regulation of gene expression is DNA methylation. Nuclear DNA is associated with histone proteins in a highly organized chromatin structure that can be divided into active euchromatin and heterochromatin, which is largely transcriptionally inert. Both forms of chromatin have distinct structural and biochemical properties that are thought to provide epigenetic marks for the formation of higher order structure and for maintaining gene activity and/or gene silencing. DNA methylation, along with diverse covalent modifications of histones and specific associations with non-histone proteins are the major determinants of

* For correspondence (Fax: +30 2310 498270; e.mail: tsaft@certh.gr).

chromatin states. The recent discovery of small RNAs able to direct DNA methylation and histone modification has provided a model for regulation of gene activity where RNA molecules play a central role (for review see TARIQ and PASZKOWSKI, 2004). Methylation in plants occurs in cytosine residues within the dinucleotide sequence CpG and the trinucleotide CpNpG (N is equal to any nucleotide except G). The extent and distribution of genomic DNA methylation is correlated with the rate of expression of many genes examined not only in plants but in all higher organisms (MATZKE *et al.*, 1989; BIRD, 2002).

Recently, it has been recognized that DNA methylation has significant implications in plant breeding, too (TSAFTARIS and POLIDOROS, 2000). In the past, genetic variation was considered only as a result of alterations in the primary nucleotide sequences due to mutations and/or gene recombination. However, it is now established that epigenetic systems like DNA methylation could generate epigenetic variation that had never been considered in plant breeding as a source of phenotypic variation (SHAKED *et al.*, 2001; HAN *et a*l., 2003). DNA methylation in maize was found to be genotype, tissue and developmental stage specific (TSAFTARIS *et al.*, 1999). In addition to endogenous (genetic) mechanisms affecting the level of DNA methylation in different tissues and developmental stages, external (environmental) signals also affect the extent of DNA methylation by their interaction with the plant (SHERMAN and TALBERT, 2002; STEWARD *et al.*, 2002). Moreover, stressful growth conditions result in more methylated DNA (less expressed) and, in general, vigorous hybrids are more resistant to such density induced methylation and suppression of genome activity in their genomic DNA (TSAFTARIS and POLIDOROS, 2000). Thus, at least to some extent methylation may underlie some heterotic phenomena.

The aim of this study was to estimate how different planting densities could affect DNA methylation in maize inbred lines and their offspring hybrids, as this could have significant implications in understanding heterosis and stability of hybrid performance. Taking advantage of the honeycomb design of planting (FASOULAS and FASOULA, 1995), and using different sets of inbreds and hybrids we estimated the effects of growth conditions (spread / dense planting) on site-specific DNA methylation with the coupled restriction enzyme digestion and random amplification (CRED-RA) of genomic DNA (CAI *et al.*, 1996). This technique allows amplification of a DNA fragment containing a cut site of a methylation sensitive restriction enzyme, only when the cytosine residue within the site is methylated and protected from digestion. Thus, presence of a PCR band reveals a methylated site(s). Unmethylated site(s) lead to absence of the amplicon (that would be present in uncut DNA) due to a digestion event(s). We report here our results indicating significant methylation differences between inbreds and hybrids, revealing that hybrids are more stable in comparison to their parents.

MATERIALS AND METHODS

Plant material

Plant material consisted of 6 sets of genotypes (Table 1). Each set included two inbred lines bred from the F2 population of the commercial hybrid PR 3183, (Pioneer Hi-Bred, Des Moines, IA) along with their respective hybrid (TOKATLIDIS *et al.*, 1998). In order to study the impact of planting density on DNA methylation, we estimated DNA methylation in 2 month old plants. This developmental stage was selected for two reasons: first because plants have grown enough to undergo density stress in dense planting; and second, in previous studies, we have shown that the highest differentiation in total methylation between different genotypes occurs at this time point (TSAFTARIS *et al.*, 1997). Plants were grown in the field under two different densities: 1.5m (spread) and 0.25m (dense) distance between individual plants with a density of 0.513 plants/m^2 and 18.5 plants/m^2 respectively, using the honeycomb design (FASOULAS and FASOULA, 1995). All the necessary cultivation treatments for plant growth under optimal conditions were performed. Sampling in the field was performed in two consecutive experiments in two years.

CRED-RA assay

Genomic DNA was isolated from the three upper leaves of each genotype according to DELLAPORTA *et. al.* (1983). DNA quantity was estimated spectrophotometrically and its quality was examined in 1.2% agarose electrophoresis. DNA (1 μg) was used for HpaII digestion. After digestion the sample was phenol/chloroform extracted and DNA was ethanol precipitated and resuspended in autoclaved distilled water. An estimated 25-50 ng of digested DNA was added as PCR template. Each set of plant material was tested with 20 random 10mer primers (AB-0320-kit 9 and10, Advanced Biotechnologies, Surrey, UK). Positive control of uncut DNA from one of the materials and negative control with no DNA was tested for each of the primers. PCR was performed according to the following conditions: denaturation at 94°C for 5 min, followed by 45 cycles of denaturation at 94°C for 1 min, annealing at 35°C for 1 min, and extension at 72°C for 2 min. The final extension step was 7 min to ensure completion of PCR in every synthesized product. In order to simplify comparisons and avoid complications due to genotype polymorphisms, PCR products were run on 1.2% agarose gels in sets of two parental inbreds and their respective hybrid, in spread and dense conditions, for each primer tested. Appearance of a PCR band in a genotype in one condition, which is not present in the other

condition, implies that HpaII did not cleave the respective recognition site in the former condition. Consequently, the cytosine residues of the HpaII recognition site were considered to be methylated. Random repetition of a subset of the reactions revealed 100% reproducibility of the results.

Statistical analysis

Analysis of data was performed using the z criterion for comparing the percentages of new methylated sites in inbred lines and hybrids under different planting conditions.

RESULTS AND DISCUSSION

The aim of this study was to record, evaluate, and compare methylation alterations in inbred lines and their hybrids when planted under spread and dense planting conditions. A representative example of recording HpaII site methylation alterations in a set of materials (1st set, Table 1) with one primer is shown in Fig. 1. A 630 bp amplicon absent in spread planting in the inbred B11-19, appeared under dense planting, demonstrating that one (or more) HpaII site(s) was unmethylated (thus cleaved) in spread planting while it was methylated (not cleaved) in dense planting. The inbred A11-7 and the hybrid did not show any changes in the band pattern under both planting densities. Table 2 summarizes the occurrence of methylated sites in both spread and dense planting regarding all the genotype and primer combinations tested. This table summarizes the results of 720 different PCRs (18 genotypes X 20 primers X 2 planting densities). Corrections of the observed numbers in inbreds were made to take into account that they resulted after testing twice as many genotypes than hybrids.

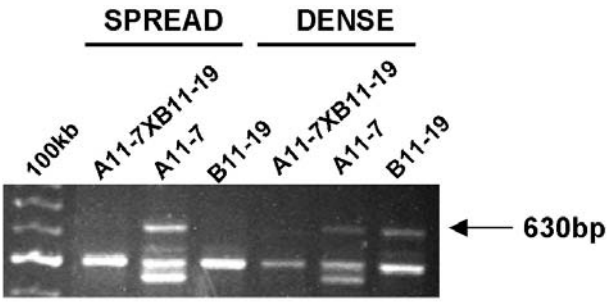

FIGURE 1 - An example of the CRED-RA analysis using one set of genotypes (two inbred lines A11-7 and B11-19 and their hybrid A11-7XB11-19), grown under spread and dense conditions. The B11-19 inbred line showed a new band at 630bp (denoting presence of one or more methylated HpaII sites). The inbred A11-7 and the hybrid maintained the same pattern in both spread and dense planting.

TABLE 1 - *Sets of plant material involving inbreds and their hybrid used for CRED-RA analysis.*

Set	Parental Inbreds		Hybrid
1st	A11-7	B11-19	A11-7 X B11-19
2nd	A5-8	B4-12	A5-8 X B4-12
3rd	A9-6	B10-19	A9-6X B10-19
4th	A3-10	B11-1	A3-10 X B11-1
5th	A7-14	B12-13	A7-14X B12-13
6th	A9-6	B5-19	A9-6X B5-19

TABLE 2 - *Occurrence of methylated sites only in spread, only in dense planting, and as total, in inbred lines and their hybrids. Observed is the number of bands recorded in each condition. For inbreds this number was divided by 2 and is shown in the corrected column, to take into account that it resulted after testing twice as many genotypes in comparison to hybrids. The percentage (%) column displays percentage of bands in each category in relation to the total number of bands recorded in this study. Percentages were estimated from the corrected value in inbreds and the observed in hybrids to the corrected total which is 45 (29 inbreds + 16 hybrids).*

	Inbreds			**Hybrids**	
	Observed	Corrected	%	Observed	%
Dense	48	24	53.4	11	24.4
Spread	10	5	11.1	5	11.1
Total	58	29	64.5	16	35.5

Statistical comparisons of genotypes under the two different planting conditions are shown in Table 3. Overall, the data show that hybrids experience significantly less methylation alterations in comparison to their parental inbred lines ($z=2,87>P_{0.01}$). Comparing the two planting conditions in inbreds, it was found that the percentage of methylated sites was significantly higher under dense than under spread planting (z=4,81>P0.01), while in hybrids the difference was not significant ($z=1,67<P_{0.05}$). Comparing inbreds and hybrids in each planting condition, it was estimated that significantly higher percentage of methylated sites occurred in dense planting conditions in the inbreds ($z=2,95>P_{0.01}$), while in spaced planting the difference between inbreds and hybrids was not signifi-

TABLE 3 - *Comparison of the percentage of methylated sites recorded in inbreds and hybrids under spread and dense planting. Statistical significance using the z criterion is indicated by two asterisks (at P0.01) or NS when non-significant. In the comparison column each condition/genotype combination is denoted by two letters meaning D: dense, S: spread, T: total (dense+spread), I: inbred, H: hybrid.*

Comparison	Z	Significance level
DI-DH	2,95	* *
SI-SH	0	NS
TI-TH	2,87	* *
DI-SI	4,81	* *
DH-SH	1,67	NS
DI-TI	–1,07	NS
SI-TI	–6,25	* *
DH-TH	–1,15	NS
SH-TH	–2,86	* *

cant ($z=0<P_{0.05}$). Consequently, when comparing the percentage of methylation changes in dense or spread planting with the total methylation changes in inbreds or hybrids, it was obvious that most of the total methylation alteration was due to increased methylation under dense planting (Table 3). In conclusion, inbred lines experience high percentage of induced methylation under dense planting, while hybrids are more stable under both planting conditions. Additionally, hybrids tend to inherit the methylation condition from the parent that shows the lower level of methylation as shown, for example, in Fig 1.

These data are in agreement with results from other studies revealing an impact of the environmental conditions on DNA methylation. Temperature changes, for instance, altered the activity and methylation state of the transposon *Tam3* in *Antirrhinum* (HASHIDA *et al.*, 2003). Planting density also affected the methylation state of the *Ac* element in maize (TSAFTARIS and KAFKA, 1998). Results obtained for three consecutive years revealed that demethylation (activation) of a methylated *Ac* element was significantly more frequent in plants grown under spread than dense planting. In addition, total DNA methylation measured by High Pressure Liquid Chromatography (HPLC) increased in inbred lines but remained stable in hybrids when compared in plants grown under spread and dense planting conditions (TSAFTARIS *et al.*, 1998).

Resistance of hybrids in induced genome methylation alterations under different stresses could be at the core of high and, maybe more importantly, F1 stable yield, especially if critical cytosine residues (e.g. regulatory genes, promoter regions of protein-coding genes) are preferably involved. Evidence has been provided that developmental changes of DNA methylation and chromatin structure at, or close to, the promoter region of a gene are responsible for epigenetic regulation of expression (HOEKENGA *et. al.*, 2000). Other regions of the genome, (e.g. heterochromatic DNA), remain highly methylated permanently, throughout plant growth. This could explain why slight changes of total methylation are concomitant with significant changes in gene expression. Results from this study support the hypothesis that hybrids perform better than inbred lines as they resist alterations in methylation under stress.

Obviously, experimental validation of this hypothesis requires analysis of higher number of possibly methylated sites than those examined. In subsequent studies we have used Restriction Landmark Genomic Scanning (RLGS) that is a method capable of screening in a single assay the methylation status of more than a thousand genes. The RLGS analysis agreed with this study demonstrating that a stable hybrid had a stable methylation pattern, that did not change significantly under stress (Kovacevic, Polidoros and Tsaftaris, unpublished results). Further experiments are underway to identify genomic regions and critical genes whose methylation is differentially affected by planting density in inbred lines and hybrids, and examine their role in the manifestation of heterosis and stability of hybrid performance.

REFERENCES

BIRD A., 2002 DNA methylation patterns and epigenetic memory. Genes Develop. **16:** 6-21.

CAI Q., C.L. GUY and G.A. MOORE, 1996 Detection of cytosine methylation and mapping of a gene influencing cytosine methylation in the genome of Citrus. Genome **39:** 235-242.

DELLAPORTA S.L., J. WOOD, J.B. HICKS, 1983 A plant DNA minipreparation: Version 2. Plant Mol. Biol. Rep. **1:** 19-22.

DE VIENNE D., J. BURSTIN, S. GERBER, A. LEONARDI, M. LE GUILLOUX, A. MURIGNEUX, M. BECKERT, N. BAHRMAN, C. DAMERVAL, M. ZIVY, 1996 Two-dimensional electrophoresis of proteins as a source of monogenic and codominant markers for population genetics and mapping the expressed genome. Heredity **76:** 166-177.

DUVICK D.N., 1997 What is yield? pp. 332-335. *In*: G.O. Edmeades, B. Banziger, H.R. Mickelson, C.B. Pena-Valdivia

(Eds.), Developing drought and low N-tolerant maize. CIMMYT, El Batan, Mexico, D.F.

FASOULA D.A., V.A. FASOULA, 1997 Gene action and plant breeding. Plant Breed. Rev. **15:** 315-374.

FASOULAS A.C., V.A. FASOULA, 1995 Honeycomb selection designs. Plant Breed. Rev. **13:** 87-139.

HAN F.P, G. FEDAK, T. OUELLET, B. LIU, 2003 Rapid genomic changes in interspecific and intergeneric hybrids and allopolyploids of Triticeae. Genome **46:** 716-23.

HASHIDA S.N., K. KITAMURA, T. MIKAMI, Y. KISHIMA, 2003 Temperature shift coordinately changes the activity and the methylation state of transposon Tam3 in *Antirrhinum majus*. Plant Physiol. **32:** 1207-1216.

HOEKENGA O.A., M.G. MUSZYNSKI, K.C. CONE, 2000 Developmental patterns of chromatin structure and DNA methylation responsible for epigenetic expression of a maize regulatory gene. Genetics **155:** 1889-1902.

JANICK J., 1998 Exploitation of heterosis: uniformity and stability considerations. pp. 319-333. *In*: J. Coors (Ed.), The genetics and exploitation of heterosis in crops. Am. Soc. Of Agronomy.

MATZKE M.A., M. PRIMING, J. TRNOVSKY, A.J.M. MATZKE, 1989 Reversible methylation and inactivation of marker genes in sequentially transformed tobacco plants. EMBO J. **8:** 643-649.

SHERMAN J.D., L.E. TALBERT, 2002 Vernalization-induced changes of the DNA methylation pattern in winter wheat. Genome **45:** 252-260.

SHAKED H., K. KASHKUSH, H. OZKAN, M. FELDMAN, A.A. LEVY, 2001 Sequence elimination and cytosine methylation are rapid and reproducible responses of the genome to wide hybridization and allopolyploidy in wheat. Plant Cell **13:** 1749-1759.

SONG R., J. MESSING, 2003 Gene expression of a gene family in maize based on noncollinear haplotypes**.** Proc. Natl. Acad. Sci. USA **100:** 9055-9060.

STEWARD N., M. ITO, Y. YAMACHUCHI, N. KOIZUMI, H. SANO, 2002 Periodic DNA methylation in maize nucleosomes and demethylation by environmental stress. J. Biol. Chem. **277:** 37741-37746.

TARIQ M., J. PASZKOWSKI, 2004 DNA and histone methylation in plants. Trends Genet. **20:** 244-251.

TOKATLIDIS I.S., M. KOUTSIKA-SOTIRIOU, A.C. FASOULAS, A.S. TSAFTARIS, 1998 Improving maize hybrids for potential yield per plant. Maydica. **43:** 123-129.

TSAFTARIS A.S., 1995 Molecular aspects of heterosis in plants. Physiol. Plant. **94:** 362-370.

TSAFTARIS A.S., A.N. POLIDOROS, 1993 Studying the expression of genes in maize parental inbreds and their heterotic and non-heterotic hybrids. pp. 283-292. *In*: A. Bianchi, E. Lupotto, M. Motto (Eds.), Proc. XVI Eucarpia Maize and Sorghum Conference. Bergamo, Italy.

TSAFTARIS A.S., M. KAFKA, A. POLIDOROS, 1997 Epigenetic modifications of total genomic maize DNA: The role of growth conditions. pp. 125-130. *In:* Tsaftaris A.S., (Ed.), Genetics, Biotechnology and Breeding of Maize and Sorghum. The Royal Society of Chemistry, Cambridge, UK.

TSAFTARIS A.S., M. KAFKA, 1998 Mechanisms of heterosis in crop plants. J. Crop Prod. **1:** 95-111.

TSAFTARIS A.S., M. KAFKA, A. POLIDOROS, E. TANI, 1998 Epigenetic changes in maize DNA and heterosis. pp. 195-203. *In*: J. Coors (Ed.), The genetics and exploitation of heterosis in crops. Am. Soc. Agronomy, Madison, WI.

TSAFTARIS A.S., A.N. POLIDOROS, 2000 DNA methylation and plant breeding. Plant Breed. Rev. **18:** 87-176.

WU L.M., Z.F. NI, F.R. MENG, Z. LIN, Q.X. SUN, 2003 Cloning and characterization of leaf cDNAs that are differentially expressed between wheat hybrids and their parents. Mol. Genet. Gen. **270:** 281-286.